The Sound of Recycling

Transfoaming glass waste into acoustic panels

Ludwika Buczyńska

TU Delft
Delft University of Technology

ABSTRACT

This thesis explores the upcycling of post-consumer glass waste into functional acoustic panels for architectural applications. Addressing both environmental concerns and indoor acoustic performance, the research investigates the potential of glass foaming and fusing techniques to transform discarded glass, such as soda lime, light bulb glass, and mixed cullet, into porous, sound-absorbing elements suitable for use in the built environment.

The study begins with a comprehensive literature review on glass recycling, classification of glass waste streams, and limitations within current recycling infrastructures, particularly regarding contaminated or mixed glass cullet. The material science behind foam glass production is examined, with a focus on how porosity, pore size distribution, and pore interconnectivity affect acoustic absorption. Kiln-based secondary casting and fusing techniques are also reviewed as accessible, energy-efficient alternatives to primary glass forming processes. In parallel, the acoustic literature is reviewed to understand key performance indicators such as reverberation time, clarity index, and sound absorption coefficient, especially in relation to porous materials. Furthermore, the review introduces the growing use of computational tools in acoustic design, including the use of simulation environments (such as CATT-Acoustic) and parametric optimization workflows (e.g., in Grasshopper), which allow for data-driven decision-making in early-stage material and geometry development.

A series of experimental trials were conducted to evaluate how various glass types respond to foaming, with particular attention paid to their level of contamination. Variables such as foaming agent type (calcium carbonate, eggshells, manganese dioxide), glass composition, particle size, and firing schedule were tested for their influence on pore development and structural integrity. Glass was successfully foamed at 860°C and 790°C. Notably, eggshells showed strong compatibility not only with clean soda lime cullet, but also with more contaminated light bulb glass and mixed cullet, yielding homogeneous pore structures. Re-foaming tests and prototype casting using 3D-printed moulds demonstrated the adaptability and scalability of the method. Selected samples were tested using an impedance tube, confirming their ability to absorb mid- to high-frequency sound, particularly around 1000 Hz, a range critical to both music and speech. The highest absorption coefficients were achieved with soda lime glass; however, the presence of contamination in other glass types did not significantly diminish acoustic performance of the developed material.

To enhance mechanical integrity, fusing trials were conducted to bond the porous layer to a solid glass surface. This was done without compromising the internal pore structure, achieving successful fusion at 705°C for samples made of both light bulb and soda lime glass paired with soda lime float glass.

To evaluate architectural performance, the panels were applied in a digital acoustic simulation of a real-world case study: the 2200 m³ Theatre Hall at TU Delft. The space suffers from excessive early reflections and high clarity index values. Field measurements were used to calibrate a model in CATT-Acoustic, which then informed a parametric optimization process in Grasshopper to determine optimal panel placement. The strategy focused on reducing C80 while preserving reverberation time, maintaining suitability for both rehearsal and performance scenarios. Although improvements in acoustic metrics were modest, they demonstrated that the porous panels successfully reduced problematic reflections without overly damping the space.

Through the integration of material science, real-world measurement, computational acoustics, and parametric design and design optimization, this thesis presents a viable, circular strategy for converting low-value glass waste into functional acoustic components. The findings point to broader potential applications in performance spaces where a nuanced balance between clarity and reverberation is required, offering a solid foundation for further research into sustainable material acoustics.

The Sound of Recycling

Transfoaming glass waste into acoustic panels

TU DELFT
MSC ARCHITECTURE, URBANISM & BUILDING SCIENCES

BUILDING TECHNOLOGY GRADUATION STUDIO

MENTOR TEAM
Dr. Faidra Oikonomopoulou
Prof. Martin Tenpierik
Dr. Gabriele Mirra

STUDENT
Ludwika Buczyńska (6068804)

PRESENTATION DATE
23 June 2025

TU Delft
Delft University of Technology

PREFACE

Completing my master's degree at the Faculty of Architecture and the Built Environment at TU Delft has been an enriching experience - academically, and personally. The past two years were filled with new challenges, but the final eight months, during which I worked on this graduation thesis, stand out particularly. My graduation project brought together two areas I've grown interested in, glass and acoustics, in a really engaging way. It was a learning process full of ups and downs, and many rewarding moments and I never had to go through it alone.

I want to thank my Mentors for their time and encouragement throughout this project. I felt their genuine interest at every step.

Faidra Oikonomopoulou has been a source of deep expertise in glass and (contagious) enthusiasm from the very beginning - already when I picked my topic with her. Faidra, thank you for your creative help in troubleshooting in the lab and your ability to treat stress with laughter. It made the whole process truly enjoyable.

Martin Tenpierik supported the room acoustics side of this thesis, helping me with the impedance tube tests and explaining complex concepts of sound propagation in such a practical and straightforward way. Martin, your quick e-mail replies and patience – especially during these meeting where I had more questions than answers- are highly appreciated.

Gabriele Mirra advised mostly on the computational and design aspects of this project. Gabriele, your openness to brainstorm, technical support (that script saved me), and sharp honesty made me really think critically of what I was doing. I'm especially grateful for the way you took my academic ambitions seriously, encouraging me as I began considering future academic paths.

Dear Mentor Team, thank you for all your help. I genuinely hope we'll stay in touch and that, even though this thesis is done, the reverberation of your support will keep echoing into whatever comes next (pun fully intended).

I would also like to thank **Telesilla Bristogianni**, whose insights were invaluable even though she was not officially part of my mentor team. Many thanks as well to **Lara**, **Menandros** and **Wilfried** for helping me get started in the lab, showing me the equipment, sharing ideas and being present throughout my experiments and presentations.

To the staff of the Stevin II and DEMO Labs - thank you for your technical assistance and for cutting my samples again and again (and again).

Lastly, thank you to my parents and friends - both in Delft and back home - for your constant emotional support. Whether through a phone call or during a shared lunch, your presence made a difference.

An unexpected highlight of this thesis process was joining Krashna Musika, the TU Delft student orchestra, which led me to choose our rehearsal room as a case study. This connection between research and personal passion turned an academic obligation into something genuinely meaningful. As a cellist with a background in architecture, I'd always dreamed of designing a concert hall, but only now do I see the possibility of doing so as an acoustician. Maybe that small, imperfect rehearsal room I have worked with may have sparked the beginning of a future in architectural acoustics?

This journey has been filled with firsts and discoveries. I've learned a lot, and I'm proud of what I've achieved. Beyond mastering new skills and research methods, I've developed a much deeper understanding of the many layers behind making building practices truly sustainable. From the challenges of recycling glass waste to the practical difficulties of material testing, I've seen how real-

world limitations influence design and how those same challenges can lead to creative solutions. This experience has made me more conscious of the environmental impact of architecture, more critical of sustainability claims, and more committed to pushing for circular solutions in the built environment.

Whether the future leads me into industry or academia, I'll carry forward this mindset so that this postgraduate path not only marks the end of a certain chapter, but opens new doors for me as a more aware and responsible engineer.

TABLE OF CONTENTS

LIST OF FIGURES

LIST OF TABLES

1 | INTRODUCTION

1. INTRODUCTION

This research explores the potential of glass waste as a raw material to produce acoustic panels, offering a solution that meets both environmental and functional demands in architecture.

In the context of a growing emphasis on circular economy principles and sustainable construction practices, the reuse of waste materials have become critical area of investigation. Glass waste represents a largely underused resource in this area. Bringing together material science, architectural acoustics, and computational design, this research explores their overlap to address new architectural challenges. By exploring the use of glass waste in acoustic panel production, the study not only seeks to divert waste from landfills but also to contribute to the development of environmentally responsible architectural components made fully of material that is currently considered waste. This approach aligns with sustainability goals, addressing functional challenges in built environment, particularly in terms of sound quality. The following sections outline the framework through which this investigation is structured.

1.1. Research framework

To situate this research within a broader context, the following section outlines its foundational elements. It begins by identifying the environmental and architectural challenges associated with glass waste and acoustic design. From there, it defines the project's objectives, research questions, and relevance. Together, these components form the framework that guides the subsequent phases of the study.

1.1.1. Problem statement

According to the European Commission, construction and demolition waste is one of the largest waste streams in the European Union, accounting for approximately 30% of total waste (Vermeulen, 2016). Among other materials, glass has a significant potential for recycling due to its unique properties, such as complete recyclability and resistance to quality loss through remelting (Bristogianni et al., 2018; DeBrincat & Babic, n.d.). Despite this, only container glass is recycled in a closed loop in Europe, while other types, including architectural, automotive, household and electronic glass waste are mostly downcycled (usually added as glass powder to other construction materials) or landfilled (Bristogianni et al., 2018; Bristogianni & Oikonomopoulou, 2023). This presents a critical environmental challenge.

One of the primary barriers to recycling glass other than container is contamination, which makes remelting difficult or unsafe. Adhesives, coatings and lamination are often impossible or uneconomical to remove. For cullet to be remelted into float glass, its origin must be known, and the purity standards are strict. Large amounts of uncontaminated glass end up in landfills due to recipe mismatch - differences in melting temperatures between types of glass further complicate recycling process (Bristogianni et al., 2018). This poses a missed opportunity, since glass recycling offers numerous benefits, including reducing landfill waste and preserving raw materials, such as sand and sodium carbonate (Hestin et al., 2016.; Surgenor et al., 2018). Therefore, alternative methods for recycling glass waste, particularly those tolerant of higher levels of contamination, are urgently needed (Bristogianni & Oikonomopoulou, 2023).

Research conducted at TU Delft has shown that contaminated glass waste can be successfully recycled through casting (Oikonomopoulou, 2019). This solution addresses challenges like contamination or recipe mismatch that are often the main reasons for downcycling or landfilling of glass. Casting not only enables mixing of different glass recipes in the same furnace but also allows for creating objects with higher tolerance for imperfections in their meso-structure, compared to thin glass standards (Bristogianni et al., 2021). Furthermore, the use of moulds in casting provides freedom in shaping the final product, allowing for the creation of customized geometries (Ioannidis et al., 2024).

Sound absorption technologies, though widely used, are often limited by traditional production methods that fail to meet customization needs or rely on synthetic materials with high environmental impact, like rockwool, glass wool or polyester (Buratti et al., 2016; Setaki et al., 2023). Research has shown that foam glass, made from recycled materials, holds promise for acoustic applications due to its porous structure (Cai et al., 2023; Cho et al., 2005; Yan et al., 2019). What is more, research by (Hesky et al., 2015) indicates that waste glass can replace up to 70% of the raw materials required for foam glass production. Foaming techniques have shown great potential for incorporating glass waste into the production of porous glass, as proven by the work of (Da Silva et al., 2021) and (Giassia, 2022). These findings, discussed in detail later in this report, highlight the potential of foam glass as a sustainable material with promising acoustic performance. In contrast, while cast glass does not naturally offer strong acoustic properties, its value lies in the use of moulds, which enable a high degree of geometric customization. This level of design flexibility is often unachievable with conventional materials typically used in acoustic applications.

Finally, an important component of this project is the integration of computational design and design optimization - the use of simulation tools adopted to predict and analyze the acoustic performance of architectural spaces. While such tools are well-established in room acoustics, research combining material engineering and acoustic performance through computational modeling is still relatively tight. This project contributes to filling that gap by combining experimental material development with digital simulation, offering a more holistic approach to the development of a sustainable, acoustically effective material, promoting manufacturing methods for recycling glass in a closed loop.

1.1.2. Objectives and boundary conditions

Project objectives

This research aims to explore the potential for upcycling glass waste into acoustic panels incorporating foaming method and investigates the influence of design parameters (such as porosity, geometry, and material composition) on material's acoustic properties. The proposed panels are planned to have a two-layer structure: a porous layer of foamed glass for sound absorption and a layer of solid glass for rigidity, fused together into a single unit. With each side exhibiting different properties, these panels provide an effective solution for the chosen case study, the Theatre Hall at TU Delft X. This venue can host both amplified and unamplified events, each of which requires different acoustic characteristics from the space. Two-sided panels are a solution to better adjust the Theatre Hall to the current function. Once the panel is prototyped, its acoustic properties are measured using impedance tube. These properties are then assigned to a digital model to perform acoustic simulations of the Theatre Hall before and after introducing the panels in the space. Optimization methods are used to determine the optimal placement of the panels within the chosen case study volume. Finally, the study aims to establish a framework for future applications of recycled glass panels in architectural acoustics, showcasing their potential as a sustainable and functional design solution.

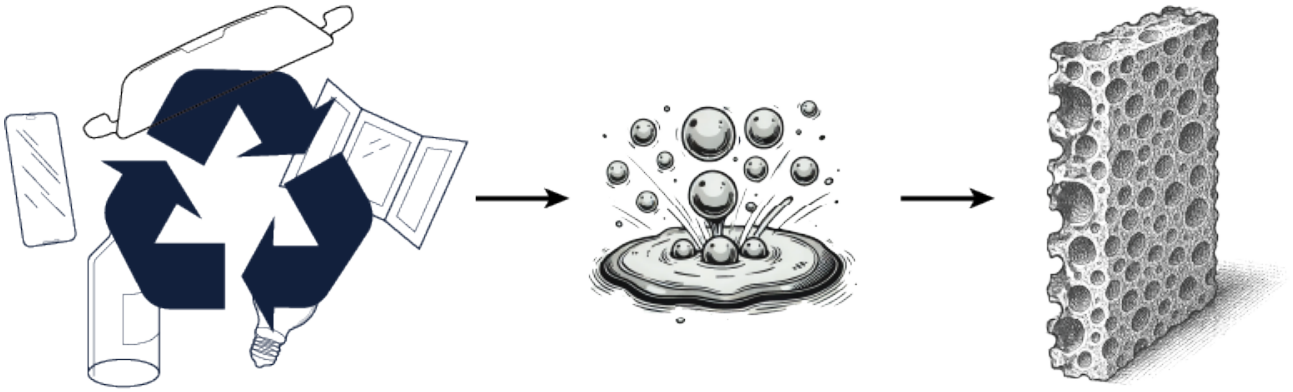

Fig. 1.1. Schematic representation of the project's main objective: upcycling mixed glass waste using the foaming method to produce porous, sound-absorbing panels for architectural applications; own work

Boundary conditions

This study focuses on evaluating the acoustic performance of glass waste panels, specifically their sound absorption coefficient, while other properties and structural considerations are excluded. The panels will be limited to laboratory-scale prototypes designed for testing. They will be virtually applied in a case study, but real-world implementation is beyond the scope of this research.

1.1.3. Research questions

Main research question

According to the stated problem, the research question of the study is formulated as follows:

What are the potential and limitations of developing a porous material from glass waste to produce acoustic panels for architectural space?

The main research question can be further subdivided into following sub-questions regarding material engineering, architectural acoustics and background questions that help guide the study – regarding the chosen case study and the research itself:

Material engineering

- What types of glass waste are suitable for acoustic panel production?
- Which glass waste streams are well suited for foaming?
- (How) do different fabrication parameters impact the porosity of the material and (how) can its porosity be controlled?
- What are the optimal physical parameters in the process of fabricating a recycled glass panel?
- How does contamination in glass waste affect the foaming reaction and resulting porosity?

Architectural acoustics

- (How) do impurities in glass waste affect the material's acoustic performance?
- What are the effects of porosity on the panel's acoustic properties?
- What are the effects of panel's geometry design on its acoustic properties?
- How to optimally integrate the panels into an existing space to improve its acoustic performance?

Background questions

Concerning the case study

- What is the current acoustic performance of the Theatre Hall?
- What functions does this space (want to) host?
- What are the ideal acoustic parameters for the Theatre Hall and its users (both the audience and performers)?

Concerning the research

- How is the acoustic performance of a material assessed?
- What are the environmental benefits of upcycling glass waste into acoustic panels?
- What metrics of acoustic performance of the room are important for classical music?
- What new applications could the manufactured material offer?

1.1.4. Relevance

The graduation studio puts focus on innovative sustainable design technologies for the built environment. This master's thesis centers on glass recycling, a major research focus at TU Delft.

Environmental relevance

This research contributes to environmental sustainability by addressing the pressing environmental challenge – the underutilization of glass waste. While container glass benefits from established closed-loop recycling, other streams, such as flat architectural, automotive or lighting glasses remain largely downcycled or landfilled. By upcycling this waste into architectural products, the study promotes circular economy principles, reducing landfill waste and resources extraction, and supports energy-efficient design and global goals for reducing carbon footprint. By demonstrating that even contaminated glass types can be transformed into functional acoustic panels, this research opens up new pathways for glass waste revalorisation.

The foaming technique employed in the study not only reduces the need for virgin raw materials but also operates at lower temperatures than traditional remelting process, decreasing energy consumption. Fusing developed in the study is used instead of employing adhesives – the resulting circular product, an acoustic panel, is made entirely of glass waste and can be re-recycled in the future.

Scientific relevance

From a research perspective, this thesis contributes to scientific knowledge filling a gap at the intersection of glass engineering and architectural acoustics – an area with significant, but underexplored potential. While foamed glass has been previously studied for insulation or structural purposes, its use as an acoustic absorber remains limited. This project not only expands the known functional applications of waste glass but also introduces new design paradigms through its hybrid porous-reflective panel concept.

Additionally, the study integrates experimental materials science with computational acoustic simulation and design optimization, reflecting a multi-scale, interdisciplinary methodology. Impedance tube testing paired with predictive modeling in CATT-Acoustic, and Grasshopper-based optimization tools (e.g. Galapagos) are used to refine panel placement in a case study venue. This cross-disciplinary approach demonstrates how digital workflow can support evidence-based acoustic interventions.

1.2. Methodology

This section of the report describes the approach adopted to finalize the project and answer the research question. The research is divided into four main parts, each corresponding to a different stage in the project. Each phase targets a specific goal and builds on the outcomes of the previous phase.

1.2.1. Phase 1: Context definition

This serves as an introduction and the foundation for the project, providing an overview and establishing the context for the research. It outlines the key issues related to glass waste and materials used in acoustics and highlights the research opportunity in combining these fields at the intersection of material engineering, computational acoustics and design optimization. The main research question is presented, and the sub-questions are formed, helping guide the research.

1.2.2. Phase 2: Literature review

This part supports the methodology with insights from prior research and experiments and establishes the theoretical framework for the study. The section provides a foundation for understanding glass recycling processes to be tested in the project, explores key acoustic aspects critical to the research, and explains computational methods for acoustic design that are crucial to complete the thesis.

The section is divided into subsections, each focused on a different aspect of the research.

- The first explores glass, including its waste streams, production methods, and relevant techniques such as kiln casting, foaming, and fusing, drawing from previous experimental studies. It also presents research on the acoustic properties of porous glass and highlights relevant findings.

- The second part of the literature review addresses architectural acoustics. It begins with an overview of sound propagation, followed by an explanation of the importance of achieving optimal acoustics in various environments. Solutions for enhanced acoustic performance are then discussed, with a focus on architectural or geometry design as well as material level. They are supported with examples of existing spaces known for their excellent acoustics.

- The third subsection of the literature review focuses on computational methods for acoustic design. It highlights the significance and limitations of computer simulations in acoustics, describes various types of acoustic simulations, and examines optimization methods used to refine acoustic performance.

1.2.3. Phase 3: Material development and testing

This phase builds upon the key takeaways and knowledge gained from the literature review. The material development process focuses on two primary techniques: foaming and fusing. The resulting panel has a dual-layer structure: a porous layer, created through foaming, for sound absorption, and a solid glass layer for structural rigidity. Once both layers are prepared, they are fused together into a single unit. The panels are then cut into smaller samples using a waterjet cutter at the Glass Lab, Faculty of Architecture, TU Delft to fit into the impedance tube, where their sound absorption coefficient is measured. The experimental process described is iterative, with adjustments made to different manufacturing parameters based on the results of each test. Guided by the literature review, special attention is given to factors such as the glass recipe (type and additives), particle size, and foaming and fusing temperatures. Data on the samples' density, porosity, and sound absorption is systematically collected and analyzed to guide the next stages of the research.

1.2.4. Phase 4a: Design application in the case study

It this phase, the acoustic potential of the glass panels is demonstrated through their virtual application in the case study, Theatre Hall at TU Delft X. Simulations in relevant software are used to predict the acoustic performance of the room after implementing the panels. The results are compared with the room's acoustic performance before applying the panels. The aim of this phase is to validate the panels' effectiveness in addressing acoustic issues in the case study which is crucial for drawing the final conclusion. To be able to perform this part, acoustic measurements have been taken in the space to gather the data needed about its current acoustic performance. The methodology and results of these measurements are described in the next chapter.

1.2.5. Phase 4b: Design optimization

In this phase the distribution of the panels is optimized by simulating alternative configurations for their placement. Genetic optimization algorithms are used to find the best design solution that fulfills the predefined set of objectives. The goal of this phase is to provide design recommendations for using the panels, and a workflow that can be re-purposed for other performance spaces with minimal adaptation.

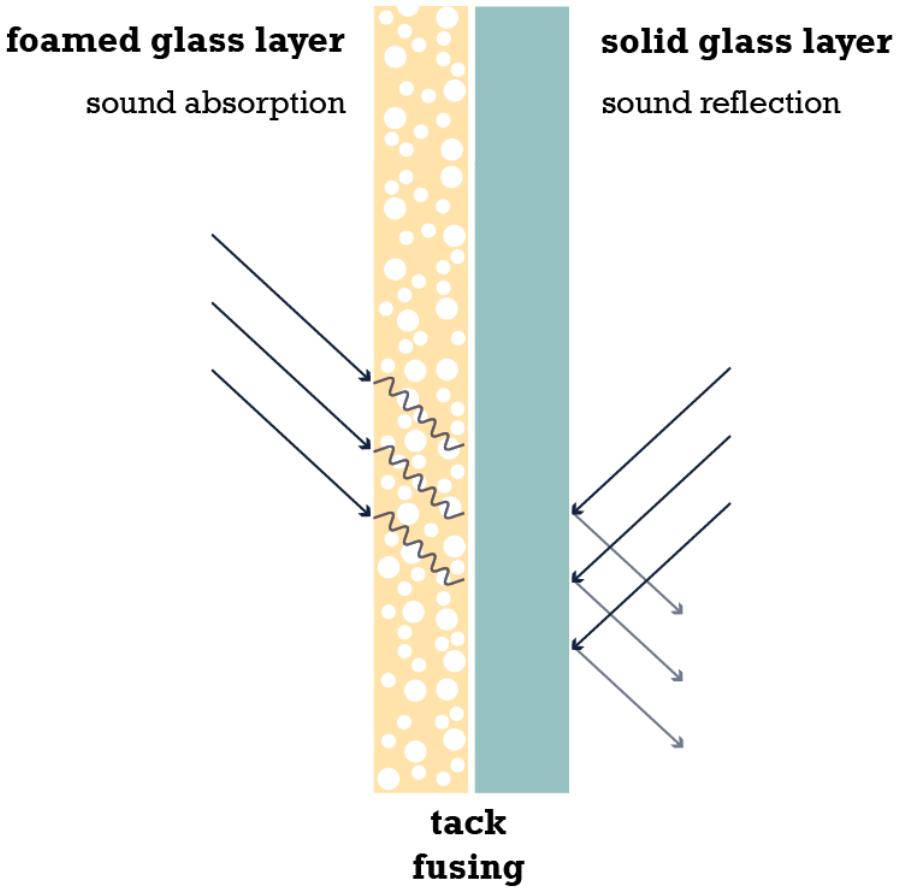

Fig. 1.2. Schematic cross-section of the dual-layer acoustic panel developed in this research, consisting of a foamed glass layer for sound absorption and a solid glass layer for sound reflection, bonded through tack fusing.

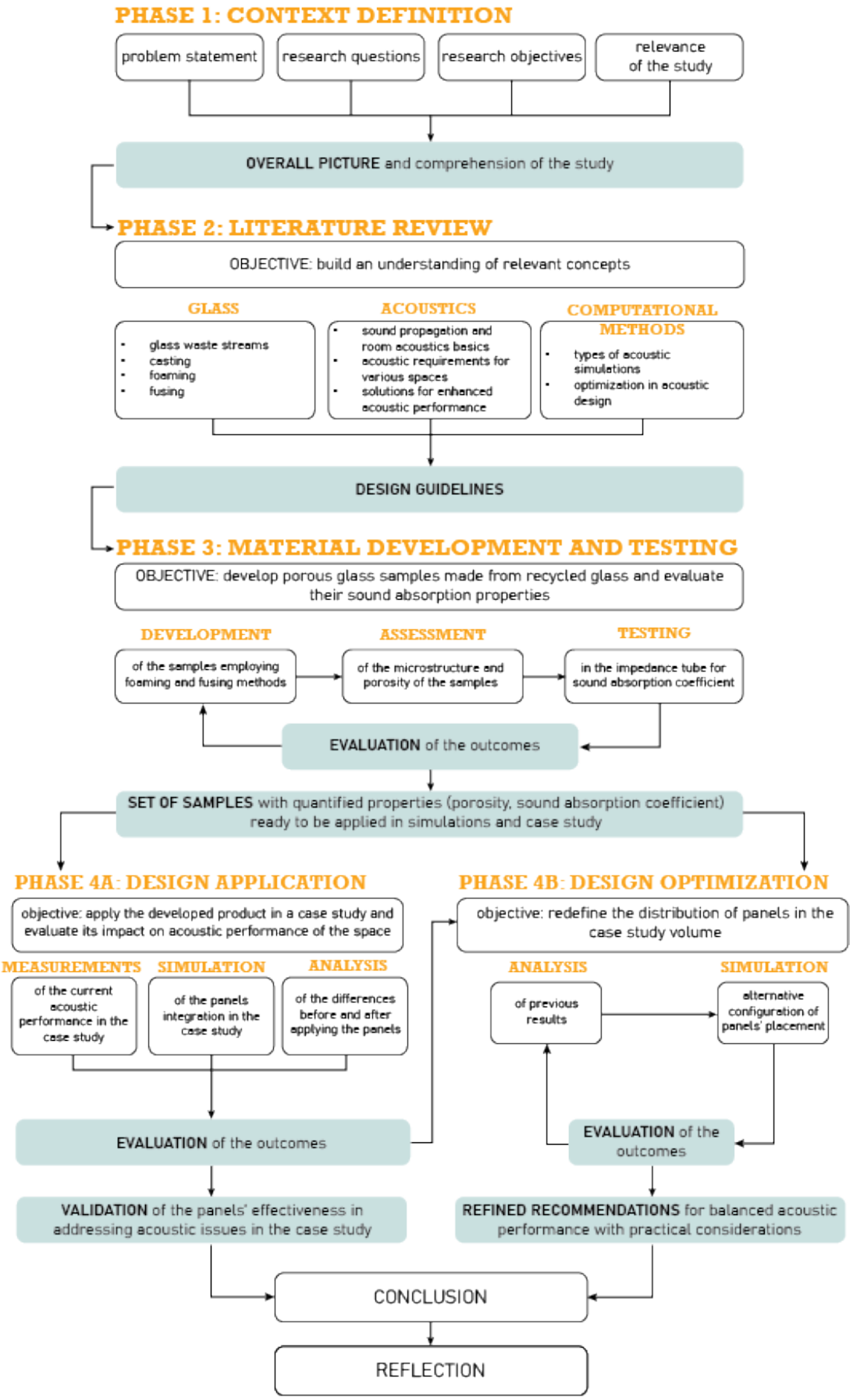

Fig. 1.3. Framework of the research, showing the overall methodology from context definition and literature review to material development, testing, and design implementation. The process is divided into four main phases: defining the research context, building theoretical foundations in the literature review, conducting material experiments, and applying the outcomes through case study integration and optimization; own work.

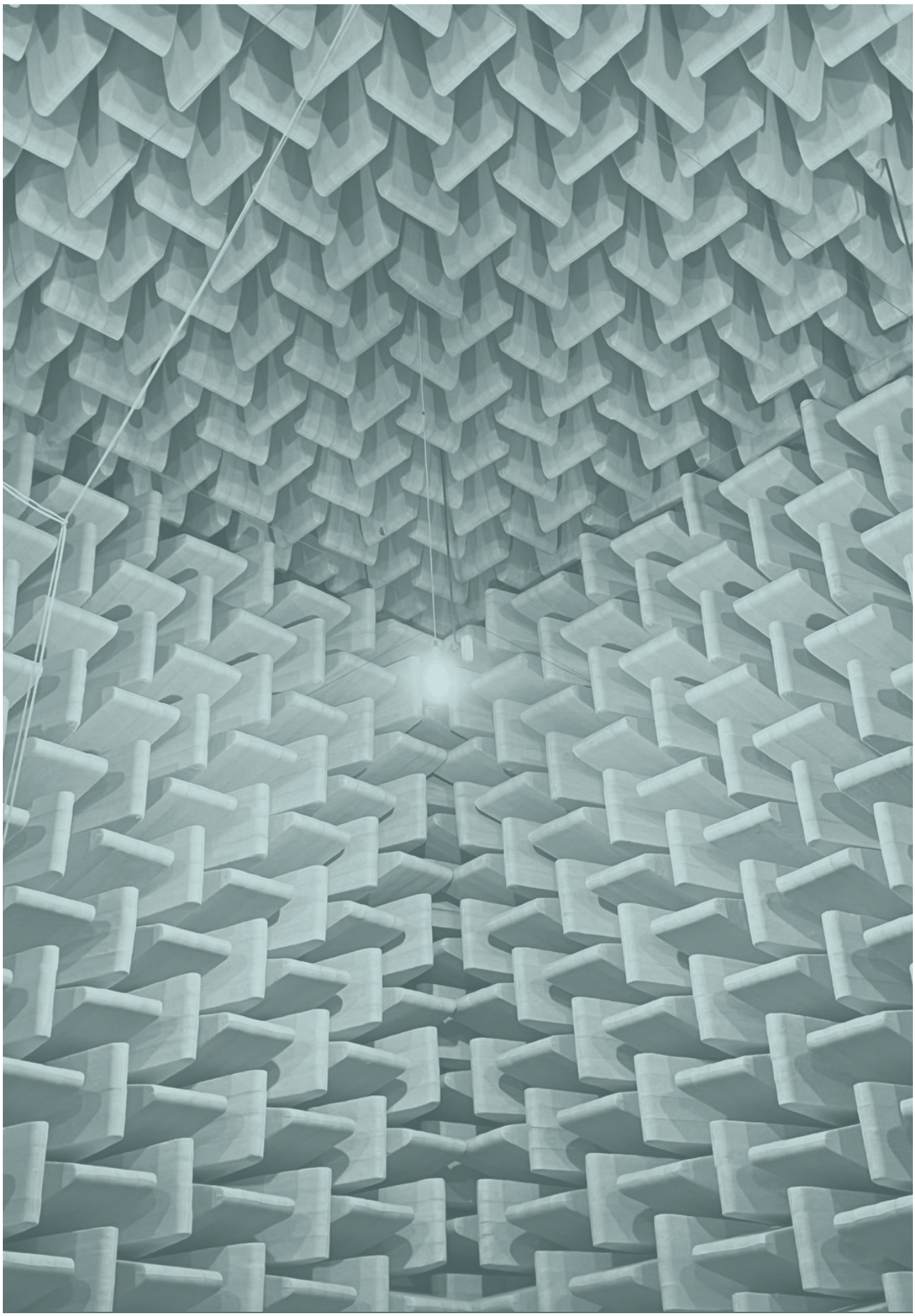

2 | LITERATURE REVIEW

2. Literature review

To establish a solid foundation for the development of the panels and their application in architectural acoustics, a comprehensive literature review was conducted. This involved analyzing resources related to sound behaviour in buildings, acoustic requirements for music spaces, material properties of glass, computational methods for simulating room acoustics. The aim was to gain understanding of the current state of the art, identify relevant methods and findings, and inform the subsequent, experimental and design, phases of this research. Each subsection of the literature review concludes with a summary of key takeaways, highlighting the most important insights from each topic that are directly relevant to the goals of this project.

2.1. Architectural acoustics

Architectural acoustics is the science of achieving a good sound environment in buildings. It encompasses the behaviour of sound within enclosed spaces and how different design elements, such as geometry, materials, and surface treatments, influence this behaviour. In the context of this research, understanding the fundamentals of sound propagation is essential for evaluating how recycled glass panels can improve room acoustics in a chosen case study. The following subsections explore the principles of sound behaviour in rooms, key performance criteria for different types of music, and strategies for acoustic treatment through both spatial design and material use.

2.1.1. Sound propagation and room acoustics

Wave character of sound

A sound wave is an oscillatory perturbation that propagates through a medium (gas, liquid, or solid) with a specific frequency, generated by the vibrations of a sound source and perceived by the human auditory system (Salter, 1998). These vibrations cause air particles to oscillate, creating a longitudinal wave in which particle motion aligns with the wave's direction of propagation. The wave's amplitude corresponds to its loudness, while its frequency determines its pitch. When both are sufficiently high, the wave is perceived as sound (Nederlof et al., n.d.). The speed of sound varies depending on the type of medium, its temperature and humidity, with an approximate speed of 343 m/s in air under standard conditions (Salter, 1998).

Frequency

Frequency refers to how many cycles a sound wave completes in one second and is the reciprocal of the period, which is the time it takes for one pressure fluctuation to complete. Higher frequencies correspond to shorter wavelengths and vice versa. The human hearing system can detect frequencies from 20 Hz to 20,000 Hz (20 kHz). Sound waves below this range are called infrasonic, and those above - ultrasonic. To simplify the analysis of such a wide range, the concept of octave bands is commonly used. It assumes grouping frequencies into broader intervals, with each band defined by upper and lower frequency boundary. For example, the 250 Hz octave band covers frequencies from 177 Hz to 345 Hz, while the 2000 Hz band spans from 1414 Hz to 2828 Hz, reflecting how the human ear perceives sound (Ermann, 2015).

Frequency enables the classification of sounds into three types: pure tones, harmonic sounds, and complex sounds. Pure tones, where all sound energy is concentrated at one frequency (e.g., car horns or whistles), are often perceived as unpleasant. Harmonic sounds, such as those produced by musical instruments, exhibit energy distributed in frequency patterns. The majority of everyday sounds, such as background noise or speech, are complex sounds, with energy across various frequencies within the hearing spectrum (Ermann, 2015).

Sound pressure (level), power and intensity

Sound is characterized by variations in air pressure caused by sound waves. These variations are perceived as loudness. The human hearing range spans from 20 micropascals, the threshold of hearing, to 200 Pascals, the threshold of pain. To accommodate this wide range, sound pressure is measured on a logarithmic scale and expressed as sound pressure level (SPL) in decibels (dB). On this scale, the threshold of hearing corresponds to 0 dB, and the threshold of pain-to 140 dB (Salter, 1998).

Sound appears as louder closer to its source than further away. To quantify the acoustic energy produced by a sound source, the parameter sound power (W), expressed in watts, is used. As the sound wave propagates from the source, it spreads over an increasingly larger area, causing the acoustic energy per unit area, known as sound intensity (I) and measured in watts per square meter, to diminish (Nederlof et al., n.d.).

Reflected sound

When sound strikes a surface, it can be absorbed (converted into heat within the material), transmitted (pass through the material), or reflected back into the room (Ermann, 2015). In most environments, reflected sound dominates, creating a diffuse sound field, where sound energy reaches the listener indirectly after multiple reflections from surrounding surfaces, unlike in a free sound field, found only in special environments like anechoic chambers, where only direct sound reaches the listener without any reflections. Reflected sound can be diffused, when it scatters into multiple weaker reflections across various angles, creating a uniform sound field. This can be achieved by shaping the surface irregularly to minimize direct reflections. This issue is explored further in the following section of this chapter.

Reflected sound that accumulates over time is referred to as reverberation, which results from late reflections-occurring more than 0.25 seconds after the direct sound (Salter, 1998). Reverberation time, a key metric in acoustics, is defined as the time it takes for a sound to decay by 60 dB (to become inaudible) after the sound source is switched off (Beranek, 1996). Reverberation influences whether a room feels acoustically “live” or “dead.” Achieving the right amount of reverberation is essential for optimizing music, speech clarity, noise reduction, and overall acoustic comfort.

Reverberation is most noticeable in spaces with hard, reflective surfaces. In contrast, smaller spaces with sound-absorbing materials experience little reverberation, as acoustic energy dissipates quickly. Excessive reverberation is common in environments like swimming pools, museums, railway stations, where hard surfaces dominate, and sound absorption is minimal, forcing people to speak louder (Cox & D’Antonio, 2017).

Reflections arriving late and heard separately from the early ones are perceived as echoes. They occur when intense reflections arrive more than 40 milliseconds after the direct sound. In auditoriums and music halls, the first rows are particularly prone to echoes due to the large distance from the rear wall, which creates a long path between the direct sound and the reflection from the rear wall. Flutter echoes arise when sound is repeatedly reflected by two parallel surfaces, travelling back and forth between them. These echoes decay more slowly compared to reflections from non-parallel surfaces. Both types of echoes significantly reduce acoustic clarity (Cox & D’Antonio, 2017).

Clarity

Clarity is a crucial aspect of both speech and music perception. To achieve good clarity, reverberation must be controlled and both direct sound and early reflections should be maximized. Early reflections are those arriving within approximately 50 milliseconds (when speech is considered) and 80 milliseconds (regarding music) after the direct sound. They improve the intelligibility and definition of sound due to the precedence effect, a psychoacoustics phenomenon, where direct

sound and early reflections (if separated by sufficiently short time) are combined into one, louder sound by the human brain. The latest studies suggest that even reflections received by the listener up to 200 milliseconds after the direct sound can contribute to improved clarity (Ermann, 2015).

Key takeaways

Sound propagates as a wave through air, liquids, or solids, generated by vibrations of a source. Its frequency describes how many cycles a sound wave completes in one second. It determines the pitch of a sound and is inversely related to wavelength. Human hearing ranges from 20 Hz to 20,000 Hz. Sound pressure level (SPL) uses a logarithmic scale to cover the full range of human hearing, from 0 dB at the threshold of hearing to 140 dB at the threshold of pain.

When sound strikes a surface, it can be absorbed, transmitted, or reflected. In most environments, reflected sound dominates and creates a diffuse sound field. In contrast, a free field contains only direct sound. Reverberation results from late reflections, defined as those occurring more than 0.25 seconds after the direct sound. It is measured as the time required for a sound to decay by 60 dB and plays a crucial role in shaping the acoustic character of a space. When strong reflections arrive after a significant delay, they may be perceived as echoes. Flutter echoes are caused by repeated reflections between parallel surfaces.

Clarity, important for both speech and music, depends on direct sound and early reflections, those arriving within about 50 milliseconds for speech and 80 milliseconds for music. Due to the precedence effect, these early reflections are merged with the direct sound by the human brain, enhancing loudness and intelligibility.

2.1.2. Acoustic requirements for music

The literature offers various definitions of music. (Rossing, 2014) describes it as "a form of art using sequences and clusters of sound". The study of music as a science falls under the domain of musical acoustics, which is closely linked to psychoacoustics, the field that explores how sound's physical properties, such as intensity, frequency, and duration, translate into how a listener perceives it in loudness, pitch, and timbre, respectively. (Ginn, 1978) highlights the difficulty of defining criteria for music due to its subjective aesthetic and emotional factors that complicate normalized assessment. However, extensive literature exists on music acoustics, particularly regarding the attributes of classical concert halls. Various literature provides acoustic metric guidelines for achieving satisfactory conditions in concert halls. In this paper, much of the focus is on classical (unamplified) music, which is strongly influenced by the physical features of the venue, such as present materials and geometry. In contrast, amplified music, for example that heard in clubs, relies mostly on electronic sound control and is less dependent on room acoustics (Lautenbach et al., 2007).

Classical music

Beranek, in numerous publications, has widely described the attributes of music halls and their corresponding acoustic metrics. The key attributes he identifies are liveness, loudness, clarity, intimacy, diffusion, and warmth, each linked to specific acoustic metrics:

- **Liveness** corresponds to **reverberation time (RT)** and **early decay time (EDT)**.
- **Loudness** is measured by **sound strength (G)**.
- **Clarity** relates to the **C80 index**.
- **Intimacy** is associated with the **initial time delay gap (ITDG)**.
- **Diffusion** is quantified by the **binaural quality index (BQI)** and the **interaural cross-correlation coefficient (IACC)**.
- **Warmth** is represented by the **bass index**.

A comprehensive summary and detailed description of these attributes and metrics can be found in (Markham, 2014). This project focuses specifically on the first three attributes (liveness, loudness, and clarity) and their corresponding acoustic metrics to describe their importance in the design and evaluation of music hall designed for unamplified music.

Reverberation time and early decay time

RT varies with the type of music being considered, with different requirements even among different periods of classical music. For instance, baroque chamber music is better suited to spaces with shorter RT, while music from the classical period benefits from longer RT (Beranek, 1992). Achieving the optimal amount of reverberation is essential for creating an acoustically pleasant environment in music halls. Too short RT can make a space feel "dry," which is particularly harmful to string instruments (Lautenbach, 2018). Recommended RT values in literature generally align around 2 seconds for classical music venues. For example, Beranek (1992) suggests an RT range of 1.7–2.2 seconds, assuming full occupancy, while (Nijs & Vries, 2005) recommend values between 2–2.3 seconds.

EDT, defined as the time it takes for the sound level to decay by 10 dB after the sound source is switched off (Beranek, 1996) is another key metric for music acoustics. Early reflections play a significant role in classical music venues, contributing to the listener's sense of being surrounded by music. These reflections should ideally come from horizontal surfaces and reach the listener before ceiling reflections (Lautenbach, 2018). For musicians, the acoustic environment should fulfill two key criteria outlined by (Ginn, 1978): the room should reflect sound back to the musicians from the audience area, enabling them to hear their own instruments, and musicians should be able to hear each other on stage. To meet those needs, (Lautenbach, 2018) emphasizes the importance of generating early reflections not only within the audience, but also from the stage area. On the other hand, (Markham, 2014) stresses that excessively strong early reflections can distract both musicians and the conductor, stressing the need for a balance.

Sound strength G

Sound strength G is a measure of loudness, defined by (Beranek, 1996) as "a function of the sound energy and the number of people who share it." Technically, it is defined as the ratio of the sound energy coming from a non-directional source to the same energy measured in a free field (e.g., an anechoic chamber) at a distance of 10 meters from the source (Beranek, 2011). Similarly to RT, different authors propose slightly varying optimal values for G strength in music halls, but they generally align around +5 dB. For instance, (Beranek, 2011) suggests a range of 4–7.5 dB, (Vercammen & Lautenbach, 2020) mention an optimal value of approximately +5 dB. (Nijs & Vries, 2005) recommend a range of 4–5.5 dB. It is important to achieve the appropriate level of G strength, as human hearing system is highly responsive to changes in this parameter. According to psychoacoustics, human ear can perceive differences as small as 0.25–0.5 dB (Ermann, 2015).

Clarity index C80

Clarity, also known as definition, regarding music, is a "degree to which the individual sounds in a musical performance stand apart from each other" according to (Beranek, 1996). He points out that this depends not only on the musicians' skill level, but largely also on the room geometry and the presence of early reflections. Technically, (Ermann, 2015) defines C80 parameter as the ratio of the sound energy that reaches the listener before the 80 milliseconds compared to the energy that arrives after that threshold. He states that the best concert halls have C80 values in the range -4 dB - +1 dB measured for an unoccupied scenario. On the other hand, unoccupied scenario (for example during rehearsals) might benefit from slightly higher clarity and then the values should be around 1 - +5 dB.

Club (amplified) music

With the rise of popular music as an industry and advancements in audio equipment, its loudness has significantly increased in recent years (Lautenbach et al., 2007; Vercammen & Lautenbach, 2020). The acoustic requirements for smaller and larger venues differ. Larger halls are prone to echoes, a common challenge for popular music concerts often held in acoustically poor venues like stadiums. In such spaces, long RT can be problematic, although features like openable roofs can help mitigate this issue by allowing the sound energy to escape to the open air rather than reflecting the sound back to the space.

Unlike classical music, which requires blending different sounds, popular music relies on electronic reproduction to achieve desired loudness, minimizing the hall's acoustic influence. Key requirements for popular music venues include a high direct-to-reverberation ratio, making the direct sound from the speakers dominate late reflections, and low reverberation, particularly in low frequencies (63–125 Hz). Excessive low-frequency reverberation can mask higher frequencies, reducing clarity. What is more, Lautenbach et al., 2007 stress that in order to reduce echoes in a pop music concert, late reflections should be reduced by at least 10 dB.

Key takeaways

The perception of sound is shaped by psychoacoustic factors such as pitch, loudness, and timbre. Classical (unamplified) music is much more sensitive to the acoustics of a room, including its geometry and materials, compared to amplified music, that usually depends more on electronic systems. For classical music venues, following acoustic attributes are considered critical: liveness (related to reverberation time and early decay time), loudness (quantified by the sound strength G), and clarity (measured by the clarity index C80).

Optimal reverberation time depends on musical style, with literature suggesting a range around 2 seconds for classical performance spaces. Early decay time, capturing the rate of sound energy decay in the first 10 dB, is also essential for a sense of envelopment and musical expression.

Sound strength G is another key metric, describing how loud sounds feel in a space. Recommended values for G in large (above 2500 seats) concert halls typically fall around +5 dB. Even small (like 0.25 dB) variations in G are perceptible to listeners, so achieving the correct balance is important.

Clarity indicates how well individual notes are distinguished from one another. It is defined as the ratio of early to late-arriving sound energy, with optimal values ranging from -4 to +1 dB in unoccupied halls. Early reflections from side walls and stage surfaces help musicians hear themselves and one another, though overly strong reflections may be distracting for the performers.

2.1.3. Solutions for enhanced acoustic performance through architectural and geometric design

This section explores methods for achieving enhanced acoustic performance, focusing on how architectural and geometric design impact acoustics, discussing the role of room shape and size on sound propagation and describing the effects of different ways of shaping diffusers surfaces.

Shape and size of the room

Room size strongly influences the acoustics inside it as it defines the sound's mean free path – the average distance that a sound ray travels before being reflected and changing its direction. (Salter 1998) stresses that in small rooms (less than 280 m^3) dimensions that are equal or exact multiplications of one another should be avoided to prevent axial standing waves – when they occur, the sound pressure adds up and overemphasizes a certain frequency. Correct room proportions are important to avoid this issue, minimizing the overlap of standing waves and ensuring consistent sound quality across the space. He also describes the important role of the ceiling in shaping overall acoustic performance in large music halls. The ceiling height should be 9-11 m for a hall with up to 500 seats, with larger halls requiring proportionally higher ceilings. Ceiling reflectors, commonly used in concert halls, should be positioned 5-10 m above the stage. Since good vision does not matter in concert halls as much as it does for example in Theatres, music halls often have flat floors that allow for rear wall reflections and a suitable sense of envelopment for the audience.

Beranek in his research categorized the world's most famous concert halls into four categories based on their shape, a summary of which was provided by (Markham, 2014). Among the types he describes: the vineyard (or terrace) hall, the fan-shaped hall, the lateral–directed hall and the shoebox, he favours the last one. Shoebox shape, a rectangular room with the stage at one narrow end, is praised by Beranek for its good acoustics due to lateral early reflections. Boston Symphony Hall and Amsterdam's Concertgebouw are well-knows examples of a shoebox hall type.

Different geometries of diffusers

A diffuser is a surface or an architectural element that scatters sound energy, minimizing strong reflections. Unlike absorbers, that quickly remove the sound energy from the space, diffusers offer an alternative way to reduce reverberation time, preserving the sound energy and distributing it uniformly in multiple directions. They can also be used to eliminate echoes. Most diffuser designs focus on breaking up the sound wavefront. Depending on architectural and acoustic requirements, diffusers can be made from materials such as wood, plastic, gypsum, or concrete. Well-optimized diffusers can serve as an alternative to basic geometric shapes, such as arcs, and are effective not only for normal sound incidence but also across a broader range of incident angles.

- **Plane surfaces (Figure 2.1.)**

Flat surfaces are common in architectural design, whether intentional or not. A rigid, non-absorbing plane surface reflects the sound in predictable ways. At high frequencies, the surface reflects sound like a mirror reflects light, producing directional reflection. At low frequencies, especially when dimensions of a surface are comparable to the acoustic wavelength, a flat surface causes diffraction at the edges of the panel. When a singular panel is used, the angle of incidence is equal to the angle of reflection, but when an array of flat panels is used, the resulting reflection is influenced by both the response of each individual panel and the arrangement of the entire array.

- **Triangles and pyramids (Figure 2.2.)**

Geometry of triangular diffusers, exactly the steepness of their slopes, defines their scattering efficiency. They can produce a range of effects, including notch effects (reducing sound in specific directions), or diffuse scattering, reducing specular reflections, especially when positioned in arrays. Strategic arrangement of these diffusers can enhance overall diffusion and prevent periodicity, which results in undesirable sound reflection patterns.

- **Curved surfaces**

Convex surfaces often blend well with modern architectural designs and are widely used as diffusers in both sound production and reproduction environments. Shapes like spheres and cylinders are particularly effective for spatial sound dispersion, especially when positioned in a correct way. Semicylinders perform well for uniform sound dispersion at normal incidence especially, but more complex curves are also effective for oblique angles. In contrast, concave surfaces pose significant challenges and are generally avoided in architectural acoustics. They concentrate sound, distributing it unevenly and creating echoes. The extent and intensity of sound focus depend on both the frequency and the curvature of the surface. For high frequencies, the focusing region is small but intense, while for low and mid frequencies the focus is more spread and therefore can be more problematic. (Cox & D'Antonio, 2017)

Fig. 2.1. Angled flat reflective panels on side walls of Baldwin High School Auditorium, Pittsburgh, PA; based on: Cox, T. J., & D'Antonio, P. (2017), Acoustic Absorbers and Diffusers: Theory, Design and Application (3rd ed., p. 378). CRC Press, Taylor & Francis Group.; source: https://hoffent.com/portfolio/baldwin-high-school/

Fig. 2.2. Pyramid ceiling at Southland Christian Church, Nicholasville, KY; the shape was used for economic, aesthetic and acoustical reasons. The pyramids are made from glass-reinforced gypsum and were designed asymmetrically with proportions of a golden ratio; source: Cox, T. J., & D'Antonio, P. (2017), Acoustic Absorbers and Diffusers: Theory, Design and Application (3rd ed., p. 386). CRC Press, Taylor & Francis Group.

Other strategies examples

Nagata Acoustics, in their design for the NOSPR concert hall in Katowice, Poland, employed cast-in-place concrete walls shaped with random, irregular patterns to create reflective surfaces that effectively diffuse high frequencies (Figure 2.3a). This not only provided an interesting, modern aesthetic, but also contributed to the hall's status as one of the most acoustically advanced concert venues in Europe.

In the Richard B. Fisher Center for the Performing Arts in New York, monolithic concrete walls are decorated with a wooden ribbon, enhancing sound diffusion and adding a unique visual element (Figure 2.3b).

Walls and ceiling of the Elbphilharmonie in Hamburg, Germany are covered with carefully designed

surfaces that are customized to the hall's specific acoustic requirements. Sound is reflected directly from flat areas and scattered by deep indentations, achieving a balanced acoustic experience. The hall features over 10,000 individually milled gypsum fiber concrete panels, each customized to meet precise acoustic and visual standards (Figure 2.3c)

As part of the Sydney Opera House refurbishment, several measures were introduced to improve acoustics. The hall previously suffered from excessive reverberation, and audience members seated further from the stage often felt disconnected from the performance. To address this, adjustable overhead reflectors were installed above the stage to enhance stage support, but they can be removed for amplified events (Figure 2.3e, f). Additionally, structured wall surfaces were added to improve diffusion and create a greater sense of musical envelopment, contributing also to the hall's visual identity (Figure 2.3d) (Engel & Reinhold, 2023).

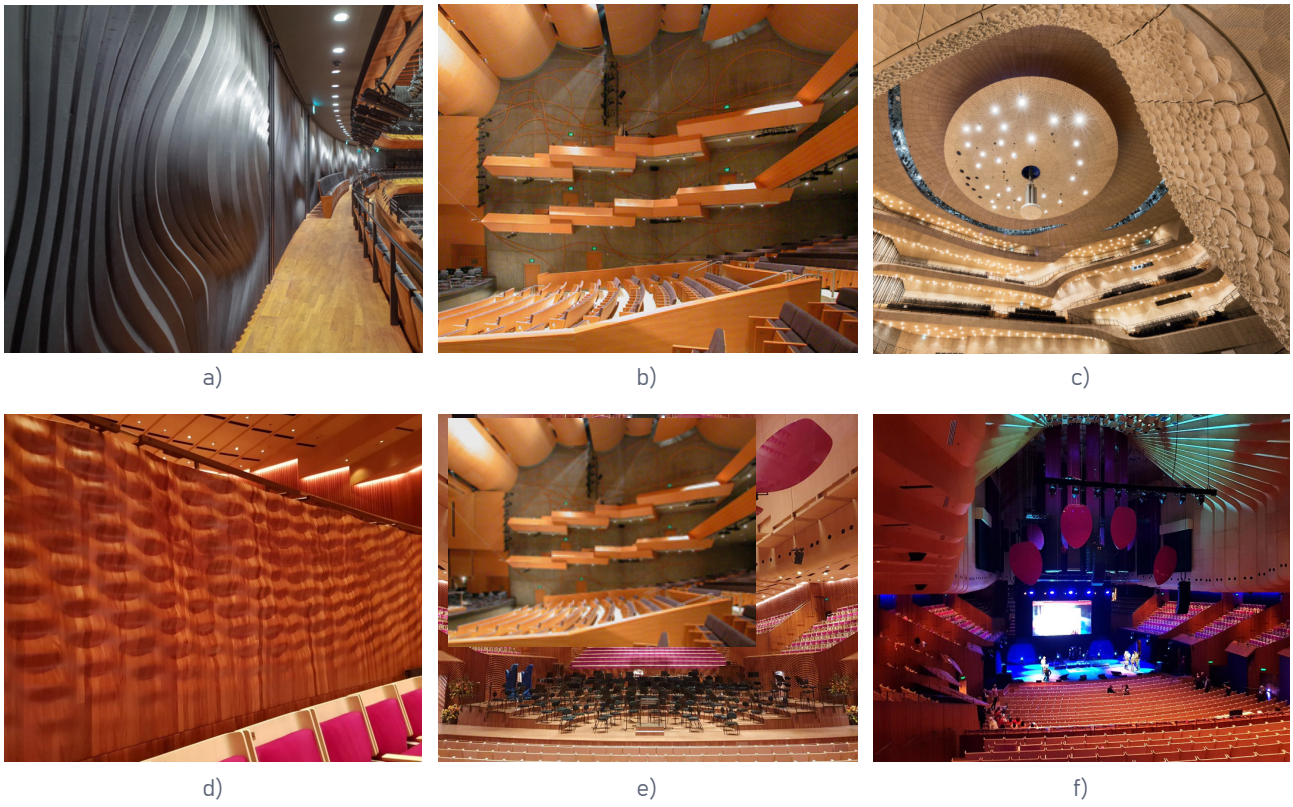

a) b) c)

d) e) f)

Fig. 2.3. a) Cast-in-place wall in NOSPR concert hall; Katowice, Poland; b) View of the main concert hall in the Richard B. Fisher Center for the Performing Arts, NY, USA; source: Toyota, Y., Komoda, M., Beckmann, D., Quiquerez, M., & Bergal, E. (2020). Concert Halls by Nagata Acoustics: Thirty Years of Acoustical Design for Music Venues and Vineyard-Style Auditoria (p. 159, 27). Springer International Publishing. https://doi.org/10.1007/978-3-030-42450-3; c) Walls of Elbphilharmonie, Hamburg, Germany; source: https://www.icmimarlikdergisi.com/2017/10/05/hamburgun-carpici-konser-binasi-elbphilharmonie/algorithms-design-concert-hall-elbphilharmonie-hamburg-germany-7-59d1dcb02a392__880/, d) Structrued surface on walls of Sydney Opera House, e), f) Movable reflective panels above the stage, that can be unfolded for unamplified event and folded up when amplified events are happening; source: https://www.ioa.org.uk/system/files/proceedings/g_engel_j_reinhold_acoustic_upgrade_for_the_concert_hall_of_the_sydney_opera_house.pdf

Key takeaways

Room size directly affects the mean free path of sound rays, influencing how sound behaves within the space. In small rooms, dimensions that are multiples of one another should be avoided to prevent standing waves that exaggerate certain frequencies. Ceiling height and reflector placement are especially important in concert halls, with ceilings typically ranging from 9 to 11 meters for up to 500 seats. Flat floors, often used in music halls, allow beneficial rear wall reflections that enhance the listener's sense of envelopment.

Different room shapes have also been studied for their acoustic qualities. Among the described types, the shoebox configuration is widely praised thanks to its ability to produce strong lateral early reflections that improve clarity and intimacy.

In addition to room geometry, diffusers play a critical role in scattering sound energy and preventing unwanted echoes. Unlike absorbers, which eliminate sound energy, diffusers preserve it, distributing it more evenly. They can be fabricated from a variety of materials and come in various forms. Flat panels reflect sound predictably at high frequencies and cause diffraction at low frequencies. Triangular and pyramid-shaped diffusers can scatter sound in many directions and are effective at reducing specular reflections. Convex curved surfaces, such as cylinders or spheres, are also effective, particularly when carefully positioned. In contrast, concave surfaces tend to focus sound, creating undesirable echoes and are typically avoided in acoustic design.

2.1.4. Material-level solutions for improved acoustics

The term "acoustical material" is broad but typically refers to materials specifically designed to absorb sound. An absorber is an acoustic element that has been designed to reduce acoustic energy. Absorbers are used to reduce noise levels and mitigate issues such as too strong sound reflections and excessive reverberation. Absorbers can be strategically placed in various locations based on the acoustic requirements of a space, such as near the sound source or close to the receiver (Arenas & Crocker, 2010). For effective acoustic design, absorbers and diffusers are often combined to create a balanced sound environment. The effectiveness of absorbers is measured with an absorption coefficient, which ranges from 0 to 1, representing no absorption to complete absorption, respectively.

Sound absorbers are typically classified into two main types - porous and resonant - each working based on different sound absorption mechanism (Cox & D'Antonio, 2017).

Porous absorbers

Porous sound-absorbing materials come in a wide variety, and their performance depends on factors such as composition, thickness, surface finish, and even the method of mounting (Arenas & Crocker, 2010). However, materials with strong sound absorbing properties are generally porous. In porous absorbers, the sound propagates through the system of interconnected channels. When a sound wave hits a porous material, the air molecules at its surface and within its pores start to vibrate, losing a part of their acoustic energy due to microscopic friction between the air and the pores' walls. This is known as thermal viscous losses. Typically, the sound absorption coefficient of purely porous absorbers increases with frequency as presented on the graph in Figure 2.6. This is due to the fact that the shorter wavelengths can enter the material more easily. Thicker panels tend to perform better, since the sound can travel deeper into the material and lose more energy along the way (Cox & D'Antonio, 2017).

Classification of porous absorbers

Porous absorbers can be categorized based on their connectivity to an external medium, for example air. Pores can be classified as open, in the form of continuous paths that connect to the material's external surface, or as closed, where they are entirely isolated from one another. Furthermore, some pores may be blind, with only one end open, while others may be through-pores, open at both ends. Effective sound absorption relies on a network of interconnected open pores, which allows air to flow through the material (Cox & D'Antonio, 2017). It is also essential to differentiate porosity from surface roughness, as a rough surface does not qualify as porous unless its irregularities are deeper than they are wide (Arenas & Crocker, 2010).

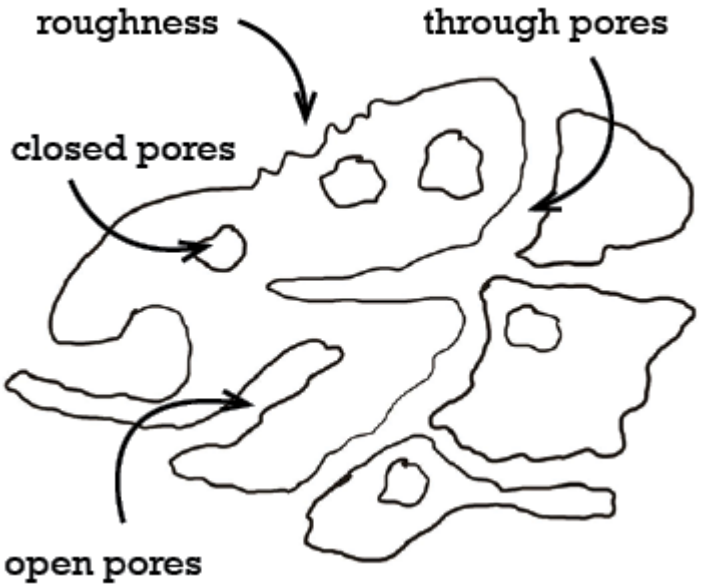

Fig. 2.4. Schematic illustration of pore types and surface features in porous materials, including open pores, closed pores, through pores, and surface roughness. These structural characteristics influence acoustic performance and material behaviour.

Porous absorbers can also be classified by their microscopic structure. Cellular absorbers, such as open-celled polyurethane or foam materials, are composed of interconnected cells. Fibrous absorbers consist of materials made from natural or synthetic fibers, including glass or mineral fibers. In contrast, granular absorbers, such as asphalt or porous concrete, are formed from rigid, microscopic particles or agglomerates, that are significantly larger in size compared to the internal voids within the material. The performance of these materials varies, with fibrous absorbers generally achieving higher porosity and thus more effective sound absorption compared to granular absorbers, which tend to have lower porosity (Arenas & Crocker, 2010). However, porous materials have the advantage in applications where fibreless materials are necessary, such as in environments where bacterial contamination must be avoided, for example food and pharmaceutical industries (Cox & D'Antonio, 2017).

Porous material properties

Porous sound-absorbing materials are characterized by several key properties that influence their acoustic performance. One of the most critical properties is flow resistivity, which varies significantly across materials and is essential for evaluating their sound absorption capability. Flow resistivity measures how easily air can penetrate the porous structure of a material and the resistance it encounters as it flows through. In simpler words, it reflects the ease with which air moves through the material. This property is expressed in rayls per meter, where the rayl is a unit of acoustic impedance.

Another important parameter is open porosity, which quantifies the volume of interconnected air spaces within the material. It is defined as the ratio of the total pore volume to the overall volume of the absorber. Only open porosity contributes to effective sound absorption, as it enables air movement through the material. High-performing absorbers can achieve porosity levels as high as 0.98. However, a trade-off often exists between porosity and flow resistivity, as these properties are interdependent and must be balanced for optimal performance.

Tortuosity, also referred to as the structural form factor, is a property that describes the complexity and orientation of pores within the material. It determines how tangled the paths for air movement are. The degree of tortuosity affects sound absorption. For simpler structures, such as cylindrical pores aligned in the same direction, tortuosity refers to the angle between the pores and the sound

wave. However, most porous absorbers have a more complex and disordered internal structure. In such cases, tortuosity must be measured or calculated from the microscopic configuration of the material (Cox & D'Antonio, 2017).

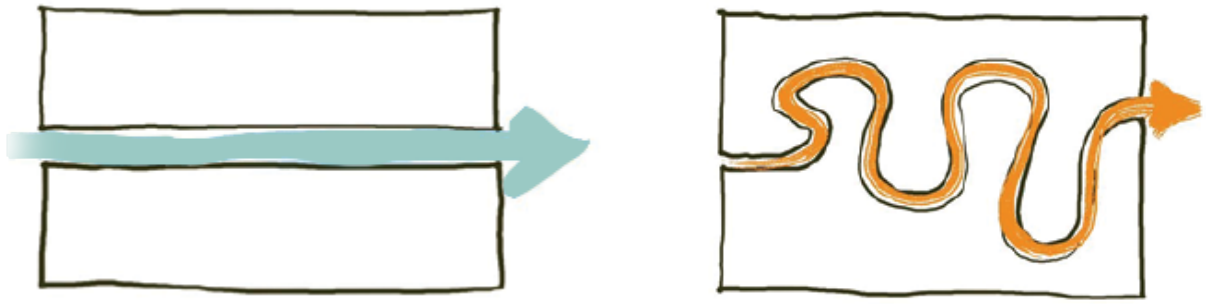

Fig. 2.5. Schematic comparison of low and high tortuosity in porous materials. On the left, air flows through a straight, low-tortuosity path; on the right, a more complex, tortuous pathway increases interaction with the pore walls, enhancing sound absorption; own work.

Resonant absorbers

Unlike porous absorbers, which are generally effective across a broad frequency range, resonant absorbers target a narrow frequency band, typically in the low to mid-frequency range, where porous materials are often less effective. Resonant absorbers rely on the principle of mass-spring resonance and are commonly categorized into two types: panel absorbers and Helmholtz absorbers.

In panel absorbers, also referred to as membrane absorbers, the vibrating mass typically consists of a flexible sheet material, such as rubber, plywood, or vinyl. Damping can be achieved by placing a porous layer, for example mineral wool, behind the vibrating membrane. In Helmholtz absorbers, on the other hand, a simple implementation involves positioning a perforated sheet in front of a porous absorber. In this system, the mass corresponds to the air plug within the perforations, and the porous layer behind the panel provides damping (Cox & D'Antonio, 2017). In both panel and Helmholtz absorbers, the air enclosed in a cavity acts as a spring.

The sound absorption coefficient curve of resonant absorbers is typically characterized by sharp peaks, as shown in Figure 2.6. These peaks correspond to the natural (or resonant) frequencies of the system, which are determined by the mass of the vibrating element and the stiffness of the air spring. The resonant frequency of an absorber can be decreased by increasing the mass (of the panel or of the air plug) and increased by decreasing the stiffness of the spring, for example reducing the air cavity (Long, 2006).

Microperforated panels

A specific type of Helmholtz absorber is the microperforated panel, which also acts as a mass-spring system, but relies on microscopic perforations and air cavity to achieve absorption. Sound energy is effectively converted into heat when air oscillates within the perforations. Unlike traditional Helmholtz absorbers, microperforated panels typically do not require a porous damping layer, as the perforations themselves provide sufficient energy dissipation.

For optimal performance, (Cox & D'Antonio, 2017) recommend that microperforations are distributed uniformly across the panel and have diameters of less than 1 mm. (Arenas & Crocker, 2010) note that perforation diameters smaller than 0.3 mm support wide-band sound absorption. However, further reducing the diameter size does not expand the absorption range. Microperforated panels are favored in architectural applications because they can be visually transparent thanks to the absence of a damping layer. Despite their advantages and development of modern manufacturing techniques (e.g. laser drilling) that make their production viable, microperforated panels remain an expensive option.

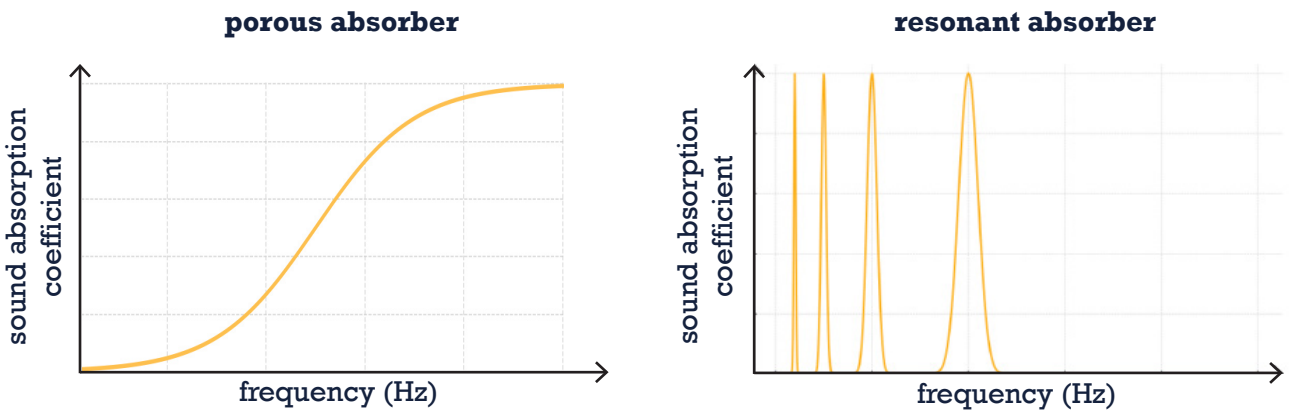

Fig. 2.6. Schematic comparison of typical sound absorption behaviour for porous and resonant absorbers. The diagram illustrates how porous absorbers gradually increase absorption with frequency, while resonant absorbers show sharp peaks at specific resonant (natural) frequencies; own work
Note: the graphs are not to scale and serve only as conceptual representations.

Evaluation of absorbers

The performance of sound absorbers can be evaluated using several methods. One common approach involves testing in reverberation chamber, which is suitable for large samples (10–12 m²). In this method, the RT of the room is measured before and after placing the sample. The absorption coefficient is then calculated from the difference in RT, but acoustic impedance cannot be measured using this approach.

Another method uses an anechoic chamber, which enables measurements at oblique incidence angles. This approach requires a large sample placed in the chamber, where sound waves are generated by a loudspeaker and monitored by two microphones. The pressure difference at the microphones is used to calculate both the absorption coefficient and impedance.

In this project, an impedance tube is used. This device allows for precise measurements of both absorption coefficient and surface impedance of the sample placed inside it under well-controlled conditions, by sending sound waves through a tube and analyzing their interaction with the sample. It is widely recognized, standardized, and requires minimal equipment. Additionally, it only needs a small sample (a few centimeters in diameter), making it efficient for testing new materials with minimal waste. While ideal for porous absorbers, the impedance tube is less effective for resonant absorbers, as the small sample size may not accurately represent the behaviour of larger samples (Cox & D'Antonio, 2017).

Key takeaways

Acoustic materials reduce sound energy by converting it into heat. Porous absorbers are the most common for broad-band control. Absorption occurs when open, interconnected pores let air move and dissipate energy. Their performance depends on factors like flow resistivity, open porosity, tortuosity, and thickness.

Resonant absorbers, such as Helmholtz resonators and microperforated panels, act as tunable mass-spring systems for specific low-to-mid frequencies.

For small, material-focused tests, the impedance tube offers precise, standardised measurements of sound absorption and surface impedance, ideal for evaluating the novel porous glass materials in this study.

2.2. Glass

Glass is a versatile material widely used in architecture and industry due to its transparency, chemical resistance, and electrical non-conductivity. Despite being fully recyclable in theory, only container glass is successfully recycled in a closed-loop system in Europe. Other types, including architectural, automotive or electronic, present significant challenges due to contamination, composite structures, and coating treatments (Bristogianni & Oikonomopoulou, 2023).

Glass production also carries a substantial environmental burden. The process is highly energy-intensive and dependent on carbon-based raw materials, accounting for 22 million tonnes of CO_2 emissions annually in Europe (European Commission, 2022).

Although glass can be categorized into many different types, for common applications it is typically divided into four main composition-based families, each with different properties influencing both their applications and recycling processes:

- **Soda lime glass**, or float glass, is the most widely used type, appearing in containers, windows, and the automotive sector.
- **Borosilicate glass** is known for its resistance to thermal shock and chemical corrosion, making it suitable for laboratory equipment and heat-resistant household items.
- **Aluminosilicate** glass is characterized by superior hardness and scratch resistance, commonly found in electronic screens.
- **Lead-barium glasses**, often used in cathode ray tubes and crystalware, are characterized by lower viscosity and require lower working temperatures, therefore are easier to recycle.

Their properties, including annealing temperature, ease of crystallization, and thermal expansion, set guidelines for recycling each type (Bristogianni et al., 2018; Bristogianni & Oikonomopoulou, 2023). Figure 2.7 presents an overview of the main glass types, their typical applications, and the waste streams they contribute to.

2.2.1. Glass waste streams

Europe produces approximately 40 million tonnes of glass products each year, resulting in various waste streams. The largest of these include container glass (~59%), flat glass (~26%), and fibre glass (~11%), with smaller contributions from domestic and special-purpose applications (Vieitez Rodriguez et al., 2011). While container glass recycling is well-established (with collection rates exceeding 80% and closed-loop recycling reaching 91%) other streams, for example flat architectural glass, automotive glazing, and lighting products, remain underutilized.

These materials often face technical and logistical challenges, including manual disassembly requirements and material contamination. For example, only about 40% of flat glass waste is collected, and less than 10% of it is recycled back into equivalent flat glass products (Hestin et al., 2016). Instead, most of this high-quality material is downcycled into aggregates or landfilled. Automotive glass presents additional complications due to its laminated structure and contamination, leading to collection rates of under 10% (Glass for Europe, 2024). Similarly, end-of-life light bulbs, particularly those with coatings or trace metals, pose treatment difficulties and are frequently excluded from closed-loop recycling systems (Magalini et al., 2014, European Parliament and Council of the European Union, 2011).

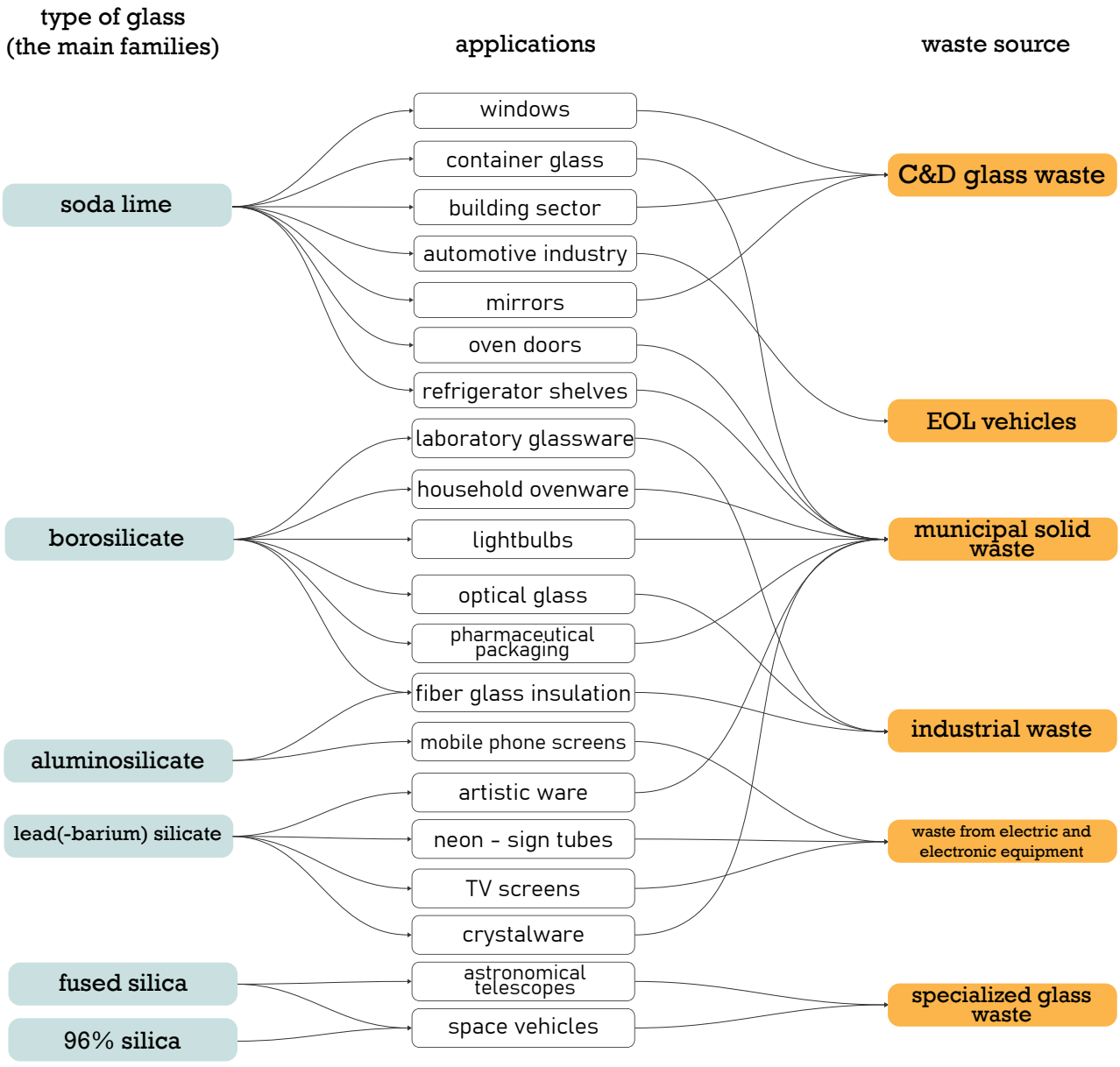

Fig. 2.7. Overview of glass families, their applications, and corresponding waste streams; own work, based on (Bristogianni & Oikonomopoulou, 2023, Oikonomopoulou, 2018, Vieitez Rodriguez et al., 2011)

Cullet types

Broken glass, or cullet, can be categorized as internal or external. Internal cullet consists of defective products and manufacturing offcuts, which are typically reused directly in production and are not considered waste. External cullet, however, originates outside manufacturing processes and can be divided into pre- and post-consumer cullet.

Pre-consumer cullet, generated during the manufacturing process before reaching consumer market, is generally more homogeneous and requires minimal treatment. In contrast, post-consumer cullet is produced after consumer use and typically requires treatment to remove contamination. Its primary sources include municipal and industrial waste, construction and demolition waste, end-of-life vehicles, and electronic waste (Vieitez Rodriguez et al., 2011).

Arup classifies cullet into three categories - A, B, and C - based on the level of contamination, as detailed by (DeBrincat & Babic, n.d.). Class A represents the purest form of cullet, free from any contamination and suitable for remelting into float glass. This class primarily consists of pre-consumer cullet, and more precisely, mostly internal cullet. Class B, also known as mixed cullet,

may contain minor contaminants, such as laminations, and is typically recycled into products like glass wool insulation. Class C includes the most contaminated cullet, containing materials such as ceramic frittings, prints, putty, or lead. This class is unsuitable for remelting and is generally downcycled and added as aggregate to other products.

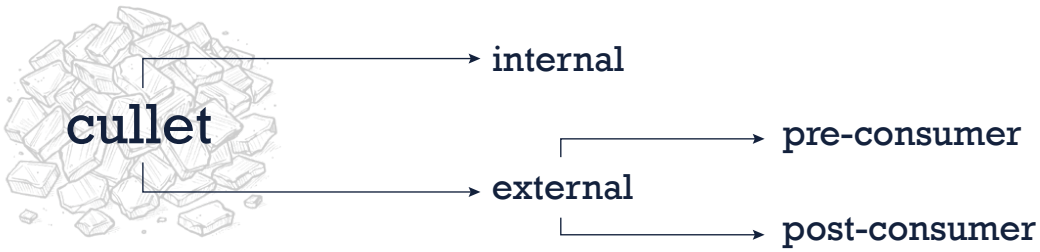

Fig. 2.8. Cullet classification scheme; Note: Internal cullet, originating from production cut-offs within factories, is not considered waste, as it is directly reused in the manufacturing process.

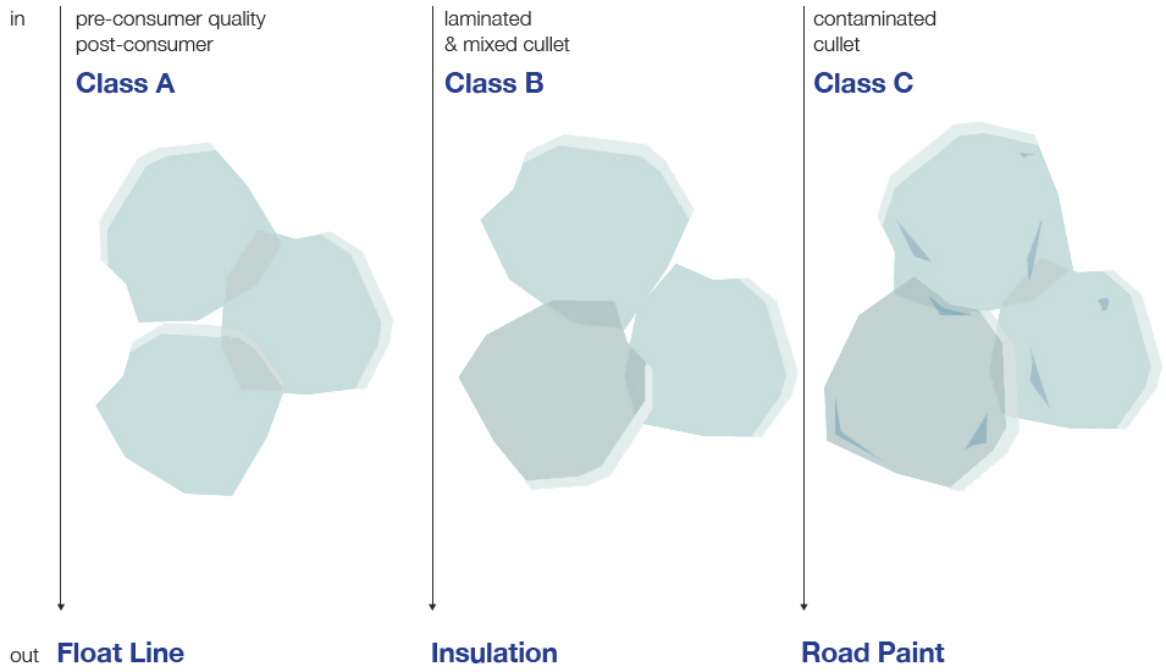

Fig. 2.9. Grades of cullet proposed; adapted and recolored from DeBrincat & Babic (n.d.), Re-thinking the life cycle of architectural glass, ARUP." figure 14, p. 34.

Challenges and benefits of recycling glass

Recycling glass faces significant challenges, primarily due to technical and supply chain barriers. Contamination of cullet, such as coatings, adhesives, and lamination, is often difficult or impossible to remove, and poses a serious issue for strict purity requirements in float glass remelting. Impurities can affect the physical properties of recycled glass, causing defects in the material or damage to the float tank. Moreover, cullet of different compositions cannot be recycled together due to variations in thermal expansion and melting temperatures (Bristogianni & Oikonomopoulou, 2023).

Supply chain barriers further complicate the problem. Regulatory restrictions, lack of standardized collection, sorting, and recycling systems, combined with the absence of automated segregation

processes prevent recycling of non-container glass. High transportation costs also reduce the economic feasibility of glass recycling (Rose & Nothacker, 2019).

Addressing these challenges is crucial, given the benefits of proper glass recycling. According to (Surgenor et al., 2018), in the EU, improved glass recycling could prevent approximately 925,000 tons of waste from being landfilled, saving over a million tons of raw materials extracted every year. Reusing one ton of cullet saves up to 1.2 tons of raw materials, including 850 kg of sand, reduces 300 kg of CO_2 emissions, and conserves 300 kWh of energy. Additionally, cullet's lower melting temperature decreases remelting energy requirements, with every 10% of cullet in a batch reducing furnace energy use by 3% and extending furnace lifespan by up to 30% (Hestin et al., 2016; Surgenor et al., 2018).

These environmental and economic benefits underscore the pressing need for innovative approaches to recycling even contaminated and mixed glass waste. One promising direction is the development of new glass products specifically designed to be made entirely from recycled glass, transforming waste into a valuable raw material.

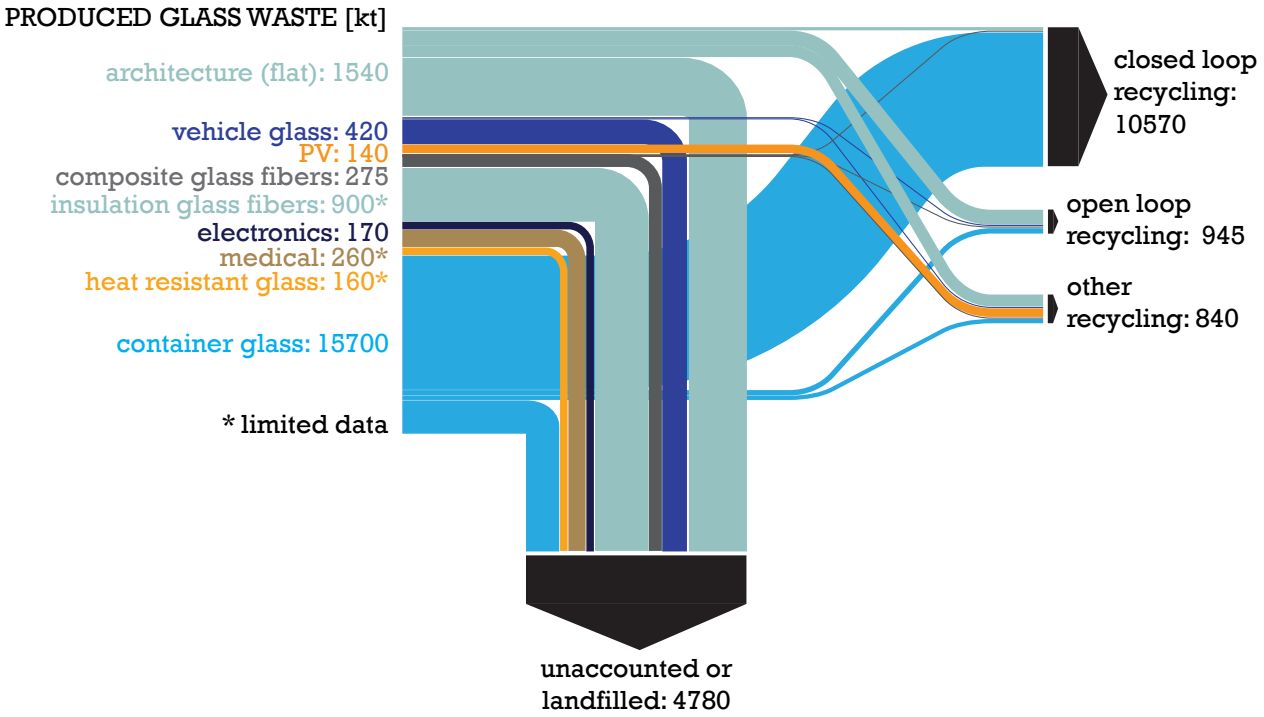

Fig. 2.10. Scheme of glass waste streams, adapted from Lara Neuhaus's presentation "Mapping Glass Waste Streams: Challenges and Incentives for Recycling," presented at the Glass Forum 2025, TU Delft, on March 19.
Note: This diagram is not to scale and serves only as a visual representation of differences in recycling rates among glass types. Recycling losses are not depicted.

2.2.2. Freeform glass panels casting

Glass casting, one of the oldest glass manufacturing techniques, is rarely used in architectural applications. From a sustainability perspective, (Oikonomopoulou, 2019) emphasizes the significance of glass casting as a key method for closed-loop recycling of glass types that are often downcycled or landfilled due to contamination or differences in their recipes. These include specialized glass such as mobile screens, ovenware, laboratory waste, light tubes, TV screens, and art glass. Despite being technically recyclable, these glass types frequently become waste due to the lack of specialized recycling facilities. Mixing them with soda lime glass, commonly used in windows and containers, is not viable because of different melting temperatures and thermal expansion coefficients. However, utilizing them to produce cast glass components provides a solution for recycling them (Oikonomopoulou, 2019). Cast glass objects are more tolerant of imperfections in their meso-structure compared to thin glass products like windows or food containers, making them more suitable for incorporating recycled materials (Bristogianni et al., 2018).

(Oikonomopoulou et al., 2018) indicate soda lime, borosilicate, and lead-barium glasses as the most frequently used for casting modular and monolithic glass objects, owing to the simplified manufacturing and post-processing.

Primary and secondary casting

Casting glass can be divided into two types: primary and secondary. Primary casting involves hot forming, where glass is created as a hot liquid directly from raw materials. These materials are melted and then poured into a mold to shape the glass. This method requires higher temperatures and more complex infrastructure, as it involves two furnaces, one for melting the glass and another for annealing, which is a controlled cooling process to relieve internal stresses.

Secondary casting, or kiln-casting, involves reheating pre-made glass until it flows and can be reshaped as desired. In this process, cullet is placed in a mold and heated in a kiln. The temperatures required for kiln-casting are lower than those for primary casting. Additionally, the process is simpler in terms of equipment, requiring only a single kiln for both melting and annealing.

Both methods have distinct requirements and applications, with kiln-casting offering a more accessible and energy-efficient option for recycling glass (Oikonomopoulou, 2019).

a) b)

Fig. 2.11. Primary vs. secondary glass casting; a) Primary (hot-form) casting: raw batch is melted in a glass furnace, poured as molten liquid into a mould, then transferred to a separate annealing furnace for controlled cooling, adapted from (Oikonomopoulou, 2021), b) Secondary (kiln) casting: recycled cullet is packed into a mould and re-melted in a single kiln, which also serves as the annealer, offering a simpler, lower-temperature route ideal for glass-recycling applications, adapted from (Bristogianni et al., 2018)

Procedure

The casting process for glass begins with a heating phase, when glass is brought to a temperature at which it is molten enough to flow into the mould. Alternatively, cullet can also be placed directly in the mould, where it melts, uniformly filling the mould. This is followed by quenching, a cooling phase to the temperature below its softening point. Quenching process may occur either gradually, cooling is then kiln-operated, or abruptly, by opening the oven's door. Following the quenching stage, annealing is conducted to relieve internal stresses within the glass. During annealing, the glass is held at a predetermined temperature for a specific time before being cooled gradually to room temperature, preventing the formation of new stresses. For 3D glass components, the annealing process is more time-consuming than for float glass, owing to their greater mass and thickness (Oikonomopoulou et al., 2018).

The size of glass cullet used in casting determines the meso-level structure of the recycled glass. When cullet is in the form of large shards (greater than 10 mm), the resulting product will exhibit glassy or crystalline structures. Alternatively, glass can be crushed into fine cullet (1–4 mm) or coarse powder (less than 1 mm). Using coarse powder improves the homogeneity of the final sample but also increases the risk of appearing bubbles due to air becoming trapped between the powder particles during the casting process (Bristogianni & Oikonomopoulou, 2023).

Moulds

Kiln-casting utilizes several types of moulds, chosen based on the desired volume and precision of the final product. Moulds are broadly categorized as disposable or permanent. Disposable moulds, typically made of soft materials like silica plaster, are cost-effective and suitable for single components or small batch production (Oikonomopoulou, 2019). These moulds offer flexibility for creating complex geometries but result in rough, opaque surfaces that require post-processing to achieve a glossy finish. This additional processing increases costs and reduces dimensional precision. Two types of disposable moulds can be differentiated: 3D-printed sand moulds and silica plaster moulds, each presents different advantages and challenges. Permanent moulds, made of steel or graphite, produce castings with smooth, glossy surfaces, eliminating the need for post-processing. However, their high cost makes them impractical for small-scale or experimental projects. The mould should be chosen to balance cost, precision, and efficiency in casting (Ioannidis et al., 2024).

The overview of glass casting experiments conducted at TU Delft has been presented in table 2.1.

Fig. 2.12. Samples produced by kiln casting glass, incorporating glasses from various waste streams; source: Glass up-casting: A review on the current challenges in glass recycling and a novel approach for recycling 'as-is' glass waste into volumetric glass components," by T. Bristogianni & F. Oikonomopoulou, 2023, Glass Structures & Engineering, 8(2), p. 299 (https://doi.org/10.1007/s40940-022-00206-9). Copyright 2023 by Springer Nature.

Table 2.1. Overview of the casting experiments found in literature

REFERENCE	TYPE OF GLASS (WASTE)	FORMING TEMP. (°C)	HEATING UP RATE (°C/h)	DWELL TIME (h)	ANNEALING TEMP. (°C)	RESULTS/REMARKS
Bristogianni et al. 2018	SL automated	860 - 1200	50°C/h	n/a	600	All samples were susceptible to crystallization, abrupt quenching helped avoid it (from 1200°C quickly to 600°C)
	SL float	860, 1200			570	Abrupt quenching required to avoid crystallization, samples resultes in a marble-like effect
	SL mouth blown	860			600	Minimal crystallization observed at top surface; samples were transparent
	BS	1200			n/a	Transparent samples crystallized locally at the top surface only. Abrupt quenching was conducted
	AS	1250, 1500				Samples cast in 1500°C were transparent, but had a high bubble content.
						Samples cast in 1250°C were prone to foam formation in the mould.
	combination of clear SL (from different producers)	1250		2h		Mechanical quenching was conducted, the part of glass in touch with the mould was more homogenous.
	combination of different colour SL	940 - 1450		n/a		At 970°C samples were partially fused, higher temperatures helped homogenize the sample (1200°C and above).
	combination of LC and float	1250		n/a		Abrupt quenching was conducted, the melt was homogenous, no crystallization occured and the sample was transparent
	combination of BS and SL (1:2 ratio)	1250		3h	560 - 340	No crystallization occurred after abrupt quenching, locally reactions with the mould were observed, sample was transparent.
Bristogianni et al. 2021	pure or contaminated SL	970 - 1120	50°C/h	10	560*	Pure cullet produced clearer glass, contaminated cullet was prone to crystallization and inhomogenities. Lower temperatures reduced crystallization but resulted in higher bubble content, while higher temperatures minimized bubbles but increased crystallization.
van Minkelen 2024	SL fritted, with pollutants	1070 for composite objects 1120 for homogenous objects	50°C/h	10	580*	No significant crystallization was observed in the homogenous objects, minor surface crystallization occurred in some composite samples.

Bristogianni & Oikonomopoulou 2023	pre- and post-consumer SL with different contaminants	970-1200	n/a	2, 6-10	n/a	Contaminants like frits and metal inclusions introduced color streaks, crystallization, and bubbles. Higher risk of crystallization when formed at lower temperatures (ca. 970°C).
	pre- and post-consumer BS	1020-1120		3, 10		Homogenous sample with minor metals inclusions in the bulk.
	pre-consumer AS	970-1200		2, 10		Transparent, yellow - tinted samples with high bubble content.
	pre- and post-consumer LB	820-1000		5, 10		Crystalline inclusions of black colour.
Matskidou 2022	SL with various contaminants	1000 - 1120	50°C/h	6	560	During quenching, a rapid drop from 1120°C to 560°C occurred at a rate of 186°C/hour. This was followed by controlled cooling phases to gradually bring the temperature to 23°C. Samples ranged from transparent to translucent, with some surface crystallization or bubbles depending on cullet type and firing parameters. Transparent samples were mostly free of imperfections.

SL - soda lime, BS - borosilicate, AS - aluminosilicate, LC - lead crystal, LB - lead barium silicate

*After reaching the maximum temperature, cooling at -160°C/h rate was conducted to 20°C above the annealing point, then slowed to -3°C/h down to the strain point, followed by rapid cooling to room temperature.

2.2.3. Glass foaming

As introduced earlier, foaming method is explored in this study to achieve porosity in glass, a key characteristic for effective sound absorption. Glass foams have been highly valued materials for thermal and acoustic insulation (Bernardo et al., 2010; König et al., 2020). They are characterized by low thermal conductivity, good mechanical properties even at high temperatures and resistance to chemical attacks. These qualities make them suitable for utilization in aggressive environments such as insulation of industrial chimneys (Ducman & Kovačević, 1997). Glass foams are non-combustible, non-toxic, and are considered more sustainable than many other thermally and acoustically insulating materials. Additionally, the production of foam glass offers an effective means of recycling waste glass (König et al., 2020). This was also proved in the master thesis of (Giassia, 2022) who produced foam glass samples for bioreceptivity, successfully incorporating large amounts of glass waste into the mixture.

Foaming process

There are various methods for producing glass foams, including replication, gel casting, incorporation, and foaming. Among these, the foaming method is the most commonly employed due to its simplicity. In the process, a foaming agent is introduced into the glass matrix (Souza et al., 2017). The mixture is then heated above the glass's softening point. During heating, the foaming agent releases gases, which create gas-filled holes within the glass. As the material cools to room temperature, it hardens with a sponge-like structure (Hesky et al., 2015).

Foaming can be performed under either dry or wet conditions. In the first one, glass cullet is mixed with foaming agents, placed in a porcelain pot and then fired. In the latter, water is added to the

mixture (approximately one-third of its weight), which is stirred and left to rest for 24 hours before being poured into a pot. Wet foaming offers several advantages: it lowers the foaming temperature, eliminates a problem with dust, improves mixture homogeneity, and simplifies the mould-filling process (Ducman & Kovačević, 1997).

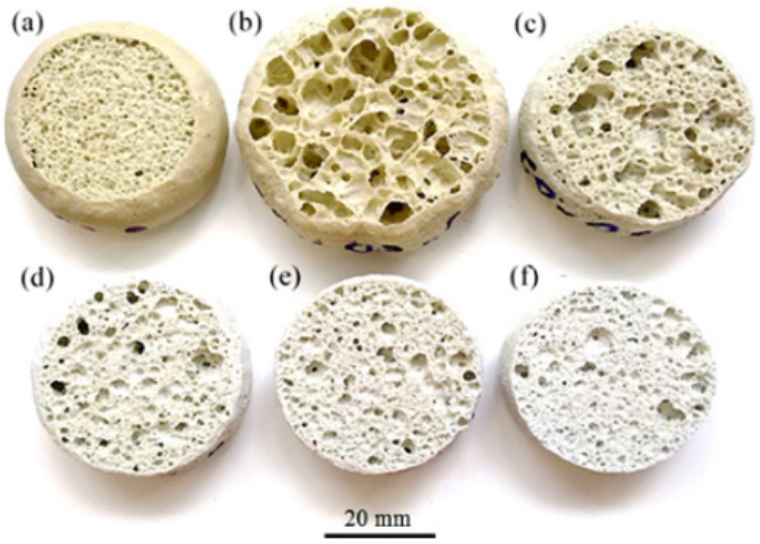

Fig. 2.13. Samples of foamed glass developed with varying amounts of eggshells: (a) 1 wt%, (b) 3 wt%, (c) 6 wt%,, (d) 12 wt%, (e) 15 wt% and (f) 30 wt% eggshells; source: Adapted glass foam production process using glass bottles and eggshell waste. Adapted from "Glass foams produced from glass bottles and eggshell wastes," by M. T. Souza, B. G. O. Maia, L. B. Teixeira, K. G. De Oliveira, A. H. B. Teixeira, & A. P. Novaes De Oliveira, 2017, Process Safety and Environmental Protection, 111, p. 64 (https://doi.org/10.1016/j.psep.2017.06.011). Copyright 2017 by Elsevier.

Glass waste types

One of the key parameters discussed in the literature on glass foaming is the type of glass used to create porous structures. Most studies focus on soda lime glass from various waste streams, including those with different levels of contamination. For instance, (Bernardo et al., 2007) successfully foamed soda lime glass from municipal waste, achieving porosity levels of up to 92%. (Cho et al., 2005) experimented with mixtures that included automotive glass, while (Ducman & Kovačević, 1997) and (König et al., 2016) investigated the foaming of glass bottles.

In a more recent study, (Giassia, 2022) explored not only soda lime glass but also combinations of soda lime and borosilicate glass, successfully achieving porosity in those mixtures. She further introduced Cyclon mix, a highly contaminated byproduct of bottle recycling collected through suction systems, containing heavily contaminated soda lime glass.

Aluminosilicate glasses, while unsustainable for recycling through casting due to the high required working temperatures and difficulty in recasting it into glossy, good quality objects, foam well due to their tendency to create bubbles (T. Bristogianni, personal communication, January 2025). Taiwanese company, Spring Pool Glass, manufactured porous glass blocks that showcased thermal and acoustic insulation, incorporating large amounts of aluminosilicate glass waste in the material.

All of these examples confirm that a variety of glass types, including mixed and contaminated waste, can be effectively transformed into porous foamed glass, offering valuable insights for the experimental direction of this project.

Foaming agents

Foaming agents are classified based on their gas-releasing chemical reactions into neutralization foaming agents (such as carbonates and sulfates) and redox foaming agents (silicon carbonate, silicon nitride, manganese dioxide, carbon) (Hubálková et al., 2017). They can also be categorized by the foaming mechanism, which may involve either oxidation - due to interaction of carbon-containing materials with the air inside the sintering furnace - or decomposition, which occurs when carbonates or sulfates release gas during heating (Bernardo et al., 2007; Hesky et al., 2015; Souza et al., 2017).

A review of the literature on glass foaming identifies calcium carbonate ($CaCO_3$) as a commonly used foaming agent due to its effectiveness and availability. Silicon carbide (SiC) is also frequently mentioned as a highly effective foaming agent because of its complex oxidation process, but its high cost prevents it from being widely used (Bernardo et al., 2007).

Foam glasses and sound absorption

The development of acoustic materials has advanced since the 1970s, shifting from asbestos-based products to modern fibers. These newer materials are safer for human health, lighter, and technologically optimized. However, they are mostly made of synthetic fibers with a high environmental footprint, contributing significantly to CO_2 emissions (Arenas & Crocker, 2010). Mineral wool, to give an example, is a widely used and highly effective sound-absorbing material with a significant environmental impact. Sheep wool could offer a potential, more environmentally friendly alternative. However, sheep wool has a lower density, meaning that it must be used in thicker layers to achieve similar acoustic performance. The interest in sustainable porous absorbent materials made from recycled or natural sources has grown in response to environmental concerns (Cox & D'Antonio, 2017).

While foam glass has been widely studied, research specifically focusing on its sound absorption properties is limited. However some relevant studies have been found. (König et al., 2020) developed low-density foamed glass with open porosity, utilized glass waste combined with additives such as carbon black, manganese or iron oxides to control porosity. Open porosity was achieved through partial crystallization of the glass, a phenomenon typically undesirable in glass casting. The produced samples exhibited homogeneous pore structures. The study proved that porosity can be controlled with additives (their type and amount) which provides a valuable insight for this thesis.

(Cai et al., 2023; Yan et al., 2019) described research on foam glass-ceramics for acoustic performance using titanium-rich slag and waste glass as raw materials. The study focused on their acoustic applications, particularly traffic noise reduction. The researchers established and refined sound absorption, accounting for factors such as pore size, open porosity and the presence of microcrystals. The results highlighted that foam glass-ceramics effectively absorbed sound within the critical 800-2000 Hz frequency range and proved that open porosity correlated to sound absorption coefficient of the samples – the sound absorption coefficient was dependent on the pore diameter. However, the study also found that excessive porosity simplified the internal structure too much and reduced multiple reflections, leading to reduced sound absorption.

(Cho et al., 2005) explored sound absorption properties of foamed glass prepared from recycled automotive window glass. It was foamed by adding sodium hydroxide (NaOH) as a foaming agent and experimenting with firing temperature to obtain optimal physical properties and high sound absorption coefficient. The study established that foam glasses with smaller pores provided better sound absorption, especially in higher frequency range. It was highlighted that porosity (size and distribution of the pores) can be controlled by changing the firing temperature and varying amounts of foaming agent and finally, that porosity affects sound absorption coefficient which is a crucial finding for this thesis.

Other studies investigating foam glasses while not solely focusing on their sound absorption, have also resulted in promising findings. For example, (Souza et al., 2017) produced glass foams from discarded glass bottles and eggshells as a foaming agent, achieving samples with porosity even up to 95%. This highlight foam glass as a potential material for applications requiring thermal and acoustic insulation. Reviewed literature suggests that cellular glass can be a sustainable alternative for conventional sound absorbing materials. For example, up to 70% of the raw materials required for foam glass production, can be substituted by glass waste (Hesky et al., 2015). Additionally, foam glass offers lower cost and environmental impact (Buratti et al., 2016). It is non-combustible (König et al., 2020) and corrosion resistant (Yan et al., 2019) which makes it perfect for indoor acoustic applications.

The overview of glass foaming experiments from the studies described in this chapter has been presented in table 2.2.

2.2.4. Glass fusing

Fusing, next to welding, is a famous method of heat bonding glass. It involves joining two or more pieces of glass through melting, achieved by global heating in a kiln. In the context of this project, fusing plays a crucial role, as it eliminates the need for adhesives to bond the two layers of the acoustic panel. Unlike welding, where the sample is heated up only locally, fusing requires uniform heating of the entire glass assembly. While primarily performed by artists for creating decorative objects, fused glass also serves functional purposes in a variety of applications, including furniture, window panes, double-glazed windows, doors, interior partitions to name a few (Bulekova & Temirgali, 2020). Fusing bases on the plasticity of glass at high temperatures, making it another technique for crafting unique products such as vases, sculptures, and architectural elements. There are three types of fusing: tack fusing, full fusing, and fusing with inclusions. Each type is defined by the degree of bonding, temperature range, and resulting effects on the glass.

Fusing methods

Full fusing assumes complete bonding of glass layers, resulting in a seamless and monolithic connection. The process adheres to the “6mm rule”, where glass thicker than 6mm tends to flatten and spread during melting (Bullseye Glass Co., 2020). A critical challenge in full fusing is managing the volume and surface area of the glass. Upper layers tend to spread more than the lower ones, potentially covering them.

Tack fusing involves stacking pieces of glass on top of one another, which are then heated and sintered to form a connection. In this process, the glass pieces do not fully combine and retain their original shapes. The footprint of the glass remains constant, though the upper layer edges soften and round slightly. Tack fusing is performed at lower temperatures than full fusing, typically between 713°C and 760°C (Beveridge et al., 2005).

Fusing with inclusions involves laminating other materials, such as decorative elements or colored glass, between two pieces of glass. Transparent or coloured glass can be used, depending on the desired aesthetic effect. The temperature required for this technique ranges between 760°C and 835°C (Beveridge et al., 2005).

Other recommendations regarding glass fusing temperatures proposed by glasscampus.com are presented in table 2.3.

Table 2.2. Overview of the foaming experiments found in literature

REFERENCE	TYPE OF GLASS (WASTE)	CULLET SIZE	FOAMING AGENT	ADDITIVES	FOAMING TEMP. (°C)	HEATING UP RATE	DWELL TIME	RESULTS/POROSITY OBTAINED	REMARKS/TAKEAWAYS
Bernardo et al., 2007	SL municipal glass waste	up to 37 µm	2.5 - 17.5 wt% silicon carbide (SiC)	MnO_2 as oxidizer	950[a)]	10 °C/min	1h	Min. density corresponded to porosity of 92%	Porosity and mechanical strength of achieved foams were comparable to commercial samples
Cho et al., 2005	60% AM glass waste, 25% zeolite, 5% sodium silicate (Na2SiO3),	powder	1 - 5 wt% sodium hydroxide (NaOH) 4 wt % calcium carbonate ($CaCO_3$)	n/a	720	n/a	30 min	pores 2 - 7 mm in diameter	The samples were cooled for 2 h. The pores became larger with increasing amounts of NaOH.
Ducman & Kovačević, 1997	waste SL glass (crushed bottles)	powder (<0.16 mm)	3 wt% calcium carbonate ($CaCO_3$)	n/a	755 - 780	5 °C/min	n/a	single pores up to 5 mm in diameter	When water was added (30wt%), the sufficient foaming temperature was lower, but the microstructure was not homogenous.
			3-10 wt% manganese dioxide (MnO_2)		855 - 880			pores up to 7 mm in diameter	Foaming process was almost completely halted with the particales larger than 0.4mm.
			up to 50 wt% waterglass		805	n/a	1 min	high porosity	
Giassia, 2022	SL	50 - 250 µm	0.33 wt% carbon black 3 - 10 wt% calcium carbonate ($CaCO_3$)	1.66 wt% calcium hydrogen phosphate ($CaHPO_4$), CM	790	50°C/h	2h	closed porosity for SL glass foamed at 960°C, open porosity for Cyclon mix	Higher foaming temperatures give a better chance for open pores.
	SL + BS / 50-50 wt%	200 - 1700 µm			840 - 960		10h		
	CM*	90 - 2500 µm			790 - 960				
Hesky et al., 2015	float glass powder	1-106 µm	sodium waterglass (sodium silicate Na_2SiO_3 and its mixtures with water)	n/a	800	4K/min	30 min	closed pores of 4 nm - 800 µm in diameter	Increasing waterglass content in the foaming agent resulted in higher porosity.
							5h		
König et al., 2016	lead/barium silicate (CRT panels)	38 - 250 µm	0.93 wt % carbon and 6.76 wt% manganese dioxide (MnO_2) mixture	n/a	835[b)]	5 - 10 °C/min	5 - 30 min	The finest powders led to larger pores (1–3 mm) during extended dwell times, rapid quenching reduced the pore size to 0.1–0.6 mm.	Slower heating resulted in better pore formation, shorter dwell time resulted in higher density of the samples.
König et al., 2020	lead/barium silicate (CRT panels)	powder	carbon black	0.44 wt% manganese oxide ($Mn3O_4$)	740 - 820[c)]	5 °C/min	40 min	closed pores 92-100%	Density of closed-porous samples was controlled by foaming temperature.
	SL glass			iron oxide (Fe_2O_3)	840 - 880[c)]	5 - 15°C/min		open pores 91-99%	
Souza et al., 2017	waste SL glass (crushed bottles)	2.9 µm	1-30 wt% calcium carbonate ($CaCO_3$, eggshells)	n/a	900	10 °C/min	30 min	porosity 83 - 92%	Foams with closed pores can be obtained by reducing the particle size of the foaming agent.
Yan et al., 2019	ca. 76% of waste SL glass, titanium - rich slag	powder	4 wt % aluminum nitride (AlN)	6 wt% fluxing agents	(1) 400	5 °C/min	20 min	Titanium slag affected the microstructure of the glass-ceramics, its sound absorption and mechanical properties	Fluxing agents were added to lower the sintering temperature.
					(2) increased to 1000[d)]	10 °C/min	30 min		

SL – soda lime, AM – automotive, BS – borosilicate, CM – Cyclon mix

* Recycling industry byproduct, containing SL glass heavily contaminated

a) Samples were cooled at -10°C/min to 600°C and then cooled at -1°C/min to 500°C, ang again cooled at ca. -5°C/min to room temperature

b) Samples were slowly cooled (-4°C/min) or rapidly quenched from foaming temperature to 530°C, and then cooled at -1°C/min to room temperature. Quenching prevented pores merging.

c) Samples were cooled at -7°C/min to 550°C and then naturally cooled to room temperature.

d) Samples were cooled at -10°C/min to 500°C and then naturally cooled to room temperature.

Table 2.3. Recommendation regarding fusing temperatures by glasscampus.com

TEMPERATURE (°C)	PROCESS	EFFECT
540	**Thermal shock range**	**Once the glass is heated above 540°C it is no longer at risk of cracking.**
650	**Slumping phase**	**The glass softens enough to sag and can be molded or draped into shape.**
705	**Tack fuse**	**Two pieces of glass in contact will bond permanently without significantly softening or losing their individual edges.**
720	**Fire polish**	The glass edges soften and become slightly rounded
760	**Almost full fuse**	The glass surfaces smooth out and approach a uniform level, though they remain slightly distinct.
790	**Full fuse**	The glass fully melts together into a single, smooth, unified surface.

A crucial factor in successful glass fusing is compatibility between the types of glass used. It is determined by many factors, the key one being the coefficient of expansion, which measures the rate at which glass expands and contracts when heated and cooled. If incompatible glasses are fused together, they can develop internal stresses at the points of contact or shatter during the cooling process.

Advantage of tack fusing in sustainable design

In this project, tack fusing will be employed as the primary method of heat bonding the layers of the panel. A significant advantage of fused glass is that it bonds on a molecular level, eliminating the need for additional materials such as adhesives (Beveridge et al., 2005). This feature is particularly relevant to this thesis as it aligns with sustainability objectives by enabling easier recycling of the panels in the future. By avoiding adhesives, the process ensures that the glass remains a fully recyclable material, reducing environmental impact. This approach highlights the potential of tack fusing as a method that not only meets the functional and design requirements of the project but also contributes to its sustainability goals.

Key takeaways

The literature review reveals that while glass is a fully recyclable material in theory, in practice only container glass is efficiently processed in closed-loop systems. Other streams like flat glass, automotive glazing, and light bulbs are underutilized due to technical and logistical barriers, including contamination. These streams, despite their volume and material quality, are often downcycled or landfilled, representing a significant loss.

Casting and foaming are two promising methods for upcycling underutilized glass waste streams. Casting enables the reuse of glass types that are typically difficult to recycle, including mixed or contaminated cullet. Foaming introduces porosity, making the material suitable for sound absorption, while also allowing large volumes of waste glass to be incorporated into foam glass production. Studies confirm the viability of using soda lime, borosilicate, and even mixed or highly contaminated glass in the foaming process. For this research, tack fusing is the preferred method of bonding, as it eliminates the need for adhesives.

Sound absorption in foam glass is possible due to open porosity. Furthermore, it is influenced by pore size, distribution, and firing conditions, parameters that can be controlled through experimental methods. This makes foam glass a sustainable alternative to synthetic sound-absorbing materials and supports the project's goal to design a recyclable, high-performing acoustic panel entirely from glass waste.

2.3. Computational methods for acoustic design and simulation

3D computer modeling has become a crucial tool in room acoustics. Modern simulation techniques offer detailed and precise analysis of acoustic performance even in complex halls. First simulation methods developed in the 1980s required entering data manually and prolonged computation. Advancements in computing power by the 1990s enabled faster and more detailed simulations. Today, various software can quickly process 3D architectural models, allowing for smooth collaboration between acousticians and architects. Innovations can be tested in real-time; the simulations are precise and help achieve goals like clarity and intimacy regardless of hall geometry (Toyota et al., 2020). Today, two types of computational acoustic simulations exist: geometrical acoustics and wave-based models (Vorländer, 2013).

2.3.1. Acoustic simulations

Geometrical acoustics

Geometrical acoustics simulations are usually efficient for middle to high frequencies and rely on two main approaches: ray tracing and image sources. Ray tracing is a commonly used statistical method that assumes sound propagation in form of rays in various directions from a sound source. They reflect off room surfaces, losing energy after each reflection based on the absorption coefficient of the surface material (Rindel, 1995). While ray tracing methods help to understand how sound spreads in space, they are based on sound energy propagation, neglecting its wave properties. Therefore, it is not possible to model phenomena like diffraction or interference with geometrical acoustics. Ray tracing results in low-resolution data, because the method is only approximation of sound behaviour It can be used only above the Schroeders frequency, where sound behaves statistically (Vorländer, 2013).

Image source methods model reflections by mirroring the sound source across the plane of the reflecting surface (Rindel, 1995). This method is used below Schroeders frequency, where sound shows modal behaviour.

The main difference between the image source and ray tracing models is the way the rays are computed; in the latter one, the rays only connect sound source and target (G. Mirra, personal communication, May 2025). Both methods remain simplified, geometry-based approximation.

Wave-based models

Wave based models' (WBM) development dates to the 1960s and, as the name suggests, they are based on the wave character of the sound, therefore they can capture phenomena characteristic of waves, like diffraction and interference, making them particularly suitable for spaces where these dominate, e.g. small rooms. They work exceptionally well for low frequencies, but detailed boundary condition input is required (Vorländer, 2013). In WBM the sound propagation is simulated by solving the wave equation, which makes them computationally expensive. Special types of wave-based models are numerical methods, allowing for analyzing complicated occurrences like reflections and vibrations by breaking down mathematical equations into shorter calculations. Three types of numerical methods are differentiated: finite-difference time-domain method (FDM), finite element method (FEM) and boundary element method (BEM) detailed description of which is provided in (Sakuma et al., 2014).

Scale model techniques

Acoustic simulations are frequently used in early design stages, being a convenient and quick method to explore different design variations. While they are extremely helpful for practical application stages, their physical modelling of sound waves is not always appropriate. That is why scale model techniques have been developed and applied to many acoustic designs of music halls and noise barriers (Sakuma et al., 2014). They are used complementary to computational methods, allowing for simulating phenomena that are challenging to be represented virtually, such as diffraction or echoes. The scale model method is typically applied in the later stages of the project, when the design is (almost) finalized. To simulate the acoustic performance of a space, a physical model of a hall is built (for large projects usually on a 1:10 scale, 1:20 can be used for smaller projects) The model is filled with nitrogen gas to imitate air absorption and measurements are conducted using speakers and binaural microphones. The recorded data is then are digitally processed to analyze the acoustics at full scale (Toyota et al., 2020).

2.3.2. Optimization

When designing spaces for optimal acoustics, trial-and-error approaches are increasingly replaced by optimization techniques based on acoustic simulation and parametric modeling. These methods, often implemented through software such as CATT-Acoustic, ODEON, or Grasshopper with acoustic plug-ins, allow designers to refine room's geometry, balance acoustic parameters such as SPL, reflections, RT or clarity or to adjust material properties (absorption, diffusion, reflection).

(Bassuet et al., 2014) described the workflow for optimizing balcony fronts to avoid late reflections in a concert hall. The process begins with defining objectives, in other words, setting specific acoustic targets. Next, the hall's geometry is parametrized, for example using tools like Rhino and Grasshopper. Simulations are then conducted, using ray tracing methods (e.g. CATT Acoustics), while optimization algorithms iteratively adjust variables to achieve the best match with the desired objective. Finally, the optimization can be validated, and the results are compared to the targets set at the beginning. Common optimization algorithms used for acoustic optimization are gradient-based methods, evolutionary (genetic) algorithms or pattern-search algorithms (Bassuet et al., 2014).

Key takeaways

Acoustic simulation tools are essential for predicting and optimizing sound performance in architectural spaces, particularly during early design stages. Geometrical acoustics methods, especially ray tracing, are widely used due to their efficiency at mid-to-high frequencies and are well-suited for modeling sound behaviour in complex geometries, such as the wall-mounted acoustic panels developed in this project. Although wave-based models offer higher precision at low frequencies and can capture phenomena like diffraction and interference, they are often too computationally demanding for iterative design workflows.

Scale model techniques remain valuable in validating acoustic performance in later design stages, but for the purposes of this research, digital simulations are more appropriate. Tools like CATT-Acoustic and parametric modeling software such as Rhino and Grasshopper (including Galapagos for optimization) allow for iterative design processes that link geometric variables to acoustic performance. In particular, evolutionary algorithms have proven well-suited for optimizing the geometry and orientation of acoustic panels, aligning well with the performance-driven goals of this thesis.

2.4. Summary and conclusions of literature review

Architectural acoustics

The literature review provided several key findings essential for this project. In the field of acoustics, fundamental concepts such as sound propagation, reverberation, clarity, and echo formation are explored. Metrics like reverberation time and clarity indices are identified as important indicators of acoustic environment, particularly in spaces designed for speech or music. Porous absorbers and their properties that are fundamental to this project were reviewed, explaining how acoustic performance can be improved through material design. Among methods described to evaluate acoustic properties of the material, the impedance tube has been identified as the most effective one and therefore has been employed in the methodology of this project. Regarding the case study, attention is drawn to RT, acoustic G strength and clarity, and the role of early reflections in achieving both speech intelligibility and a pleasant perception of music.

Glass

In the field of glass recycling, literature review stresses significant challenges, including contamination and the lack of infrastructure for recycling non-container glass. Methods such as glass casting and foaming are described as promising in addressing these issues. Glass casting offers a sustainable solution by incorporating mixed or contaminated glass types unsuitable for conventional recycling. Glass foaming presents a method for creating porous materials with strong potential for acoustic applications. The overview of both casting and foaming experiments found in literature is provided and serves as a baseline for future experiments that are going to be conducted in this project.

Most importantly, the literature review allowed for the identification of glass types most suitable for foaming, which is further explored during the experimental phase of this project. The literature recommends that focus should be put on post-consumer cullet excluding container glass that is already successfully recycled in closed loop in Europe. Soda lime, borosilicate, and lead barium glasses were found to be better suited for casting, while aluminosilicate glass shows potential for foaming. Given that flat glass is the second-largest glass waste stream in Europe, and that much of it originates from architectural and automotive sources, it deserves more attention and investigation. These applications primarily involve soda lime glass, which is also the base composition for most of the waste types explored in this study - including architectural glazing, automotive glass, and light bulb glass (which may also contain borosilicate). This common chemical basis and the high volume of waste generated helped guide the selection of glass types for experimental investigation.

Moreover, key parameters such as firing schedule and cullet size are found to have a significant influence on the results. Crystallization, undesired in casting, is accepted in foaming for achieving open porosity, crucial for sound absorption.

Among other methods found, tack fusing was identified as a sustainable way of joining glass pieces without the need for adhesives. The findings regarding manufacturing parameters for both casting and foaming are summarized in Table 2.4.

Computational methods for acoustic design

In the area of computational methods, the review identifies geometrical acoustics, wave-based models, and hybrid approaches as tools for simulating and optimizing acoustic performance. While geometrical acoustics are better suited for high-frequency sounds, wave-based methods are preferred for simulating low-frequency sounds. These computational techniques are essential for evaluating the acoustic properties of the designed panels, enabling iterative improvements before experimental validation. Also, an understanding of optimization algorithms was gained, giving

options for the future to choose from the optimization algorithms that can be used for acoustics.

To summarize, findings from the literature review highlight the potential for combining recycled glass with advanced acoustic design. They establish a theoretical basis for the project's next stages, demonstrating how porous glass panels can address both environmental and acoustic challenges.

Table 2.4. Overview of recommended manufacturing parameters for foaming and casting, along with the rationale behind the selection of glass types used in this project's experimental phase.

PRODUCTION METHOD	GLASS WASTE TYPE	REASON/PREVIOUS STUDIES	CULLET SIZE	FIRING SCHEDULE		FOAMING AGENT	CRYSTALLIZATION DESIRED
				MAX TEMP.	DWELL TIME		
FOAMING	clean soda lime	It will serve as a reliable baseline for comparison with other, more contaminated types of soda lime glass.	powder	700 - 900°C	<1 h	calcium carbonate, eggshells, sodium hydroxide, manganese dioxide, carbon black	yes
	light bulbs	A niche and more contaminated type of soda lime waste, potentially containing traces of borosilicate glass - a combination shown to be effective for foaming by Giassia (2022). This waste stream presents a growing recycling challenge due to the need to separate coated glass and concerns over possible mercury contamination, making it unsuitable for reuse in the glass industry.					
	automotive	Glass excluded from closed-loop recycling due to challenges such as manual disassembly and the presence of lamination layers. Successful sound absorption in foam glass produced from automotive glass waste was reported by Cho et al. (2005).					
	aluminosilicate	A type of glass excluded from closed-loop recycling, but known for its tendency to form bubbles, an attribute that may support effective foaming, making it a promising candidate for testing.					
	cyclon mix	Severely contaminated byproduct of recycling glass bottles, successfully transformed into porous glass samples in the experiments by Giassia (2022), demonstrating its potential despite poor initial quality.					
CASTING	soda lime borosilicate lead-barium	Indicated by (Oikonomopoulou et al., 2018) as the most frequently used for casting modular and monolithic glass	powder , medium shards, large shards	800-1500°C	2-10 h	-	no
	aluminosilicate	While technically recyclable through casting, as demonstrated by Bristogianni (2018), this type of glass presents sustainability challenges due to the high processing temperatures required and the difficulty of achieving high-quality, glossy finishes in cast products.					

3 | EXPERIMENTAL RESEARCH

3. Experimental research

This chapter presents the experimental phase of the research, in which recycled glass waste was processed into material samples and their acoustic performance was evaluated. Building on the theoretical framework established in the literature review, the experiments aimed to translate conceptual strategies, foaming and fusing, into practical outcomes. This part of the research is guided by one of the project's primary objectives: to explore **how different fabrication parameters affect the porosity and resulting sound absorption of foamed glass materials**, and whether these properties can be effectively controlled for architectural applications. The chapter is structured to first describe the experimental setup and methodology, followed by the development of foam glass samples, fusing techniques, and ultimately, the acoustic testing of selected specimens.

3.1. Set up equipment and methodology

To stay within the project's timeframe and match the resources and facilities available at TU Delft, a series of experiments was designed, putting the strongest focus on variables that the literature identifies as critical: glass waste composition, foaming agent type and concentration, foaming temperature. These factors are expected to govern porosity and the sound-absorption of the foam glass panels.

A repeatable manufacturing process was established and conducted in the Stevin II laboratory, using the ROHDE 1000 S kiln located at the Faculty of Civil Engineering. Each experimental batch was designed to isolate a single variable while keeping all other parameters constant, allowing for effective comparative analysis. The experiments began with the production of foam glass samples, informed by insights from the literature review. Findings from each test cycle guided adjustments in the subsequent phases of the experiments.

Once foamed, the samples were cut into test specimens using waterjet cutting machine: a Sanken 5-axis unit in the Glass Lab or the cutter in the DEMO Lab at the Faculty of Electrical Engineering, Mathematics and Computer Science. Normal incidence sound absorption coefficients were then measured with a Brüel & Kjær PULSE impedance tube (Type 4206) in the Faculty of Architecture; the tube's two diameters, 100 mm and 29 mm allowed for measuring sound absorption coefficient in the frequencies range 50 Hz to 1600 Hz and 1600 Hz to 6400 Hz, respectively.

Experimental batches were designed in such way so that parameters are isolated and their influence on a final result can be clearly stated. Data from every test cycle guided the choice of parameters for the following cycle, allowing for better informed decisions and with time, also control over porosity. From each series the most promising specimens, judged on their pore structure assessed visually, were reproduced in a larger moulds for acoustic testing. In this way, the experiments examine how individual fabrication variables affect porosity and acoustic response.

Finally, after measuring the sound absorption coefficients of the developed samples, the panels were virtually implemented in the chosen case study to assess their effectiveness. A digital model of the space was created, and the panels (using the measured acoustic data) were integrated into the model. Acoustic simulations were then conducted, and the results were compared to the baseline scenario to evaluate the impact of the panels on the room's acoustic performance.

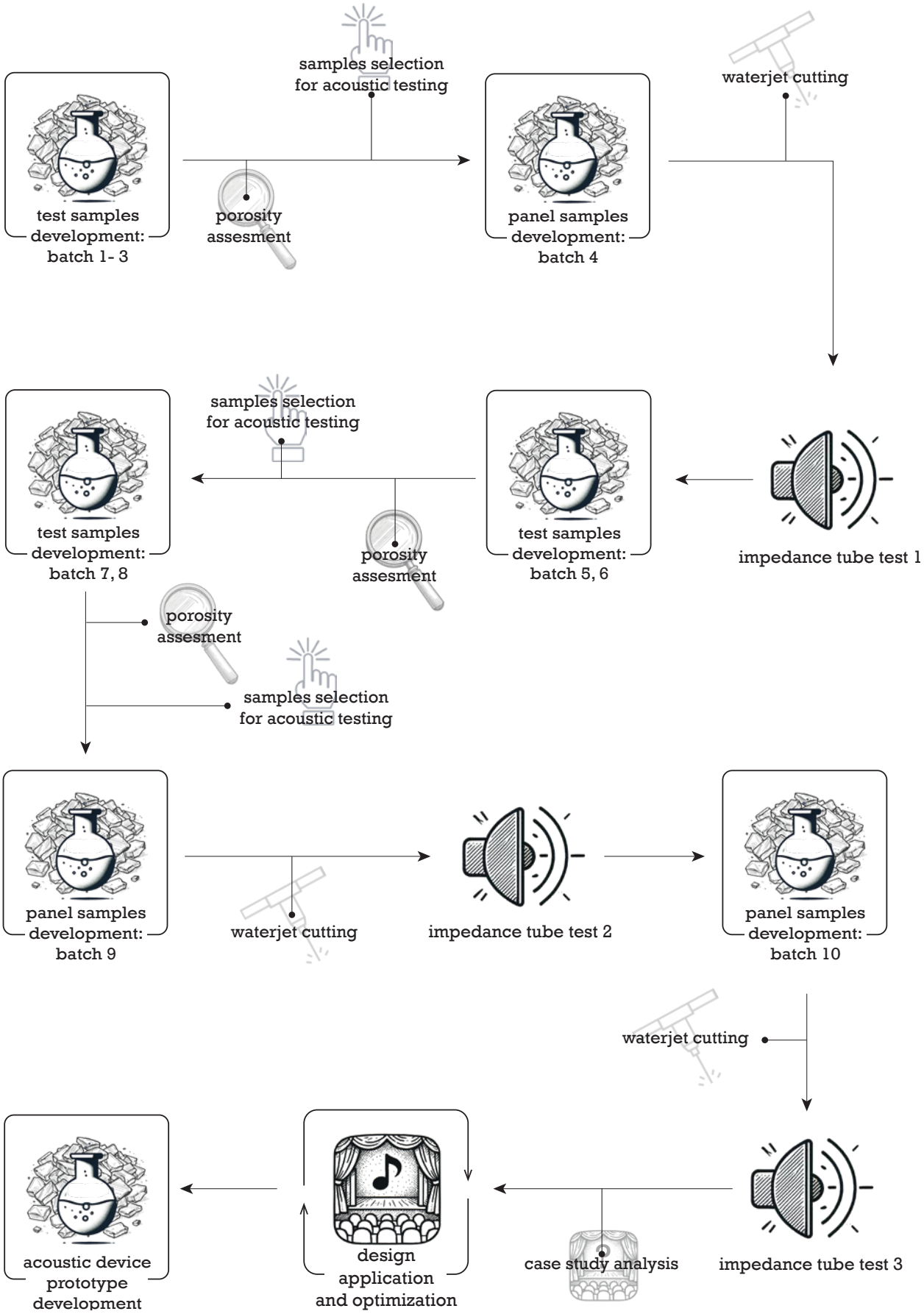

Fig. 3.1. Workflow of sample development, testing, and design integration throughout the research process. The diagram outlines the iterative procedure of producing and refining foamed glass samples across multiple batches. It includes porosity assessment, waterjet cutting, impedance tube testing. The process ends with design application, optimization and case study validation.

3.2. Foam glass samples development

This section details the process of developing foamed glass samples using various combinations of waste glass and foaming agents. The aim was to identify which parameters most significantly influence the resulting porosity and, by extension, the acoustic performance of the material. The development process was iterative and exploratory, with each batch informing adjustments to subsequent samples. The following subsection outlines the specific parameters that were varied and tested during this phase.

3.2.1. Tested parameters

Literature studies have shown that various fabrication parameters influence the properties of foam glass in different ways. Building on these findings, selected parameters were tested to explore their relationship with sample porosity and their impact on sound absorption performance. Starting-point values for each parameter were drawn from literature, with later modifications guided by the results of already conducted tests.

Glass waste type

The principal element for the experiments is the glass waste source. Since container glass is currently the only type of glass successfully recycled in closed loop system, the initial question stated in this research was whether other types of glass waste could be repurposed for foaming and manufacturing of acoustic panels. A range of waste glass types was collected and tested for their feasibility in the foaming process used to manufacture acoustic panels. The selection of glass waste types for the experimental phase was grounded in literature findings and was guided by their level of contamination, representativeness of real-world recycling challenges and cullet availability.

The types of glass tested were:

- **low iron soda lime:** A clean, high-purity material commonly sourced from architectural glazing. It provided a widely available baseline for early experiments due to its chemical consistency.

- **light bulbs glass:** A composite waste stream made up of soda lime and borosilicate glasses, often contaminated with plastics, ceramics, rubber, and metallic parts. It highlights a niche yet growing challenge in separating treated or coated glass types and is often excluded from closed-loop recycling.

- **automotive glass:** Laminated soda lime glass with embedded PVB layers, posing separation challenges during recycling, included based on literature indicating successful foaming outcomes with laminated automotive glass waste, despite its complexity due to embedded lamination layers.

- **aluminosilicate glass:** Chemically durable thin glass from mobile phone screens, which is difficult to remelt and recycle due to its high processing temperature, selected because of its known tendency to create gas bubbles during heating (Bristogianni, personal communication, January 2025), a property considered advantageous for foam formation.

- **mixed glass:** Severely contaminated glass containing a variety of inclusions, such as CRT fragments, wire mesh, or laminated particles, representing typical end-of-life demolition waste. According to Maltha Glass, the cullet provider, a maximum of 25g per metric ton of ceramic, stone or porcelain, 100g per metric ton of plastic and few grams per metric ton of concentrations of iron, aluminum and other residual metal may be present.

- **Cyclon mix:** A byproduct of bottle-recycling processes. This highly contaminated material

includes fine glass particles and non-glass residues collected through the suction system during sorting, tested following insights from the master thesis of (Giassia, 2022), which reported promising porosity results using this material.

By including these categories, the experimental work aims to explore the feasibility of transforming even the most heterogeneous, difficult-to-recycle, low-quality glass waste into functional porous materials.

Due to the most promising results that will be detailed later in the paper, low iron soda lime and light bulb glass were selected for a significant number of experiments. As the study progressed, the use of clean low-iron soda lime cullet was replaced with the more contaminated, mixed glass, to assess the feasibility of using less pure waste streams in acoustic panel manufacturing.

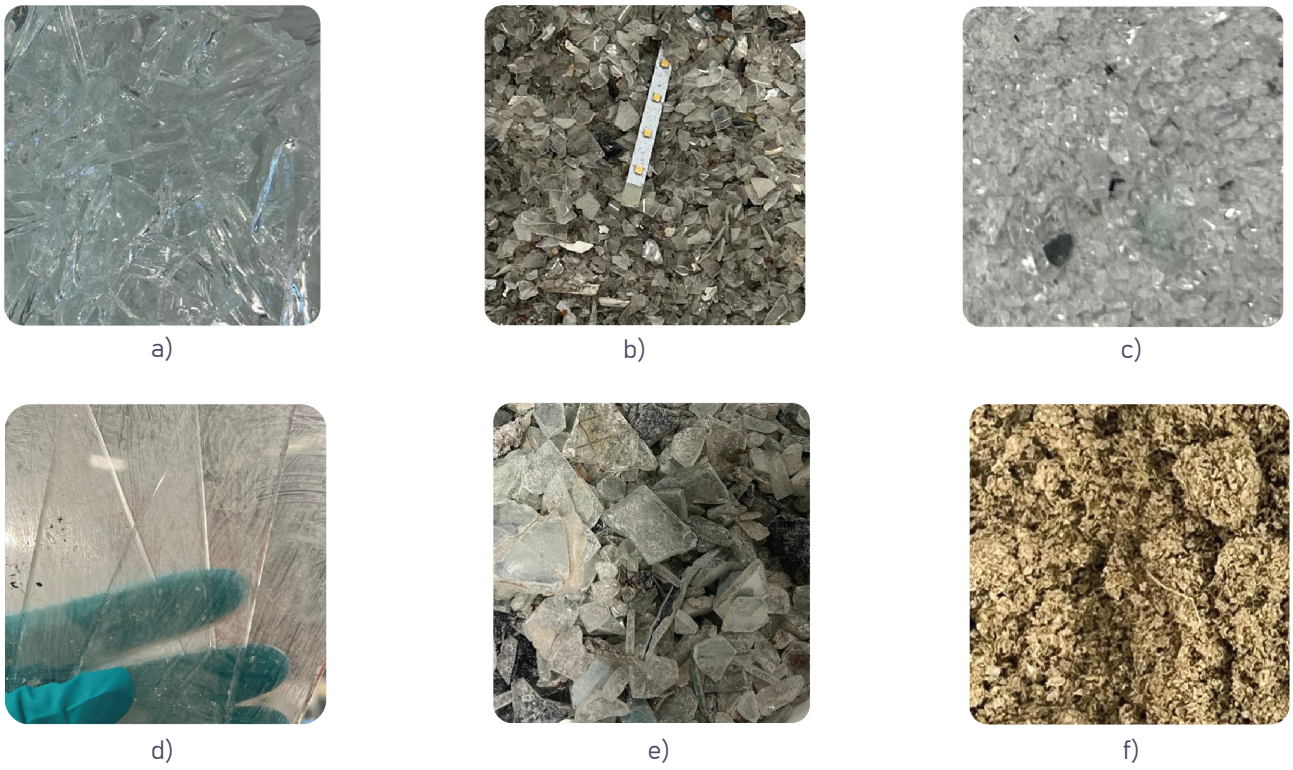

Fig. 3.2. Types of glass waste used in the experiments: a) low iron soda lime, b) mix glass waste from light bulbs, c) soda lime automotive glass, d) aluminosilicate glass from mobile phone screens, e) severely contaminated mixed cullet, f) Cyclon mix

Foaming agent

Since the traditional way of achieving foam glass is adding a foaming agent to it, this was the second parameter. The literature review highlighted that the amount of foaming agent added has a major influence on the foaming behaviour and the resulting properties of foam glass. For this reason, the type and quantity of foaming agent were identified as another key parameters to be tested. Several foaming agents were tested in different concentrations:

- **calcium carbonate ($CaCO_3$)**, 1- 15 wt%
- combination of **carbon black (C)** and **calcium hydrogen phosphate ($CaHPO_4$)**, 0.3 – 1.6 wt %
- **manganese dioxide (MnO_2)** 5 – 10 wt%
- **eggshells**, 1 – 5 wt%

The initial assumptions regarding the foaming agent choice and its concentration were based on the studies researched during literature review: a study by (Souza et al., 2017) that proved effective foaming of glass waste using eggshells, master thesis of (Giassia, 2022) who experimented with

combination of carbon black (C) and calcium hydrogen phosphate ($CaHPO_4$) and achieved desired in this project open porosity crucial for sound absorption.

Manganese dioxide (MnO_2) was used in only a few experiments, exclusively with clean soda lime cullet, due to its high cost and limited availability. In contrast, calcium carbonate demonstrated good compatibility with various types of glass waste and was therefore used extensively. It was later substituted with eggshells, which were also included in a significant number of experiments.

Eggshells consist of up to 95% of calcium carbonate, with the remaining 5% comprising calcium phosphate, magnesium carbonate and other organic compounds (Fernandes et al., 2014, Souza et al., 2017). The comparison between samples foamed with pure calcium carbonate and those using eggshells revealed interesting differences in performance, offering an important insight into how effective waste-derived foaming agents can be.

Glass and foaming agent particle size

When glass cullet is finely powdered, the foaming agent can act more effectively within the molten phase, as smaller particles become a liquid quicker than larger ones. Alternatively, larger particles may not fully melt but instead - partially fuse, creating interconnected pore channels between them (Bristogianni, personal communication, February 2025). These two ways of achieving porosity were examined. Glass waste was finely powdered in almost all the experiments - tests using larger particle sizes produced less effective results.

All foaming agents were used only in powder form. Only eggshells offered opportunity to investigate how the particle size of the foaming agent affects foaming process. Therefore, eggshells were tested both as a fine powder and as manually crushed, larger particles, approximately 2 mm in diameter.

Fig. 3.3. Overview of different glass cullet sizes tested in the early stages of the project.
Initial experiments explored various particle sizes, but powdered glass was quickly identified as the most effective for achieving uniform foaming results and was used in subsequent testing.

Firing schedule

The firing schedule has a significant influence on the microstructure of foam glass. Correct programming of the kiln at each stage of the firing process is crucial for achieving consistent foaming results. Among the firing parameters identified for testing, the maximum temperature and dwell time - the duration for which the sample is held at the peak temperature - were considered the most critical. Although the heating and cooling rates can also affect the microstructure, these were kept constant across all firing schedules tested.

Three firing schedules were developed and tested, with the initial attempts based on literature review, specifically the work of (Giassia, 2022) and (Konig et al., 2020). The first trials used a maximum temperature of **860°C with a dwell time of one hour**, which successfully produced foamed glass. Building on this result, subsequent tests were performed at lower temperatures to reduce energy consumptions needed for heating the oven. Every time the temperature was reduced, the dwell time was elongated by one hour to ensure sufficient foaming. As a result, samples were fired at **790°C for two hours**, and later at **720°C for three hours**. These adjustments were made based on the outcomes of each trial while remaining withing the temperature ranges reported in the literature. Rather than starting with the highest tested values, the focus was on exploring the lower end of the successful temperature spectrum used by other researchers.

All firing schedules followed the same initial procedure: samples were heated to 160°C at a rate of 50°C/h and held at this temperature for two hours to dry the glass and the moulds. Afterwards, the temperature was increased at the same rate to the maximum temperature (860°C, 790°C, or 720°C) and held at that temperature for the corresponding dwell time. Then, the temperature was lowered toward the annealing point at a rate of -160°C/h, where the samples were held for four hours to relieve internal stresses. Finally, the temperature was gradually reduced to room temperature at a slow rate of -25°C/h. The firing schedules are illustrated in the diagram presented in Figure 3.4.

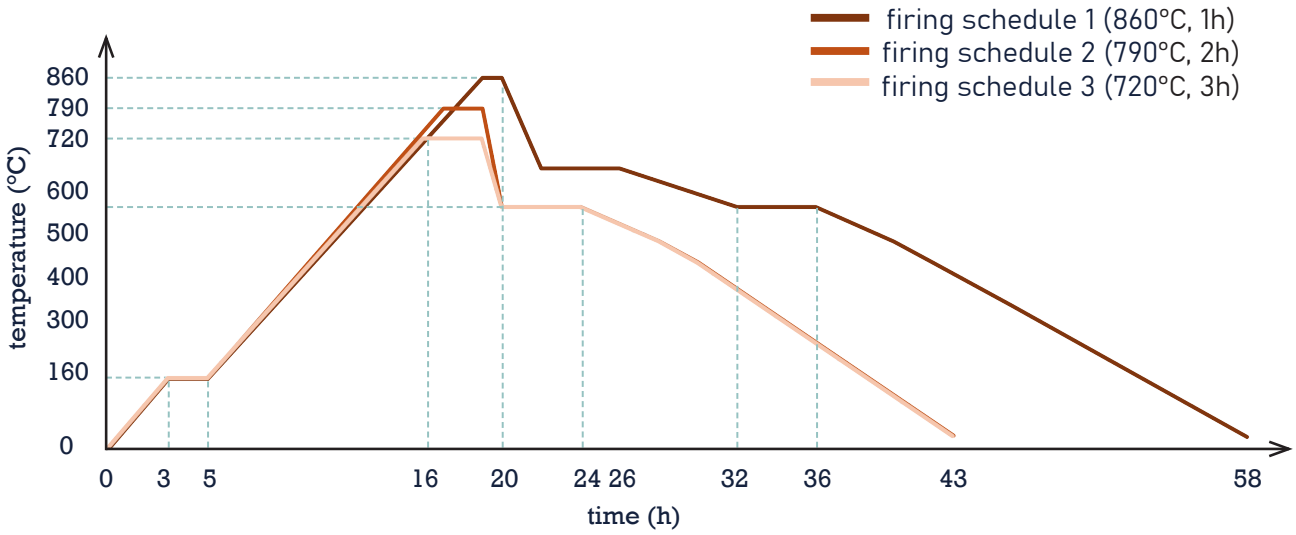

Fig. 3.4. Diagrams presenting the firing schedules tested in the project; firing schedule 1 (860°C, 1h), firing schedule 2 (790°C, 2h), firing schedule 3 (720°C, 3h). Exact diagram of each one can be found in Appendix.

Mould geometry

Although mould geometry was not initially considered a test variable, observations during the experiments revealed its influence on the foaming results. Two mould types were used in the study. Initially, all samples were foamed in cubic moulds measuring 5 x 5 x 5 cm. The samples that demonstrated the most promising porosity were selected for acoustic testing and had to be reproduced in larger moulds (12 x 12 x 6 cm). In some cases, samples produced in different moulds

showed noticeable differences in porosity structure, which are discussed in detail in the results section of this chapter.

a) b)

Fig. 3.5. a) Two types of mould used in the project; the small one (5 x 5 x 5 cm) for samples initial testing and the large one (12 x 12 x 6 cm) for development of larger samples for impedance tube testing, b) Extraction of the sample after firing.

The experiments were structured to test one parameter at a time, allowing the specific impact of each change to be isolated and analyzed. This method proved effective, as the individual influences of the parameters became observable through the results. However, it became evident that successful foaming was ultimately dependent on the combination of glass type, foaming agent mixture, and firing schedule. The combination of these three factors guided the direction of the research. An overview of the tested combinations is presented in the experiment overview scheme in Figure 3.6, while detailed documentation of all experiments is presented in table 3.1

3.2.2. Samples development process

Mould preparation

Samples were fired in crystal-cast moulds, chosen for their ability to withstand the high temperatures required for foaming. These moulds are disposable, and, in most cases, they had to be destroyed to extract the sample after firing. Although the mould preparation process is time-consuming, it is relatively straight-forward procedure. A 3D-printed positive of the desired mould shape was first created. A formwork was then constructed around the positive using wooden slabs and sealed with clay to prevent leakage of the casting mixture. The crystal-cast mixture was prepared using a 2.4:1 ratio of crystal cast to water and poured into the form. After approximately 30 minutes, once the material was fully solidified, the wooden formwork could be removed and 3D printed positive taken out of the mould. The mould was then cleaned to remove any clay residues and left to dry for at least 24 hours before use.

For moulds for firing aluminosilicate glass, a protective layer was applied, as aluminosilicate glass is known to chemically react with the mould during firing.

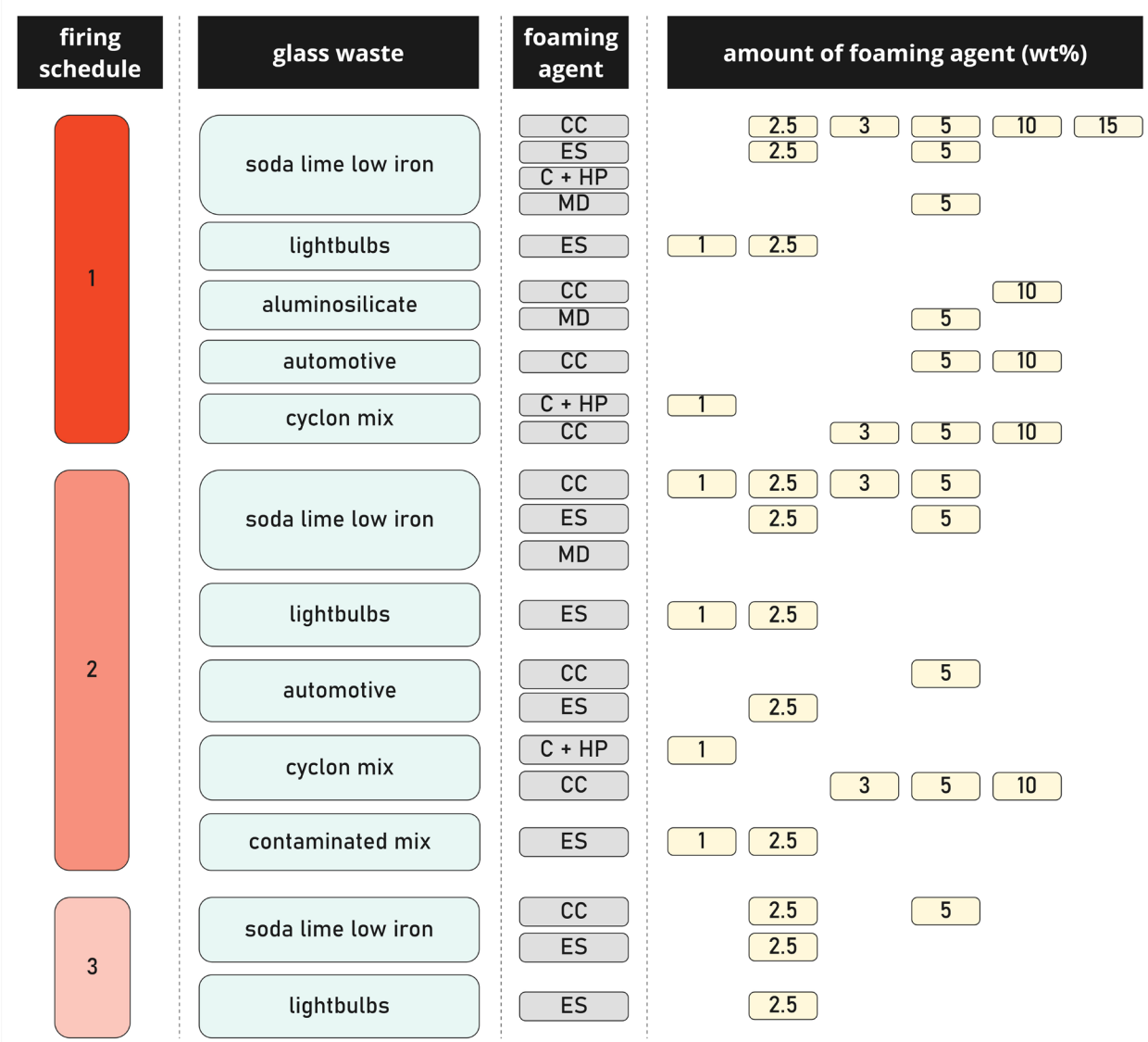

Fig. 3.6. Schematic overview of the experiments conducted during the development of foam glass samples. The diagram summarizes the combinations of glass waste types, foaming agents, their respective quantities (wt%), and firing schedules tested; CC – calcium carbonate, ES – eggshells, C – carbon black, HP – calcium hydrogen phosphate, MD – manganese dioxide.

Mixture preparation

First, glass waste streams were first screened for their sustainability in foaming. For each experiment, a specific type of glass was selected and processed either by powdering or by crushing the cullet into smaller particles using a milling machine. The low iron soda lime cullet, the cleanest cullet available, was cleaned beforehand with isopropanol to ensure high purity. Other, more contaminated types of glass were milled as received, together with any present contaminants. After milling, the material was sieved to remove oversized particles, such as large fragments of plastic, metal, or rubber that could not be effectively milled. Once the powdered glass was prepared, it was weighed together with the appropriate amount of foaming agent. The materials were then thoroughly mixed and placed into moulds for firing.

The small test samples consisted of approximately 100 g of the total mixture, while the larger samples for acoustic testing required around 1000 g of the mixture. An exception was made for samples prepared with Cyclon mix. Due to the material's form and loose structure, much less mixture could be placed into the moulds, approximately half the usual amount, as the Cyclon mix was not compressed before firing.

Fig. 3.7. a) Low iron soda lime cullet before and after milling in the Herzog milling machine. The cullet for almost all of the samples was milled for 6 seconds unless specified differently, b) Cyclon mix weighed with carbon black and dicalcium phosphate before mixing

Firing

Moulds containing the prepared mixtures were labelled and placed into the kiln. To ensure traceability, each batch was photographed before firing, allowing samples to be identified even if the labels were burned off during the firing process. The kiln was programmed according to the selected firing schedule. After the firing cycle, the moulds were again photographed, removed from the furnace, and the samples were carefully extracted, typically by breaking the moulds.

To maintain consistent documentation of all recipes, variables, and experimental trials, a systematic labelling method was developed. This system ensured that each sample could be easily tracked and referenced throughout the project. The labelling approach is illustrated in Figure 3.8.

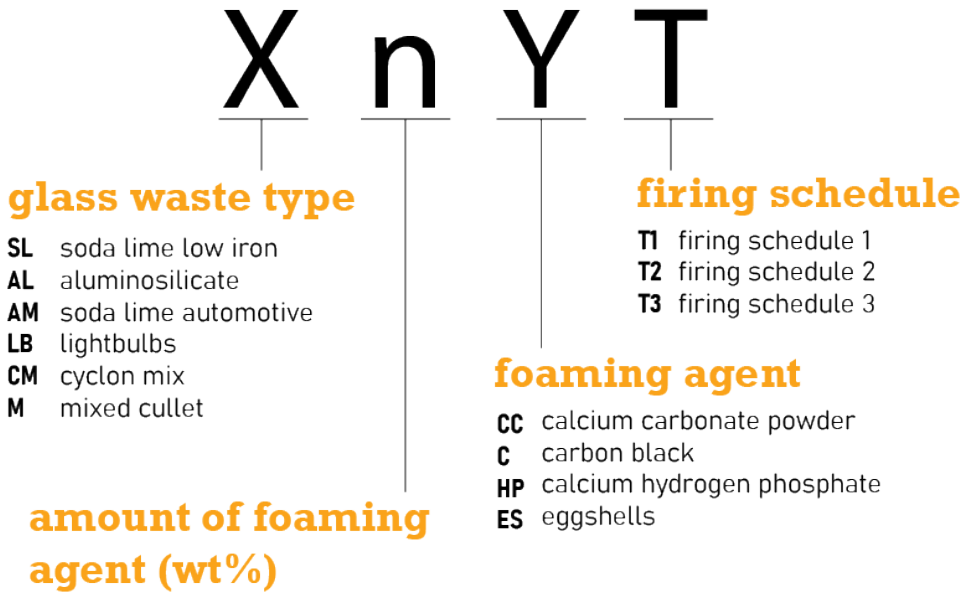

Fig. 3.8. Samples labeling scheme; own work

Porosity assessment and sample selection for acoustic testing

While the top surfaces of the samples generally exhibited clear foaming, the surfaces in contact with the mould remained unfoamed. To gain a more accurate understanding of the internal pore structure, the samples were cut using a diamond saw. Small test specimens had their edges trimmed to expose the cross-sectional porosity, while larger samples had both the top and bottom surfaces removed to reveal an open porous structure through the full thickness of the material. All cutting procedures were carried out at the Stevin II Laboratory, Faculty of Civil Engineering and Geosciences. Based on this combination of visual and cross-sectional assessment, the samples with the most consistent and well-developed internal porosity were selected for subsequent acoustic testing.

Sample selection for acoustic testing was based on a qualitative assessment of foaming quality. Initial evaluation was conducted through visual inspection, focusing on the presence, size, and distribution of pores. This visual assessment was guided by reference images from previous research on foam glass for sound absorption (e.g., König et al., 2016; Giassia, 2022), allowing for informed comparisons with established examples of successful porosity.

Fig. 3.9. Overview of the foamed glass sample production process.
The procedure includes three main stages: mould making using a 3D-printed positive and castable mixture; cullet preparation, where waste glass is crushed, milled to powder, and mixed with a foaming agent; and firing, when the mixture is heated in the mould over approximately 50-60 hours (depending on a firing schedule chosen) to produce porous samples.

Samples preparation for impedance tube testing

The manufacturing parameters and experimental results were documented continuously throughout the process. After the initial assessment of porosity, the most promising samples were reproduced using larger moulds measuring 12 × 12 × 6 cm. Once fired, the top and bottom surfaces of these larger samples were cut off using a diamond saw to fully expose the internal pore structure.

The next step involved preparing the samples for acoustic testing. A 10 cm diameter circular specimen was cut from each large sample using a waterjet, allowing it to fit tightly into the impedance tube. As two different specimen sizes are required for complete acoustic testing, and to ensure consistency of material properties between the tests, the smaller samples were in most cases not produced separately. Instead, they were also cut from the same large circular specimen using the waterjet, ensuring that both sample sizes originated from the same foamed material.

The small samples required for high-frequency impedance tube testing (29 mm diameter) were too small to be safely cut using the waterjet cutting machine at the Glass Lab of Architecture Faculty. Specimens of such small size risked falling between the machine's ribs, causing potential damage.

To work around this issue, the small samples were cut from the larger ones as two connected circles, joined by a small bridge, as shown in Figure 3.10a. After cutting, the samples were taken to the glass laboratory, where the bridge was manually broken - a simple process due to the natural brittleness of foam glass. Any remaining residue from the break was then polished off using a polishing machine.

Although ideally the cutting process would avoid the need for this extra step, this method was the only effective solution to obtain small-diameter specimens necessary for full-spectrum frequency measurements.

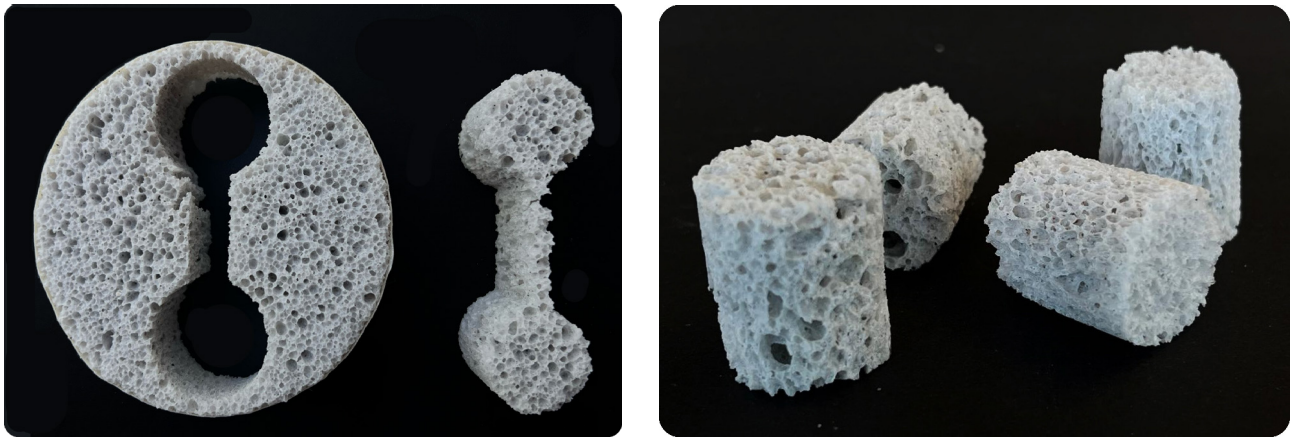

a) b)

Fig. 3.10. a) Method used to cut small samples from larger ones to prevent their loss during in the waterjet cutting machine; b) Small samples after post-processing, prepared for impedance tube measurements at high frequencies.

Fig. 3.11. Different types of pores obtained throughout the study, mixing different manufacturing parameters; from the left: SL2.5ES, LB2.5ES, SL5ES, SL5CC, SL/CM5050

3.2.3. Results interpretation

This section presents the findings from the sample development phase and discusses how each manufacturing parameter influenced the final properties of the foam glass samples - most importantly porosity (including pore size and distribution), but also aspects such as color, brittleness, and other characteristics. For each parameter discussed, the included images show samples produced under identical conditions, with only that single variable changed, allowing a clear comparison of its impact.

Table 3.1. The overview of all the conducted experiments

BATCH	FIRING SCHEDULE	PICTURE	SAMPLE	TYPE OF GLASS WASTE	AMOUNT (WT %) AND TYPE OF FOAMING AGENT		RESULTS/REMARKS
1 (10.02)	1		SL5CCT1	SL	5	$CaCO_3$	Extensive foaming at the top with interconnected pores reaching up to 15 mm.
			SL10CCT1	SL	10	$CaCO_3$	No foaming observed; horizontal surface cracks present.
			SL15CCT1	SL	15	$CaCO_3$	No foaming occurred.
			SL0.3CBT1	SL	0.33	C	No foaming occurred.
			SL1CBT1	SL	1	C	No foaming occurred.
			A10CCT1	AS	10	$CaCO_3$	Small cullet (milled 1 s) used; no foaming observed.
2 (14.02)	1		SL2.5CCT1	SL	2.5	$CaCO_3$	Rough, interconnected pores (1–5 mm) throughout depth.
			SL5CCT1	SL	5	$CaCO_3$	Glass powder–cullet mix (60:40) used; no foaming. Powder alone performed better under same conditions.
			SL3CCT1	SL	3 0.33 1.66	$CaCO_3$ C $CaHPO_4$	Rough surface, no foaming; denser and heavier than samples with only calcium carbonate.
			SL5MDT1	SL	5	MnO_2	Top surface cracked open; section shows small pores (≤1 mm).
			A5CCT1	AS (small cullet)	5	$CaCO_3$	Small cullet (milled 1 s); glossy surface with singular crystals on top.
			A5MDT1	AS (small cullet)	5	MnO_2	Small cullet (milled 1 s), slight foaming; section shows tiny pores (<1 mm).
3 (20.02)	2		SL2.5CCT2	SL	2.5	$CaCO_3$	Pores up to 5 mm, larger than the same sample fired in T1.
			SL3.5CCT2	SL	3.5	$CaCO_3$	CC added at mould bottom; no effect observed.
			SL2CCT2	SL	2	$CaCO_3$	CC added at mould bottom; no effect observed.
			MCT2M	SL	mixed (5 bottom, 2 top)	$CaCO_3$	2.5% top part foamed; 5% bottom part did not. Visible line at concentration change.
			SL10MDT2	SL	10	MnO_2	Tiny pores (< 1 mm) , shrinking occurred.

			AM5CCT2	AM	5	$CaCO_3$	Powder mixed with small cullet (unspecified ratio); minimal foaming, tiny pores in section, deep horizontal surface crack
4 (3.03)	2		SL1CCT2	SL	1	$CaCO_3$	Small pores (~1.5 - 3 mm).
			SL2.5CCT2	SL	2.5	$CaCO_3$	Medium pores (~ 3 - 4.5 mm).
			SL3.5CCT2	SL	3.5	$CaCO_3$	Larger, circular pores (up to 7 mm).
			SL5CCT2	SL	5	$CaCO_3$	Didn't foam like the same recipe in smaller mould; result confirmed on repeat.
			AM2.5EST2	AM	2.5	ES	Closed pores up to 5 mm; particles ca. 2mm were added
			SL2.5EST2	SL	2.5	ES	Interconnected pores up to 2 mm; more homogeneous than the same sample with CC.
			SL10CCT2	SL	10	$CaCO_3$	No foaming; rough, stone-like texture with some tiny surface crystals.
5 (7.03)	2		C0.3CB1.6PT2	CM	0.3 1.6	C $CaHPO_4$	Bonded better than other C samples, but still brittle.
			C3CCT2	CM	3	$CaCO_3$	Poor bonding; extremely brittle.
			C5CCT2		5	$CaCO_3$	No bonding occurred.
			C6.5CCT2	CM	6.5	$CaCO_3$	Cyclon mix was compressed in the mould; no bonding occurred.
			C10CCT2		10	$CaCO_3$	No bonding occurred.
			SL2.5EST2	SL	2.5	ES	Smaller pores than in SL2.5CCT2.
			MCT2M	SL	mixed (5 bottom, 2 top)	$CaCO_3$	Only upper 2.5 cm foamed; clear line at concentration boundary.
			LB2.5EST2	LB	2.5	ES	Interconnected pores, larger than in SL2.5CCT2.
6 (14.03)	1		LB5EST1	LB	5	ES	Very large pores (up to 20 mm); less vertical growth than SL glass.
			LB2.5EST1	LB	2.5	ES	Pores larger than in the same sample fired at T2.
			SL5EST1	LB	5	ES	Gradient porosity: smaller pores at bottom, larger (up to 3 mm) on top.
			SL2.5EST1	SL	2.5	ES	Gradient porosity: smaller pores at bottom, larger (up to 1 mm) on top.
			C0.3CB1.6PT1	CM	0.3 1.6	C $CaHPO_4$	Less brittle than the same sample fired at T2

			C3CCT1	CM	3	$CaCO_3$	Higher calcium content increases brittleness: 3–5 samples are very brittle and crumbly; 10 sample didn't bond at all.
			C5CCT1		5	$CaCO_3$	
			C10CCT1	CM	10	$CaCO_3$	
7 (21.03)	2		SL2.5EST2	SL	2.5	ES	Two pore types, both nearly circular: dense tiny pores (<1 mm) on surface, larger ones (~2.5 mm) deeper in the sample.
			SL5CCT2	SL	5	$CaCO_3$	Rough, porous structure with horizontal and vertical interconnections; larger central void formed by merging smaller pores (up to 17 mm) with finer pores near the edges.
		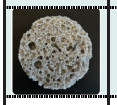	LB2.5EST2	LB	2.5	ES	Homogeneous structure with pores 5 - 11 mm, slight variation in depth.
			LB1EST2	LB	1	ES	Pores vary in size; spaces between large ones filled with smaller, shallow pores. Thin walls separate deep-reaching pore corridors.
			MCT2M	SL	mixed (2.5 bottom, 5 top)	$CaCO_3$	Visible transition line at foaming agent shift; larger pores (up to 5 mm) at bottom, smaller (<1 mm) on top.
			SL/CM_20/80	SL + CM	5 (soda lime part)	$CaCO_3$	Very brittle, crumbles easily.
			SL/CM_50/50	SL + CM	5 (soda lime part)	$CaCO_3$	Much more solid than the same sample with a 20/80 soda-lime to Cyclon mix ratio.
			CM0.3C3.2HT2	CM	0.3 3.2	C $CaHPO_4$	Decomposes more than the same sample with 1.6 $CaHPO_4$.
8 (28.03)	3		SL2.5EST3	SL	2.5	ES	Foamed less than the same sample at higher temperatures.
			SL2.5CCT3	SL	2.5	$CaCO_3$	Foamed less than the same sample at higher temperatures.
			SL5CCT3	SL	5	$CaCO_3$	Shrinking in the top surface occurred.
			LB2.5EST3	LB	2.5	ES	Foamed less than the same sample at higher temperatures.
			LB5EST3	LB	5	$CaCO_3$	Shrinking in the top surface occurred.
9 (4.04)	2		M + M1EST2	M	1	ES	No pores within 5 mm of the surface; small (<1 mm), shallow, densely packed pores in the centre.
			M + M2.5EST2	M	2.5	ES	Pores ~2 mm, some closed, others interconnected with deeper layers; shapes vary.
			SL +SL2.5EST2	SL	2.5	ES	Visible pore line at mould overflow; larger pores (~2 mm) above, ~1 mm below.
			SL + LB1EST2	LB	1	ES	Interconnected pores up to 5 mm; larger voids formed by merging smaller pores; rich structure with varied pore depth.

			SL/CM_50/50	SL + CM	10	ES	Sandy, rough finish; no pores like other glass types; denser sample.
			SL5EST2	SL	5	ES	Densely packed, circular pores 4 - 6 mm.
10 (11.04)	2		M + LB1ES	LB	1	ES	Wide pore size range (~5–20 mm), with significant variation in depth.
			SL thick + M2.5ES	M	2.5	ES	A lot of small pores (~1.5 mm), evenly distributed and densely packed, few larger pores up to 6 mm
			M + M5EST2	M	5	ES	Numerous densely packed pores, ranging from ~2–5 mm, with occasional larger ones in between.
			SL thin + M5CCT2	M	7.5	ES	More foaming near the surfaces; central pores are <1 mm, densely packed, with a visible crack.

SL - low iron soda lime, AS - aluminosilicate, AM - automotive, CM - cyclon mix*, LB- lightbulbs, M - mixed cullet

$CaCO_3$ - pure calcium carbonate, ES - eggshells, C - carbon black, MnO_2 - manganese dioxide, $CaHPO_4$ - dicalcium phosphate

Recipe

Recipe variations combining different types of glass waste and foaming agents led to the development of a wide range of samples, each exhibiting different colours, pore sizes, structures, distributions, and degrees of brittleness. Promising foaming behaviour was observed in samples made from soda lime glass, light bulb glass, and even contaminated mixed glass cullet. Even when the same foaming agent and quantity were used, the pores in the light bulb glass samples were visibly larger, with the largest pores 10 mm in diameter, than in other glass types.

Samples made from light bulbs consistently exhibited a glossy finish, with visible pores on the top surface, specifically in the areas that expanded beyond the mould, indicating successful foaming. In contrast, soda lime glass samples showed higher variability: in some cases, the foamed structure extended visibly beyond the mould, while in others, the surface expanded significantly but the spongy, porous texture remained confined within the mould and did not reach the surface.

Soda lime glass and mixed glass cullet worked effectively with various foaming agents, resulting in matte finish and porosity characterised by smaller, more uniform pores ranging from approximately 1 up to 5 mm.

The Cyclon mix did not foam in the same manner as the samples based on other glasses. Although the final material was still porous, the structure resembled more of a sandy, stone-like material rather than a typical foamed glass with discrete pores. A similar outcome was observed when soda lime powder was mixed with Cyclon mix at different proportions. A 20/80 soda lime/Cyclon mix ratio produced a very brittle material that disintegrated easily, meanwhile a 50/50 ratio resulted in a sturdier sample.

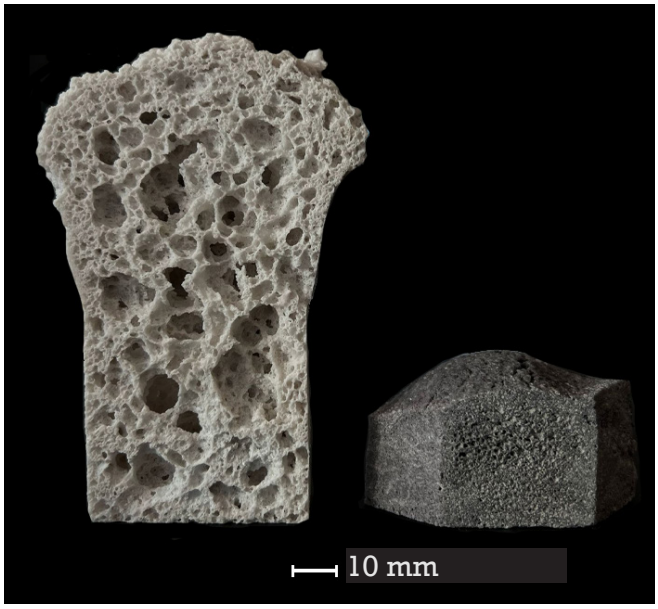

Fig. 3.12. Comparison of samples made from the same soda lime glass waste and foamed at the same temperature, using different foaming agents. Left: SL5CCT1, Right: SL5MDT1

Amount of foaming agent

The amount of foaming agent influenced pore size across all tested glass types. In general, higher concentrations led to larger pores, aligning with the literature review findings. However, there is a threshold beyond which increasing the amount no longer enlarges pores but instead prevents foaming. This threshold appears to decrease with rising temperature.

Soda lime glass was tested with various amounts of calcium carbonate. Figure 3.13c shows clear differences in pore structure of samples fired in 860°C due to different foaming agent concentration. Figure 3.13b compares samples foamed at 720 °C with 2.5 wt% and 5 wt%, where the higher concentration resulted in no pores, though the same amount produced rich porosity at 860°C. Following the literature review insights, higher concentrations were also tested (10% and 15%), but led to foaming failure in low-iron soda lime glass.

Light bulb glass showed the opposite trend: less foaming agent resulted in larger pores (Figure 3.13d).

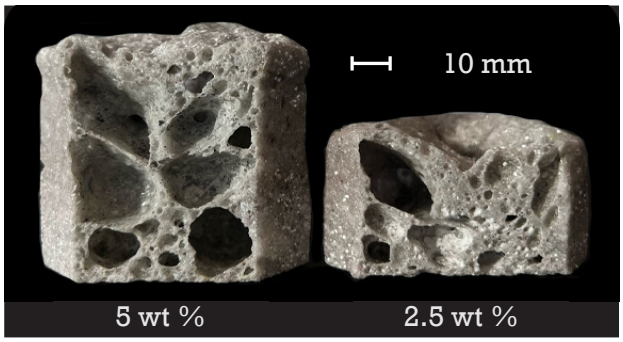

a)

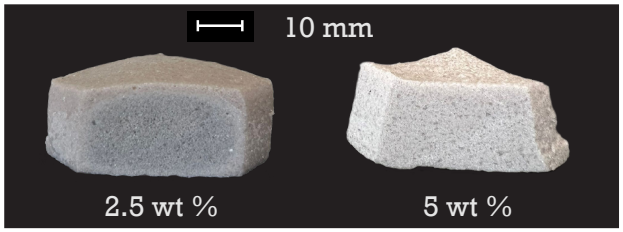

b)

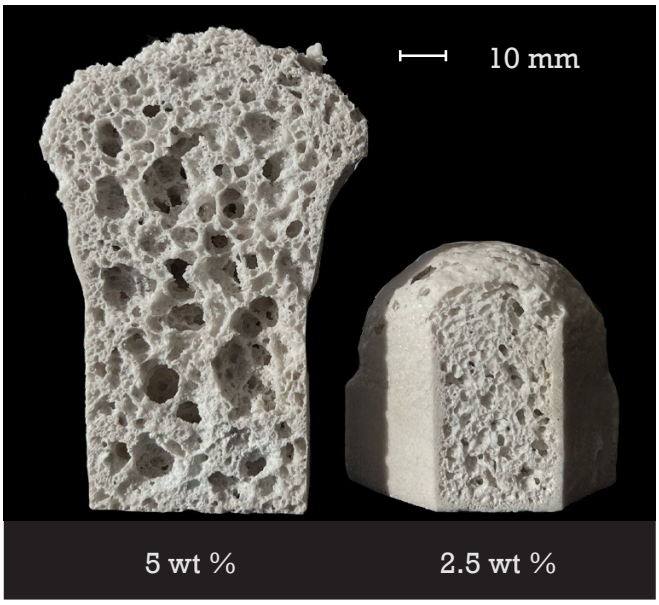

c)

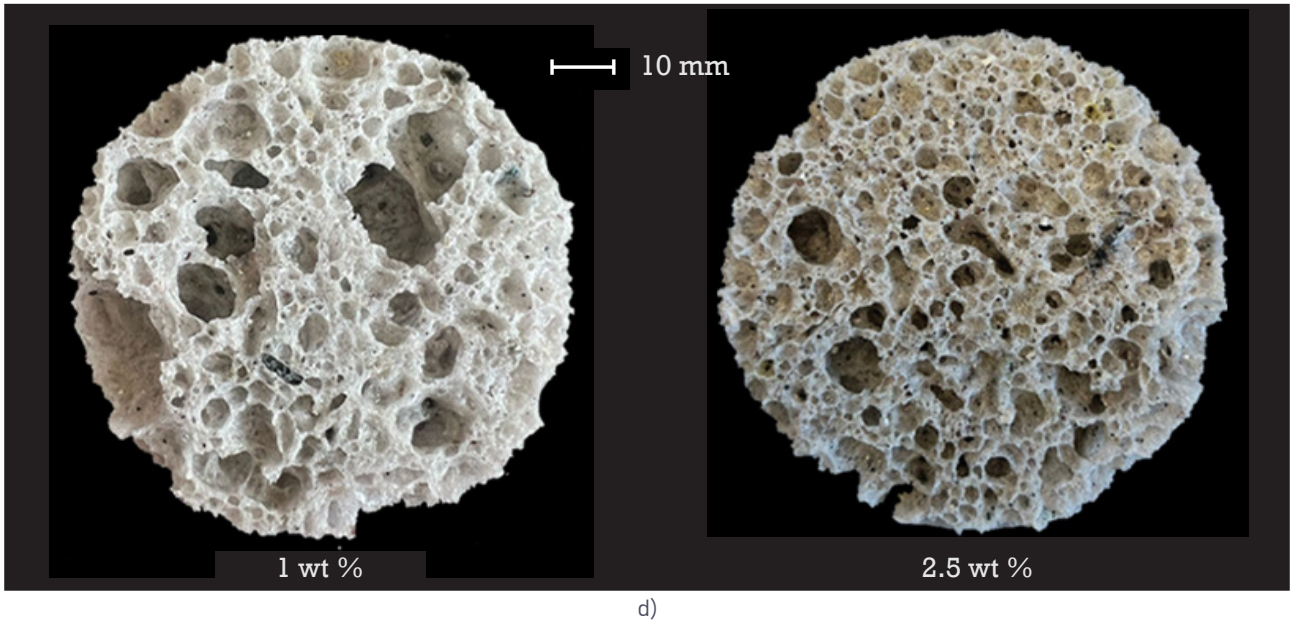

d)

Fig. 3.13. Samples made of the same glass waste, foamed in the same temperature with different amount of the same foaming agent; a) From the left: LB5EST1, LB2.5EST1, b) From the left: SL5CCT1, SL2.5CCT1

Glass particle size

As mentioned earlier, experiments were also conducted using different glass particle sizes to explore whether this could help achieve open pores in the samples. A few tests were performed with larger glass particles (up to 2 mm in diameter), but these samples did not foam in the same way as those made with powdered glass. This may be because the larger particles were too heavy for the gas bubbles produced by the foaming agent to lift. Instead, the larger particles partially fused together, forming pores with a very different structure compared to the properly foamed samples. This difference is illustrated in Figure 3.14, which compares the structure of the samples. Both soda lime samples were made using the same recipe and firing schedule; the only difference was that the sample on the right in Figure 3.14b used a mixture of glass powder and smaller cullet (around 2 mm) in a 40:60 ratio.

Additional samples using larger glass particles included automotive and aluminosilicate glass. While these did not foam, they still showed signs of porosity, proved by their ability to absorb water.

Overall, powdered glass proved to be much more effective, allowing the foaming agent to work as intended. As a result, further experiments with larger cullet sizes were not pursued, and nearly all the successful tests used glass in powder form (milled in the milling machine for 6 seconds).

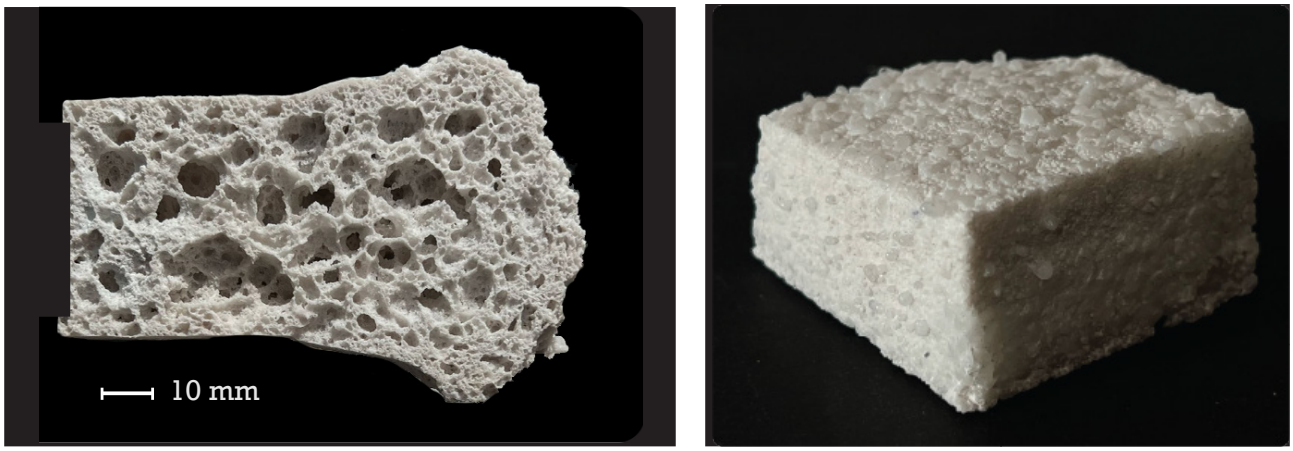

a) b)

Fig. 3.14. Samples manufactured using the same recipe and fired at the same temperature differ only in the grain size of the material used: a) was made entirely with fine glass powder, while b) used a 40/60 mixture of powder and larger particles. Both samples are labeled SL5CCT1.

Foaming agent particle size

The variation of foaming agent particle size could only be tested with eggshells. Figure 3.15 shows samples produced from low-iron soda lime glass cullet with 2.5 wt% eggshells. In one sample, the eggshells were added as a fine, flour-like powder; in the other, they were manually crushed into particles approximately 2 mm in size.

The sample prepared with powdered eggshells exhibits a fine, homogeneous pore distribution. The pores are small, densely packed, and similar in size. The structure appears smooth, suggesting the even distribution of the foaming throughout the mixture.

In contrast, the sample made with larger eggshell particles shows more irregular pore structure. Pores are larger and unevenly distributed. Some have merged into larger cavities, indicating local over-foaming due to the uneven distribution of the foaming agent particles. This sample has fewer pores overall, but they are larger and closed, not interconnected.

A similar effect was observed when larger eggshell particles were used with automotive glass; the resulting pore structure resembled that of the soda lime glass sample. All other experiments with

different foaming agents were conducted using only fine powder forms. It is important to note that only these two experiments used eggshells in a form other than powder. Therefore, while initial observations suggest foaming agent's particle size significantly impacts pore structure, further experiments would be necessary to draw definite conclusions.

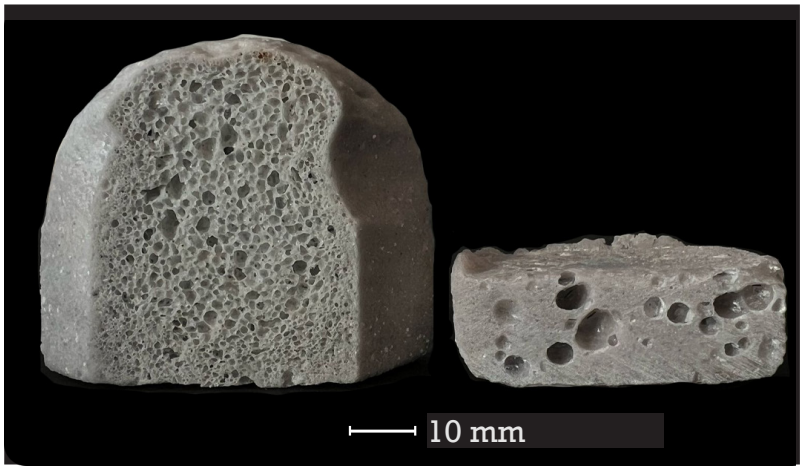

Fig. 3.15. Samples made from the same glass waste, foamed at the same temperature and with the same amount of foaming agent, differing only in the form of the foaming agent. From left: SL2.5EST2 with eggshells added in powder form; right: sample made with the same recipe, but eggshells added as larger particles.

Fig. 3.16. Glass mixed with eggshells – larger particles of the foaming agent can be observed in the mixture

Eggshells vs calcium carbonate

Initially, calcium carbonate powder was used as the foaming agent. As the study progressed, it was replaced with eggshells, which performed comparably in terms of foaming effectiveness. Eggshells present a more sustainable choice, considering the environmental need for new methods of recycling this waste material.

This comparison was chosen because eggshells are chemically similar to calcium carbonate, consisting of approximately 95% $CaCO_3$. However, despite their chemical similarity, the results between the two materials were noticeably different.

The comparison between calcium carbonate and eggshells was based on multiple foaming tests conducted using low iron soda lime cullet, with identical amounts of either foaming agent and varied firing schedules.

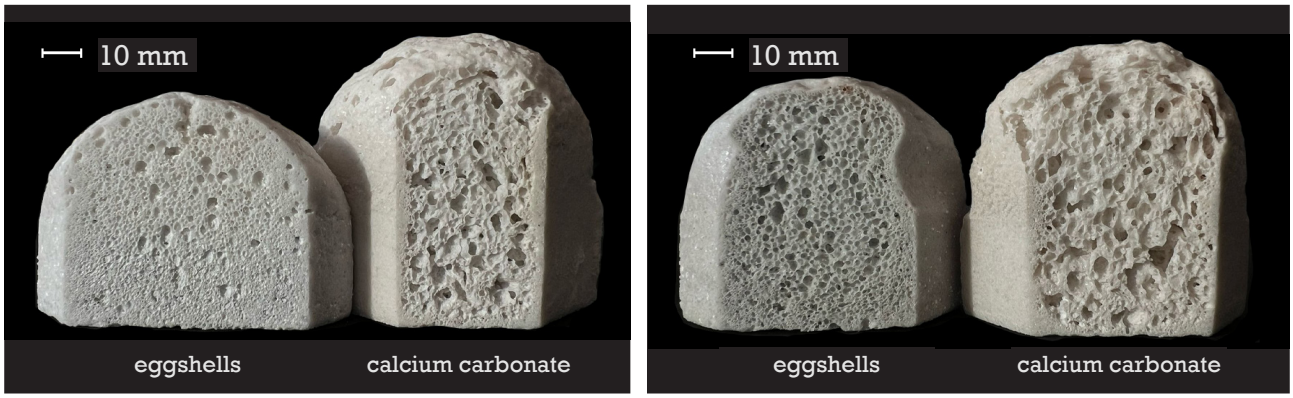

Fig. 3.17. Comparison of samples made using the same recipe and firing schedule, differing only in the type of foaming agent used - pure calcium carbonate (right in each image) and eggshells (left); a) SL2.5EST2 and SL2.5CCT2 b) SL2.5EST1 and SL2.5CCT1

Firing schedule

The impact of the firing schedule on foaming was clearly visible across all samples. Both light bulb glass and soda lime glass were tested in all three firing schedules designed in the study. These two materials responded differently to the same firing conditions, highlighting the material-specific nature of the foaming process.

For the light bulb glass samples, higher firing temperatures resulted in samples with large, highly irregular pores and thin pore walls, leading to a fragile and open structure. As the firing temperature was reduced and dwell time adjusted, the pore structure became gradually smaller. Even at lower firing temperatures, the foamed structure remained relatively coarse and open. This behaviour suggests a lower viscosity in the molten state, which aligns with expectations, as borosilicate glasses typically require higher working temperatures.

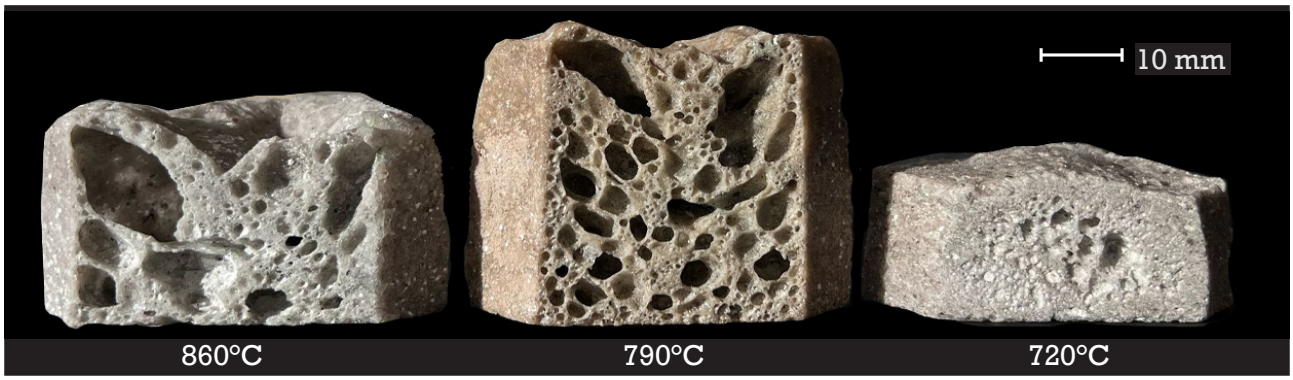

Fig. 3.18. Samples manufactured with the same recipe, fired in different firing schedules; From the left: LB2.5EST1, LB2.5EST2, LB2.5EST3

In contrast, soda lime glass samples responded more consistently to changes in the firing schedule. At higher temperatures or shorter dwell times, they exhibited moderate foaming with medium-sized pores. As the firing temperature decreased and dwell time increased, the pore structure became finer and more uniform. However, the samples fired at 860 °C and 790 °C (firing schedules 1 and 2), shown in Figure 3.19, displayed similar pore characteristics.

Compared to light bulb glass, soda lime glass maintained better structural integrity and allowed for more reliable control over pore development through the foaming agent. Nonetheless, light bulb glass proved more sensitive to firing temperature, showing greater responsiveness in pore formation.

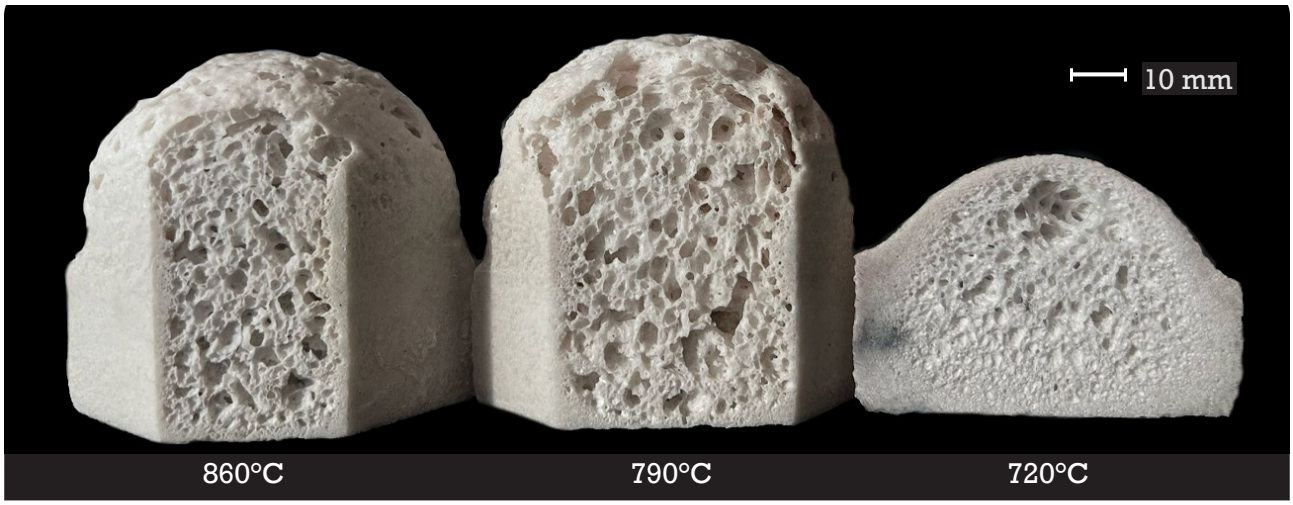

Fig. 3.19. Samples manufactured with the same recipe, fired in different firing schedules; From the left: SL2.5EST1, SL2.5EST2, SL2.5EST3

Cyclon mix samples displayed a different behaviour from all the other types of glass waste tested. This material did not foam in the traditional sense observed with soda lime or light bulb glass. Instead, the Cyclon mix samples developed a rough, grainy structure rather than well-defined pores. The firing schedule had a major influence on the degree of bonding between the particles. At higher firing temperatures, the particles fused together more strongly, resulting in a sturdier, more cohesive material. Lower firing temperatures, on the other hand, produced weaker, less bonded samples that were more fragile – some of them didn't even bond at all as presented in Figure 3.20b. All the Cyclon mix samples were prone to crumbling. This behaviour indicates that for Cyclon mix, the primary effect of the firing schedule is not to achieve foaming, but to control the cohesion of structure.

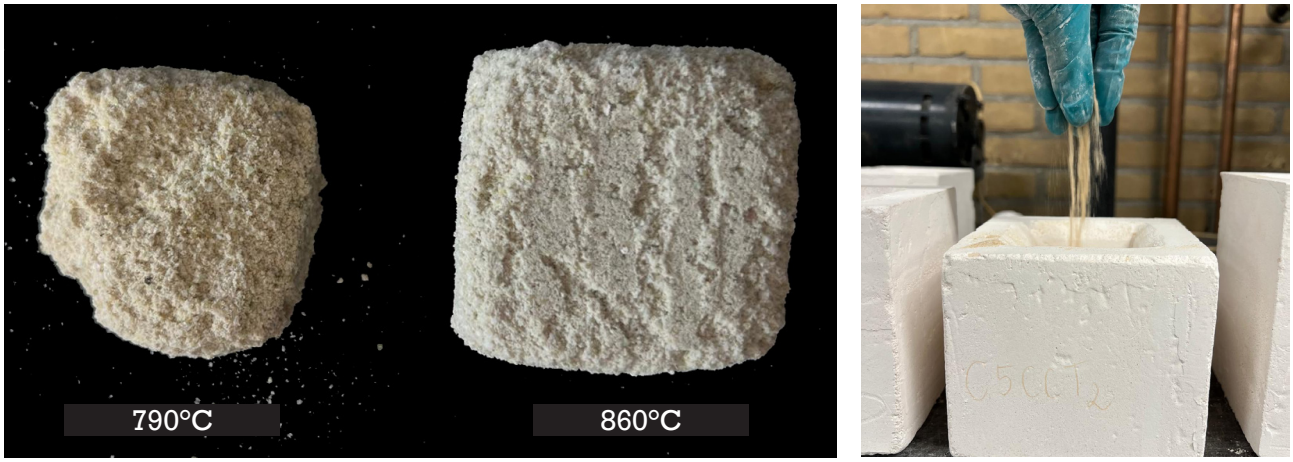

a) b)

Fig. 3.20. a) Cyclon mix samples fired at different temperatures. Unlike other glasses, they did not foam, and required higher temperatures just to bond properly. At lower temperatures, the samples were prone to crumbling or, as shown in image b), failed to bond entirely.

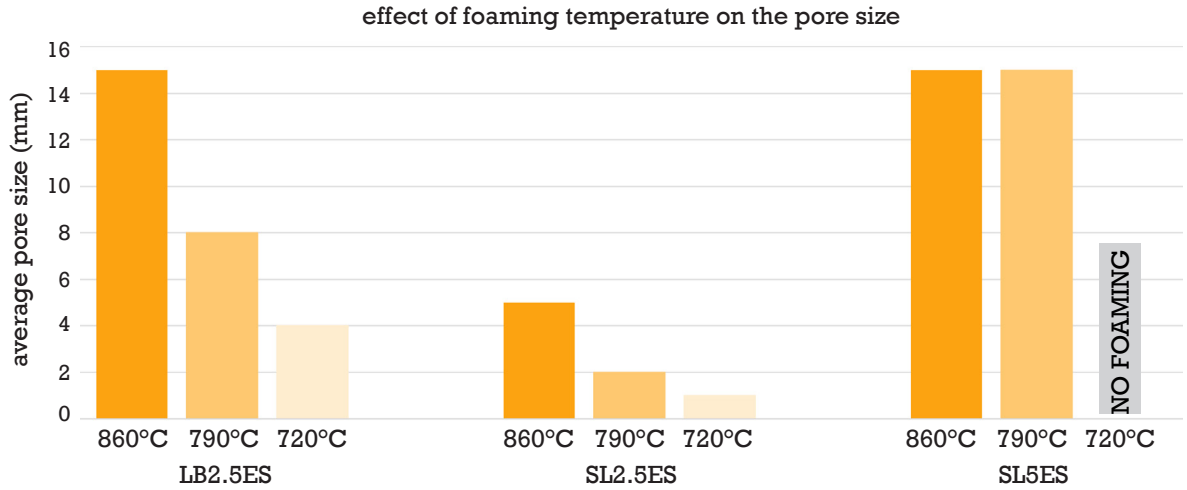

Fig. 3.21. Effect of foaming agent on pore size – higher temperatures consistently lead to the development of larger pores.

Mould size or shape

Although mould geometry was not originally planned to be tested as a variable in this study, the use of two different mould types during the experiments revealed that it does influence the foaming outcome, even when the same recipe and firing schedule are applied. Figure 3.22 presents a low iron soda lime glass sample with 2.5 wt% eggshells manufactured in different types of mould.

The sample made in the larger mould displays a greater ratio of open pores relative to the total area of the section and deeper pore structures. However, it also foamed less overall compared to the sample made in the smaller mould.

An additional observation was that some larger moulds were taller than necessary, which may have physically supported the vertical growth of foaming glass. In contrast, the shallower moulds did not support this upward growth, which may explain the observed differences in porosity between the samples.

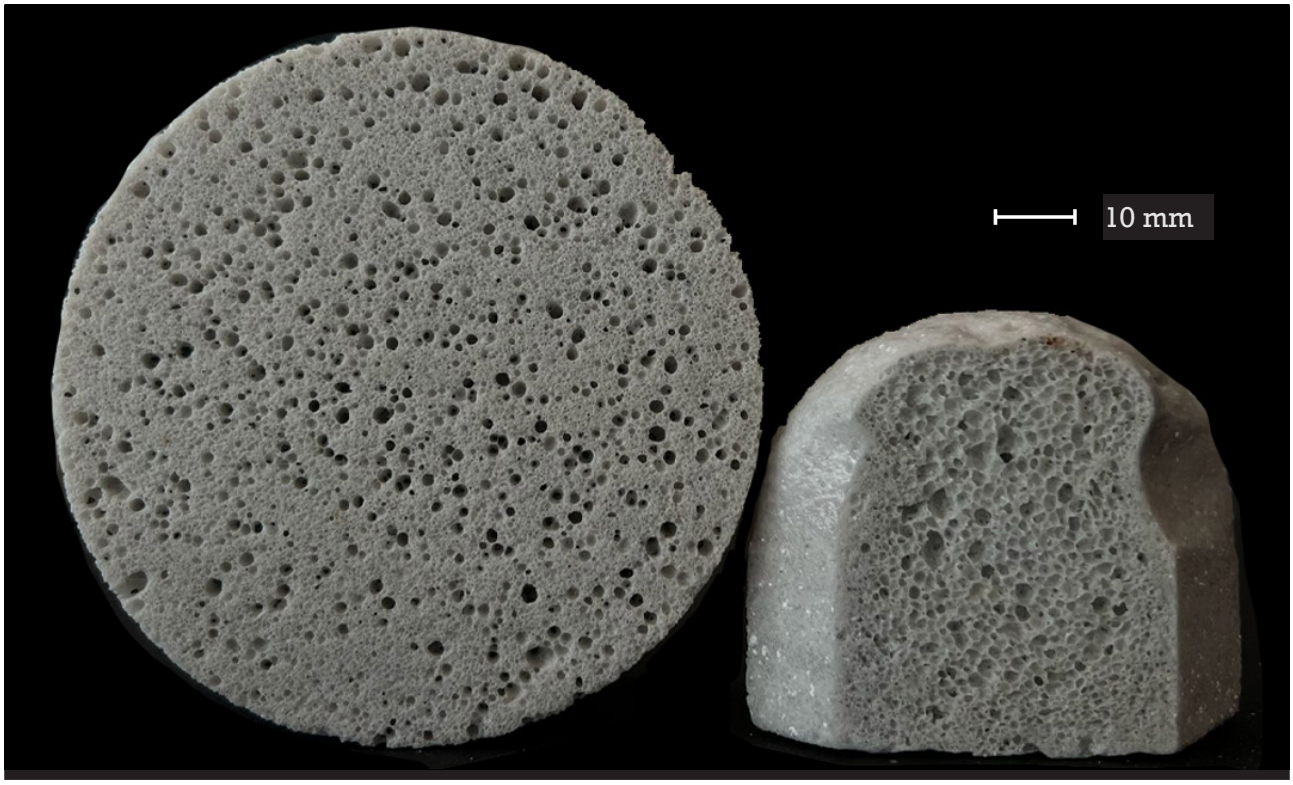

Fig. 3.22. Samples manufactured with the same recipe, and fired in the same firing schedules, but in different moulds; Both labeled SL2.5EST2

Gradient porosity within a sample

The porosity within the samples varied significantly, not only with depth but also across the height and surface of each section. As a result, some samples exhibited very different pore sizes on their opposite sides.

In general, pores tend to be much smaller near the surface of the samples. This pattern is consistently visible in all cut samples, as well as in Figure 3.23, which illustrates the differences in pore size across sample's horizontal sections.

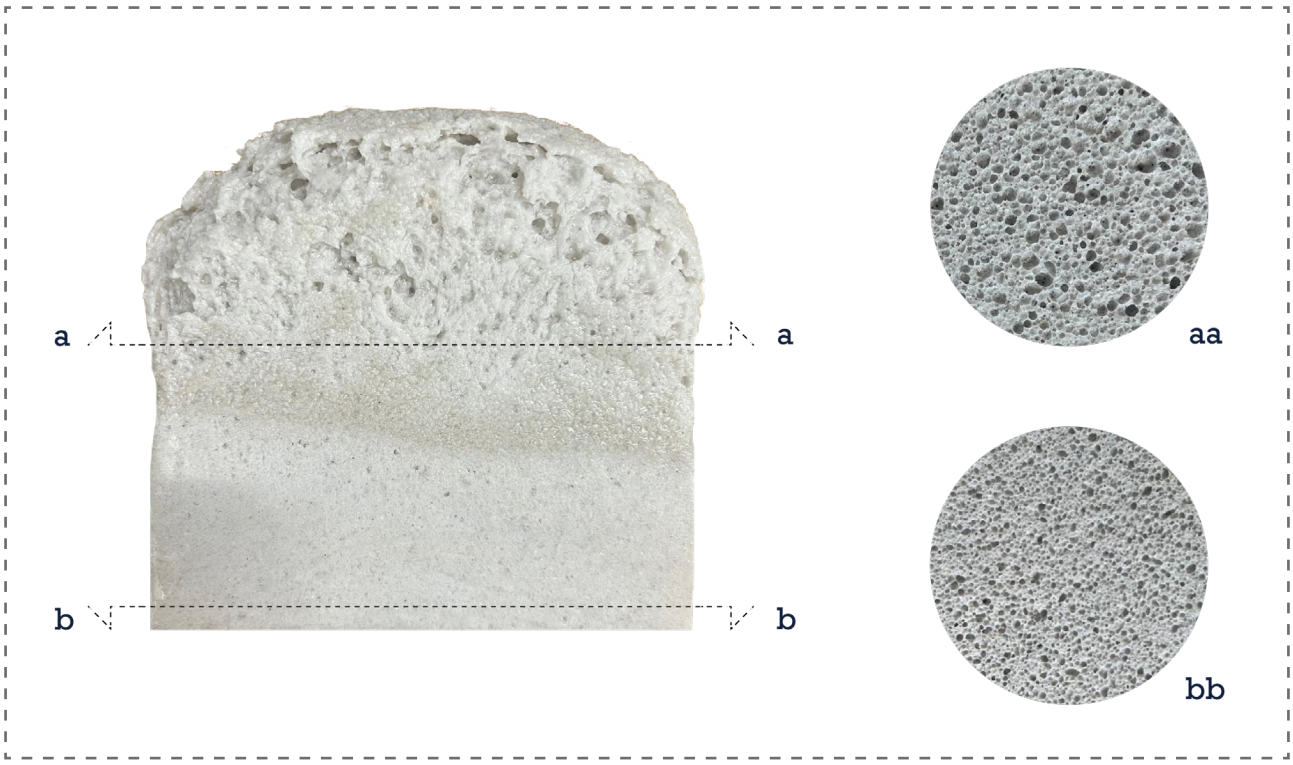

Fig. 3.23. Variation in pore size within a single sample, depending on the height of the section. Pores are typically smaller near the surface - where expansion is constrained by the mould - and larger in areas where the mixture was able to foam and expand freely outside the mould.

Other findings

Mixing different foaming agent concentrations

An experiment was conducted to explore the effect of mixing two foaming mixtures with different foaming agent concentrations. A 50/50 mixture was prepared, combining one batch with 2.5 wt% calcium carbonate and another with 5 wt% calcium carbonate, using low iron soda lime cullet as the base material in both cases.

In the sample shown on the left in Figure 3.24, the 2.5% mixture was placed at the bottom of the mould, with the 5% mixture layered on top. In this configuration, the bottom part did not foam at all, and a clear line is visible where the upper, higher-concentration mixture began to foam.

In contrast, when the arrangement was reversed - with the 5% mixture at the bottom and the 2.5% mixture on top (sample on the right in Figure 3.24) - both parts foamed. A transition is visible between the two layers, although the separation line is less distinct than in the first sample.

Initially, the lack of foaming in the bottom layer was suspected to be an error. However, a second firing under the same conditions produced identical results, confirming that the issue was related to the material behaviour rather than a mistake.

These results suggest that simply mixing different concentrations is not sufficient to achieve a gradient in porosity. However, layering, with the higher concentration at the bottom, may offer a more reliable approach, though further investigation is needed to understand the mechanisms behind these results.

Cracks

Some samples developed wrinkle-like cracks on their surfaces, resulting in a very irregular and rough texture, likely due to only partial foaming. These defects appeared mostly in samples made with larger glass particles - this could be caused by an uneven distribution of the foaming agent, or possibly because in such cases, foaming may have occurred only in areas where the particles were small enough to allow it. These samples have a stone-like finish, as shown in Figure 3.25.

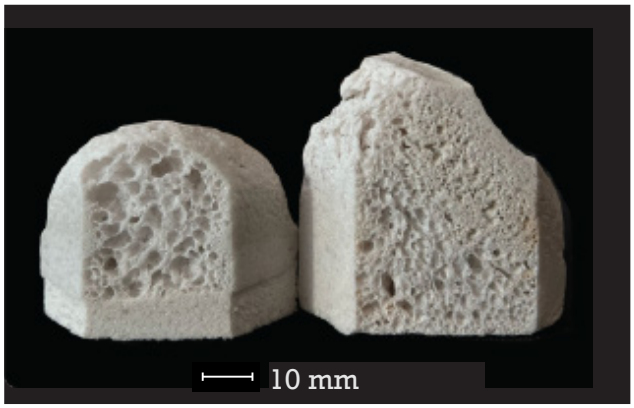

Fig. 3.24. Samples made from low-iron soda lime glass with mixed foaming agent concentrations, combining 2.5 wt% and 5 wt% mixtures; Left: 2.5% concentration at the bottom, 5% at the top; Right: 5% concentration at the bottom, 2.5% at the top.

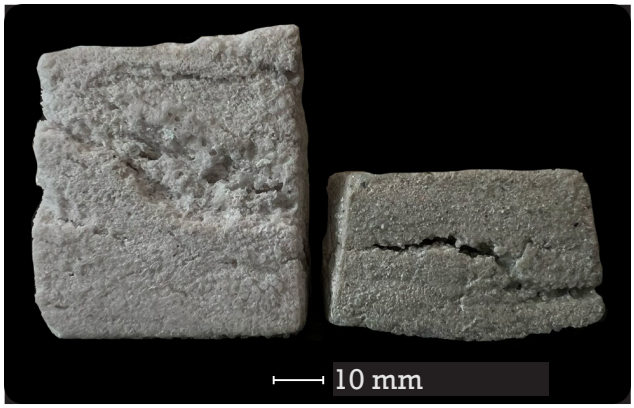

Fig. 3.25. From the left: SL10CCT1 and AM5CCT1. Horizontal cracks are visible on both samples. Additionally, shrinkage is observed on the automotive glass sample (AM5CCT1).

3.3. Fusing

After successfully developing porous samples through foaming, the next phase of the research focused on integrating these with a solid glass layer to form a structurally stable, hybrid panel. This dual-layer configuration aimed not only to preserve the sound-absorbing qualities of the porous glass but also to enhance mechanical performance for architectural application. Additionally, the solid layer was expected to contribute acoustically by functioning as a reflective surface, complementing the absorptive behaviour of the foam. Two fusing strategies were investigated: one involving the bonding of pre-foamed samples to flat glass, and another combining foaming and fusing in a single firing process. The following subsections present each approach and assess their feasibility and results.

3.3.1. Two-step fusing: bonding foamed samples to flat glass

Fusing is a heat bonding technique used to join glass elements together. It plays an important role in this research, as the panels require a solid layer for both mechanical rigidity and their dual functional nature (sound absorption versus reflection). An ideal solution is to tack fuse the layers, rather than using adhesives, in order to allow easier panels' recycling in the future.

While extensive research exists on glass fusing in general, little work has been done on fusing porous glass with solid float glass pieces. Some guidelines were available to follow, but a critical requirement for this project was that the fusing process needed to bond the glass layers at a molecular level without changing or destroying the pore structure, which is essential for maintaining the acoustic performance of the panels.

Several fusing firing schedules were tested, experimenting only with selected types of porous glass. An overview of these fusing experiments is presented in Figure 3.27.

First, fusing was attempted during the foaming of other samples, using firing schedule 2 (790 °C with two hours dwell time), the same schedule as used for foaming samples. Soda lime and light bulb porous panels were fused with a solid low-iron soda lime glass piece.

Next, a lower temperature of 705°C for one hour was tried, following recommendations presented in the literature review. Again, soda lime and light bulb porous layers were fused with a low-iron soda lime solid piece.

Finally, an even lower firing schedule of 600°C for 1 hour was tested to fuse soda lime, light bulb, and Cyclon mix porous layers with low-iron soda lime solid pieces.

3.3.2. Single-step fusing: simultaneous foaming and bonding

Alternative approach tested was placing the solid layer of glass and the foaming mixture together in one mould, so that in the same firing cycle the glass would foam and fuse with the solid layer. This was tested either by placing a whole pane of glass (cut to the size of the mould) or by placing glass cullet at the bottom of the mould as presented in Figure 3.26. However, this method with cullet would probably be less effective structurally, as the connections between individual glass pieces create weak points in the panel.

Generally, single step fusing can help to save both energy and time since the whole panel can be manufactured in only one firing cycle.

Fig. 3.26. Glass placed at the bottom of the mould to serve as the base layer for the foaming glass; a) Soda lime glass, later covered with foaming mixture, b) Mixed cullet, manually selected to include wiring and colorful glass pieces, then covered with foaming mixture, c) Mixed cullet, covered with foaming mixture (without manual selection)

max temp./ dwell time		elements fused		results
		foam glass piece	solid layer	
790°C	2h	low-iron soda lime	low-iron soda lime	layers fused, pore structure remained unchanged
			light bulbs	LB piece melted, pore structure was damaged
705°C	1h	low-iron soda lime	low-iron soda lime	layers fused, pore structure remained unchanged
			light bulbs	layers fused, pore structure remained unchanged, slumping occured
600°C	1h	low-iron soda lime	low-iron soda lime	neither bonding nor change in shape occured
			light bulbs	
			Cyclon mix	

Fig. 3.27. Fusing experiments overview, own work

3.3.3. Fusing results interpretation

The experiments demonstrated that the success of fusing porous glass with float glass depends significantly on the firing temperature and the type of porous material used.

At 790 °C, soda lime porous glass fused successfully without damaging the pore structure, but light bulb porous panels collapsed due to remelting.

At a reduced temperature of 705 °C, both soda lime and light bulb porous layers fused successfully without compromising their porous structure, making it the most suitable firing schedule for delicate porous glasses.

At 600 °C, no bonding occurred between any of the tested materials, indicating that this temperature was too low for effective bonding.

The approach of fusing and foaming simultaneously showed promising results presented in Figure 3.28. Using cullet provided visually interesting effects, but most likely compromised the structural integrity of the panels due to weak connection points between glass fragments. Using a single, continuous glass sheet resulted in strong, uniform bonding of the layers.

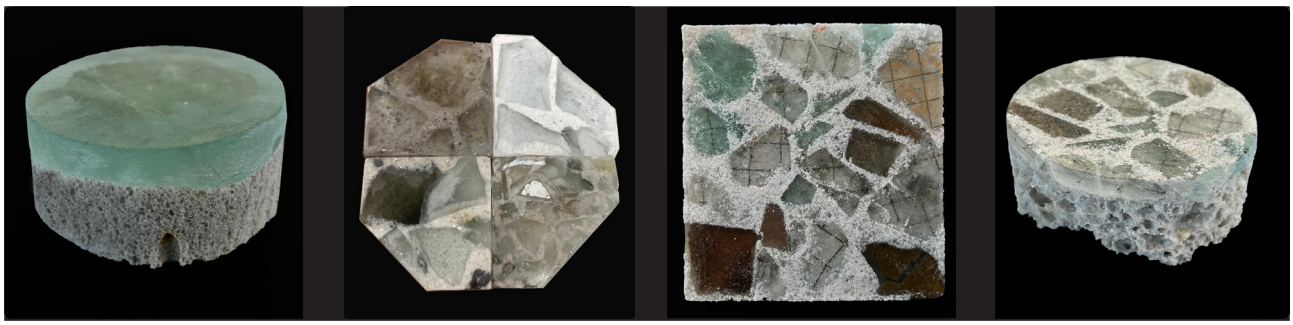

Fig. 3.28. Samples fused with solid glass during the same firing process as the foaming; a) Surface of mixed cullet placed at the bottom of the mould; a) Sample for impedance tube testing: foamed light bulb glass fused with solid pane of 10 mm float glass placed at the bottom of the mould; b) Test samples with soda lime cullet or mixed glass cullet at the bottom of the mould, resulting in a mosaic-like aesthetic, c), d) mixed cullet at the bottom covered with the foaming mixture with light bulbs glass

3.3.4. Summary of experimental work with glass

The experimental phase confirmed the feasibility of repurposing various types of glass waste, particularly soda-lime, light bulb glass, and mixed cullet, into porous structures. The foaming process proved to be highly sensitive to manufacturing parameters, including the type of glass and foaming agent used, particle size, and the firing schedule. In general, increasing the amount of foaming agent resulted in larger pores for low-iron soda lime and mixed cullet, whereas light bulb glass showed the opposite trend.

Across all glass types, higher firing temperatures consistently led to the formation of larger pores. The most promising and controllable results were achieved with soda-lime glass in combination with either calcium carbonate or eggshells. Low-iron soda lime glass, in particular, exhibited high sensitivity to the amount of foaming agent added. Light bulb glass, tested only with eggshells, also produced satisfactory results - this combination led to larger pores than other glass types. However, in this case, pore size was more effectively controlled through firing temperature than by adjusting the foaming agent concentration, unlike clear soda lime with calcium carbonate, where both variables had clearer effects.

Pure calcium carbonate and eggshells, even though they are almost the same material, showed notably different results with eggshells resulting in more homogenous, even pores structure. Notably, powdered glass cullet foamed most effectively, and higher foaming agent concentrations generally produced larger pores, although this was also influenced by the glass type and firing temperature.

Fusing experiments demonstrated that a tack fusion of porous and float glass is achievable without compromising the pore structure, particularly at 705 °C with one hour dwell time. Simultaneous foaming and fusing in a single firing cycle also proved successful with both cullet pieces on the bottom of the mould or the whole glass pane.

Collectively, the foaming and fusing experiments highlight fabrication challenges of recycled glass panels. The findings provide a strong foundation for further development of elements that combine porosity for sound absorption with structural solidity for architectural integration.

3.4. Acoustic testing

To evaluate the acoustic performance of the developed foam glass samples, a series of standardized sound absorption measurements was conducted. Given the experimental scale and material constraints, the impedance tube method was selected for its precision, repeatability, and minimal sample size requirements. This approach enabled the systematic comparison of different glass compositions, foaming agents, and firing schedules. The following section outlines the measurement procedure and presents the results of the acoustic tests, which served as the basis for further simulation and design integration.

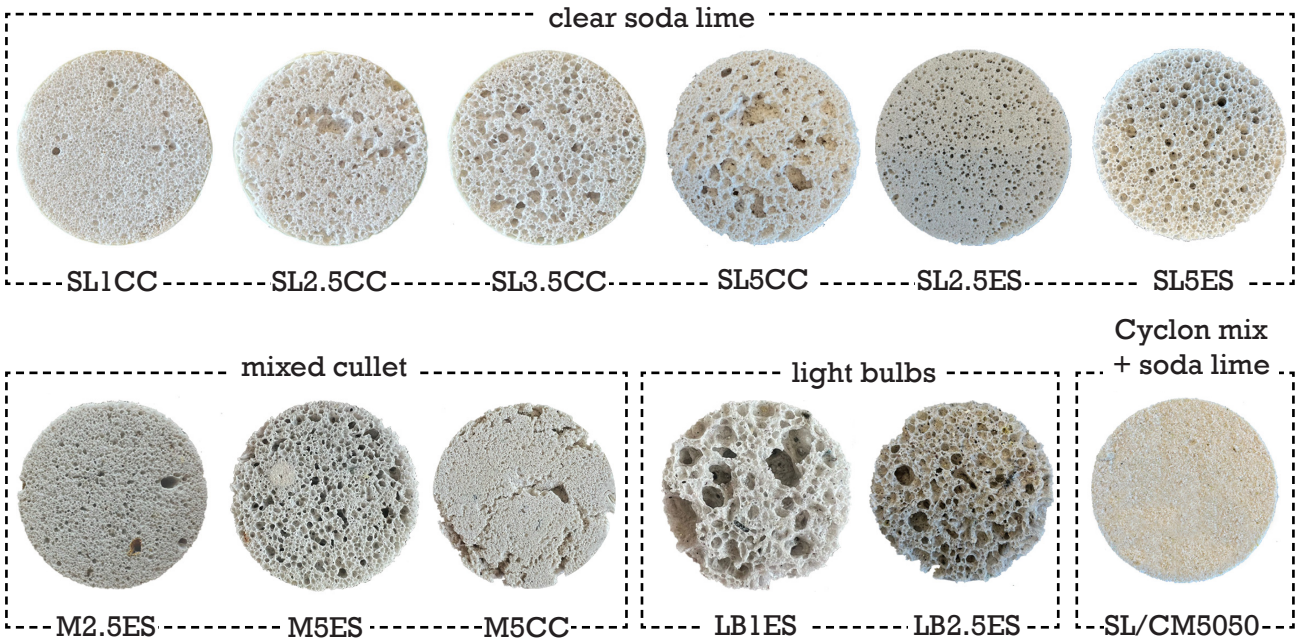

Fig. 3.29. Samples chosen to be remade in larger size so that circular specimens could be cut out for impedance tube testing.

3.4.1. Impedance tube measurements procedure

The impedance tube is a device used to measure a material's acoustic impedance and sound absorption coefficient (SAC). It can also determine the reflection coefficient and impedance. This method is especially well-suited for testing new materials, as it requires only a small sample - unlike measurements performed in anechoic chambers or reverberation rooms. The impedance tube setup consists of a speaker positioned at one end of the tube and two microphones placed along the tube's length. These microphones record the sound pressure level before and after the sound wave interacts with the sample. The final result is derived by comparing these two measurements.

In order to assess the SAC accurately, the samples must fit tightly within the tube, requiring them to be cut to precise dimensions. The impedance tube setup allows measurement of SAC up to 6400 Hz. For frequencies between 50–1600 Hz, the main body of the tube is used, requiring samples with a diameter of 10 cm. To measure higher frequencies, an extension tube is mounted, and samples must then be smaller, with a diameter of 2.9 cm. Both types of samples tested were 3.5 cm thick.

For each batch of samples, measurements at lower frequencies were performed first. Afterwards, the same sample was cut to smaller dimensions using a waterjet cutting machine to ensure that the small-diameter sample matched the original as closely as possible, saving both time and material.

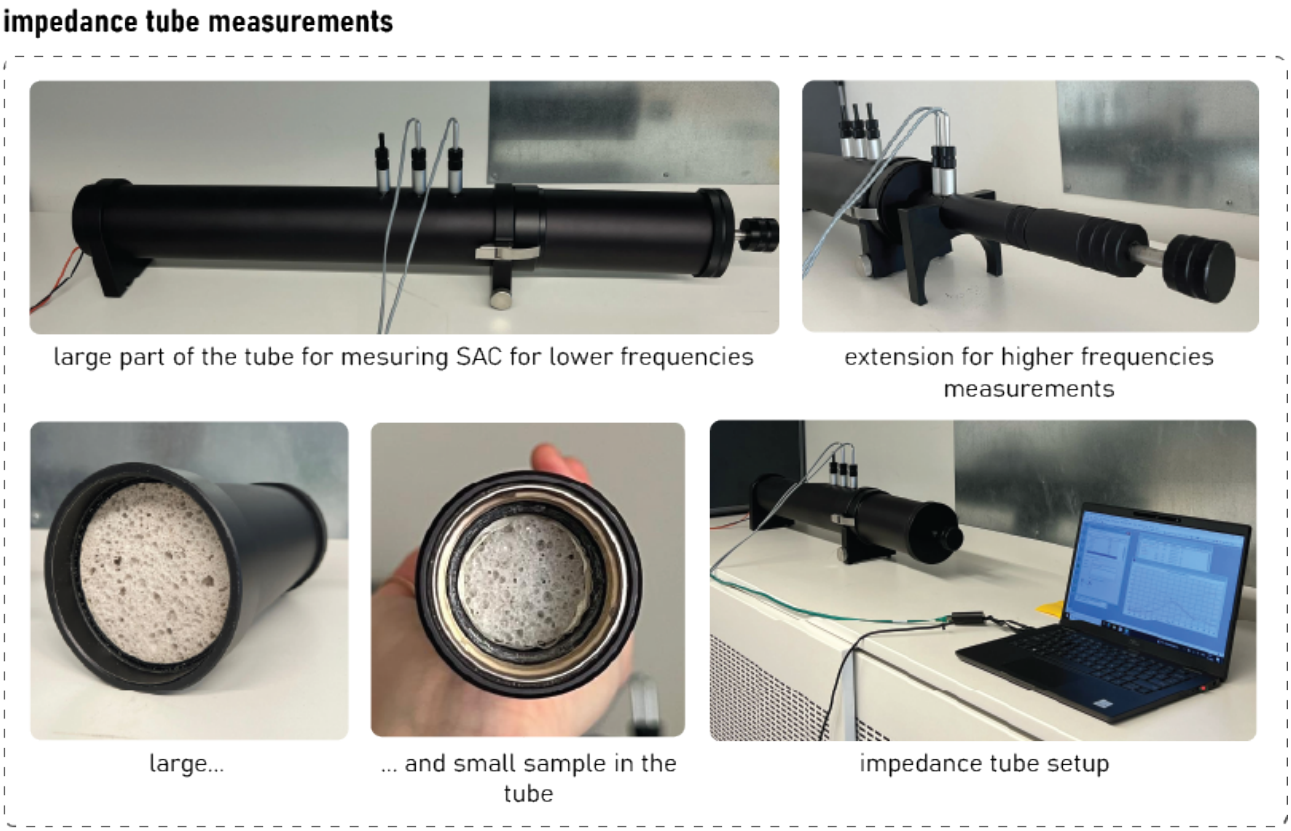

Fig. 3.30. Impedance tube setup used for measuring the sound absorption coefficient (SAC) of glass samples. The system includes a large-diameter tube for low-frequency measurements and an extension for higher frequencies. Both large and small cylindrical samples were tested by inserting them into the tube. The setup was connected to a laptop for data collection and analysis.

3.4.2. Results interpretation

Thirteen samples depicted in Figure 3.29 were tested using the impedance tube, each varying in glass type, foaming agent, and its concentration. The firing schedule was kept constant during this phase of the experiment: all samples manufactured for acoustic testing were fired using firing schedule 2 (maximum temperature of 790°C with dwell time of two hours), being the lower of the two effective firing temperatures tested earlier.

The results showed that different samples exhibited varying SACs across the tested frequency range. Most samples displayed a peak SAC at a specific frequency, where sound absorption was particularly high. This sharp peak may not have been expected, but it aligns with the general understanding that materials rarely offer high absorption across the entire frequency spectrum. The frequency at which this peak occurs varies between samples.

The SAC was recorded every 2 Hz up to 1600 Hz, and every 4 Hz from 1600 Hz onward. In typical acoustic analysis, SAC is not reported with such a fine resolution; instead, results are commonly presented in standard octave bands. To align with this convention, the raw data was converted into SAC values for the 125, 250, 500, 1000, 2000, and 4000 Hz octave bands. The full set of absorption coefficient results for all the samples is shown in Figure 3.31.

As discussed in the literature review, the sound absorption mechanism of porous absorbers relies on microscopic friction between air particles and the internal pore surfaces. Because of this interaction, the energy of the sound waves is converted into heat as they travel through the material. According to (Cox & D'Antonio, 2017), the SAC curve of a typical porous absorber follows a characteristic shape: low absorption at low frequencies that gradually increases with frequency, often reaching high absorption at higher frequencies. This is because higher frequencies have

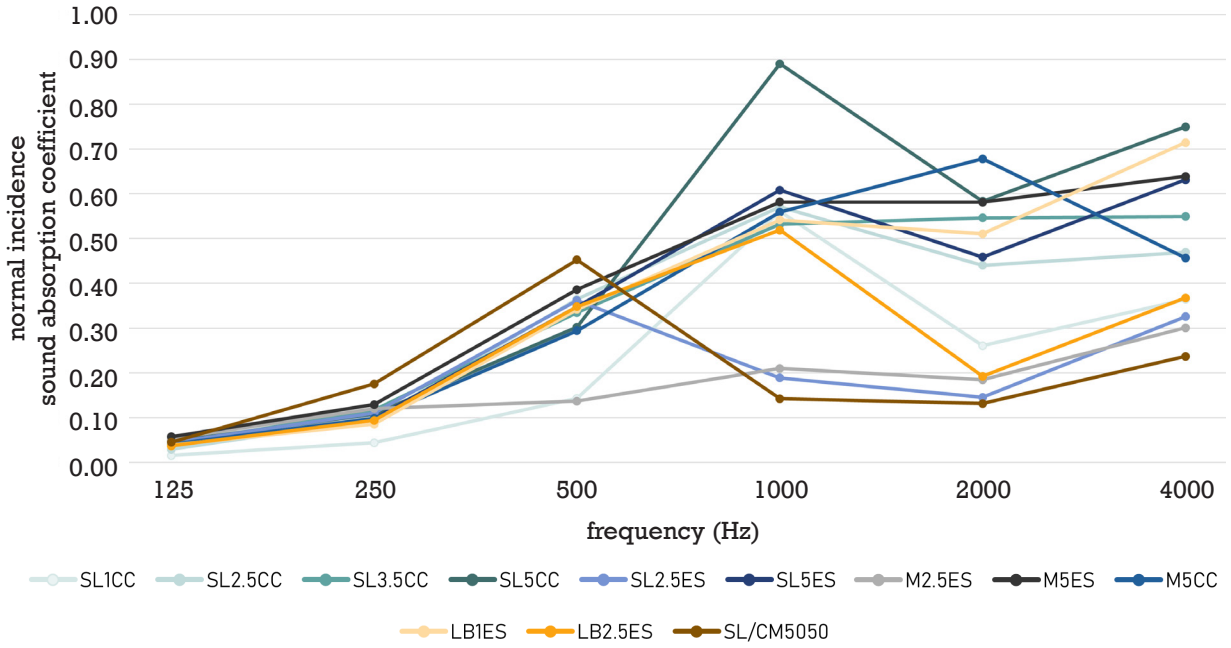

Fig. 3.31. Sound absorption coefficients of all tested glass foam samples, presented in standard octave bands. Raw measurements were recorded at 2 Hz intervals up to 1600 Hz and at 4 Hz intervals beyond, then averaged into octave bands to align with conventional acoustic reporting standards: 125 Hz (88-177 Hz), 250 Hz (177 – 355 Hz), 500 Hz (355 – 710 Hz), 1000 Hz (710 – 1420 Hz), 2000 Hz (1420 – 2840 Hz) and 4000 Hz (2840 – 5680 Hz)

shorter wavelengths, which makes it easier for sound waves to penetrate the material.

On the other hand, resonant absorbers display a different absorption pattern. They function as mass-spring systems, where a vibrating mass (such as a membrane or air plug) oscillates against an elastic element, typically a volume of trapped air and they are typically more effective at lower frequencies, with distinct peaks at specific values known as resonant or natural frequencies - the points at which the mass-spring system resonates.

None of the tested samples showed a SAC curve typical of purely porous absorbers (Figures 3.32 - 3.39). Instead, they exhibited irregular patterns with noticeable peaks and dips across frequencies, more characteristic of resonant behaviour. In the case of the manufactured samples, the pores within the glass likely act as cavities. The air trapped in these cavities behaves like a spring, while the air mass in the neck vibrates in response to incident sound waves. These mass-spring systems resonate at specific frequencies, accounting for the peaks observed in the absorption curves.

However, unlike typical resonant absorbers, the peaks are broader, indicating that the material also exhibits porous absorption characteristics. This suggests that sound absorption in the manufactured samples results from a combination of both porous and resonant mechanisms.

This hybrid behaviour is characteristic of a lumped mass-spring system, where the pore network contributes to resonant behaviour, while friction between air and pore surfaces leads to thermal-viscous losses. As a result, the peaks are broader and less sharp and the absorption is distributed across a wider frequency range, producing the irregular SAC profiles observed in the graphs (M.J. Tenpierik, personal communication, May 2025).

Soda lime

Six soda lime glass samples were tested in the impedance tube, each using different concentrations of calcium carbonate or eggshells as the foaming agent.

For the soda lime and calcium carbonate combination, sound absorption begins to be effective (SAC exceeds 0.2) at around 300 Hz (Figure 3.32). The sample SL1CC (1 wt% CC) showed two absorption peaks: one at approximately 850 Hz with a SAC of 0.7, and another reaching 0.6 at around 3600 Hz. SL2.5CC (2.5 wt% CC) exhibited its main peak slightly earlier, with a SAC of 0.6 around 680 Hz. After a brief dip, the SAC climbed again to 0.6 near 1700 Hz. SL3.5CC (3 wt % CC) followed a similar pattern to SL2.5CC, though its peaks occurred at slightly higher frequencies: it reached about 0.6 SAC at around 900 Hz and nearly 0.7 around 1800 Hz. The highest concentration sample, SL5CC (5 wt % CC), demonstrated the most effective sound absorption overall. It reached a SAC of 1 at around 850 Hz, dropped around 1600 Hz, and then climbed again to approximately 0.95 at 3000 Hz. While there are some frequency ranges where this trend does not hold, the general pattern indicates that increasing the foaming agent concentration tends to enhance sound absorption, likely due to the formation of larger or more interconnected pores.

A similar trend was observed in the samples made from low iron soda lime glass with eggshells as the foaming agent. Two samples were tested: SL2.5ES and SL5ES (with 2.5 and 5 wt% eggshells, respectively). As seen in Figure 3.33, the sample with the higher eggshell content (SL5ES) consistently exhibited better sound absorption across most of the frequency range. SL5ES clearly outperformed SL2.5ES, reaching a peak SAC of 0.73 around 820 Hz, dipping near 1500 Hz, and rising again to approximately 0.7 at 3500 Hz.

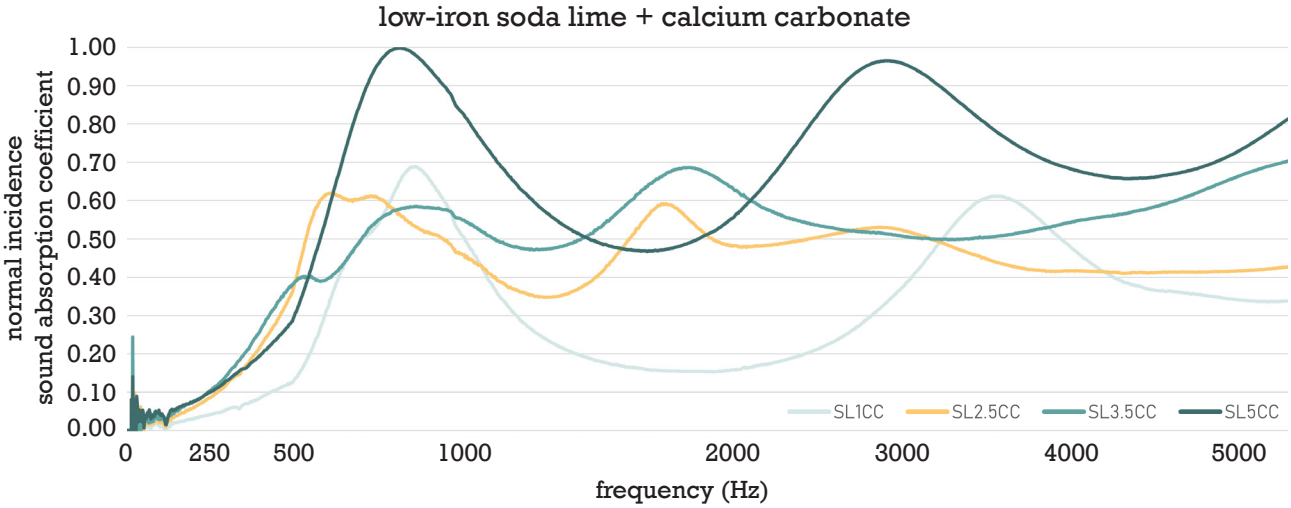

Fig. 3.32. Impedance tube measurement results for soda lime glass waste samples foamed with calcium carbonate. The results show a clear trend: increasing the amount of foaming agent (which led to larger pores in soda lime glass) improves sound absorption. The SL5CC sample exhibited the highest sound absorption coefficient of all tested samples, approaching a value of 1 at both ~1000 Hz and ~3000 Hz. Notably, 1000 Hz is a particularly relevant frequency, as it lies within the core range of both orchestral sound and human speech.

Mixed glass cullet

Mixed glass cullet samples were tested with both calcium carbonate and eggshells as foaming agents. The sample with 5 wt% eggshells (M5ES) showed the best overall acoustic performance above 1500 Hz, and featured a sharp SAC peak of 0.83 around 600 Hz. The calcium carbonate sample (M5CC) performed similarly up to 500 Hz and reached a SAC of 1 near 1100 Hz, but its performance dropped off at higher frequencies, falling below that of M5ES.

In contrast, the sample made with 2.5 wt% eggshells (M2.5ES) did not exhibit absorptive behaviour below 2000 Hz, as its SAC remained below 0.2. Beyond 2000 Hz, the absorption improved slightly but did not exceed a SAC of 0.38, with the peak occurring around 4200 Hz.

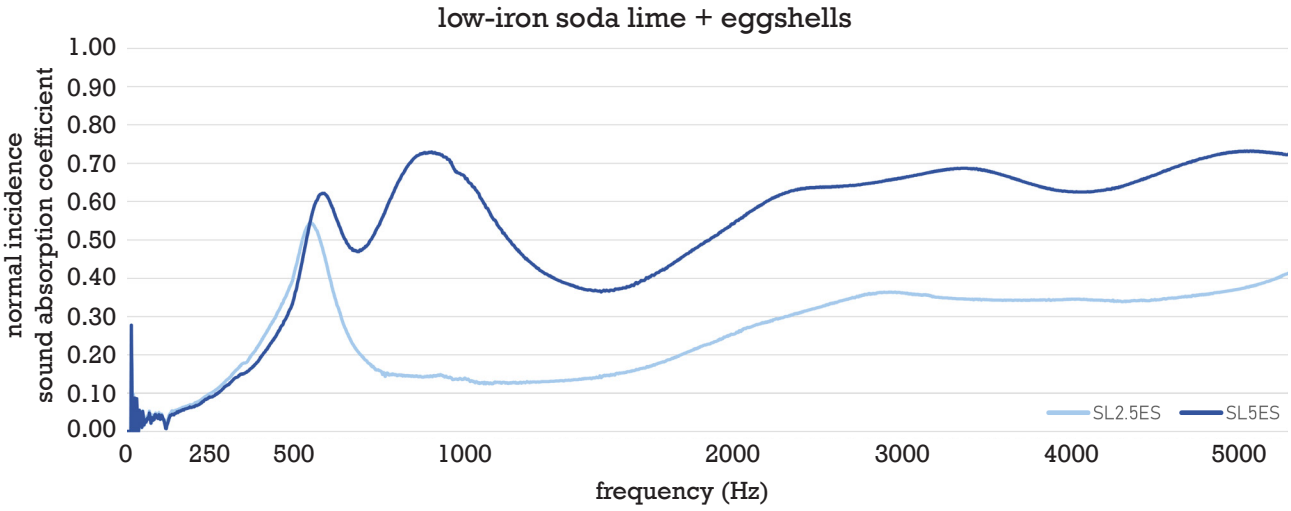

Fig. 3.33. Impedance tube measurement results for soda lime samples foamed with eggshells. Both samples showed similarly low performance below 500 Hz. At higher frequencies, as with calcium carbonate, the sample with more foaming agent – resulting in larger pores – demonstrated improved sound absorption.

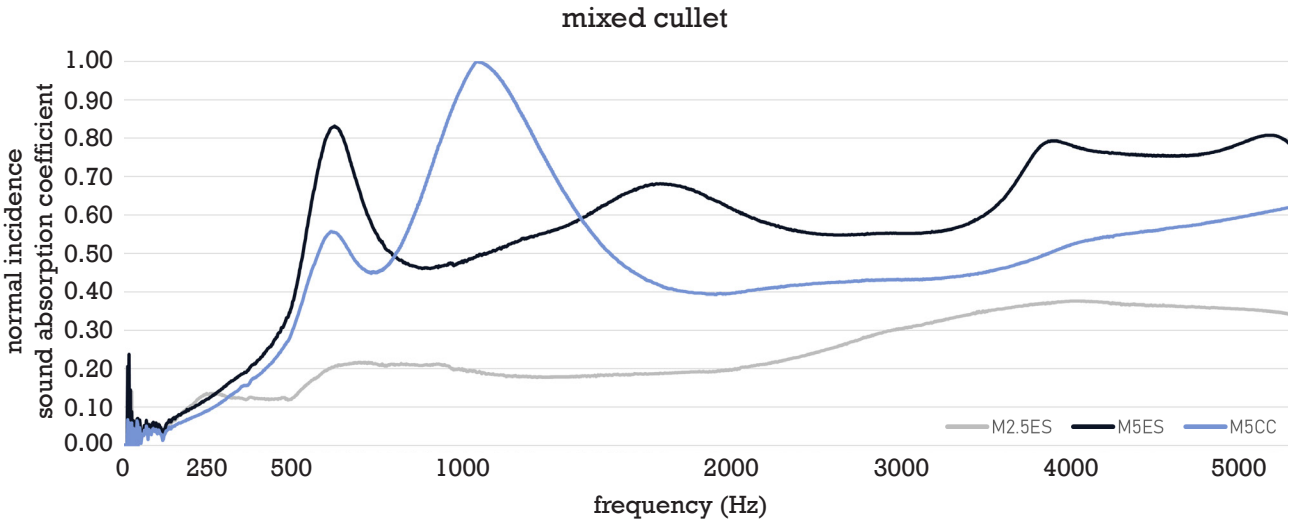

Fig. 3.34. Impedance tube measurement results for samples made with mixed, highly contaminated glass cullet. The chart compares two samples foamed with eggshells (M2.5ES and M5ES) and one with pure calcium carbonate (M5CC). M5CC shows the best performance around 1100 Hz, reaching a SAC close to 1. The M5ES sample slightly outperforms it above 1500 Hz, while the M2.5ES sample, with the lowest foaming agent content, performs poorly across all frequency ranges.

Light bulbs

Two samples made from light bulb glass were tested for their SAC, incorporating 1 wt% and 2.5 wt% of eggshells as the foaming agent, respectively. The results of this test are presented in Figure 3.35. Both samples exhibited similar SAC values up to approximately 700 Hz, where they reached a peak of around 0.8. Beyond this point, the sample with 1 wt% eggshells (LB1ES) demonstrated better acoustic performance compared to the one with 2.5 wt% (LB2.5ES). This suggests that, in the case of light bulb glass, a lower foaming agent concentration resulted in more favorable porosity for sound absorption. These findings are consistent with earlier observations, where larger pores contributed to improved acoustic performance. However, unlike low-iron soda lime glass, in the case of light bulb waste, lower foaming agent content lead to larger pores.

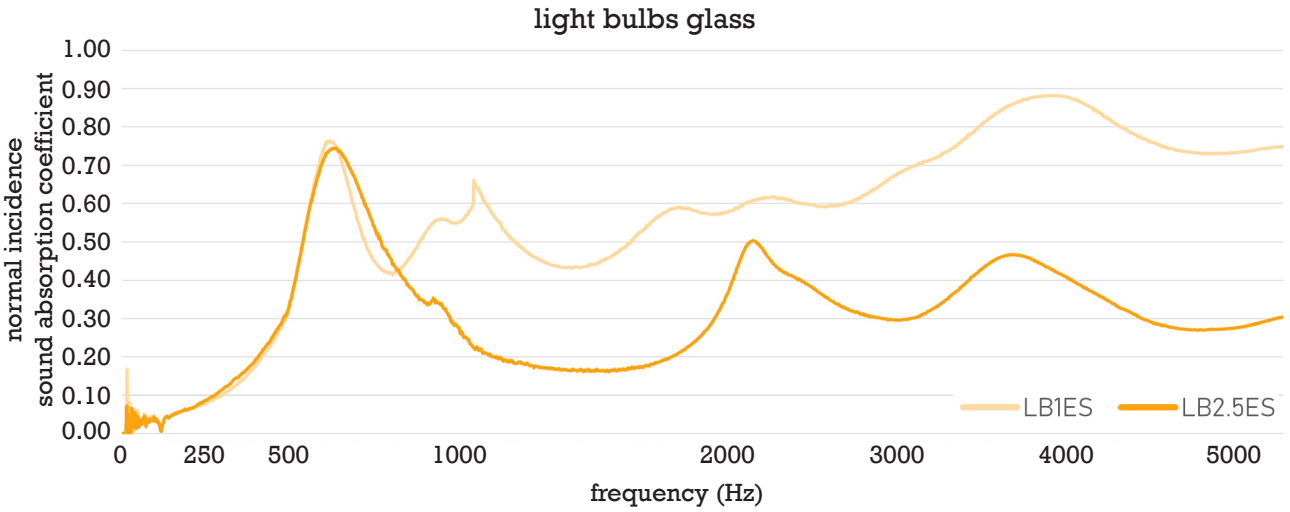

Fig. 3.35. Impedance tube comparison of light bulb and eggshell samples. Unlike the clear soda lime and mixed cullet series, the sample with a lower foaming agent content (LB1ES) achieved a higher sound absorption coefficient, likely due to the formation of larger pores compared to samples with 2.5 wt% foaming agent (LB2.5ES).

Cyclon mix

The Cyclon mix was tested in only one sample, combined in a 50/50 ratio with clear low-iron soda lime cullet. Attempts to use Cyclon mix alone, or in a 20/80 ratio with soda lime glass, resulted in extremely brittle samples that crumbled easily and therefore were not suitable for acoustic testing. As noted earlier, this type of glass did not foam in the conventional sense but was still clearly porous.

Among all the tested samples, this one was the densest and demonstrated the best sound absorption performance at the lowest frequencies. It reached its peak SAC of 0.6 at around 500 Hz. After that, the SAC dropped significantly to 0.15 around 800 Hz, then gradually increased again with frequency like pure porous absorbers, reaching approximately 0.35 by the end of the tested range (Figure 3.36).

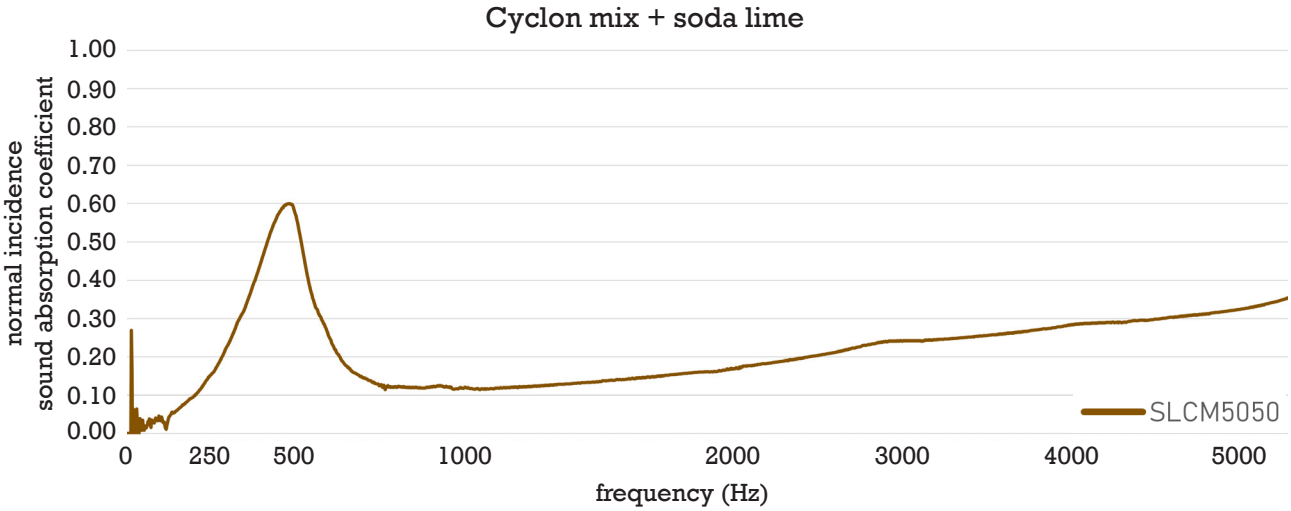

Fig. 3.36. Impedance tube results for the only tested sample made with Cyclon mix, combined in a 50:50 ratio with clear soda lime cullet due to its brittleness and limited foaming capacity. The sample showed the highest sound absorption coefficient at low frequencies (~500 Hz), but significantly lower performance at higher frequencies.

Type of glass vs sound absorption

Samples made with different glass types but the same amount of foaming agent (SL2.5ES, M2.5ES, LB2.5ES) were compared to assess how glass composition affects sound absorption (Figure 3.37). Up to around 600 Hz, the performance of low-iron soda lime (SL2.5ES) and light bulbs glass (LB2.5ES) samples is very similar. Beyond that point, up to approximately 1000 Hz, the sample made from light bulb glass demonstrated the highest sound absorption performance among all tested materials. This sample also exhibited the largest pore sizes. Notably, the light bulb glass was heavily contaminated, containing fragments of metal and plastic that were milled together with the glass in its received state. Despite this, its strong acoustic performance suggests that such contamination does not significantly impair the material's sound-absorbing behaviour.

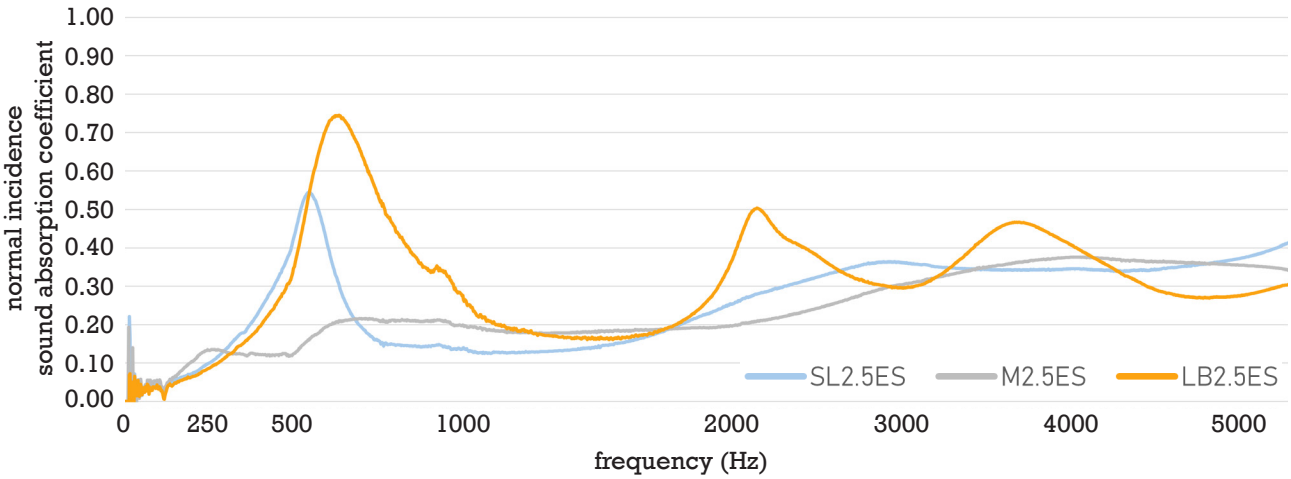

Fig. 3.37. Graphs showing the SAC of samples produced with the same amount of foaming agent but different types of glass waste. While the overall performance is similar across samples, light bulb glass shows slightly better absorption between 500–1000 Hz and around 2200 Hz.

To further investigate the impact of contamination in glass on sound absorption, two samples were compared, both manufactured using the same type and concentration of foaming agent (5 wt% of calcium carbonate), but differed in the quality of glass cullet used (Figure 3.38). One sample employed low-iron soda lime glass, considered the cleanest cullet available, while the other utilized a highly contaminated cullet mix containing fragments of other glass types (such as CRT panel glass), metal, plastic, and rubber inclusions. Both samples demonstrated excellent performance

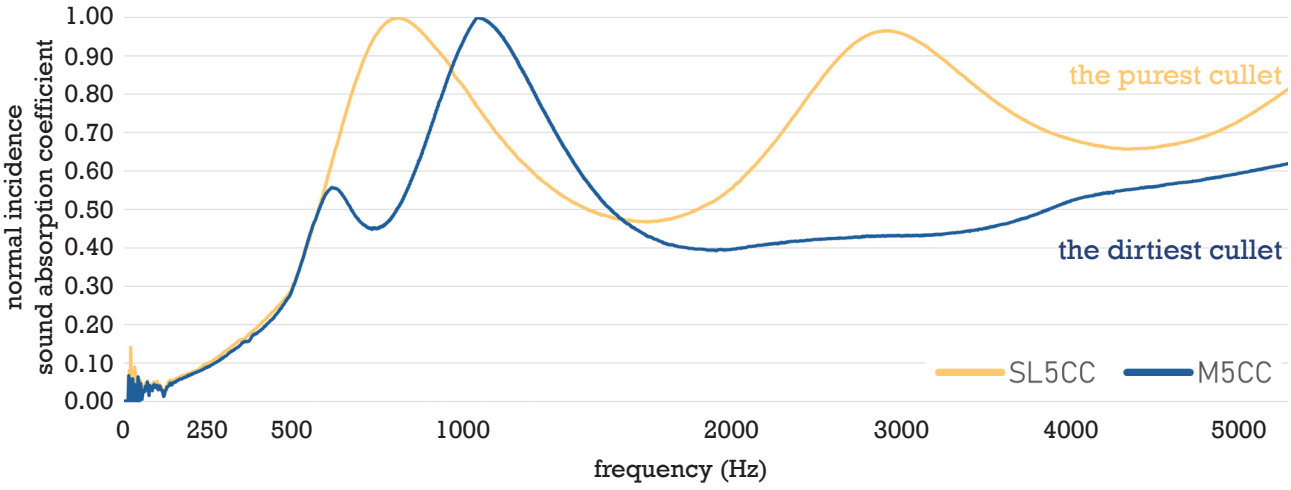

Fig. 3.38. Graphs showing SAC of samples made with the same foaming agent amount but different glass types: the cleanest (SL5CC) and a highly contaminated one (M5CC). Both reach SAC ≈ 1, suggesting contamination does not hinder absorption, though only the clean sample shows a secondary peak.

around 1000 Hz, with SAC approaching 1. This may suggest that contamination does not significantly impair sound absorption at mid-range frequencies. However, at higher frequencies, the sample made from clean cullet exhibited a second peak in SAC, which was not present in the contaminated sample. This difference could potentially be due to contamination. Nonetheless, as this observation is based on a comparison of only two samples, further testing would be necessary to confirm any definitive conclusions.

Eggshells and pure CC comparison

This section focuses specifically on comparing the performance of eggshells (ES) versus pure calcium carbonate (CC) as foaming agents regarding sound absorption. Samples made with the same type of glass but using different forms of the foaming agent were analyzed: SL2.5CC and SL5CC were compared with SL2.5ES and SL5ES, each at 2.5 wt% and 5 wt% concentrations (Figure 3.39).

In both cases, samples using pure CC consistently demonstrate better sound absorption. For the 5 wt% samples (b), the difference becomes particularly noticeable at frequencies above 2000 Hz. For the 2.5 wt% samples, the CC-based sample performs better than the ES-based one across nearly the entire tested frequency range. Nonetheless, the overall trend is clear: samples foamed with pure CC show better sound absorption characteristics.

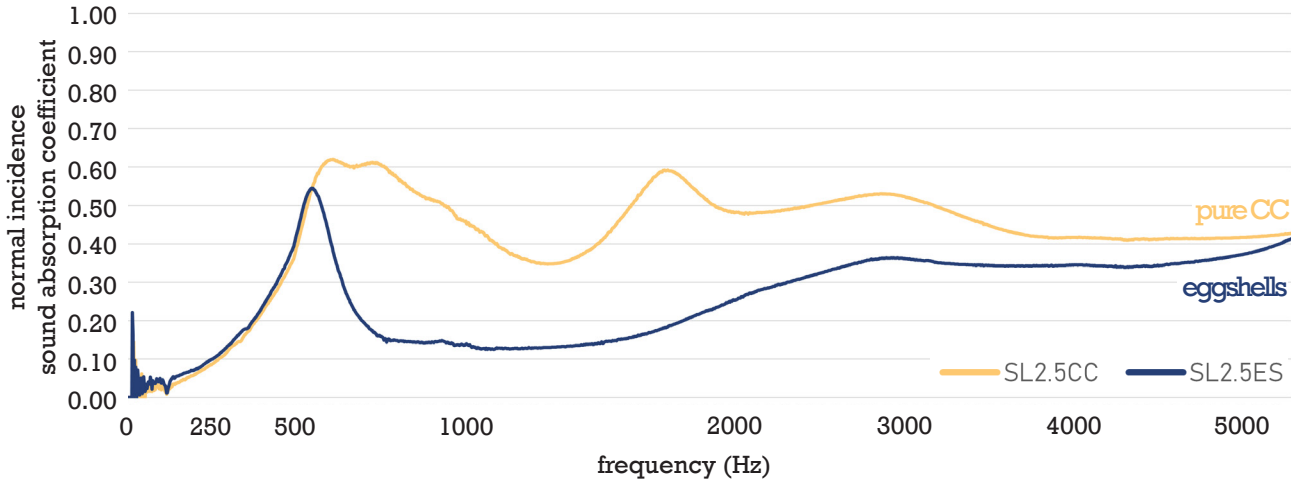

a)

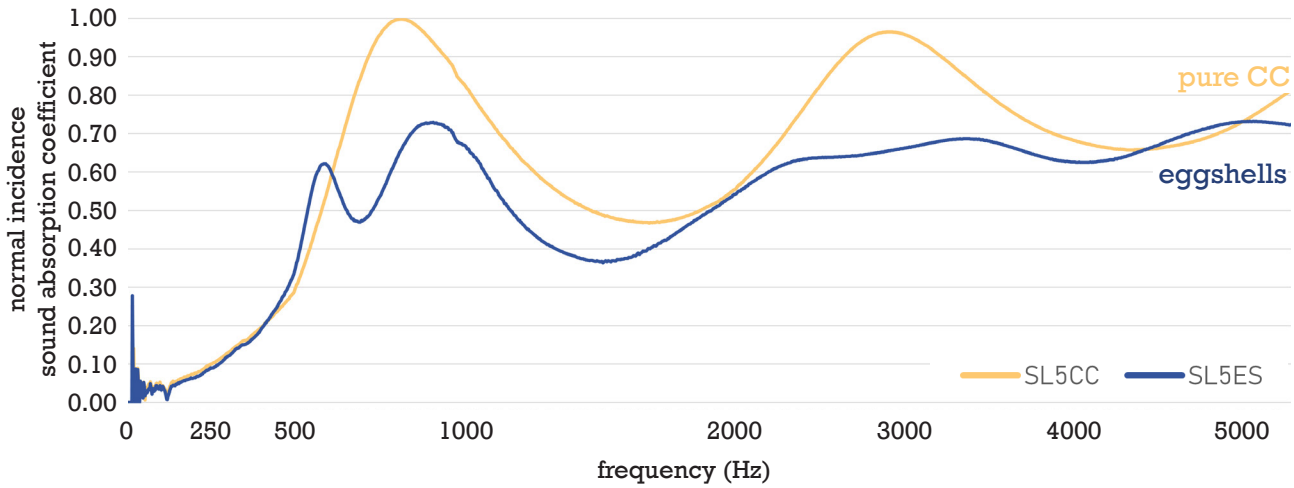

b)

Fig. 3.39. Graphs illustrating the difference in SAC between samples manufactured using the same process and glass type, differing only in the form of the foaming agent - eggshells versus pure calcium carbonate; a) Low-iron soda lime glass with 2.5 wt% foaming agent, b) Low-iron soda lime glass with 5 wt% foaming agent

This difference aligns with observations from the manufacturing process, where samples made with pure CC developed a rougher, more tortuous pore structure that penetrated deeper into the material. This complex internal structure enhances acoustic performance by increasing the path length for sound waves and thus the potential for sound energy loss through friction.

1-layer vs 2-layer samples

fused

Most samples in this study were tested in a single-layer configuration, consisting only of the porous foamed glass layer. However, since the final panel design requires fusing a rigid solid glass layer to the porous one, it was important to investigate whether, and how, this influences acoustic performance.

As presented in Figure 3.40, the SAC values for single-layer and double-layer samples are generally comparable. This is particularly evident at lower frequencies (125 Hz and 250 Hz), where both configurations exhibit poor absorption performance. At higher frequencies, slight differences can be observed: the SAC of the double-layer LB1ES sample is minimally higher, while that of the M5ES sample is slightly lower. However, these deviations are negligible and fall within a margin that does not indicate a significant shift in acoustic behaviour.

The most notable difference is observed in the M5CC sample at 2000 Hz, where the single-layer configuration shows approximately twice the SAC compared to its double-layer version. Despite this variation, the overall comparison suggests that the fusing process used to join the solid and porous glass layers does not meaningfully deteriorate the acoustic performance. Visual inspection of the fused samples supports this conclusion, as the pore structure described before in the report, remains mostly unchanged.

glued

In addition, four experiments were conducted to compare single-layer versus double-layer samples, joined using adhesive. Although this approach deviates from the previously stated goal of avoiding adhesives through fusing, it was included as a supplementary investigation.

The results presented in Figure 3.41 indicate that the performance of single- and double-layer samples was largely comparable, with the latter occasionally exhibiting slightly improved absorption. It is important to note, however, that these tests were carried out using only the small impedance tube, meaning that the results are reliable only within the 1600–6400 Hz frequency range.

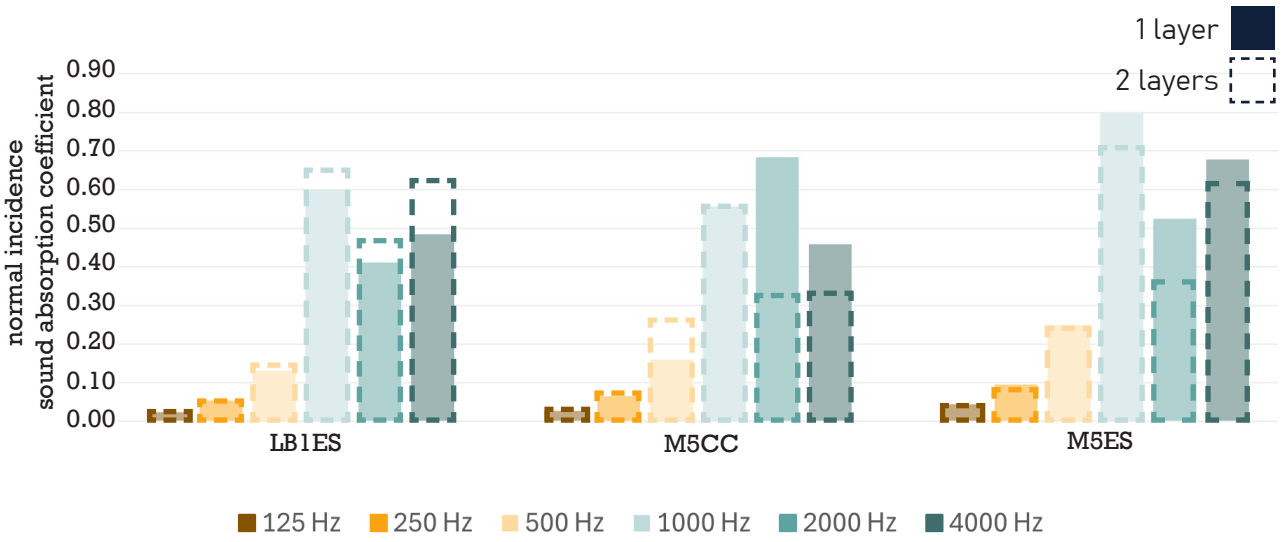

Fig. 3.40. Sound absorption comparison between single-layer and **fused** double-layer foam glass samples. The SAC values are generally comparable. SAC curves for these samples are shown in the Appendix.

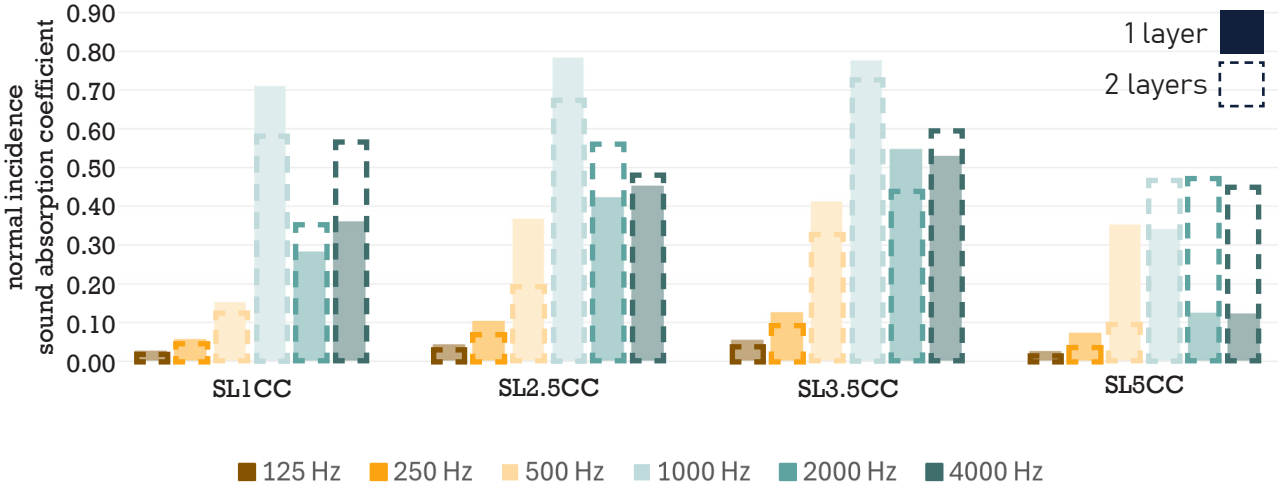

Fig. 3.41. Sound absorption comparison between single-layer and **glued** double-layer foam glass samples. The SAC values are generally comparable, with the double-layered samples occasionally showing slightly improved performance. SAC curves for these samples are shown in the Appendix.

Different porosity within one sample

As previously shown in Figure 3.23, a gradient in porosity was observed within a single foam glass sample. The lower section, in contact with the mould, exhibited smaller and denser pores, and the upper section, where the material expanded freely, developed much larger pores. To examine how these variations impact acoustic performance, two specimens were extracted from the same block: one from the bottom and one from the top. Despite their different pore structures, the measured SAC curves were similar, as illustrated in Figure 3.42. This indicates that, within the tested frequency range, pore size variation may not influence the overall acoustic performance.

Nonetheless, further investigation is needed to verify whether this finding holds true with a larger number of samples or at a larger scale, as the current conclusion is based on a single test. It is also important to note that this test was conducted only in the main body of the impedance tube, providing results only up to 1600 Hz. A full frequency range is necessary to draw more reliable conclusions.

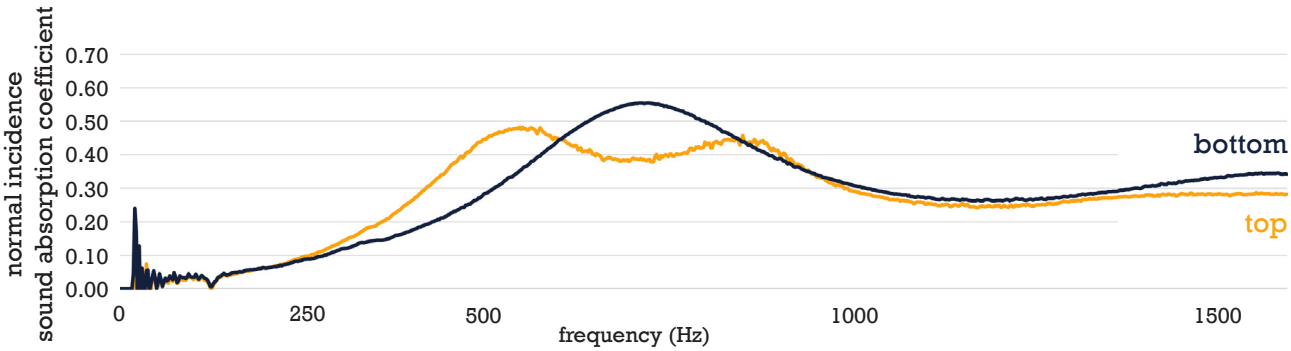

Fig. 3.42. Comparison of normal incidence SAC between top and bottom sections of the same foam glass sample (SL5EST2). Despite visible differences in porosity, both samples exhibit similar acoustic behaviour. The bottom sample (finer pores) shows higher absorption in the mid-frequency range (~700 Hz), while the top sample (larger pores) performs slightly better at lower frequencies.

Sample's thickness vs SAC

The literature review highlighted that material thickness significantly affects the performance of porous absorbers. To investigate this effect, two samples (SL2.5CC and SL3.5CC) were tested in both their typical 35 mm thickness and a thinner version of approximately 10 mm. These measurements were conducted using only the main body of the impedance tube, limiting the frequency range to 1600 Hz. In both cases, the same trend was observed: the thicker samples performed better at lower frequencies (up to around 1000 Hz), while the thinner ones showed improved absorption in the higher frequency range (from approximately 1000 Hz to 1600 Hz).

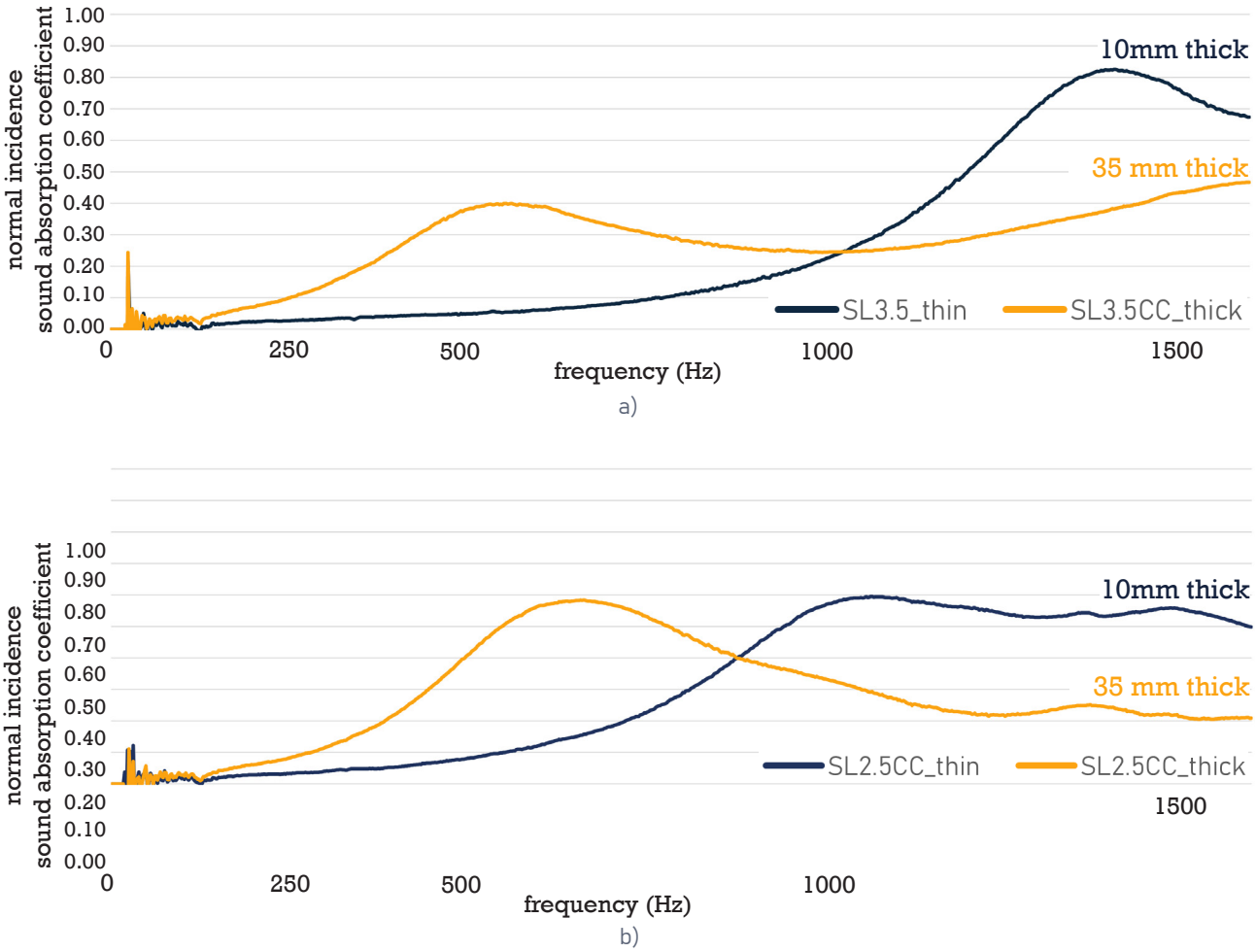

Fig. 3.43. Comparison of sound absorption between standard (~35 mm) and reduced (~10 mm) thickness samples, highlighting how material thickness influences SAC across different frequency ranges; a) SL3.5CC, b) SL2.5CC

3.4.3. Summary of acoustic testing

The impedance tube tests provided insights into the acoustic performance of the developed foam glass samples. A total of thirteen samples were evaluated across a frequency range of 50–6400 Hz. This approach enabled accurate measurement of the SAC with minimal material use, allowing for a detailed assessment of how variables such as glass type, foaming agent concentration, and particle size influence acoustic behaviour.

The majority of samples demonstrated strong absorption in the mid-to-high frequency range, with peak SAC values reaching up to 1.0 in certain cases (e.g., SL5CCT2, M5CCT2). A key observation was the correlation between larger pore structures and improved sound absorption performance, as summarized in Figure 3.44 for low-iron soda lime and light bulb glasses.

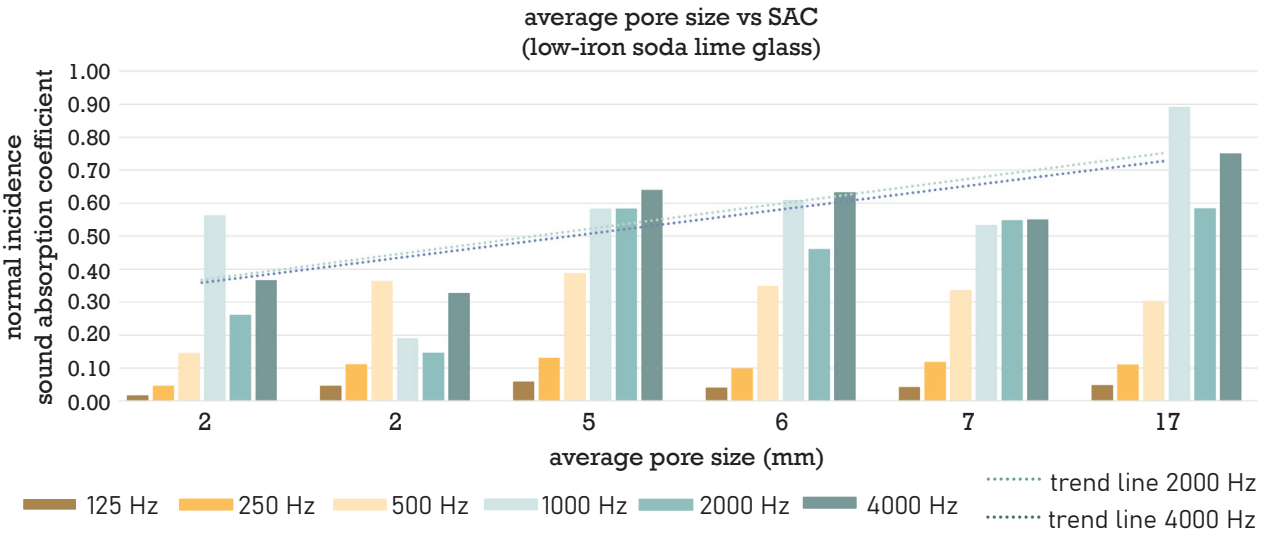

a)

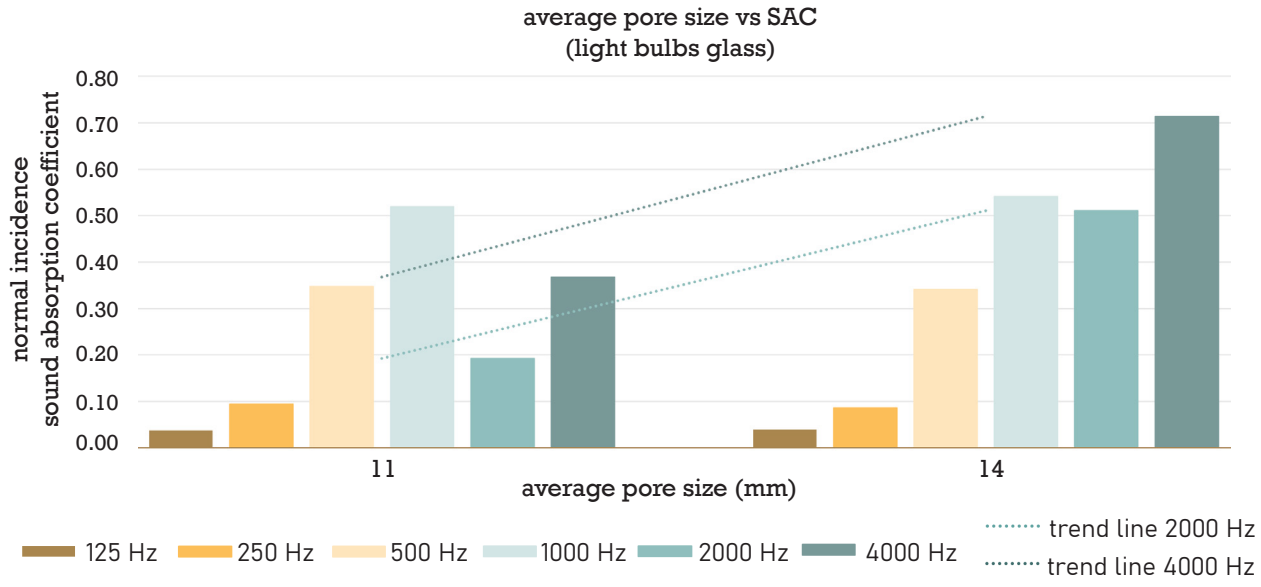

b)

Fig. 3.44. Pore size versus sound absorption: Graphs illustrate the relationship between average pore size and SAC for samples made from (a) low-iron soda lime glass and (b) light bulb glass. The trend - larger pores resulting in higher sound absorption - is particularly evident at 1000 Hz and 4000 Hz for soda lime, and at 2000 Hz and 4000 Hz for light bulb glass.

Samples foamed using pure calcium carbonate generally performed better than those using eggshells due to more tortuous pore structure. This finding indicates that the choice of foaming agent significantly influences the internal pore network and, consequently, the acoustic response.

In terms of glass type, clean soda lime glass exhibited the highest SAC overall. However, highly contaminated mixed cullet and light bulb glass also achieved excellent performance, with SAC values reaching up to 1.0 and 0.9 respectively. These findings confirm that even impure or mixed glass waste streams can be effectively transformed into sound absorbers.

Interestingly, the SAC curves did not follow the trend for purely porous absorbers. Instead, most samples exhibited irregular frequency-dependent peaks, suggesting a hybrid absorption mechanism that combines both porous and resonant behaviour. This is likely due to the presence of narrow pore necks and internal voids that form mass-spring systems within the material.

Additionally, tests on samples with a fused solid backing layer showed minimal impact on SAC across the frequency range. This is particularly relevant to the design goals of the project, as the rigid layer provides necessary structural support and aesthetic value without significantly diminishing acoustic performance.

The samples performed well across relevant frequency ranges, particularly in the mid to high frequencies. Notably, two samples exhibited a peak SAC close to 1 around 1000 Hz, which is especially promising. As illustrated in Figure 3.45, this frequency is common across many orchestral instruments, making it highly relevant to the case study, but it also lies at the center of the human voice range. As such, the panels would also be well-suited for broader applications, such as noise control in other architectural contexts.

In summary, the impedance tube tests validate the potential of foamed glass waste as a viable acoustic material for architectural applications. The observed hybrid absorption behaviour, shaped by composition and processing parameters, proves the viability of reusing diverse and contaminated glass waste streams for acoustic panels manufacturing.

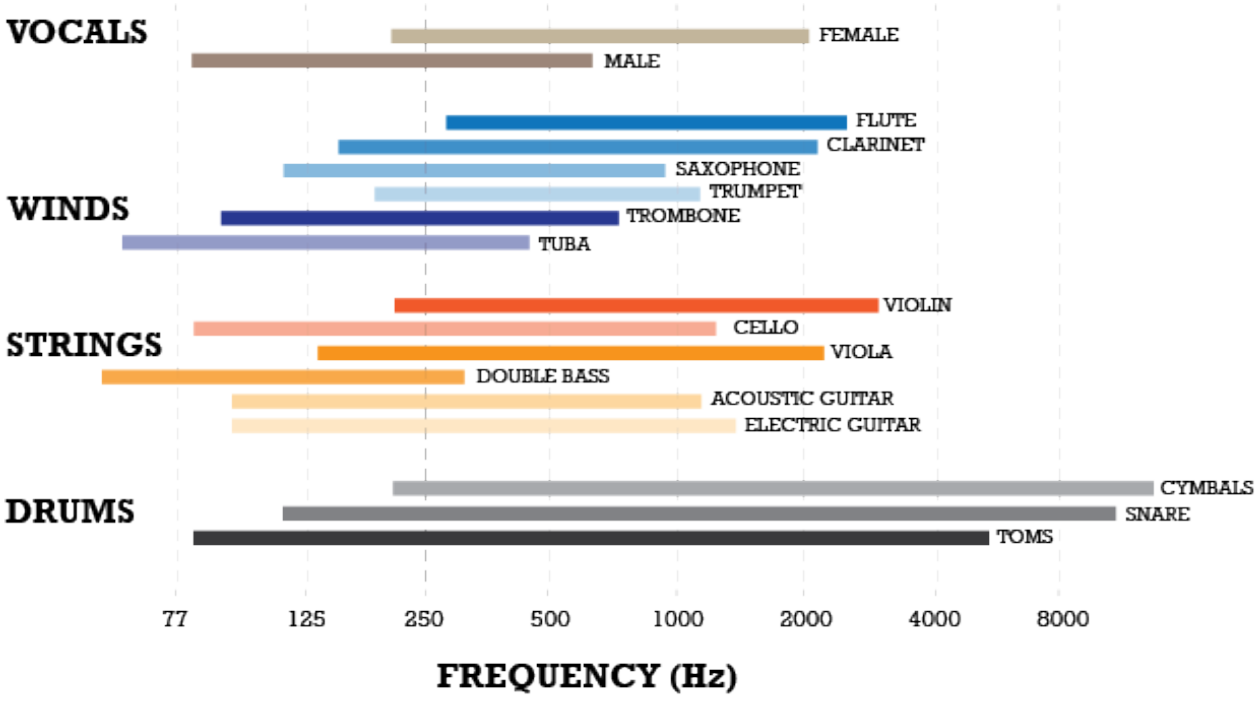

Fig. 3.45. Frequency ranges of musical instruments and voice types. Notably, many instruments, including strings, winds, and percussion, as well as female voice, concentrate energy around 1000 Hz. This emphasizes the acoustic relevance of that frequency range, especially in the context of performance spaces and the case study discussed.

4 | DESIGN APPLICATION

4. Design application

Following the successful development and testing of the glass panels, this chapter explores their architectural integration and acoustic performance in a real-world context. The aim is to evaluate how the material innovation developed in the lab can improve the acoustics of an existing performance space. Applying the panels in a virtual model allows for simulating their impact and assessing their effectiveness without the constraints of full-scale construction. The selected case study, a multipurpose Theatre Hall at TU Delft, provides a representative setting with known acoustic challenges. This design application phase bridges material research with computational acoustic analysis and design optimization, validating the panels' performance and informing their ideal placement through simulation-based evaluation.

4.1. Case study: Theatre Hall at X TU Delft

To evaluate the real-world applicability of the developed panels, this research included a case study conducted in the multipurpose Theatre Hall located within the TU Delft campus. This venue accommodates a wide range of events, including speech, amplified performances, and unamplified musical performances - most relevant to this study. Each of these uses imposes distinct acoustic requirements, making the hall an ideal testing ground for assessing how the hybrid panels can enhance clarity, reduce undesirable reflections, and tailor the room's acoustic response to varying functional demands. The following subsection outlines the spatial and acoustic characteristics of the hall that informed the simulation process and guided the panel placement strategy.

4.1.1. Room

Theatre Hall is regularly used for orchestra and choir rehearsals, as well as for chamber music concerts. It has a seating capacity of 175. Additionally, to host amplified events, the space is equipped with two large speakers suspended from the ceiling and directed towards the audience. These features make the Theatre Hall an ideal setting for the analysis. Before conducting acoustic measurements, the physical characteristics of the Theatre Hall were documented, including its geometry and surface materials. These data are crucial to create a virtual model of the Theatre Hall and proceed with simulations.

Fig. 4.1. Photograph of the Theatre Hall; own work. The image shows the interior of the Theatre Hall, capturing its spatial layout and material finishes as they appear in the existing condition.

4.1.2. Room geometry

The hall has a rectangular shape, measuring approximately 16.2 meters in width, 15.25 meters in length, and 9 meters in height. Its dimensions were measured with a laser device. The auditorium, located in the center of the hall, is curved and divided into three sections. Its foundation spans for the entire width of the room, with the widest part extending 3.3 meters into the room's length. Under the floor there is a basement used for storing instruments and other equipment.

4.1.3. Surface materials

The walls of the Theatre Hall are clad with wooden panels. Three of the walls can be covered with a heavy curtain, providing more absorption. The floor is wooden, while the ceiling is covered with various installations and professional spotlight system on steel construction, contributing to the scattering of the sound. Auditorium benches are padded with fabric, adding absorption, and the audience elevated foundation is made of plywood.

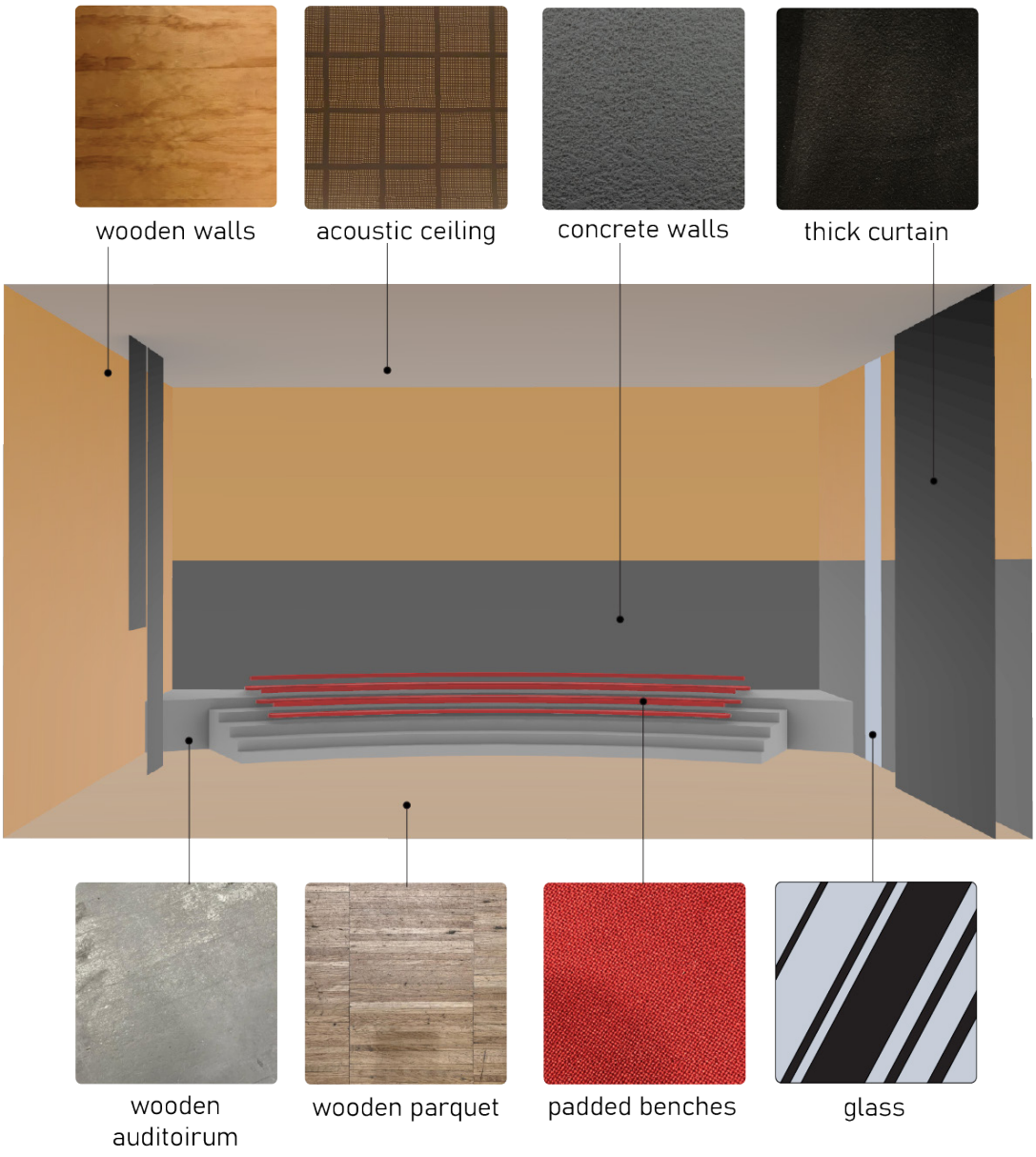

Fig. 4.2. Schematic representation of materials appearing in the Theatre Hall, own work

4.1.4. Measurements

To enable accurate simulation and performance analysis of the Theatre Hall, a series of on-site acoustic measurements were conducted. These measurements were essential for capturing the hall's existing acoustic conditions and providing reliable baseline data to calibrate the simulation model, ensuring it reflects the real-world scenario as closely as possible.

Methodology and equipment

Measurements were performed using a Norsonic Nor140 Class 1 sound pressure level meter together with a NOR 276 omni-directional sound source, which generated sound waves at various frequencies with the support of a NOR 280 power amplifier. An electronic sweep signal was used for the measurements, repeated four times to ensure accuracy. The sound source and receiver were connected to a laptop via a Behringer UCA222 audio interface. Measurements were taken at ten different points throughout the hall, both in the stage environment and the audience area and are presented on the measurements scheme in Figure 4.4. To avoid disturbance, the measurements were conducted in the empty room. For all points, measurements were carried out with the walls exposed (curtains fully open). For one specific point, additional measurements were taken in three scenarios: with all curtains opened, with curtains covering only the wall behind the stage area (facing the audience), and with all curtains fully closed.

Several acoustic metrics were recorded, including early decay time (EDT), which describes the initial drop in sound energy, RT values across different decay intervals: T-1→11, T-5→25, T-5→35 and T-5→45, which is the time needed for sound energy to decay from 1 to 11 dB, 5 to 25 dB, 5 to 35 dB and 5 to 45 dB below the initial sound level, respectively.

In addition to these metrics, many other acoustic parameters were recorded. The focus in this study is put, except reverberation time, also on acoustic strength (G), which is the measure of loudness and clarity index for music (C80). All the metrics were measured for the standard octave frequency bands: 125, 250, 500, 1000, 2000, and 4000 Hz.

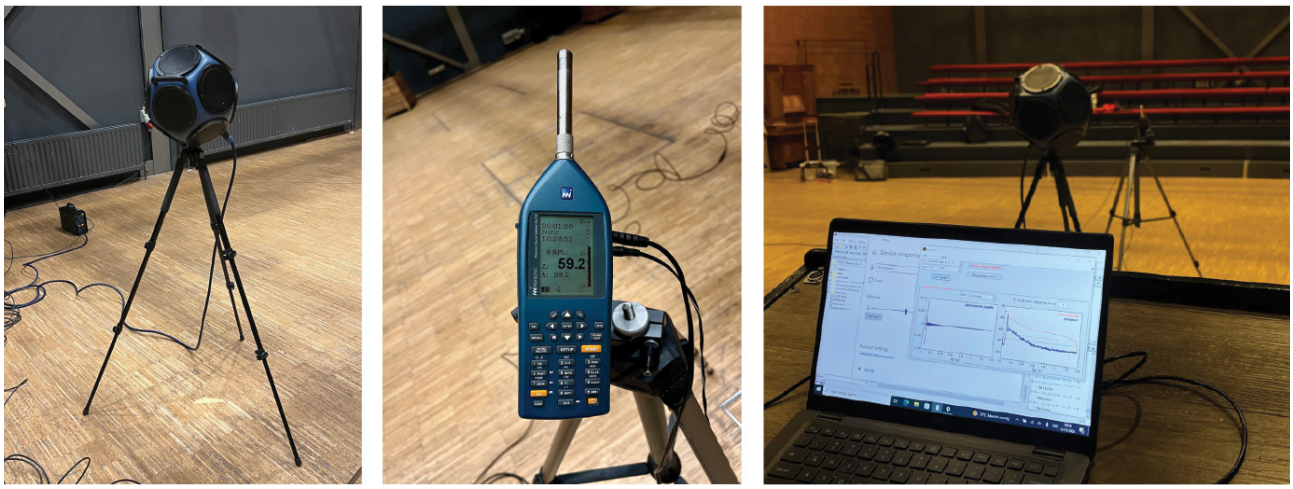

dodecahedron speaker | microphone | set up

Fig. 4.3. Equipment used in in-situ acoustic measurements in the Theatre Hall

Results analysis and comparison with recommended values

The T-1 →11 and T-5→25 metrics provided the most accurate results across most points and frequency bands, while other RT values had lower regression correlation coefficients and T-5→25 values were used to assess the acoustic performance on the Theatre Hall.

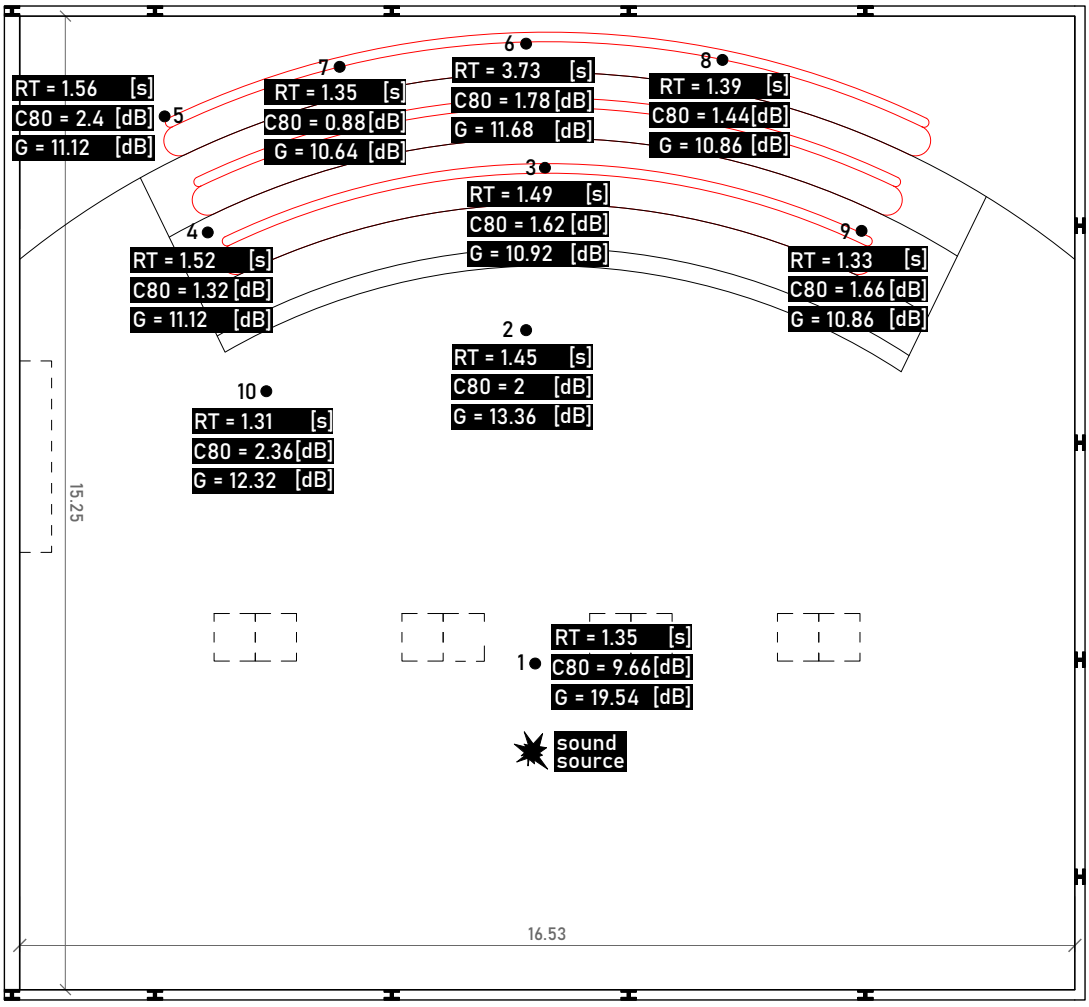

RT - reverberation time, G - acoustic strength, C80 - clarity index

Fig. 4.4. Schematic plan of the Theatre Hall indicating the positions of the sound source and receivers. The diagram includes measurement results for each receiver position, showing average values (across all measured frequencies) for reverberation time, clarity index C80 and acoustic strength G; The values are averages from 125 – 2000Hz for each receiver position.

The acoustic analysis of the Theatre Hall is based on three key metrics: RT, G - strength and the clarity index C80. These measured values, averaged for frequencies 125-2000 Hz for each listener positions, are presented in Figure 4.4.

The measured values were compared against recommended values found in the literature. Most of these recommendations, however, concern large classical music venues. (Nijs & Vries, 2005) discuss "ideal" acoustic values for smaller music halls, which are more comparable to the Theatre Hall, given its relatively small capacity of 175 seats. The authors present a G-RT diagram, illustrating the relationship between G and RT as functions of room volume and mean sound absorption coefficient. They propose an "ideal" curve on this diagram, which was used as a reference for assessing the acoustic performance of the Theatre Hall. The G-RT diagram showing both the measured and target values for the Theatre Hall is presented in Figure 4.5.

Reverberation time

In the Theatre Hall, the average measured RT is approximately 1.4 seconds, which is slightly below the recommended values typically suggested for larger music halls in literature. Also, based on the G-RT diagram analysis, it can be concluded that the RT in the Theatre Hall could be slightly longer but should not be much shorter. A risk associated with excessively short RT is that the room may sound too dry, which, while beneficial for speech intelligibility, is generally undesirable for classical

music performances. Nevertheless, as noted by (Meyer and Hansen, 2009), changes in RT are more perceptible to musicians than to the audience.

Acoustic G-strength

Literature suggests that an optimal G value for large music halls is approximately 5 dB. Based on that it can be concluded that G measured in the Theatre Hall is consistently too high across all receiver points and frequency bands. This is a common issue in small rooms, where the limited volume causes excessive accumulation of sound energy. On the other hand, the G-RT diagram proposed by (Nijs & Vries, 2005) allows for slightly higher G values in smaller venues. Personal experience as a practicing musician in the Theatre Hall supports the conclusion that the space often feels excessively loud, contributing to discomfort and fatigue for performers and likely for the audience as well. This may be a key reason why the venue is used primarily for rehearsals rather than orchestra concerts. Consequently, it was concluded that the G-strength should not be further increased.

As noted by (Ermann, 2015), the human brain is highly sensitive to changes in G - strength, capable of perceiving differences as small as 0.25–0.5 dB. This highlights the importance of carefully fine-tuning this parameter but also suggests that even small improvements can have a perceptible impact for occupants of the Theatre Hall.

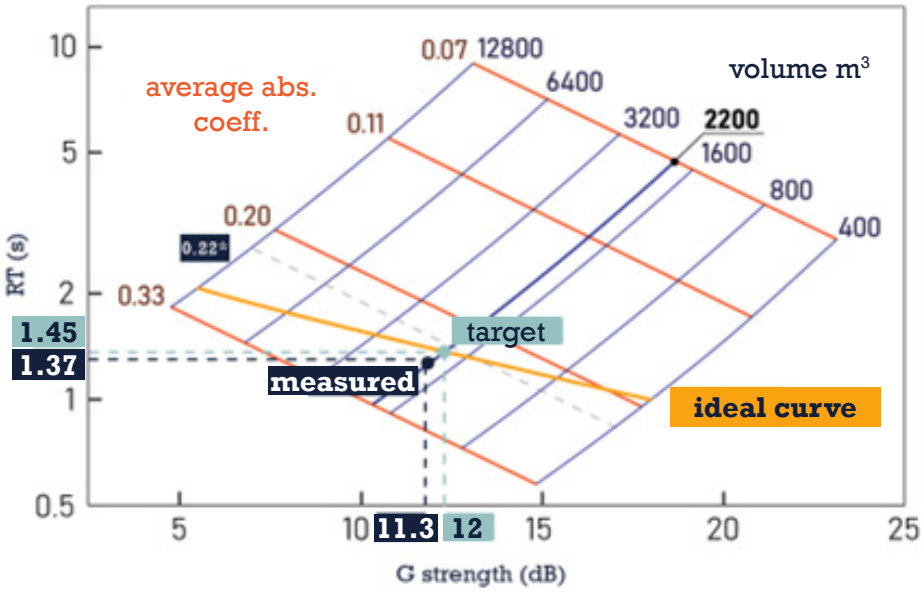

Fig. 4.5. The G-RT correlation scheme, adapted from Niels and de Vries (2005). The graph plots the G strength against RT, illustrating how the hall's acoustic response deviates from the ideal balance between loudness and reverberation. It compares measured acoustic values from the Theatre Hall with ideal reference values based on the curve; From this comparison, it can be observed that the measured RT is slightly too high, while the G-strength is slightly too low for the case study volume of 2200 m³.

Clarity index C80

It is common in smaller rooms for too high G-strength and too high C80 to go hand in hand, and this pattern also occurs in the Theatre Hall. The risk associated with a too high C80 index is that the listener may perceive the sound as overly dry or dead. A high C80 value indicates a lack of richness normally contributed by later sound reflections, which in turn reduces the sense of envelopment in the space, beneficial for classical music. This happens because a large amount of early, strong sound energy reaches the listener shortly after the sound has been emitted. The room is not large enough to spread the sound energy or delay the reflections. Following the literature review, it was concluded that the ideal C80 values are between –1 dB and 5 dB for rehearsal spaces and slightly

lower, typically around –4 dB to 1 dB for performance spaces.

In the Theatre Hall, the mean measured C80 value is slightly over 2 dB, with even higher values observed at the low (125 Hz) and high (2000 Hz, 4000 Hz) frequency bands.

In their work, (Nijs & Vries, 2005) mention that a diagram similar to the G-RT diagram can be created, but with RT replaced by the C80 values. Although such a diagram was not found elsewhere in the literature, an attempt was made to create one for the Theatre Hall. Using formula [1] for clarity derived from (Salter, 1998), corresponding C80 values were calculated.

$$C_t = 10\,log_{10}\left[\frac{Ve^{(0.4r+13.82t)/T)}}{312Tr^2} + e^{(13.82t)/T)} - 1\right] \quad [1]$$

Where:

- C_t is clarity; t is the time defining the extent of the early sound field (here: 80ms)
- T is the reverberation time
- r is the distance from the sound source; for the purposes of constructing the C80–G diagram, the average source-to-receiver distance was used (10 meters)

In this analysis, RT values were replaced with the corresponding computed C80 values. The resulting diagram is shown in Figure 4.6. In the modified version, both G and C80 should ideally be expressed as functions of the mean absorption coefficient and room volume. However, the calculations were conducted only for a single room volume of the Theatre Hall - 2200 m³. As a result, while the plot does not reflect how C80 would vary with changing volume, the correlation between G and C80 is accurate for the given room volume.

The adapted diagram suggests that the C80 value should ideally be around 1. While the authors of the referenced paper do not distinguish between optimal values for performance versus rehearsal scenarios, a C80 of 1 appears to be a balanced target. According to the literature, a C80 value of approximately 1 dB can be a compromise, representing the upper limit of what is typically

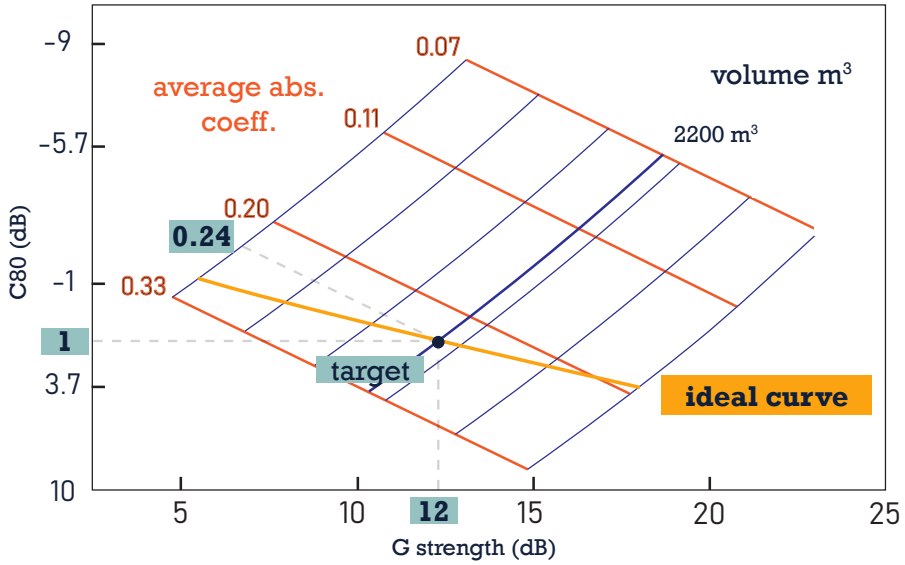

Fig. 4.6. Adapted C80–G correlation diagram for the Theatre Hall; own work, based on (Salter, 1998) and (Niels and de Vries, 2005). The diagram presents the relationship between the calculated C80 and G values for a fixed room volume of 2200 m³, using a modified version of an existing correlation model. While the original formulation includes RT, here it has been replaced with computed C80 values.

recommended for performance spaces and the lower limit for rehearsal scenario. This makes it a suitable baseline for multi-purpose halls like the Theatre Hall, where both activities may take place.

However, if only the reverberant field is considered, the first term within the brackets can be omitted, and as a result, the room volume is no longer included in the calculation.

$$C_t = 10\,log_{10}(e^{(13.82t)/T)} - 1) \qquad [2]$$

C80 was recalculated based on the modified formula [2]. As a result, the C80–G correlation diagram presented in Figure 4.7 excludes volume as a parameter. With this revised approach, the "ideal" C80 value is approximately 0.6, slightly lower than the value previously derived when volume was included, yet still representing a reasonable balance between rehearsal and performance scenarios.

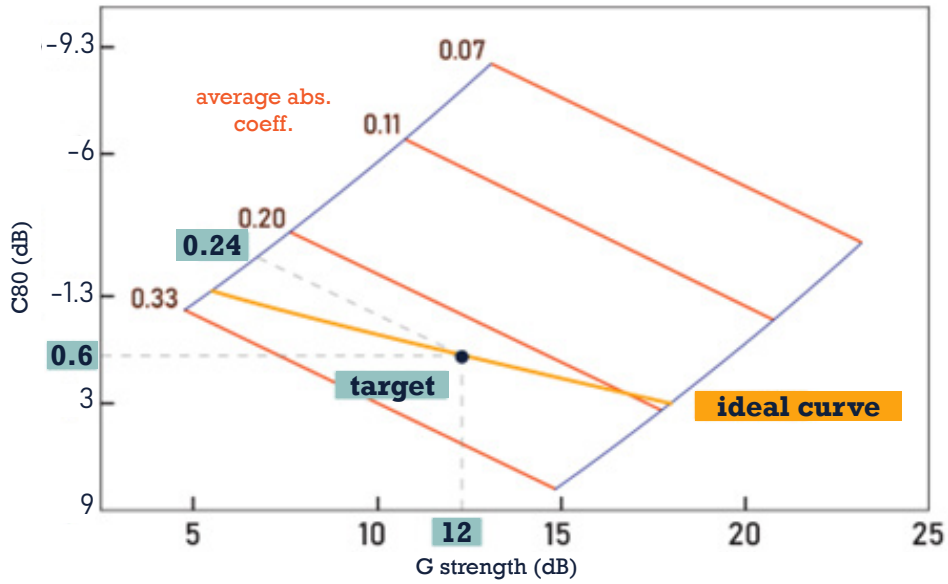

Fig. 4.7. C80–G correlation diagram based on the modified formula excluding room volume; own work, based on (Salter, 1998) and (Niels and de Vries, 2005). This diagram presents the recalculated correlation between G and C80 using a simplified model that omits room volume as a parameter, focusing solely on the reverberant field.

Conclusion

This evaluation identifies the key acoustic issues in the Theatre Hall and outlines potential strategies for improvement, with particular focus on reducing the clarity index C80 and possibly also G-strength. While a slight increase in RT may be beneficial, it is crucial to avoid any further reduction, as this could negatively impact the room's acoustic character.

Figure 4.8 summarizes the primary acoustic issues, proposed solutions, and possible implementation methods.

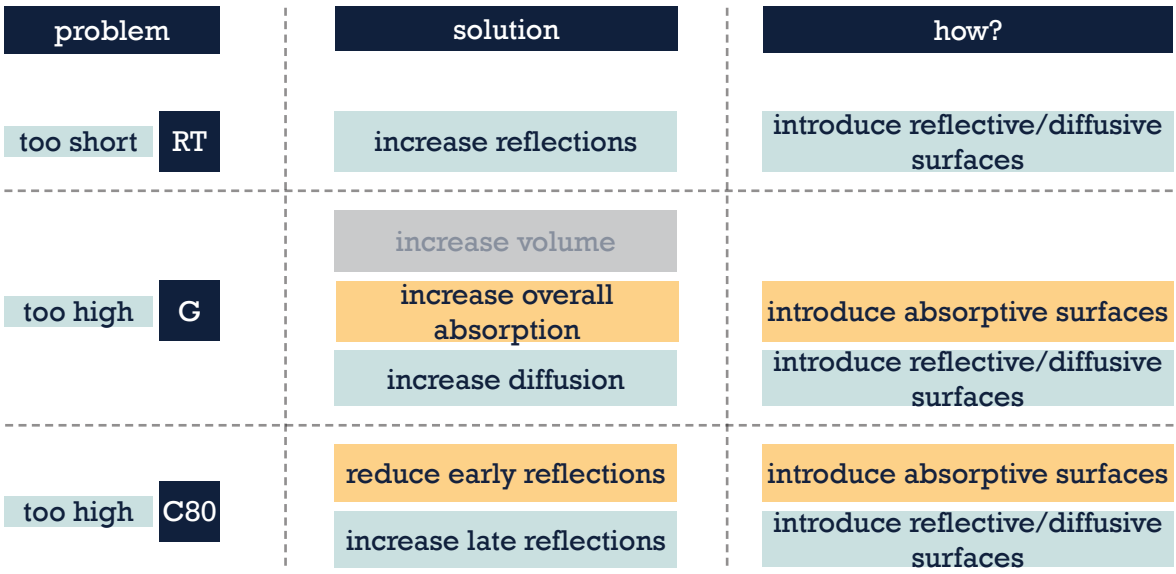

Fig. 4.8. Acoustic issues identified in the Theatre Hall, proposed solutions for mitigating these problems, and corresponding implementation strategies; own work

Since excessive C80 has been identified as the main issue, this parameter becomes the focus of the intervention. C80 measures the ratio of sound energy arriving within the first 80 ms to that arriving later. To reduce high C80 values, strategies include minimizing early reflections and/or enhancing later ones.

In typical sound reproduction spaces like recording studios, absorption is commonly used to reduce reflections. However, in performance venues, excessive absorption is avoided, as it can create an acoustically "dry" environment lacking warmth (Cox & D'Antonio). The Theatre Hall, however, presents a unique case. Due to its strong early reflections and high clarity, which may cause listener fatigue, this project proposes the use of targeted porous absorption.

Instead of damping the entire space, specific reflective zones will be treated to reduce problematic reflections. This tailored approach addresses the hall's acoustic challenges while preserving its dual function for both rehearsal and performance. Reducing early reflections will help lower C80 and may also reduce G-strength, as both are influenced by similar acoustic factors.

In parallel, strategically placed reflectors will be used to reinforce later reflections, counteracting the RT reduction that absorption might cause. While absorption effectively lowers C80 and G, it risks over-dampening the space if applied excessively.

By carefully combining targeted absorption with added reflectors, this strategy aims to correct the acoustic imbalances without compromising reverberation, maintaining an overall balanced sound quality in the Theatre Hall.

4.2. Acoustic simulations

With the material properties validated through impedance tube testing, the next phase involved assessing the panels' impact on room acoustics through digital simulations. Using the measured absorption coefficients, the foamed glass panels were integrated into a 3D model of the case study space, the Theatre Hall at TU Delft, developed in CATT-Acoustic and Grasshopper. The goal was to evaluate whether and how these panels could improve acoustic parameters such as C80, G-strength, and RT. This section outlines the development and calibration of the acoustic model, followed by simulation results comparing the baseline condition and various panel configurations.

4.2.1. CATT-A model development

To virtually implement the proposed acoustic solutions in the case study, a digital model of the Theatre Hall was developed using CATT-Acoustic (CATT-A), a room acoustics prediction software based on geometrical acoustics. The initial geometry of the hall was created in Rhino and Grasshopper, where a custom Python script by G. Mirra was used within Grasshopper to translate the geometric data into a format compatible with CATT-A. This script automatically generated the required files for setting up the simulation. To optimize simulation efficiency, the model geometry was simplified wherever possible without compromising acoustic relevance. Figure 4.9 presents the digital models created in Rhino/Grasshopper and their imported versions within the CATT-A environment.

CATT-A requires several files to set up a project, including:

- **MASTER.GEO** file containing information about the hall's geometry. First, all vertices of the surfaces in the project are defined by their X, Y, and Z coordinates and assigned unique numbers. In the later part of the file, surfaces are described by referencing the corresponding vertex numbers.

- **REC.LOC** file, defining the locations of the receivers, specifying their X, Y, and Z coordinates. The receiver points correspond to the positions where real-life acoustic measurements were conducted in the Theatre Hall.

- **SRC.LOC** file, providing information about the sound source, including its X, Y, Z coordinates, orientation, and the SPL at a distance of 1 meter along one of the axes. This SPL value was obtained during the actual measurements. For this simulation, a single source was used, placed in the center of the area typically occupied by the orchestra during rehearsals, corresponding with the location used in the real-life measurements. The source was modeled as omnidirectional, emitting sound uniformly in all directions. In the in-situ measurements, the dodecahedron loudspeaker was used, which exhibits near-omnidirectional behaviour.

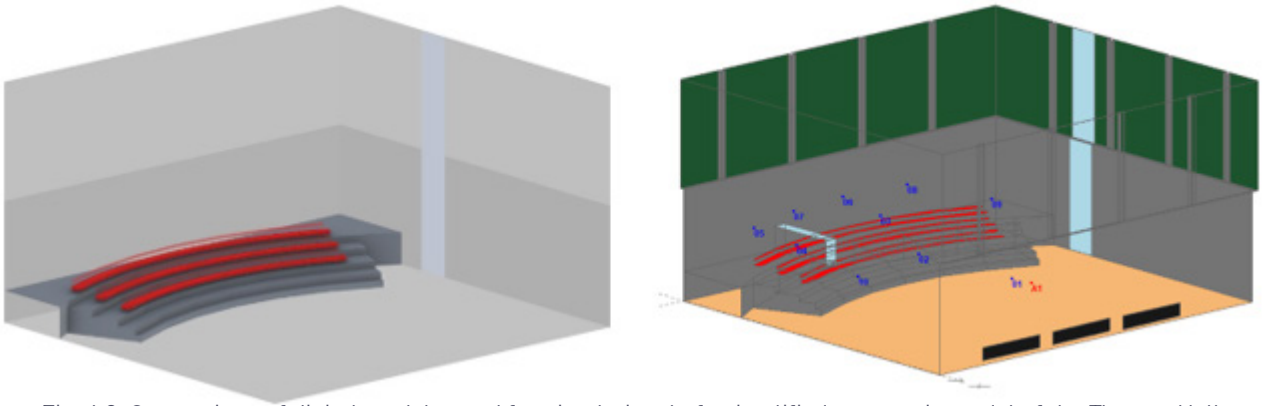

Fig. 4.9. Comparison of digital models used for simulation. Left: simplified geometric model of the Theatre Hall developed in Rhino/Grasshopper. Right: corresponding acoustic model prepared in CATT-Acoustic, including material definitions, source positions, and receiver points for acoustic analysis.

In CATT-A, surfaces are organized based on their material. Each material is defined by two key acoustic parameters: the absorption coefficient, which is the ratio of sound energy absorbed by a surface to the total incident energy, and the scattering coefficient, which represents the ratio of energy scattered in a diffuse manner (non-specular) to the total reflected energy (Cox & D'Antonio, 2017).

To manage the model's complexity and reduce computational load, the geometry of the hall was simplified. Elements, such as lighting rigs, speakers, and acoustic equipment suspended from the ceiling (visible in Figure 4.1), were not individually modeled. Instead, the scattering coefficient of the ceiling was increased to account for the additional diffusion these elements introduce in reality. This is a common practice in geometrical acoustics modeling, especially in ray-tracing or image-source methods, where detailed geometry can drastically increase simulation time without significantly improving accuracy.

Additionally, several 3D elements were simplified into single surface representations. For example, benches and curtains were modeled as flat planes rather than volumetric objects. The orchestra was represented as a double-sided surface, using an estimated surface area of 1.5 m² per musician, with the sound source placed at the center of this surface to reflect its typical location during rehearsals. The absorption and scattering coefficients for all materials, including the auditorium, benches (for both occupied and unoccupied scenario), floor, ceiling, curtains, and orchestra - were based on data provided by (Cox & D'Antonio, 2017).

4.2.2. CATT-A model calibration

Measured vs simulated values comparison

To ensure reliable simulation results, the CATT-A model required calibration - aligning the simulated RT values with those measured in the Theatre Hall. The calibration process began with an empty-room simulation, and results were compared against in-situ acoustic measurements. RT20 (RT 5→25) was chosen as the indicator for this comparison due to its high correlation coefficient.

Initial simulations resulted in significantly lower RT values than those measured. To improve accuracy, the absorption coefficients of various surfaces were adjusted, either increased or reduced, until the simulated RTs better reflected the measured data. At some frequencies, simulated RTs were too high at certain receiver positions and too low at others; in these cases, average RTs were calculated across all receivers for each frequency. The model was considered successfully calibrated once the difference between simulated and measured average RT values remained within 5% across the frequency range.

Then, C80 and G-strength were compared between measured and simulated results. These were not always aligned: measured C80 values were slightly lower than simulated ones at 250 Hz, 500 Hz, and 1000 Hz, while G values were slightly higher than the simulated ones across the entire frequency range. However, these minor differences fall within acceptable margins and confirm that the calibrated model accurately represents the acoustic behaviour of the Theatre Hall.

Following calibration, a simulation was conducted for the occupied-room scenario and RT, C80 and G were documented and are presented in the Appendix.

Simulation parameters

The number of rays in an acoustic simulation plays a critical role in determining the reliability and resolution of the results. There is no fixed or "magical" number that guarantees accuracy across all scenarios. The optimal ray count depends on both the geometric complexity of the room and the desired precision of the outcomes. In general, increasing the number of rays leads to more accurate and detailed simulations. However, there is a threshold beyond which additional rays

provide negligible improvement, significantly increasing computation time.

For this project, the model was initially calibrated using 500,000 rays, being a good balance between accuracy and performance. For final simulations, the ray count was increased to 1,000,000.

The impulse response length was set to 2500 milliseconds, which is sufficient given the moderate reverberation of the Theatre Hall. In more reverberant spaces, longer impulse response times would be necessary to capture the full decay of sound energy. In this case, 2500 ms was enough to ensure that the entire reverberation tail was included in the echogram, allowing accurate analysis of RT and other parameters.

All other simulation parameters related to air properties were kept at the default CATT-A settings, with temperature set to 20°C, relative humidity at 50%, and air density at 1.2 kg/m³.

4.2.3. Current state simulations analysis

CATT-A analysis

A preliminary acoustic analysis based on in-situ measurements identified key issues in the Theatre Hall. To gain better insight into the reasons for these problems, further analysis was conducted using CATT-A, which applies ray-tracing methods to simulate sound propagation in the space.

In music performance venues, early reflections play an important role in ensuring both clarity and stage support (the ability for musicians to hear themselves and one another). However, in smaller rooms like the Theatre Hall, the ratio of early to late reflections becomes too high. A large portion of strong, early-arriving sound energy reaches the listener almost immediately after the direct sound and the room's limited volume prevents the development of later reflections.

The time trace function in CATT-A was used to identify these critical reflection paths. This function visualizes how sound rays travel through the room over time, enabling precise spatial and temporal analysis of reflection patterns.

As shown in Figure 4.10, the direct sound wave from the stage reaches the audience area approximately 24 milliseconds after emission. At nearly the same moment, early reflections from the rear wall behind the orchestra reach the musicians, followed by a strong ceiling reflection.

By 40 milliseconds after the sound is emitted four primary first-order reflections reach the audience area, originating from the wall behind the orchestra, the wall behind the audience and the side walls. These early reflections are key targets for acoustic treatment. By introducing selective absorption on these surfaces, the aim is to reduce the intensity of early reflections without significantly reducing the reverberation.

Aeolus analysis

Aeolus is a Grasshopper plugin for acoustic analysis that uses image source modeling method, working by tracing sound reflections starting from a specified target point and working backwards, toward the sound source. Once the reflection order is defined (i.e. the number of times sound is allowed to bounce off surfaces), the method calculates all possible reflection paths up to that order, evaluating each combination of surface interactions. The number of paths it considers depends on how many surfaces are in the room and the reflection order. This is especially useful because it can calculate accurate SPLs at one or more specific target points (Mirra et al., 2023). Another advantage is the plugin's integration with Grasshopper, enabling direct interaction with parametric geometry. This makes it especially useful for iterative design processes, where geometry and acoustic analysis can be linked and updated automatically.

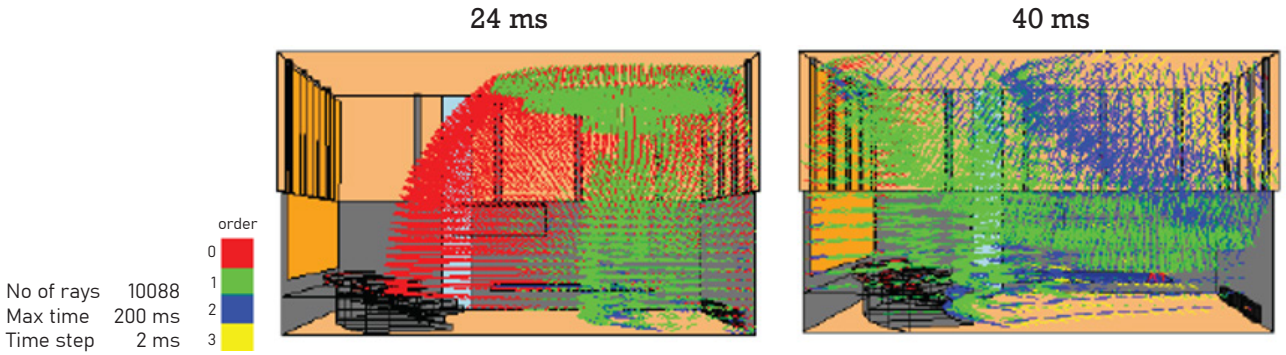

Fig. 4.10. Analysis of the current acoustic performance in the Theatre Hall using the time trace function in CATT-A; a) The direct sound wave reaches the audience approximately 24 ms after being emitted; b) Around 40 ms after emission, four first-order reflections reach the audience, originating from the ceiling, rear wall behind the audience, rear wall behind the orchestra, and the side walls, shortly following the arrival of the direct sound.

Similarly to CATT-A, Aeolus requires the definition of sound source and receiver points, and the construction of an acoustic scene. However, the simulation method differs: in CATT-A, sound rays lose a portion of their energy upon reflection, according to the absorption coefficient of the material. In contrast, Aeolus does not differentiate between material types. All reflections, regardless of the surfaces they interact with, carry the same amount of energy as the direct sound. This simplification makes Aeolus less accurate in modeling later reflections, but it is still highly effective for predicting the early sound energy and visualizing reflection paths.

In Aeolus reflection paths (rays) are visualized as curves. Using the lengths of these curves and assuming a speed of sound of 343 m/s, the arrival times of each reflection were calculated. These reflections were then categorized into two groups: early and late reflections, arriving before or after 80 milliseconds of the sound being emitted, respectively, as illustrated in Figure 4.11.

This classification enables a clear visualization of how sound energy is distributed within the space, helping to identify surfaces contributing to excessive early reflections.

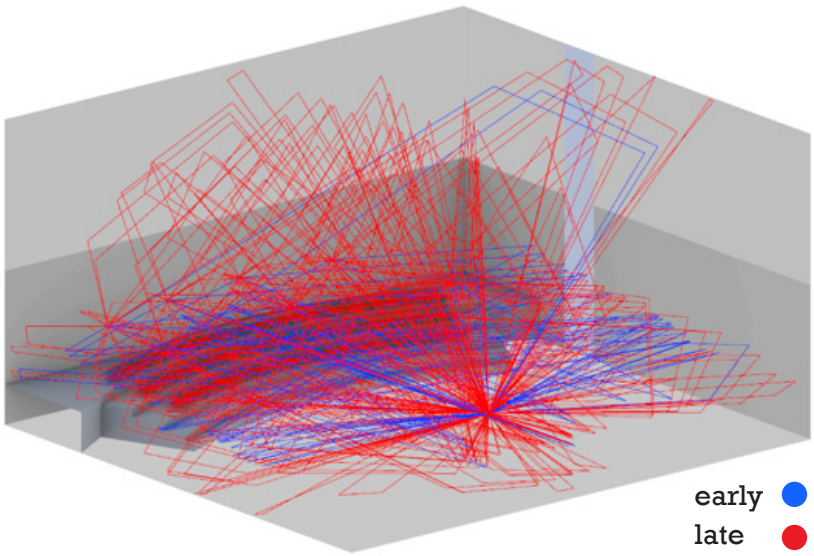

Fig. 4.11. Visualisation of reflection paths in Grasshopper, Aeolus. The paths were divided based on the arrival time to the source point that was calculated based on the lenght of these curves - assuming speed of sound 343 m/s, their arrival time was calculated and the paths were divided into early/late based on whether they come before or after 80ms after sound emmisoin.

4.2.4. Potential solutions for acoustic improvement

Targeted absorption

Deterministic test of the approach

As discussed earlier in the report, one way to reduce early reflections is by absorbing them at the points where they first occur. The challenge with this approach is to target only the early reflections without significantly affecting the overall RT, which means avoiding the absorption of later reflections. To achieve this, Aeolus was used to identify the specific surfaces responsible for the earliest reflections. Rather than covering large areas with absorbers, precisely selected spots were covered. By visualizing reflection paths in Aeolus described before, the intersection points between rays and the hall's surfaces were identified (Figure 4.12). These points marked where early reflections were directed towards the listeners, and absorbing panels were proposed only at those locations.

However, many of these early reflection points overlapped with paths of valuable later reflections. To avoid reducing RT, a compromise solution was implemented: absorbing areas were designed to target the early reflection paths only, while leaving closest areas exposed to allow late reflections to occur. This was done by removing absorption material around the intersection points related to late reflections.

The effectiveness of this approach was then evaluated using CATT-A simulations. Compared to the initial rehearsal scenario (orchestra only, no audience), this treatment resulted in only a slight reduction in RT, still within acceptable limits, and a noticeable reduction in both G-strength and C80 values, particularly at 500 Hz and 1000 Hz, where improvements were close to the just noticeable difference (JND) threshold for clarity (1dB). This suggests that listeners and performers would likely perceive a small but audible improvement in clarity.

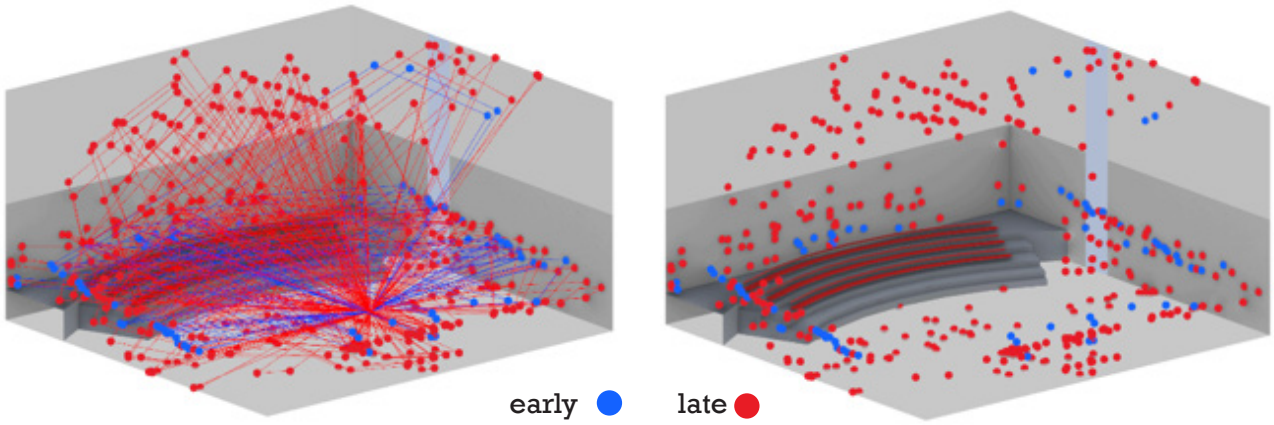

Fig. 4.12. Reflection points mapped onto the surfaces of the Theatre Hall, divided into early reflections (arriving before 80ms) that should be absorbed and late (arriving after 80ms) that should be preserved. The points were determined by defining the early and late reflections path with the surfaces – they are the exact spots of the bounces, c) absorption applied only there, where the early reflections occur, d) the same amount of absorbing material distributed randomly across walls in Theatre Hall

To confirm that the observed improvements were indeed the result of carefully placed absorption, and not simply due to the addition of absorptive material in general, a control experiment was conducted. The same amount of absorption (approximately 13 m²) was added to the room, but this time it was placed randomly, without considering whether the covered surfaces were responsible for early or late reflections (Figure 4.13).

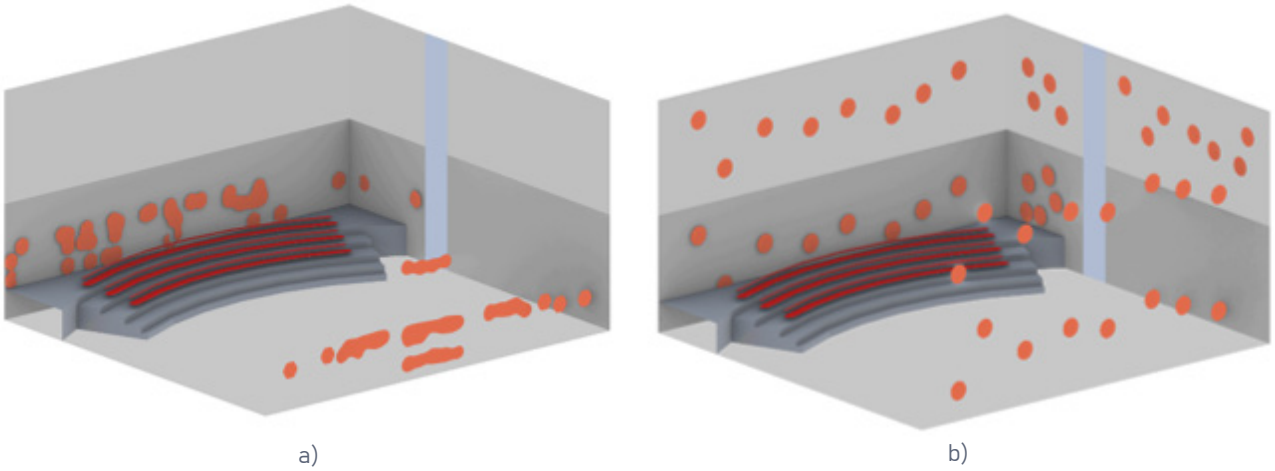

Fig. 4.13. a) Absorption applied only there, where the early reflections occur, b) The same amount of absorbing material distributed randomly across walls in Theatre Hall

The results of this random placement clearly demonstrated worse performance. In fact, in the case of C80, the values were even slightly worse than those simulated before any panels were applied.

This outcome confirms that it is not just the presence of absorption, but its strategic placement, that effectively reduces both C80 and G-strength. A full comparison of acoustic metrics across scenarios is presented in Figure 4.14.

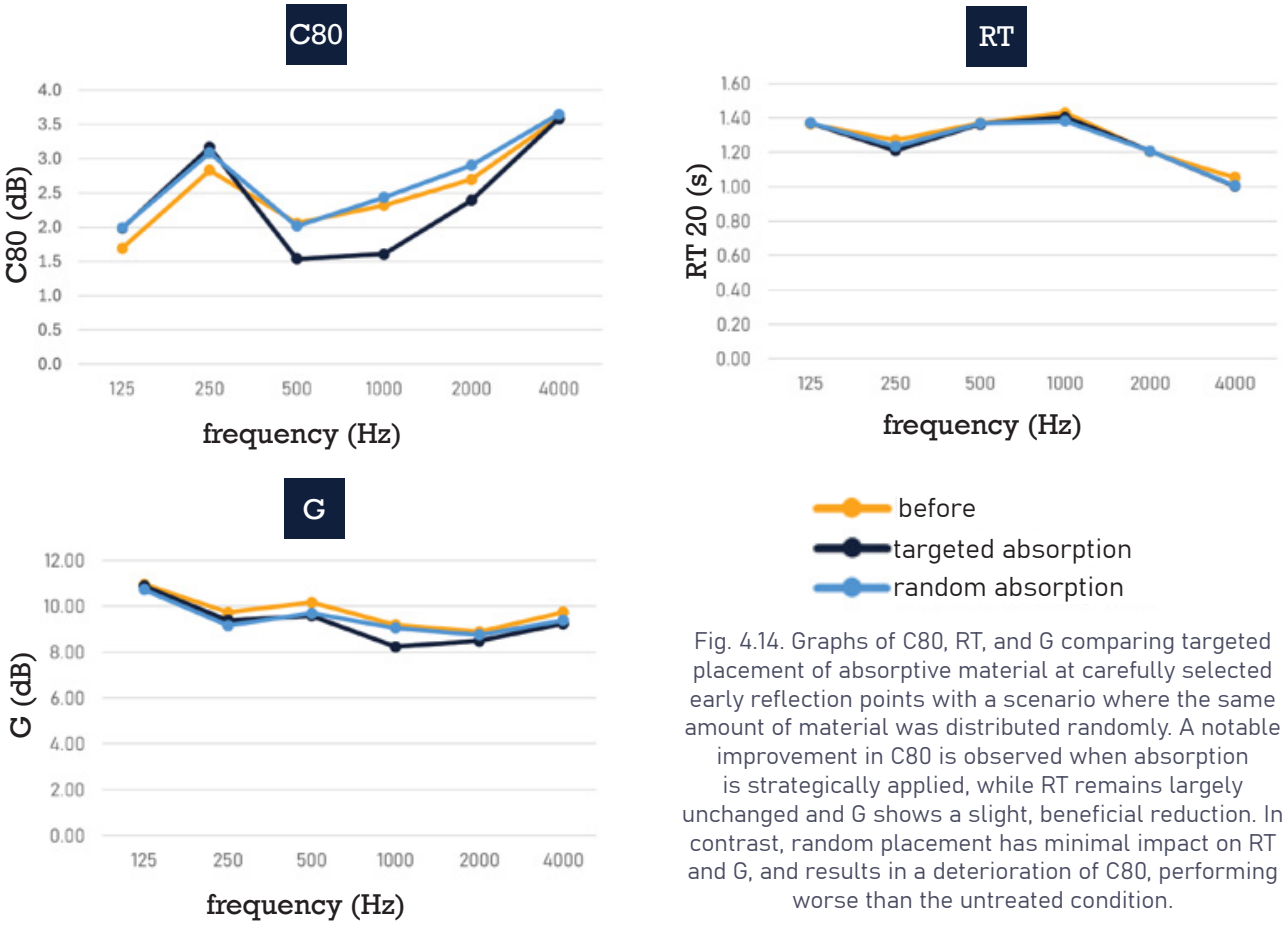

Fig. 4.14. Graphs of C80, RT, and G comparing targeted placement of absorptive material at carefully selected early reflection points with a scenario where the same amount of material was distributed randomly. A notable improvement in C80 is observed when absorption is strategically applied, while RT remains largely unchanged and G shows a slight, beneficial reduction. In contrast, random placement has minimal impact on RT and G, and results in a deterioration of C80, performing worse than the untreated condition.

Stochastic test of the approach

In real-world scenarios, the position of a sound source is rarely fixed. It is subject to variation due to factors such as the performer's movement on stage, instrument directivity, playing height (e.g., seated versus standing), and the overall ensemble layout. To reflect this variability and ensure a more realistic acoustic treatment, 50 sound source positions were sampled within the stage area of the Theatre Hall. The same analysis was applied to each position to determine which wall and ceiling surfaces are most likely to contribute to early reflections reaching the audience and which are more involved in delivering late reflections. This approach enables absorber placement to be optimized across multiple performance conditions, resulting in a more balanced and adaptable design. It also reduces the occurrence of excessive early reflections from acoustically critical surfaces, regardless of the precise source location, making the design better for real-world applicability.

To implement this, the stage area in the digital model was defined and populated with 1000 candidate points, varying in both horizontal (X, Y) and vertical (Z) coordinates to reflect differences in sound source height. Since performers are more likely to be positioned near the center of the stage rather than near its edges or near to the walls, a probabilistic sampling method was applied. A custom Python script was developed to select 50 sound source locations based on a Gaussian-weighted distribution, giving points closer to the center a higher likelihood of being chosen, while reducing the probability for points further away from the center. This ensures a realistic spatial distribution of sources, better representing typical performance conditions.

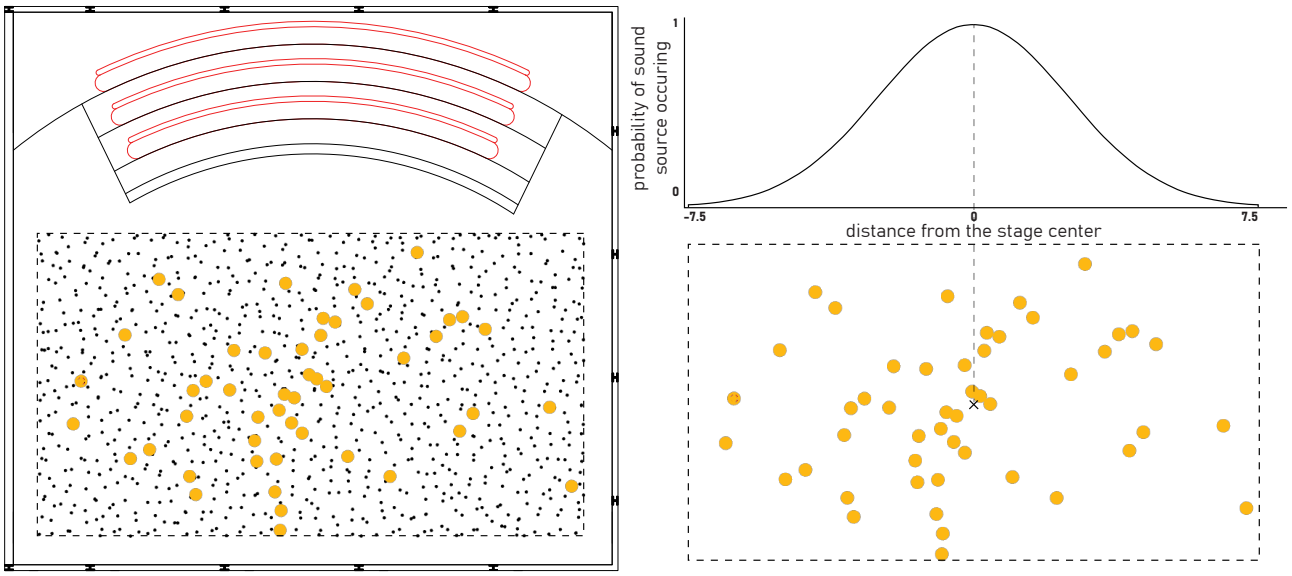

Fig. 4.15. Scheme of randomly selected 50 sound sources from 1000 generated points within the stage area. The selected sources vary in height and follow a Gaussian distribution, with points nearer to the center of the manually defined stage area having a higher probability of being chosen.

A similar analysis was conducted, this time taking into account reflection points from all 50 sound source positions. While it was expected that the general locations of early reflections would remain relatively consistent, the distribution of reflection points became noticeably denser compared to the single-source scenario. As a result, a greater area of absorptive material was applied. Another simulation was performed in CATT-Acoustic. Despite the use of nearly three times more absorbing surface, the RT and G-strength G showed minimal change. A further reduction in C80 was observed, particularly in the 500–1000 Hz frequency range, supporting the effectiveness of the applied strategy.

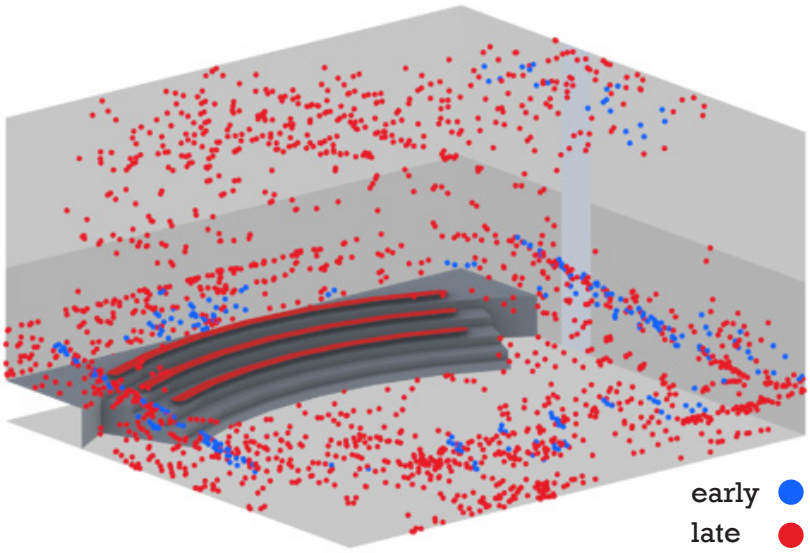

Fig. 4.16. Reflection points with 50 random sound sources.
Including 50 source positions resulted in a denser distribution of early reflection points and a broader application of absorptive material

Panel geometry design

Building upon the previous analysis and aiming to develop a solution that is also architecturally engaging, the wall surfaces of the Theatre Hall were subdivided into a hexagonal pattern. By mapping the early reflection points onto these surfaces, only the wall areas receiving early sound energy were marked for treatment. A similar mapping was conducted for later reflections.

However, in many cases, points of early reflections overlapped with those of valuable late reflections. To avoid undesired reductions in reverberation time, a compromise was introduced: absorbing elements were applied only in areas exposed predominantly to early reflections, while regions contributing to beneficial late reflections were excluded. In practice, this was done by removing segments of the pattern that intersected with late reflection paths. The step-by-step shaping process is illustrated in Figure 4.17.

After identifying all hexagonal cells where early reflections occurred, a total of 125 panels were selected, covering approximately 73 m² of absorbing surface. However, covering such a large area with absorptive material had the opposite effect than intended, resulting in a deterioration of the C80 index (Figure 4.19). To refine the approach, the selection criteria were tightened by considering only cells where early reflections were denser - intersected by more than one sound path. This reduced the number of panels to 81 and the absorbing area to about 43 m², but the C80 value was still worse than in the untreated scenario.

In a final iteration, only cells intersected by more than three early reflection paths were retained, resulting in 51 panels and approximately 29 m² of absorbing surface. As shown in Figure 4.19, this configuration led to a noticeable improvement in C80 in mid-frequencies, a slight increase in RT, and minimal impact on G-strength. Based on these balanced results, the configuration with 51 panels was selected for further development.

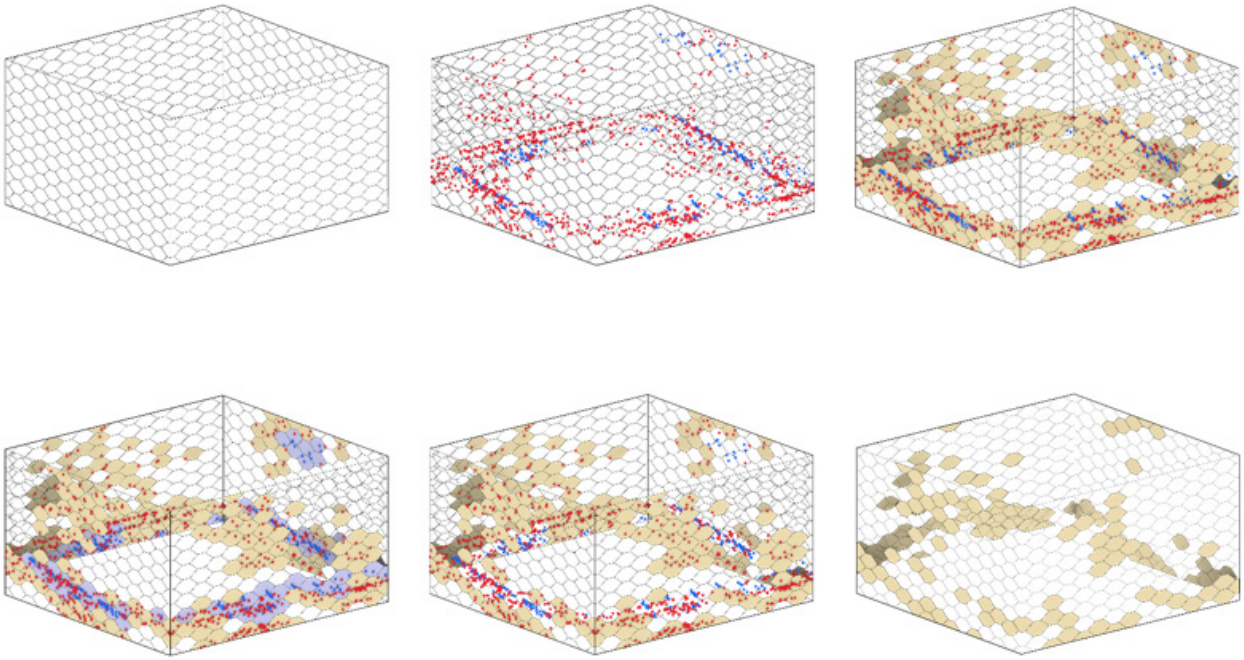

Fig. 4.17. Scheme illustrating the panel shaping process: a) division of the walls into a hexagonal cell pattern; b) mapping of points where both early and late reflections occur; c–e) selective placement of panels in regions exposed to early reflections, avoiding areas with predominantly late reflections; f) resulting panel distribution.

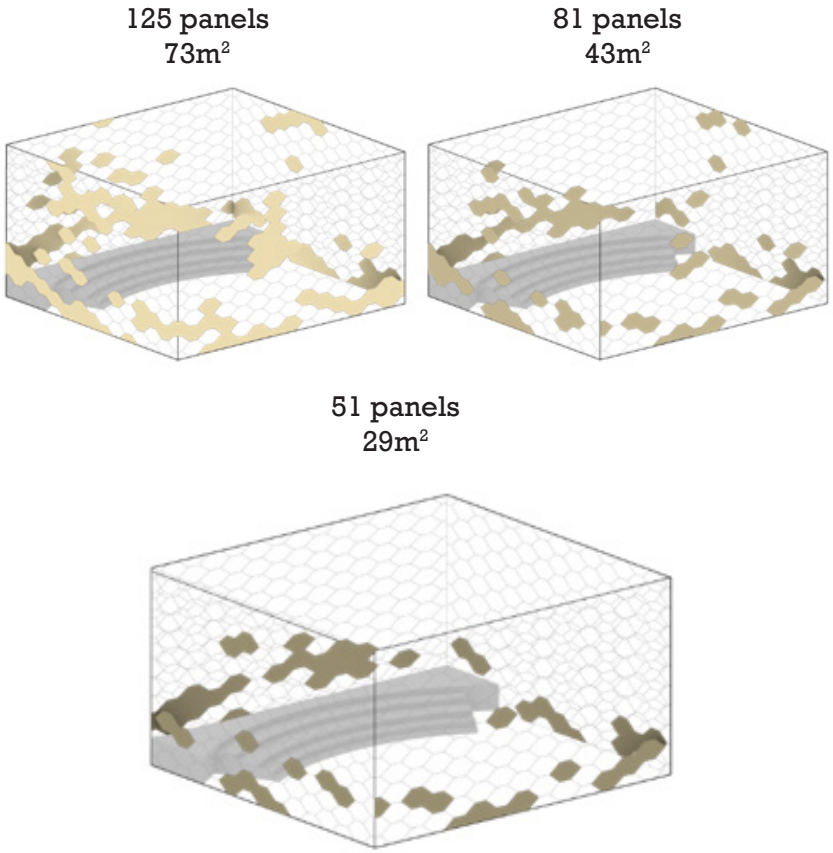

Fig. 4.18. Number of panels selected based on the intensity of early sound reflections. A total of 125 panels are included when at least one intersection point with early reflection paths occurs; this is reduced to 81 panels for more than two points, and to 51 panels for more than three points.

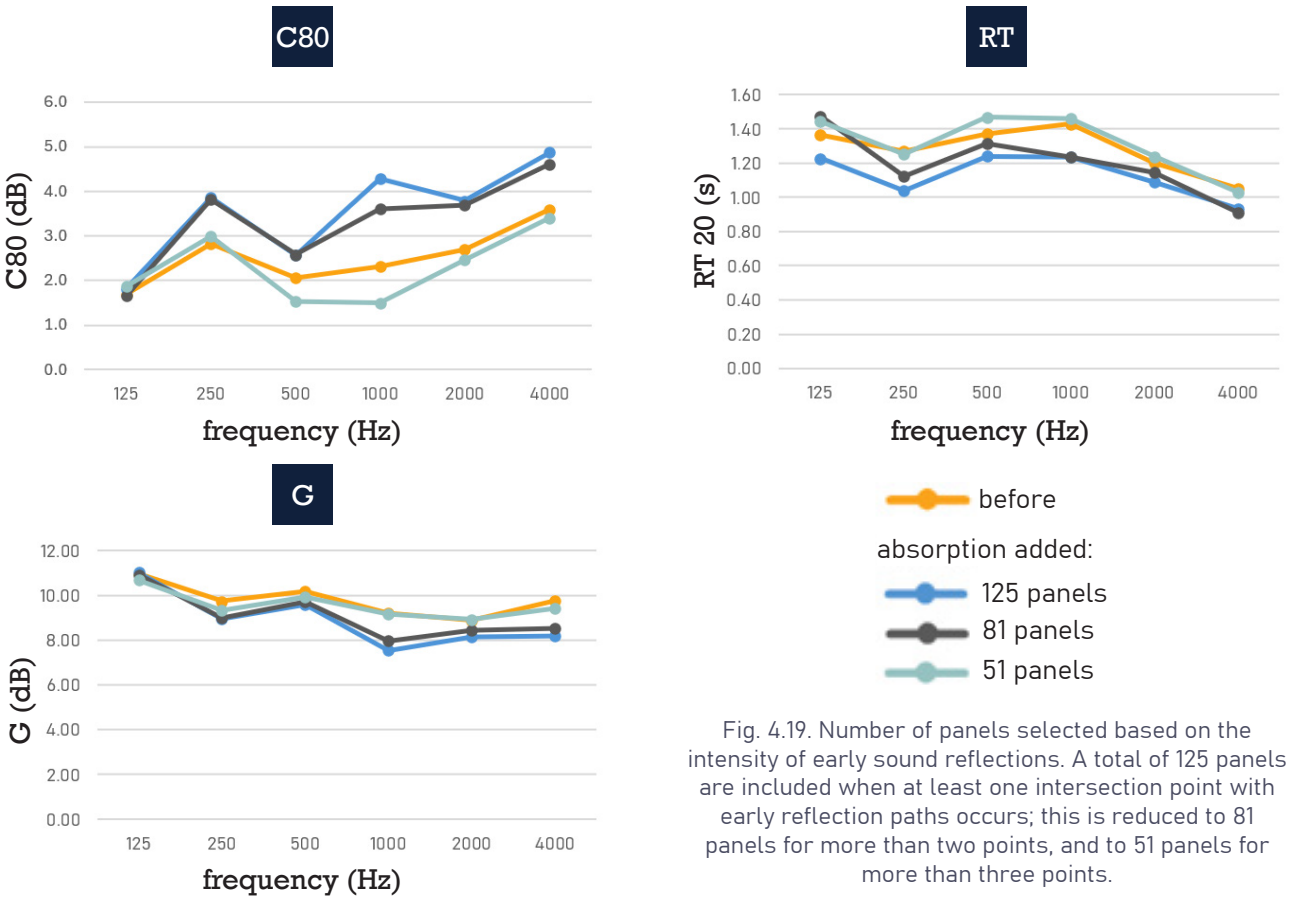

Fig. 4.19. Number of panels selected based on the intensity of early sound reflections. A total of 125 panels are included when at least one intersection point with early reflection paths occurs; this is reduced to 81 panels for more than two points, and to 51 panels for more than three points.

Previously, the absorptive panels were considered flat elements. As demonstrated above, these panels are most effective in the mid-to-high frequency range; however, they do not absorb all incident sound. To further reduce C80, and potentially the G-strength as well, reflected sound can be diffused by scattering it into multiple weaker reflections across various directions, thereby promoting a more uniform sound field. This can be achieved by introducing geometric irregularities that minimize strong, direct reflections. To incorporate this, once the absorptive surface areas were identified, their geometry was further articulated. Each hexagonal cell was subdivided into triangles, and the central point of the hexagon was moved inward. This caused all triangular segments connected to that point to rotate toward the room's interior, forming pyramid-like structures as presented in Figure 4.20. Constructed from the same absorptive material, these shaped panels could not only target early reflections more effectively but also introduce spatial depth, texture, and architectural rhythm to the wall surfaces. Additionally, they may function as diffusive elements, contributing positively to the room's acoustic environment.

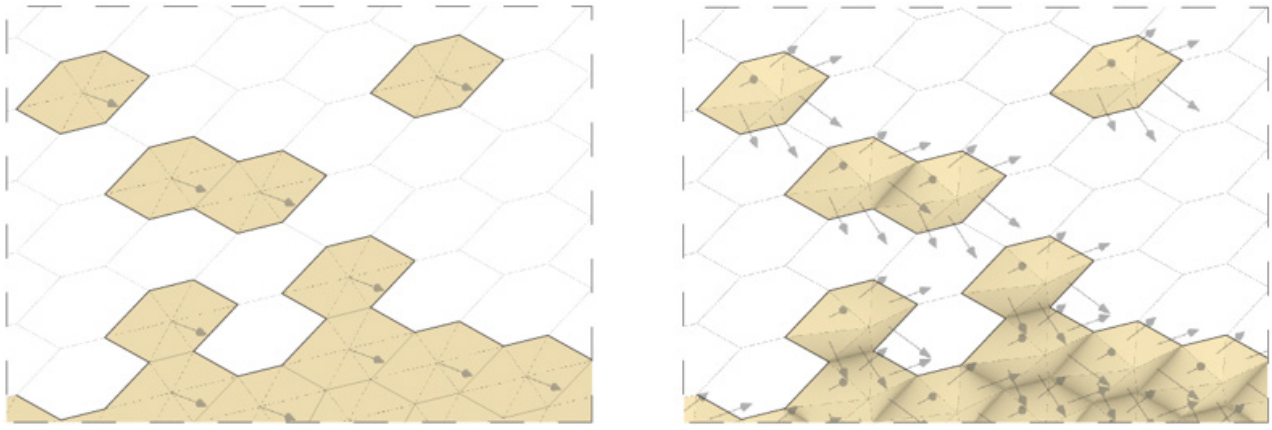

Fig. 4.20. Scheme illustrating the shaping of concavo-convex wall surfaces by forming pyramid-like panels through inward displacement of each hexagon's center point.

While this shaping strategy helped reduce the G- strength, it increased C80, likely due to the shortened reflections paths caused by the pyramidal geometry.

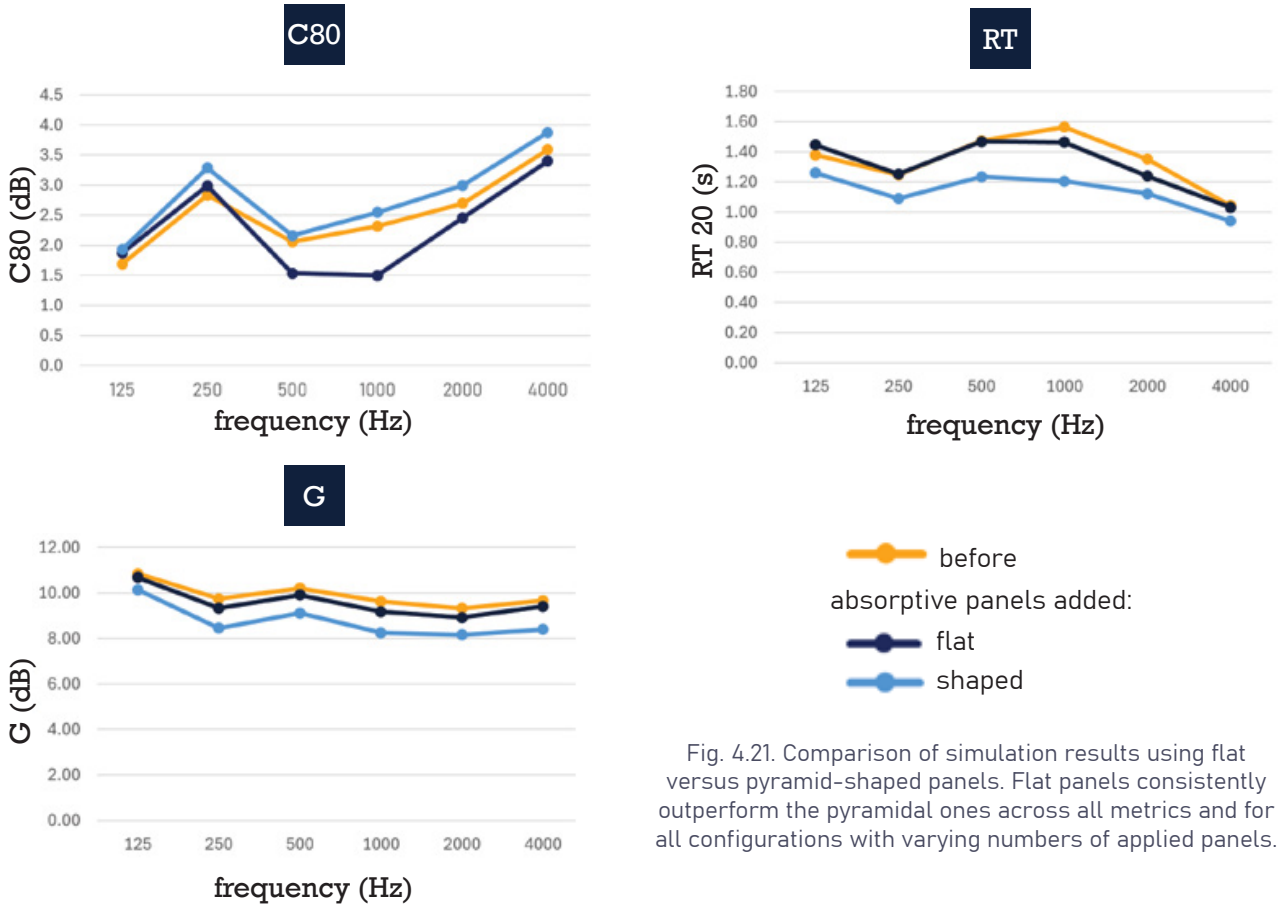

Fig. 4.21. Comparison of simulation results using flat versus pyramid-shaped panels. Flat panels consistently outperform the pyramidal ones across all metrics and for all configurations with varying numbers of applied panels.

Reflective surfaces placement suggestions

In contrast to the previously discussed approach, where absorptive material was introduced to reduce C80 by minimizing early reflections, this part of the study aims to achieve the same goal, but through introducing reflective surfaces. They are designed to either redirect early reflections away from the audience or extend their paths, so that they arrive later than 80 ms after sound emission. This would help balance the early-to-late energy ratio and thereby reduce C80. The search for effective solutions followed a trial-and-error approach, though the options tested were not random. Using the time-trace function in CATT-A and drawing inspiration from well-regarded acoustic spaces, panel placements were strategically explored to either extend the sound path or delay its arrival at the listener, thereby reducing early reflections.

The key strategies tested included:

- Canopies placed above the orchestra to block reflections toward the ceiling, or above the audience to capture and redirect early ceiling reflections (Figure 4.22c, 4.22d),
- Reflective side wall panels to lengthen the path of lateral reflections and promote later energy arrival,
- Reflective barriers between the stage and audience to bounce early reflections back towards the orchestra, delaying their arrival to the audience (Figure 4.22a, 4.22b),
- Diffusive elements placed on rear or side walls (behind both the audience and orchestra) to scatter intense reflections and promote a more even sound field.

Most options produced only minor improvements, some of them didn't even improve the situation at all, stressing the difficulty of changing the ratio of early to late reflections in such a small room. A

full overview of all tested configurations and their simulation outcomes is included in the Appendix.

The stage-audience panels seem to be the most effective for reducing C80 in the occupied scenario (Figure 4.22b). Their application resulted also in a slight reduction in G-strength, and a minor influence on RT.

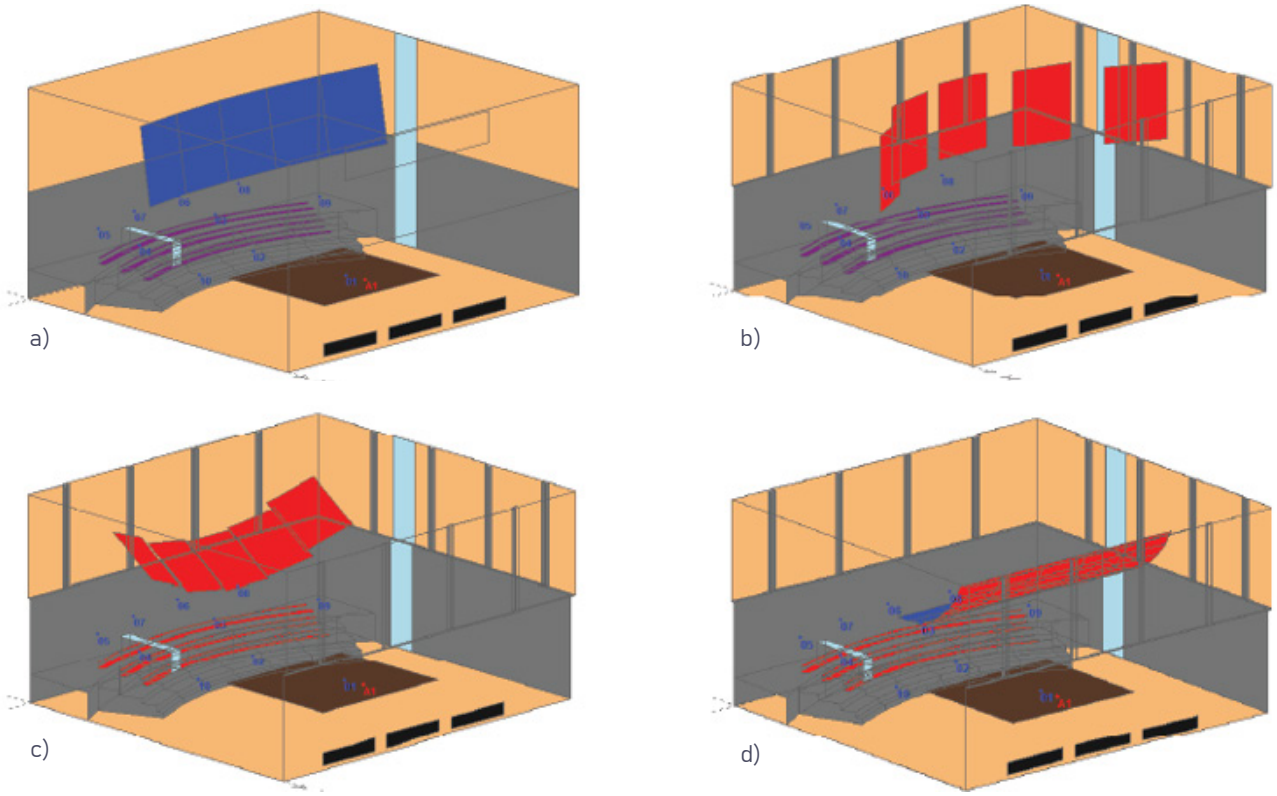

Fig. 4.22. Selected design options tested for improving clarity in the Theatre Hall.
All configurations, along with their corresponding results, are presented in the Appendix.

Design optimization

Using the early/late reflections classification described earlier in this chapter, the SPL was calculated separately for early and late reflections. The ratio between these two served as a simplified estimate of the C80 clarity index within Aeolus. To evaluate the performance of each panel configuration, the mean squared error (MSE) was calculated based on a target early-to-late energy ratio corresponding to C80 = 0.6 dB. This target was previously identified as the "ideal" value for the Theatre Hall, derived from the adapted C80–G correlation diagram. Higher MSE values indicated greater deviation from this values. MSE values exceeding 1 suggested that most tested configurations remained far from the optimal option.

To optimize panel performance, Galapagos was employed within Grasshopper. Galapagos is a single-objective evolutionary solver based on a genetic algorithm. The solver requires the definition of a fitness function, which in this case was the minimization of the MSE. The number of solutions evaluated in each generation (population size) was set to 50. Each individual in the population was defined by a set of genome values.

The input geometry for optimization consisted of reflective panels that were added to the acoustic scene. These panels were parametrically controlled in Grasshopper. The genes (variables subject to optimization) included the angle of rotation of the surface around the orchestra (0–45° in 1° increments) and the curvature of the panel, defined by an arch shape (-0.5 m to 0.5 m in 0.1 m increments) and rotation of each panel around its vertical symmetry axis (0 - 90° in 1° increments) as illustrated in Figure 4.23. Each genome was controlled with sliders in Grasshopper and evaluated

based on its effect on the acoustic performance (fitness function).

After running the solver, the difference between the best and worst solutions was slight, the change was of the order 0.1 in the MSE. The optimized option was checked for its effectiveness in CATT-A and compared against a scenario where the reflective panels were placed randomly.

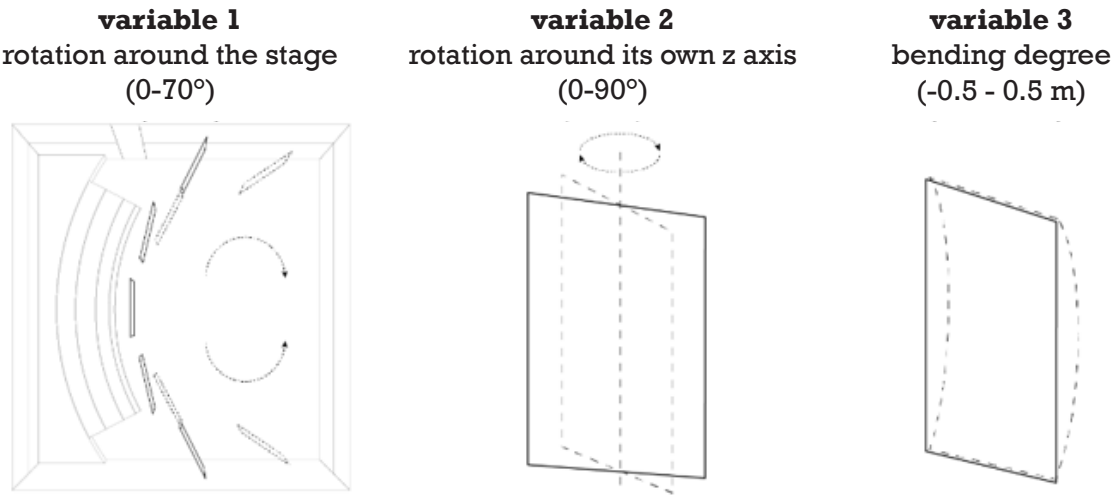

Fig. 4.23. Scheme of variables used in the optimization of reflective panels: symmetrical rotation around the stage area, independent rotation around each panel's vertical axis, and the degree of bending applied to the panel surfaces.

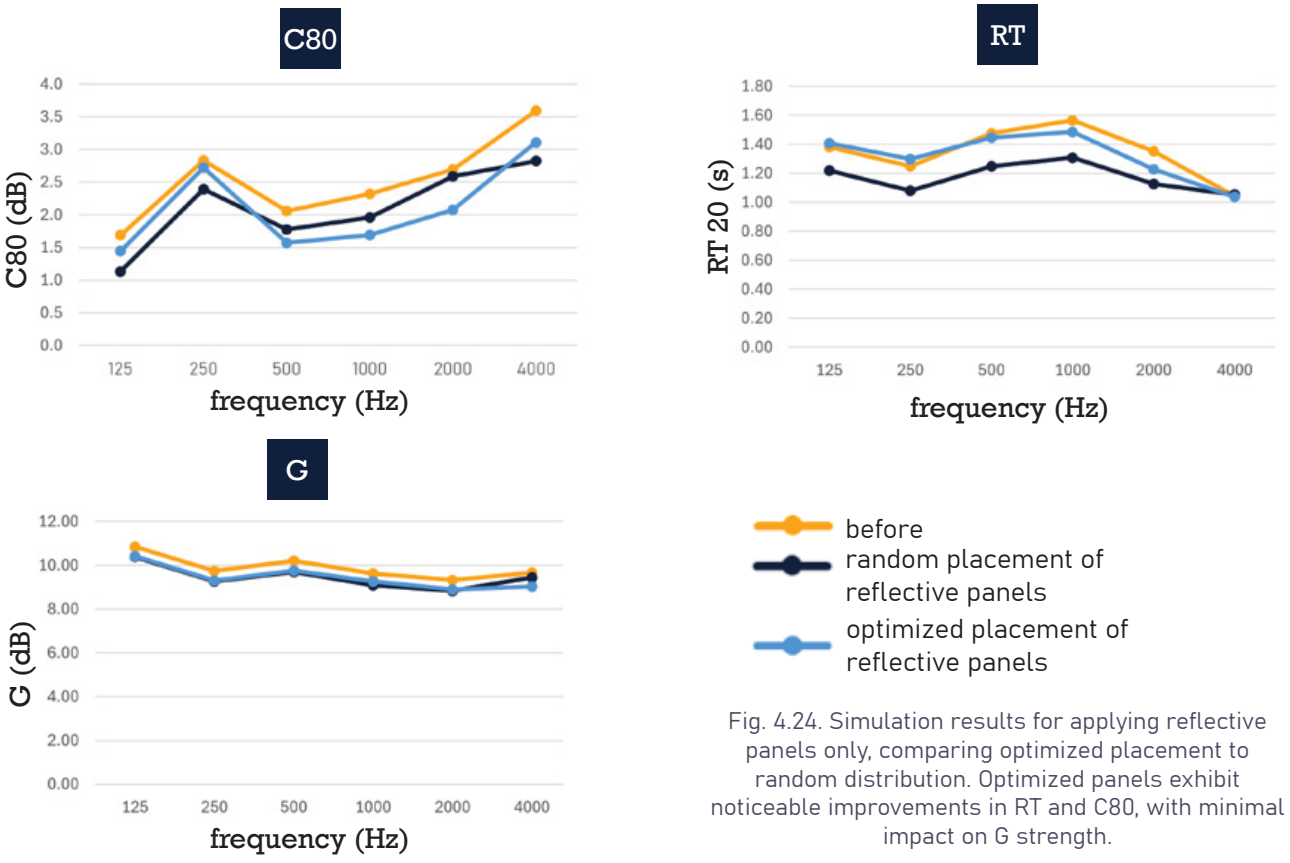

Fig. 4.24. Simulation results for applying reflective panels only, comparing optimized placement to random distribution. Optimized panels exhibit noticeable improvements in RT and C80, with minimal impact on G strength.

As shown in the graphs in Figure 4.24, both random and optimized panel distributions led to improvements across all three evaluated metrics, with the optimized configuration performing more effectively overall. For C80, a significant improvement is observed from the 500 Hz octave

band and above. In terms of RT, the random panel placement caused a noticeable reduction, an undesirable effect, whereas the optimized configuration had minimal impact, with only a slight decrease around 2000 Hz. Regarding G, both configurations resulted in slight improvements, likely negligible or just at the threshold of the JND according to psychoacoustic criteria.

The design application combined material science, computational acoustics, and design optimization in a holistic approach to address the specific acoustic challenges of the Theatre Hall. The primary objective was to reduce C80 without significantly compromising RT, a critical balance in spaces designed for musical performance.

The goal was partially achieved, as the resulting C80 values remained above the previously defined optimal target of 0.6 dB. However, the optimized panel configuration and the targeted placement of absorption, described in the report, resulted in a measurable reduction in C80 within its JND range at key mid-frequency bands (500, 1000, and 2000 Hz), while preserving RT within acceptable bounds. Although the overall improvements were moderate, this reflects the acoustic constraints of the chosen case study. In alternative settings, such as lecture halls where lowering RT for clearer speech is the priority, better acoustic improvements would likely be achievable.

Crucially, the integration of a computational workflow made this outcome possible. The combination of parametric design tools, simulation software, and design optimization enabled rapid iteration and evaluation of panel configurations. This digital approach was grounded in real-world acoustic measurements, which were used to calibrate and validate the simulation model, ensuring its accuracy and reliability.

Together, this workflow facilitated a data-driven, performance-oriented design process. It allowed for the development of a targeted acoustic intervention, carefully placed panels that effectively reduce excessive clarity without over-dampening the space, demonstrating how digital methods and experimental validation can be successfully merged in architectural acoustics.

In the context of the Theatre Hall, careful attention had to be paid to avoid over-absorption and the risk of creating an acoustically dry space. The developed panels proved effective in addressing this need, offering targeted acoustic treatment that mitigates problematic reflections without negatively impacting the hall's reverberant qualities.

Fig. 4.25. Visualization of the proposed acoustic panel design integrated into the Theatre Hall, own work. The image illustrates the final design application of the porous panels within the Theatre Hall.

4.3. Production process

Even though understanding was gained on how different manufacturing parameters affect the sample, controlling foam properties proved to be complex, with occasional unexpected results that couldn't always be expected or explained. Whenever unusual results occurred, experiments were repeated to verify outcomes. For instance, the first SL5CCT2 sample turned out denser and less foamed than expected, despite using the same material and conditions that had worked in smaller moulds. A second attempt produced much better foaming and ultimately the best sound absorption result. This experience highlights the inherent randomness in foaming, despite careful control, results were not always repeatable. Factors such as uneven foaming agent distribution, possibly local temperature fluctuations, or unpredictable chemical reactions during firing likely contributed to these inconsistencies. The variability of recycled glass waste and the unpredictability of the foaming process pose challenges for standardizing production.

From a design perspective, some of the proposed panel geometries in this thesis include more complex forms, for example curved. While these are feasible with cast glass, they raise a crucial question: to what extent can such geometries be achieved with foam glass? Given its brittle nature, foam glass may offer less flexibility in terms of shaping compared to cast glass.

This leads to additional considerations around the fusing process. While single-step fusing (foaming the porous layer and combining it with the solid one in one firing) proved promising in reducing energy use and processing time, it may not always be viable, particularly when the solid layer requires complex geometry. In such cases, a two-step approach may be necessary: casting the solid layer first at a higher temperature, then adding the foaming mixture in a secondary firing cycle on top of the solid glass geometry. A possible alternative could involve casting the lower glass layer at its required high temperature, then partially cooling the kiln before introducing the foaming layer and continuing the process at the foaming temperature. While theoretically plausible, this approach would require careful thermal control and logistical coordination.

Beyond manufacturing considerations, several practical limitations emerged regarding the real-world applicability of the panels. While they hold a strong potential for indoor acoustic use, their open-porous structure makes them prone to dust accumulation and difficult to clean. That would be an important challenge when considering their commercial release. This issue also raises the question of whether such panels could be adapted for outdoor environments, where exposure to moisture, dirt, and pollution could further compromise their durability. In addition, while the Cyclon mix samples were particularly prone to crumbling, all tested (foamed) panels exhibited some degree of surface degradation. This observation highlights the need to improve the mechanical integrity of the material to ensure reliable, long-term performance in architectural applications. Without such reinforcement, surface wear and structural fragility could limit the panels' durability, especially in high-traffic or exposed environments.

4.3.1. Feasibility check

Prototype

A prototype was developed to address geometry considerations, using a curved form as the basis for testing. As detailed earlier in the report, the mould was 3D printed and cast with Crystal Cast, featuring a curved base to shape the glass accordingly. Two fabrication approaches were explored.

In the first, single-step method, a flat solid glass piece was placed into the mould (Figure 4.26), with the foaming mixture, composed of light bulb glass and 2.5 wt% eggshells, poured on top. The sample was fired using firing schedule 1 (860 °C with a one-hour dwell time), allowing the slumping of the solid layer, foaming, and fusing to occur simultaneously. During firing, the solid glass conformed to the mould's curvature while the foaming mixture expanded, resulting in a cohesive, curved panel. The layers bonded successfully, with the porous texture clearly visible through the solid layer,

producing a visually appealing aesthetic. The outcome of this process is shown in Figure 4.27 (before post-processing) and Figure 4.28 (after polishing the solid surface).

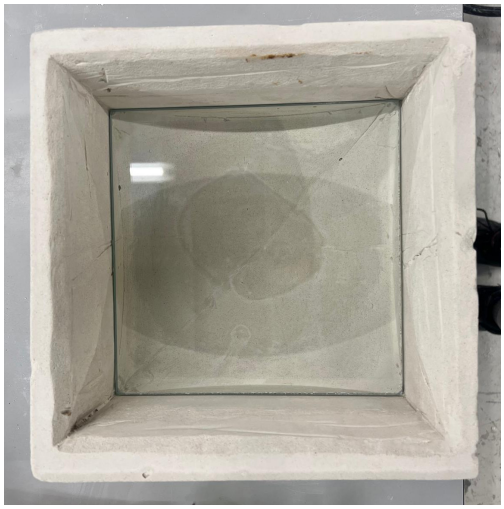

Fig. 4.26. Curved mould with a flat glass layer positioned inside to enable slumping, prior to adding the foaming mixture on top.

Fig. 4.27. Prototype of a single-step fused and foamed panel before post-processing. A curved panel produced by placing solid glass at the bottom of the mould and the foaming mixture on top. This image shows the result prior to polishing the solid surface.

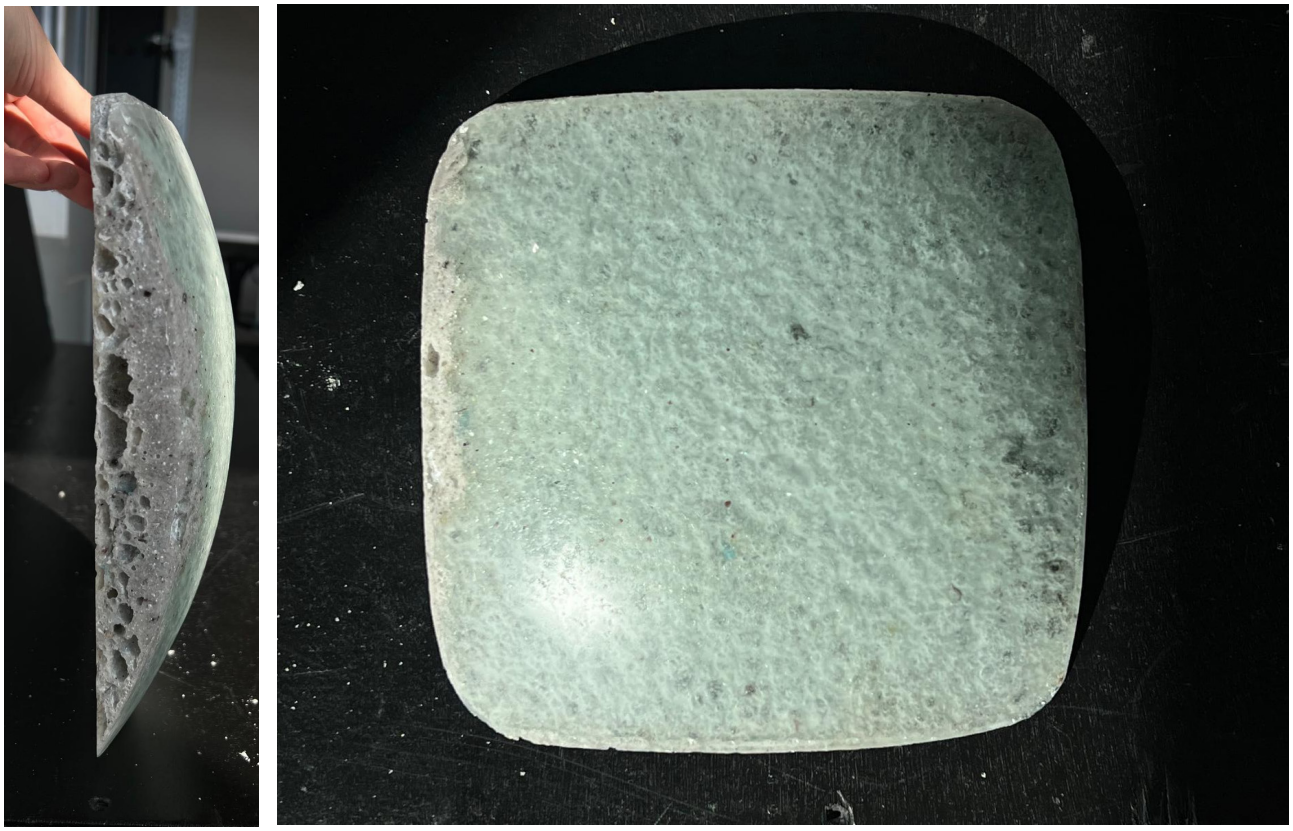

Fig. 4.28. Final prototype after post-processing. The single-step fused and foamed panel after polishing the solid glass surface. The result is a unified, curved element combining a transparent solid layer with a porous backing, demonstrating both structural integrity and acoustic potential.

In the second, two-step method, the foaming mixture, this time consisting of mixed cullet and 2.5 wt% eggshells, was first fired alone in the curved mould using the same firing schedule 1. Although the composition and temperature were identical to those used successfully in earlier tests, the sample exhibited only minimal foaming, forming a denser structure with small, sparsely distributed pores. Afterward, the porous layer was placed back into the kiln with a flat solid glass layer on top and re-fired in 705 °C for one hour to enable slumping and tack fusing, as presented in Figure 4.29. While the solid glass slumped as intended to follow the curvature of the porous layer (Figure 4.30), the layers did not successfully bond. This outcome may suggest that, although the firing schedule was effective for smaller-scale samples, it is insufficient for larger or more massive elements. A higher temperature or extended dwell time might be required to ensure proper tack fusion in this configuration.

Fig. 4.29. Setup for two-step fabrication approach using a curved mould (own work). The foamed porous layer was first created separately, then reinserted into the kiln with a solid glass sheet on top for slumping and tack fusing.

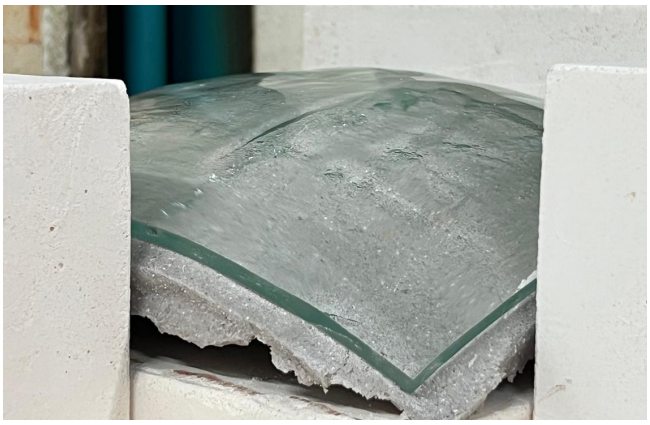

Fig. 4.30. In the two-step fusing process, after the second firing, the solid glass layer successfully slumped and conformed to the curved shape of the underlying foamed layer. However, the two layers did not bond together.

Refoaming potential

As part of the experimental exploration, an attempt was made to refoam previously foamed samples to assess whether additional porosity could be introduced in a second firing without adding more foaming agent. Two types of pre-foamed materials were tested: light bulb glass and low-iron soda lime glass. The light bulb glass samples showed promising results, after being crushed and re-fired without additional foaming agent, the material exhibited further expansion, suggesting that foaming potential remained (Figure 4.31).

In contrast, the low-iron soda lime sample did not respond to refoaming. After the second firing, the material retained the cubic shape of the mould and was opaque, rough in texture outside, but smooth on the inside, lacking a glossy surface (Figure 4.32). This suggests that, in the case of soda lime glass, the initial firing likely exhausted the foaming capacity, and additional porosity cannot be achieved without reintroducing a foaming agent. However, these conclusions are based on a single test, and further experiments would be necessary to fully evaluate the refoaming potential of both materials.

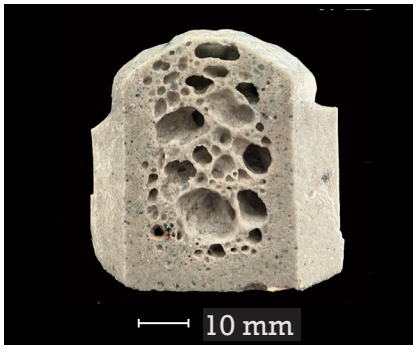

Fig. 4.31. Light bulb glass after refoaming – visible porous structure indicates successful secondary foaming.

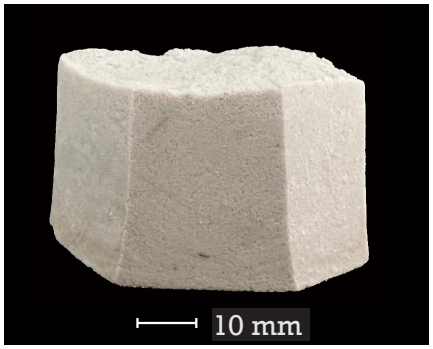

Fig. 4.32.Low-iron soda-lime glass after refoaming; no visible pores formed, but the sample retained a smooth and uniform internal structure.

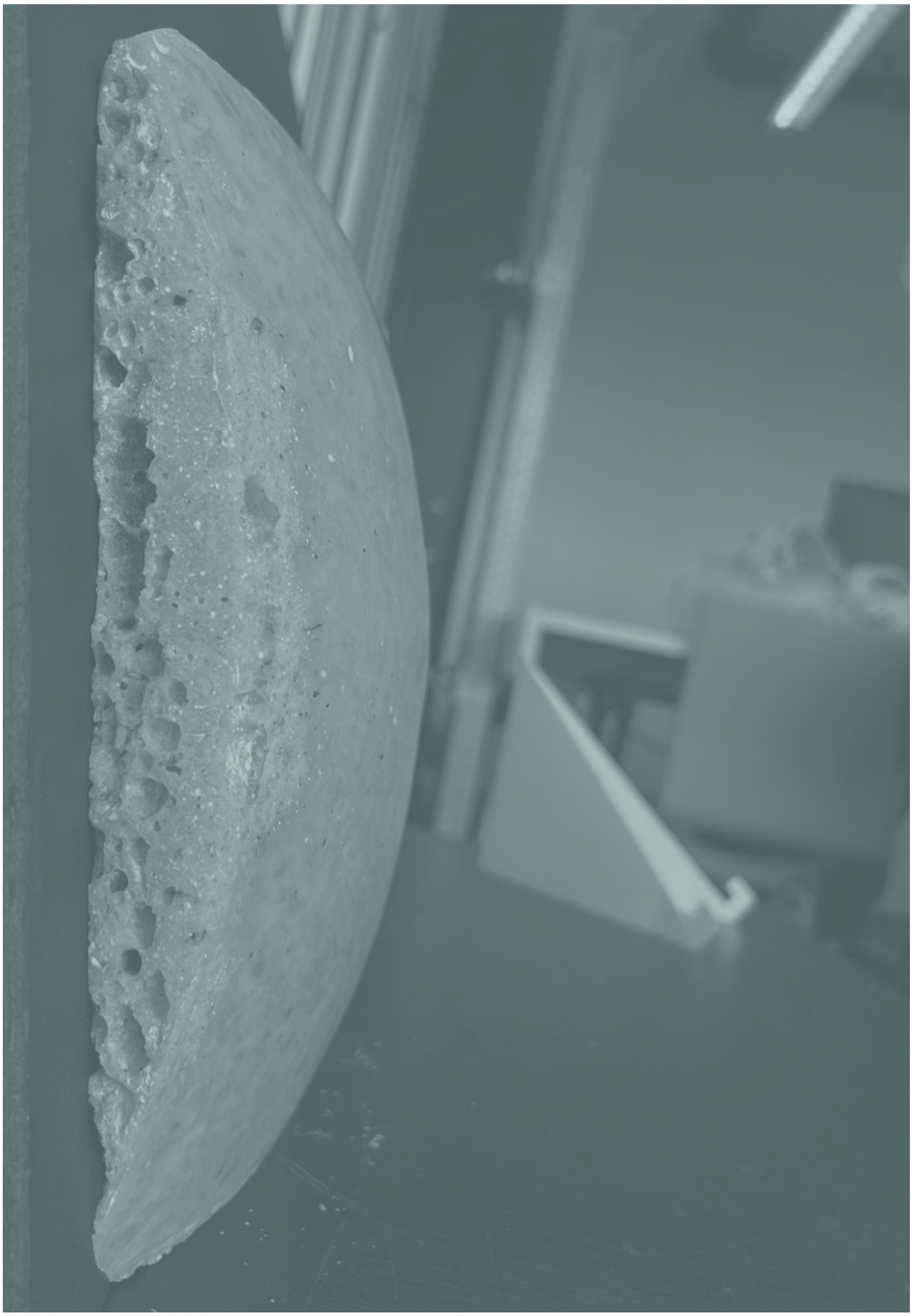

5 | CONCLUSION

5. Conclusion

This chapter synthesizes the insights gained throughout the research, connecting the experimental material development with its architectural implementation. The objective was not only to prove that glass waste can be repurposed into acoustically functional panels, but also to test whether such material innovation can address real world performance needs in architectural spaces.

5.1. Key findings summary

By integrating physical prototyping with computational simulations and design optimization, this study evaluated both the feasibility and performance of the proposed solution within a real-world case study. The following sections summarize the key findings from each stage of the project, including foaming and fusing experiments, acoustic performance testing, and architectural application, addressing the corresponding sub-questions of the research and finally leading to an answer to the main research question.

5.1.1. Foaming

Foaming was chosen as a method of obtaining porosity in glass crucial for sound absorption. It was achieved by introducing different foaming agents into glass and firing the mixtures at controlled temperatures.

Regarding foaming, the research focused on **glass waste streams are well suited for foaming**. To identify suitable candidates, five types of waste glass were tested: soda lime (low-iron float glass), light bulb glass, automotive windshield glass, aluminosilicate phone screens, and Cyclon mix. The selection was guided by both the volume of waste produced and the specific challenges each type poses to recycling. Soda lime glass was included due to its high prevalence, while the other types were chosen for their recycling complexity, including contamination with metals and coatings, composite structures, and the lack of established infrastructure for separation and recovery.

Among the tested foaming agents, both pure calcium carbonate and eggshells proved effective in generating porosity across various glass types. The most consistent and controllable results, however, were achieved by combining low-iron soda lime cullet with either of the two foaming agents. These combinations offered the best responsiveness to adjustments in foaming agent concentration and firing schedules, making them a reliable option for further development.

Nonetheless, low-iron soda lime cullet represented the cleanest glass type used in the study, serving as a reliable reference material. Light bulb glass and mixed cullet should be considered promising alternatives, as one of the core objectives was to evaluate **whether contaminated glass waste could perform comparably to clean cullet**. Despite their high levels of contamination, both glass types exhibited the ability to develop well-structured porosity and offered some degree of control over pore formation, highlighting their potential for upcycling into functional acoustic materials.

In terms of pore structure, while both foaming agents, pure calcium carbonate and eggshells, were similarly effective in creating porosity, eggshells tended to produce more homogeneous pore networks compared to pure calcium carbonate.

(How) do different fabrication parameters impact the porosity of the material and (how) can its porosity be controlled?

The experiments demonstrated that manufacturing parameters significantly influence the quality and structure of the foamed samples. Variables such as the type of glass waste and foaming agent, particle sizes of these components, the firing schedule, and the foaming temperature, all played critical roles in determining the final outcome.

Three types of glass waste (low-iron soda lime cullet, light bulb glass, and contaminated mixed cullet) were used extensively in testing. All three materials were shown to foam effectively when combined with either pure calcium carbonate or eggshells as foaming agents. Across all tested samples, an increase in the foaming agent concentration consistently resulted in the formation of larger pores for low-iron soda lime and mixed cullet, but the opposite trend was observed in light bulb glass.

The firing schedule had a significant impact on the foaming outcomes. For soda-lime and mixed cullet light bulb glass, higher temperatures generally resulted in smaller pores. In contrast, the Cyclon mix, although it did not foam in the same way as the other glass types, showed a strong dependency on temperature in terms of structural integrity: at lower firing temperatures, the samples were more prone to crumbling, while higher temperatures improved their cohesion.

Additionally, the particle size of the foaming agent influenced the porosity type. When the agent was used in powder form, pores were more evenly distributed throughout the sample. In contrast, coarser foaming agent particles produced larger, irregular, and closed pores, as foaming occured only locally. Optimal foaming results were obtained using powdered glass; larger fragments of cullet did not foam successfully.

What are the optimal physical parameters in the process of fabricating a recycled glass panel?

Based on the conducted experiments, the optimal manufacturing parameters for successful foaming across all tested glass types were identified as follows: using 2.5 wt% of a foaming agent (either eggshells or pure calcium carbonate) combined with a firing schedule reaching a maximum temperature of 790 °C and a dwell time of 2 hours. This parameter set proved effective for foaming low-iron soda lime glass, light bulb glass, and mixed cullet, and may serve as a reliable baseline for further experimentation.

To assess the impact of contamination on the foaming process, the cleanest cullet (low-iron soda lime) was compared with the most contaminated waste streams used in the study (mixed glass cullet and light bulb glass). Despite differences in composition and impurity levels, all three types successfully foamed, resulting in distinct yet well-developed porous structures. Among them, the light bulb glass samples exhibited the largest pores, indicating that even highly contaminated glass waste can be transformed into effective porous materials suitable for further application.

5.1.2. Fusing

Porous glass samples were successfully produced through foaming techniques to enable sound absorption, while fusing them with a solid glass layer provided the necessary rigidity. However, the structural performance of the resulting panels was not validated through mechanical testing; future studies will be needed to confirm their suitability and safety for architectural applications.

The fusing experiments confirmed the feasibility of producing dual-layer glass panels by bonding porous foam glass to a solid float glass layer. Two methods were explored: tack fusing performed after foaming, and a combined foaming–fusing process conducted in a single firing cycle. In both cases, porous samples made from either light bulb glass or low-iron soda lime glass were fused with flat float glass. Tack fusing, performed at a relatively low temperature of 705 °C with a dwell time of one hour, successfully preserved the porous structure, ensuring adhesion between the layers.

Simultaneous foaming and fusing was also achievable, both when using continuous glass sheets and cullet. These findings confirmed that a structurally integrated panel could be fabricated without compromising the acoustic functionality of the porous layer. While the mechanical performance of the fused units has not been structurally validated, the process opens promising possibilities for producing architecturally applicable, self-supporting acoustic elements from glass waste.

5.1.3. Acoustic testing

Acoustic testing confirmed that the selected foam glass samples achieved satisfactory levels of sound absorption, particularly in the mid-to-high frequency range. The results indicate that higher open porosity and the presence of larger pores correlate with improved acoustic performance.

In terms of foaming agents, samples produced with pure calcium carbonate consistently outperformed those made with eggshells. Several tested samples exhibited sound absorption coefficients comparable to those of conventional sound absorbing materials like mineral wool, reinforcing the acoustic viability of glass waste-based foams for indoor applications. When considered alongside findings from the foaming experiments, these results help address one of the key research questions guiding this project:

What types of glass waste are suitable for acoustic panel production?

The low-iron soda lime cullet, considered the most reliable option, and the more contaminated mixed cullet both achieved peak sound absorption coefficients (SAC) of 1.0 at mid-to-high frequencies, specifically around 1000 Hz and 4000 Hz for the clean cullet, and around 1000 Hz for the mixed cullet. Additionally, light bulb glass, a niche waste stream typically excluded from conventional recycling, also demonstrated promising acoustic performance, reaching SAC values of up to 0.8. This suggests its potential as a viable alternative for sound-absorbing applications.

While before the contamination was assessed in terms of foaming and porosity and was found to not be harmful, the samples made of cleanest and the dirtiest cullet were compared in terms of SAC to asses:

(How) do impurities in glass waste affect the material's acoustic performance?

The results indicate that contamination in the glass does not necessarily hinder sound absorption performance. Both the clean low-iron soda lime and the highly contaminated mixed cullet samples exhibited the highest peak SAC values among all tested materials, reaching up to 1. Light bulb glass, also considered a contaminated waste stream, performed slightly less effectively but still achieved a sound absorption coefficient of up to 80%, proving its potential as a viable acoustic material.

What are the effects of porosity on the panel's acoustic properties?

Across all tested samples, a clear trend was observed: larger pore sizes correlated with improved sound absorption performance. Additionally, samples produced using pure calcium carbonate exhibited a more tortuous, irregular, and rough pore structure, which consistently resulted in higher SAC values compared to the more uniform and homogenous pore networks formed in samples manufactured with eggshells.

5.1.4. Design application

In the design phase, the measured acoustic properties from impedance tube tests were applied to panels integrated into a 3D model of the Theatre Hall, developed using CATT-Acoustic and Grasshopper, to evaluate:

How to optimally integrate the panels into an existing space to improve its acoustic performance?

First, the key acoustic issues in the Theatre Hall were identified by focusing on three main performance metrics: clarity index C80, reverberation time RT, and G-strength G. Among these, the clarity index was found to be excessively high, particularly in the simulated occupied scenario, indicating a disproportion in early-to-late energy distribution. As a result, targeted design strategies were implemented to reduce C80, while carefully monitoring RT and G-strength to avoid compromising overall acoustic quality. The aim was to achieve a balanced sound environment suitable for both

rehearsal and performance conditions.

To address the excessive C80 problem, absorbing panels were placed on the walls of the Theatre Hall in areas most responsible for directing early reflections toward the listener - the primary factor influencing C80. In order to asses:

What are the effects of panel's geometry design on its acoustic properties?

two geometric approaches were tested: flat panels and pyramid-shaped extruded panels designed to enhance diffusion. The latter configuration, however, performed worse, likely due to its tendency to shorten reflection paths and thereby increase C80 rather than reduce it. Although this outcome was unintended, it confirmed the correctness of the panel placement strategy.

In parallel, reflective panel configurations were explored. Several strategies were evaluated, including overhead canopies above the orchestra and audience, reflective side wall panels to lengthen reflection paths, stage-audience barriers to delay early reflections, and rear wall diffusers to scatter strong reflections. These tests demonstrated that panel geometry has a significant impact on acoustic performance.

Among these strategies, the introduction of reflective panels between the stage and audience yielded the most meaningful reduction in C80 in the occupied scenario. This setup provided a balance between C80 and G-strength with minimal impact on RT. Nevertheless, the extent of improvement remained modest, reflecting the challenge of achieving optimal acoustic conditions in a relatively small hall.

To further enhance the design and placement of the panels, a parametric optimization process was conducted using Galapagos. The goal was to approach a target early-to-late energy ratio (C80 ≈ 0.6 dB). The optimization's fitness function was defined as the mean squared error (MSE) from this ideal value, and the algorithm explored variations in panel rotation and curvature to fine-tune performance.

In summary, this research demonstrated the potential of upcycling glass waste, often considered non-recyclable, into acoustic panels using foaming and fusing techniques. It showed that by adjusting parameters such as glass composition, foaming agent, and firing schedule, porosity can be tailored to influence acoustic performance. Impedance tube measurements confirmed the material's sound-absorbing capabilities, and its digital application in a case study proved its architectural viability. Nonetheless, further refinement is needed to address durability concerns, particularly the risk of crumbling in the porous layer, even when fused to a solid backing. Despite these challenges, the study lays a strong foundation for rethinking glass waste as a valuable resource in acoustically demanding environments, advancing both sustainable design and innovative material use. Taking all that into consideration, the answer to the main research question:

What are the potential and limitations of developing a porous material from glass waste to produce acoustic panels for architectural space?

can be summed up as follows:

Potential:

- **Circular material use:** Described approach enables the upcycling of post-consumer and hard-to-recycle glass waste (e.g., soda-lime, light bulbs, and mixed cullet), aligning with sustainability goals and circular economy principles. It reduces landfill waste while providing a functional architectural product made entirely of glass waste that can be re-recycled.

- **Acoustic performance:** The foamed glass panels developed in this study demonstrated effective sound absorption in the mid- to high-frequency range, particularly around 1000 Hz. This makes them well-suited not only for environments requiring musical clarity but also for spaces where speech intelligibility is essential or where excessive reverberation needs to be controlled. Given that this frequency range is acoustically critical for both voice and music, the results underscore the panels' versatility. Notably, even panels produced from contaminated glass types exhibited satisfactory acoustic performance, highlighting the potential for using lower-quality waste streams without compromising functionality.

- **Architectural adaptability:** The combination of foaming, fusing, and parametric design enabled a high degree of geometric flexibility that is difficult to achieve with conventional sound-absorbing materials. This study demonstrated that porous glass panels can be shaped, layered, and configured to meet architectural constraints while also offering strong visual appeal. When designed intelligently, these panels can function not only as absorbers, but also as diffusers or hybrid reflectors, expanding their acoustic functionality and aesthetic potential within interior spaces.

- **Integration with computational design:** The method integrates real-world acoustic measurements with simulation tools like CATT-Acoustic and parametric modelling in Grasshopper, enabling iterative design and optimization of panel placement and geometry. This allows targeted acoustic interventions that improve clarity without compromising reverberation or spatial aesthetics. Tools like Galapagos automate the search for optimal configurations, supporting data-driven decisions. By combining material science, acoustic performance tuning, and architectural design, the workflow enables scalable solutions for complex acoustic environments.

Limitations:

- **Foaming sensitivity:** The foaming process is highly sensitive to multiple variables, including glass composition, particle size, foaming agent type and concentration, and the firing schedule. Even small changes in these parameters can lead to foaming failure or overly dense structures, limiting both predictability and scalability. Although valuable insights were gained into how these factors influence the final outcome, a degree of randomness remains in the foaming reactions, introducing an element of unpredictability that lies beyond human control.

- **Low absorption in low frequencies:** Like most porous absorbers, these panels perform best at higher frequencies. Their effectiveness drops in the low-frequency range, limiting their utility in spaces that require bass control, such as recording studios.

- **Manufacturing challenges:** Achieving consistent pore structures and scaling the production process beyond laboratory conditions presents challenges, particularly in controlling temperature gradients during firing or performing fusing - the creation of double-layer panels adds further complexity, especially in ensuring reliable adhesion between the porous and solid layers, as demonstrated by the prototype tested using the two-step fusing method. Moreover, even samples that achieved successful fusion showed signs of decomposition at their surface. This issue would need to be addressed before the panels can be considered for commercial or architectural deployment.

5.2. Further research suggestions

While this research focused on developing and testing recycled glass panels for their acoustic properties, several additional areas could be explored to broaden the material's architectural applicability. The following suggestions outline potential directions for further research:

5.2.1. Real-scale acoustic testing

While impedance tube is an easy and convenient method for SAC measurements under well controlled conditions, further research could explore the acoustic performance of full-scale panels in other environments such as reverberation chamber that would validate and build upon the laboratory findings, accounting for effects that cannot be caught in the impedance tube such as oblique sound incidence.

5.2.2. Life Cycle Assessment

Conducting a full LCA would allow for environmental evaluation of the recycled glass panels, from waste collection to manufacturing, usage and end-of-life scenarios. This would validate the sustainability of claims, check whether the energy needed for manufacturing the panels at each step of the process do not kill the benefits of recycling glass this way, and allow for better comparison with conventional acoustic materials such as mineral wool panels.

5.2.3. Thermal performance evaluation

Foamed glass is already known for its low thermal conductivity; therefore, future studies should investigate the capabilities of the foamed and cast glass panels serving as a thermal barrier in vertical applications. Then, if possibly such a panel would be a part of the façade, its mechanical strength should be assessed (both the porous and solid layers, as well as the fused unit) to ensure safe architectural implementation.

5.3. Reflection

This chapter reflects on the overall trajectory of the thesis project, from its initial conception to the final outcomes. It assesses the graduation process, addresses ethical considerations, and explores the potential societal impact of the work. The aim is to highlight the strengths and limitations of the chosen approach, examine how challenges were navigated throughout the development, and evaluate the project's broader significance within both architectural and scientific contexts.

5.3.1. Graduation process

The chapter is divided into three parts: the first reflects on the graduation journey and the relationship between the project and the broader context of the Building Technology track; the second examines the research strategy, tools, and methods employed; and the third evaluates the outcomes in relation to the initial goals and research question, with a focus on the interplay between research and design. Together, these reflections offer insights into the effectiveness of the project and the methodology applied.

Relationship between the thesis topic and the Building Technology track

This thesis is situated within the Building Technology Graduation Studio at TU Delft, where it contributes to the broader discussion on sustainable materials and circular design strategies in architecture. The focus on transforming waste glass into functional acoustic panels aligns with the track's emphasis on environmental responsibility and material innovation.

The Building Technology master track at TU Delft integrates architectural and engineering disciplines, with a strong emphasis on sustainability and innovative design thinking. Within this context, glass stands out as a material of both everyday presence and architectural significance.

Glass has long been recognized for its unique properties - its ability to visually connect interior and exterior spaces through transparency, its structural strength, and its excellent performance in compression when cast, all of which have been extensively researched within the AE+T department at TU Delft. I am glad to contribute to this body of work by adding acoustic performance to the list. This material's versatility, combined with its potential for infinite recyclability without degradation, makes it a strong candidate for advancing a circular built environment. Aligned with ongoing research into innovative glass recycling strategies, this graduation project demonstrates that glass can serve as both a smart and sustainable material in the future of architecture.

Research approach and outcomes

The research approach combined material experimentation, acoustic measurements, computational simulation and design-optimization techniques. This interdisciplinary strategy turned out to be a major strength.

- **Strengths:** This approach enabled a holistic investigation of the problem. The iterative experimental process allowed for continuous material refinement based on real measurements and extensive hands-on experience, truly a case of learning by doing. It was especially rewarding to implement the panels I had personally manufactured (even if only in a virtual model), using absorption coefficients I had measured myself, and to see the acoustic performance improve. Furthermore, by focusing on the reuse of glass waste, this project addresses a key technical challenge in glass recycling: contamination. It demonstrates that even low-quality, severely contaminated cullet can be effectively repurposed for sound-absorbing applications, turning a problematic waste stream into a valuable resource.

- **Weaknesses:** Time constraints limited the scope of real-world validation, such as testing in a

reverberation chamber, which could account for oblique sound incidence, unlike the impedance tube that measures only normal incidence. Although the lab process was time-consuming, I managed to produce more samples than initially expected and gained valuable insight into how manufacturing parameters influence both material structure and acoustic performance. However, further testing is needed, particularly for fused samples. So far, only those fused simultaneously with the foaming process have been measured. While this project shows that technical barriers in glass recycling, especially contamination, can potentially be overcome, it does not address supply chain challenges, such as the separation and collection of different types of glass waste.

- **Opportunities:** There is significant potential to expand this research by investigating the structural and thermal performance of the material and by developing panel designs suitable for industry application. Further opportunities lie in the integration of machine learning within the design and simulation workflow. Strengthening the connection between parametric modeling environments such as Rhino/Grasshopper and acoustic simulation tools like CATT-Acoustic could greatly enhance both this project and future studies, given the widespread use of these platforms in architectural and acoustic design contexts.

- **Threats:** Even though understanding was gained on how different manufacturing parameter affect the sample, controlling foam properties proved to be complex, with occasional unexpected results that couldn't always be expected or explained. The variability of recycled glass waste and the unpredictability of the foaming process pose challenges for standardizing production. Whenever unusual results occurred, experiments were repeated to verify outcomes. For instance, the first SL5CCT2 sample turned out denser and less foamed than expected, despite using the same material and conditions that had worked in smaller moulds. A second attempt produced much better foaming and ultimately the best sound absorption result. This experience highlights the inherent randomness in foaming, despite careful control, results were not always repeatable. Factors such as uneven foaming agent distribution, possibly local temperature fluctuations, or unpredictable chemical reactions during firing likely contributed to these inconsistencies. While the panels show potential for indoor use, their porous structure makes them prone to dust accumulation and difficult to clean – an important consideration before launching them as a product. This also raises the question of whether such panels could be adapted for outdoor use. Additionally, even the rigid, solid samples showed some surface crumbling, which would need to be addressed to ensure durability and long-term performance in a commercial application.

Research-design relationship

In this project, research directly informed design. The relationship between research and design was iterative and mutually reinforcing. Rather than treating research and design as separate phases, they informed and evolved next to each other throughout the project.

Material testing provided performance data that guided design decisions for the panel system. In turn, the architectural case study allowed the simulated testing of these materials in a realistic context. This interplay between material research and spatial design exemplifies the iterative relationship between experimentation and application.

The design of the glass panels was driven by insights gained from material research. Early-stage literature review and experiments on foaming provided a scientific foundation for understanding how different glass types and fabrication parameters influenced the physical and acoustic properties of the material. These findings informed critical design decisions - such as the two-layer composition of the panel (porous foamed layer for absorption and solid cast layer for structure), the choice of tack fusing to bond layers without adhesives, and the focus on open porosity to optimize sound absorption.

At the same time, the design goals - creating an acoustic panel suitable for a dual-use performance

hall - set clear functional requirements for the material: sound absorption in specific frequency ranges and structural integrity. These goals guided the research process by narrowing down which acoustic properties to measure, what fabrication parameters to test, and how to define success.

Moreover, the use of computational acoustic simulations created a bridge between material-level findings and spatial performance. Laboratory measurements of the prototype were translated into absorption coefficients, which were then implemented in digital models of the Theatre Hall at TU Delft. This allowed the panel's real-world effectiveness to be evaluated in context, and further informed adjustments to design and panels' placement in the case study volume.

Ultimately, the project demonstrates that research is not just a foundation for design - it is an active part of the design process itself.

5.3.2. Ethical and moral considerations

One ethical consideration I had throughout this project was the feeling that, at times, my results might not be enough to draw broad conclusions, because truly proving a pattern would likely require hundreds of experiments like the ones I conducted. Still, I'm confident that the work I've done contributes to the core problem I defined to address. That's why I chose to present my findings honestly and confidently, always making sure to explain exactly what was done, even if some outcomes didn't fully support the expected or "positive" result. A key part of that was not overstating the environmental benefits of the panels. While the project promotes the reuse of waste glass, I did not conduct a Life Cycle Assessment which would be essential to formally support sustainability claims. Instead, I based these claims on literature and clearly positioned an LCA as a necessary step in future research. I also deliberately avoided using binders or chemical additives that could hinder recyclability, in line with circularity principles.

Another concern relates to the impedance tube measurements. Some of the samples were slightly too small for the tube, which needs a tight fit to ensure accurate readings. To address this, I sealed the gaps with tape or a rubber strap, which may have introduced minor inaccuracies. That said, the resulting SAC curves didn't show any unusual artifacts, so I remain optimistic (but cautious) about their reliability. Still, I would repeat those specific tests if the time allowed, manufacturing new samples, cutting them precisely to size, and re-measuring, to ensure the validity of the data.

Lastly, over the course of the project, I intentionally narrowed down the number of variables I tested. Early on, I made decisions about which samples and parameter combinations to continue with, focusing on those that showed promising results and would eventually need to be tested for sound absorption. As the study progressed, I concentrated on materials and settings that performed better. This is why, for example, low iron soda lime glass appears in far more experiments than automotive or aluminosilicate glass. Similarly, calcium carbonate proved effective with most glass types and was eventually replaced with eggshell as a more sustainable alternative.

That said, the samples or combinations I set aside at the early phase of the project may still have potential, perhaps under different firing conditions or with alternative foaming agents. It wasn't easy to let go of these possibilities, but it allowed me to develop a deeper understanding of what was working and why.

5.3.3. Societal Impact

Practical Applicability

While still in the prototype stage, the panels developed in this research show strong practical potential. The methods explored: foaming and fusing (potentially also casting) are scalable and adaptable to architectural production. Their simulated application in the Theatre Hall demonstrated

their ability to enhance acoustic performance in real-world scenarios. I believe that acoustic glass panels like these could eventually become a viable product, and not only for boutique spaces such as concert halls, where both aesthetics and acoustic quality are critical. Similar concepts have already been applied in outdoor settings for traffic noise control, suggesting broader applicability.

However, there are still challenges to overcome before these panels could be considered commercially viable. One of my major concerns is dust accumulation. The porous structure, while essential for acoustic absorption, easily traps dust, particularly problematic if panels are mounted overhead with the porous side facing upward. Cleaning would be difficult, and this issue needs to be addressed in future development. Additionally, although the panels may be water-resistant, some samples absorb significant moisture, especially after being cut in wet conditions. From experience, I found that drying takes quite a long time, and wiping the surface is not enough.

Another issue is material degradation. Even the rigid, solid samples tend to release fine dust and decompose slowly, which would be unacceptable in a commercial product. Improving crystallization, (possibly through the use of $CaHPO_4$), could enhance durability and reduce dust formation.

From a manufacturing standpoint, I see strong potential for optimization. Combining fusing and foaming in a single kiln run is particularly promising, as it saves both energy and time. This method works well when the solid glass layer (for example float glass) remains flat or needs to be curved: it can be placed at the bottom of the mould, with the foaming mixture added on top. After firing, only the top surface needs to be trimmed to expose the porous layer.

However, more complex designs, such as shaped or diffusive back layers, may introduce complications. In those cases, a deeper mould would be required to fit both layers, with the casting cullet placed below and the foaming mixture above. A challenge here is that the foaming temperature may not be sufficient to cast the bottom layer. One possible solution is a two-stage firing: first heating to a higher temperature to cast the base, then lowering the temperature, opening the kiln to add the foaming mixture, and reheating for the foaming process. While more complex and potentially riskier, this method could allow for more customized designs.

That said, if both fusing and foaming can be successfully combined in a single, well-controlled firing, this remains the most energy- and time-efficient approach.

I am also aware that the proposed panel application is somewhat specialized, focused more on comfort than safety (however I do believe that these should be equally important in a built environment) and intended for very special, acoustically sensitive environment like performance space. Still, I believe that proving the panels' effectiveness in such a demanding context shows even greater potential for their use in more common acoustically problematic spaces, such as sports halls, swimming pools, train stations, or museums, where issues like excessive reverberation are often present.

Innovation achieved

The project successfully innovated by combining two contrasting forms of glass (rigid and porous) into a single, recyclable panel system. The use of waste streams not traditionally recycled, and the development of acoustic panels from them, presents a novel contribution to both material science and architectural acoustics. This research aligns with sustainable goals also, addressing the need to reduce construction waste, reuse materials, and minimize dependence on synthetic, non-recyclable acoustic materials.

Socio-cultural and ethical impact

By proposing a sustainable material made from locally sourced glass waste, this project helps shift how we think about materials, challenging the idea that waste has no value. It also raises

awareness (hopefully both among the manufacturers and architecture enthusiasts) about the challenges of glass recycling and promotes a more circular approach to design. The methodology employed in the project is clearly explained, so that the research can be built upon in the future in a responsible way. The work connects with growing concerns about waste, climate change, and sustainable construction, and offers a practical, creative solution for reusing difficult waste materials. This supports wider goals in Europe to move toward more circular and sustainable building practices.

Impact on architecture and the built environment

This thesis proposes a new material strategy that integrates acoustic performance, sustainability, and aesthetic flexibility. Its potential impact on architectural practice lies in encouraging designers and manufacturers to think outside-the-box, move beyond conventional materials and to embed environmental responsibility from the early stages of material and system design. At the same time, it allows for a high degree of customization and aesthetic experimentation - aspects that are equally important in architecture.

References

1. Arenas, J., & Crocker, M. (2010). Recent Trends in Porous Sound-Absorbing Materials.

2. Bassuet, A., Rife, D., & Dellatorre, L. (2014). Computational and Optimization Design in Geometric Acoustics. Building Acoustics, 21(1), 75–85. https://doi.org/10.1260/1351-010X.21.1.75

3. Beranek, L. (1996). Acoustics and musical qualities. The Journal of the Acoustical Society of America, 99(5), 2647–2652. https://doi.org/10.1121/1.414808

4. Beranek, L. (2011). Concert hall acoustics. Architectural Science Review, 54(1), 5–14. https://doi.org/10.3763/asre.2010.0059

5. Bernardo, E., Cedro, R., Florean, M., & Hreglich, S. (2007). Reutilization and stabilization of wastes by the production of glass foams. Ceramics International, 33(6), 963–968. https://doi.org/10.1016/j.ceramint.2006.02.010

6. Bernardo, E., Scarinci, G., Bertuzzi, P., Ercole, P., & Ramon, L. (2010). Recycling of waste glasses into partially crystallized glass foams. Journal of Porous Materials, 17(3), 359–365. https://doi.org/10.1007/s10934-009-9286-3

7. Bristogianni, T., & Oikonomopoulou, F. (2023). Glass up-casting: A review on the current challenges in glass recycling and a novel approach for recycling “as-is” glass waste into volumetric glass components. Glass Structures & Engineering, 8(2), 255–302. https://doi.org/10.1007/s40940-022-00206-9

8. Bristogianni, T., Oikonomopoulou, F., de Lima, C. J., Veer, F. A., & Nijsse, R. (2018). Structural cast glass components manufactured from waste glass: Diverting everyday discarded glass from the landfill to the building industry. 2018.

9. Bristogianni, T., Oikonomopoulou, F., Justino De Lima, C., Veer, F., & Nijsse, R. (2018). Cast Glass Components out of Recycled Glass: Potential and Limitations of Upgrading Waste to Load-bearing Structures. Challenging Glass Conference Proceedings, 151-174 Pages. https://doi.org/10.7480/CGC.6.2130

10. Bristogianni, T., Oikonomopoulou, F., & Veer, F. A. (2021). On the flexural strength and stiffness of cast glass. Glass Structures & Engineering, 6(2), 147–194. https://doi.org/10.1007/s40940-021-00151-z

11. Bulekova, A., & Temirgali, G. (2020). Processing of Glass Containers Using Fusing Technology. https://easychair.org/publications/preprint/THMr

12. Bullseye Glass Co. (2020). Heat & glass: Technotes 4 – Understanding the effects of temperature variations on Bullseye Glass. Bullseye Glass Company. https://www.bullseyeglass.com

13. Buratti, C., Belloni, E., Lascaro, E., Lopez, G. A., & Ricciardi, P. (2016). Sustainable Panels with Recycled Materials for Building Applications: Environmental and Acoustic Characterization. Energy Procedia, 101, 972–979. https://doi.org/10.1016/j.egypro.2016.11.123

14. Cai, L., Tian, J., Feng, K., Liu, Y., & Jiang, Q. (2023). Sound absorption model of foam glass-ceramics based on microstructure. Journal of Non-Crystalline Solids, 604, 122136. https://doi.org/10.1016/j.jnoncrysol.2023.122136

15. Cho, H. Y., Choi, C. H., Kim, J. Y., Choi, D. H., & Lee, S. W. (2005). Sound Absorbing Properties of

Foamed Glasses. Materials Science Forum, 486–487, 578–581. https://doi.org/10.4028/www.scientific.net/MSF.486-487.578

16. Cox, T. J., & D'Antonio, P. (2017). Acoustic absorbers and diffusers: Theory, design and application (Third edition). CRC Press, Taylor & Francis, CRC Press is an imprint of the Taylor & Francis Group, and informa business.

17. Da Silva, R. C., Puglieri, F. N., De Genaro Chiroli, D. M., Bartmeyer, G. A., Kubaski, E. T., & Tebcherani, S. M. (2021). Recycling of glass waste into foam glass boards: A comparison of cradle-to-gate life cycles of boards with different foaming agents. Science of The Total Environment, 771, 145276. https://doi.org/10.1016/j.scitotenv.2021.145276

18. DeBrincat, G., & Babic, E. (n.d.). Re-thinking the life-cycle of architectural glass.

19. Ducman, V., & Kovačević, M. (1997). The Foaming of Waste Glass. Key Engineering Materials, 132–136, 2264–2267. https://doi.org/10.4028/www.scientific.net/KEM.132-136.2264

20. Engel, G., & Reinhold, J. (2023). Acoustic upgrade for the Concert Hall of the Sydney Opera House. Proceedings of the Institute of Acoustics, 45(2). Müller-BBM Building Solutions.

21. Ermann, M. A. (2015). Architectural Acoustics Illustrated.

22. European Parliament and Council of the European Union, Directive 2011/65/EU of the European Parliament and of the Council of 8 June 2011 on the restriction of the use of certain hazardous substances in electrical and electronic equipment (recast). 2011: Official Journal of the European Union.

23. Giassia. (2022). Bio-host glass.

24. Ginn, K. B. (1978). Architctural acoustics (2. Aufl). Brüel & Kjaer.

25. Glass for Europe Dismantling automotive glass is a mandatory step to increase recycling of end-of-life vehicles - Position on the revision of the End-of-Life of Vehicles Directive. 2024).

26. Hesky, D., Aneziris, C. G., Groß, U., & Horn, A. (2015). Water and waterglass mixtures for foam glass production. Ceramics International, 41(10), 12604–12613. https://doi.org/10.1016/j.ceramint.2015.06.088

27. Hestin, M., deVeron, S., & Burgos, S. (2016). Economic study on recycling of building glass in Europe. 2016, Deloitte.

28. Hubálková, J., Voigt, C., Schmidt, A., Moritz, K., & Aneziris, C. G. (2017). Comparative Phenomenological Study of Fracture Behaviour of Ceramic and Glass Foams under Compressive Stress Using In Situ X-Ray Microtomography. Advanced Engineering Materials, 19(9), 1700286. https://doi.org/10.1002/adem.201700286

29. Ioannidis, M., Oikonomopoulou, F., Bristogianni, T., Bilow, M., & Koniari, A. M. (2024). Surface and finishing quality exploration of complex cast glass forms produced on disposable moulds. Glass Structures & Engineering. https://doi.org/10.1007/s40940-024-00264-1

30. König, J., Lopez-Gil, A., Cimavilla-Roman, P., Rodriguez-Perez, M. A., Petersen, R. R., Østergaard, M. B., Iversen, N., Yue, Y., & Spreitzer, M. (2020). Synthesis and properties of open- and closed-porous foamed glass with a low density. Construction and Building Materials, 247, 118574. https://doi.org/10.1016/j.conbuildmat.2020.118574

31. König, J., Petersen, R. R., & Yue, Y. (2016). Influence of the glass particle size on the foaming process and physical characteristics of foam glasses. Journal of Non-Crystalline Solids, 447, 190–197. https://doi.org/10.1016/j.jnoncrysol.2016.05.021

32. Lautenbach, M. (2018). Musis Sacrum Arnhem: Acoustics of the Parkzaal and the Muzenzaal. Peutz BV. https://www.peutz.nl/downloads/Musis_Arnhem_E.pdf

33. Lautenbach, M., Heringa, P., & Vercammen, M. (2007). Acoustics for large scale indoor pop events. International Symposium on Room Acoustics, Satellite Symposium of the 19th International Congress on Acoustics, Seville, Spain.

34. Long, M. (2006). Architectural acoustics. Springer. https://archive.org/details/ArchitecturalAcoustics_201901

35. Magalini, F., et al., Study on Collection Rates of Waste Electrical and Electronic Equipment (WEEE) - Possible Measures to be initiated by the Commission as Required by Article 7(4), 7(5), 7(6) AND 7(7) of Directive 2012/19/EU on Waste Electrical and Electronic Equipment (WEEE). 2014, European Commission: ec.europa.eu.

36. Markham, B. (2014). Leo Beranek and concert hall acoustics. The Journal of the Acoustical Society of America, 136(4_Supplement), 2162–2162. https://doi.org/10.1121/1.4899823

37. Matskidou. (2022). RE-FACADE GLASS PANEL made by Construction & Demolition Recycled Glass.

38. Mirra, G., Mack, M., & Pugnale, A. (2023). Aeolus: A Grasshopper plugin for the interactive design and optimisation of acoustic shells.

39. Nederlof, L., Cauberg, J. J. M., & Tenpierik, M. (n.d.). A brief introduction to the wave character of sound. In Room Acoustics: Fundamentals. Delft University of Technology, Delft.

40. Nijs, L., & Vries, D. D. (2005). The young architect's guide to room acoustics. Acoustical Science and Technology, 26(2), 229–232. https://doi.org/10.1250/ast.26.229

41. Oikonomopoulou, F. (2019). A+BE | Architecture and the Built Environment, No. 9 (2019): Unveiling the third dimension of glass. A+BE | Architecture and the Built Environment. https://doi.org/10.7480/ABE.2019.9

42. Oikonomopoulou, F., Bristogianni, T., Barou, L., Veer, F. A., & Nijsse, R. (2018). The potential of cast glass in structural applications. Lessons learned from large-scale castings and state-of-the art load-bearing cast glass in architecture. Journal of Building Engineering, 20, 213–234. https://doi.org/10.1016/j.jobe.2018.07.014

43. Rindel, J. H. (1995). Computer Simulation Techniques for Acoustical Design of Rooms

44. Rossing, T. D. (Ed.). (2014). Springer Handbook of Acoustics. Springer New York. https://doi.org/10.1007/978-1-4939-0755-7

45. Sakuma, T., Sakamoto, S., & Otsuru, T. (Eds.). (2014). Computational Simulation in Architectural and Environmental Acoustics: Methods and Applications of Wave-Based Computation. Springer Japan. https://doi.org/10.1007/978-4-431-54454-8

46. Setaki, F., Tian, F., Turrin, M., Tenpierik, M., Nijs, L., & Van Timmeren, A. (2023). 3D-printed sound absorbers: Compact and customisable at broadband frequencies. Architecture, Structures and Construction, 3(2), 205–215. https://doi.org/10.1007/s44150-023-00086-9

47. Souza, M. T., Maia, B. G. O., Teixeira, L. B., De Oliveira, K. G., Teixeira, A. H. B., & Novaes De Oliveira, A. P. (2017). Glass foams produced from glass bottles and eggshell wastes. Process Safety and Environmental Protection, 111, 60–64. https://doi.org/10.1016/j.psep.2017.06.011

48. Surgenor, A., Holcroft, C., Gill, C., & DeBrincat, G. (2018). Building glass into the circular economy. How to guide.

49. Toyota, Y., Komoda, M., Beckmann, D., Quiquerez, M., & Bergal, E. (2020). Concert Halls by Nagata Acoustics: Thirty Years of Acoustical Design for Music Venues and Vineyard-Style Auditoria. Springer International Publishing. https://doi.org/10.1007/978-3-030-42450-3

50. Vercammen, M., & Lautenbach, M. (2020). Variable Acoustics without Compromise: Concert Halls for both Symphonic and Pop Music. 5 pages. https://doi.org/10.48465/FA.2020.0257

51. Vermeulen, J. (2016). EU Construction & Demolition Waste Management Protocol.

52. Vieitez Rodriguez, E., Eder, E., Villanueva, P., & Saveyn, A. (2011). End-of-Waste Criteria for Glass Cullet.

53. Vorländer, M. (2013). Computer simulations in room acoustics: Concepts and uncertainties. The Journal of the Acoustical Society of America, 133(3), 1203–1213. https://doi.org/10.1121/1.4788978

54. Yan, Z., Feng, K., Tian, J., & Liu, Y. (2019). Effect of high titanium blast furnace slag on preparing foam glass–ceramics for sound absorption. Journal of Porous Materials, 26(4), 1209–1215. https://doi.org/10.1007/s10934-019-00722-0

Appendix

Results of acoustic measurements in the Theatre Hall

RT 1 - 11

	Frequency (Hz)					
	125	250	500	1000	2000	4000
Receiver	RT -1->11					
P1	0.67	0.74	1.06	1.13	1.18	0.24
P2	1.18	0.94	1.22	1.41	1.12	0.97
P3	1.03	1.36	1.34	1.20	1.11	0.96
P4	1.01	1.43	1.13	1.40	1.25	0.96
P5	1.29	1.23	1.61	1.93	1.74	1.06
P6	1.06	1.17	1.49	1.22	1.22	0.90
P7	1.02	1.08	1.36	1.32	1.17	0.98
P8	1.25	1.22	1.45	1.41	1.23	1.06
P9	1.14	1.32	1.20	1.32	1.19	0.97
P10	1.13	1.42	1.65	1.42	1.35	1.02
P11 OP	1.09	1.06	1.19	1.19	1.07	0.86
P11 CL	1.13	1.42	1.65	1.42	1.35	1.02
P11 BA	0.99	1.05	0.98	1.05	0.83	0.73

RT 5 - 25

	Frequency (Hz)					
	125	250	500	1000	2000	4000
Receiver	RT -5->25					
P1	1.17	1.18	1.48	1.49	1.45	0.99
P2	1.34	1.20	1.42	1.74	1.55	1.03
P3	1.37	1.37	1.47	1.71	1.53	1.01
P4	1.32	1.34	1.56	1.66	1.72	1.06
P5	1.42	9.97	9.29	9.84	11.13	3.93
P6	11.31	1.26	1.54	1.80	2.75	1.05
P7	8.82	1.25	1.46	1.42	1.27	1.00
P8	1.66	1.20	1.40	1.44	1.25	1.04
P9	7.23	1.15	1.46	1.47	1.23	1.04
P10	4.58	1.18	1.40	1.41	1.25	1.04
P11 OP	1.54	1.50	1.51	1.49	1.28	1.06
P11 CL	4.58	1.18	1.40	1.41	1.25	1.04
P11 BA	1.38	1.10	1.11	1.27	1.07	0.84

C80

	Frequency (Hz)					
	125	250	500	1000	2000	4000
Receiver	C80					
P1	9.1	10.1	10.1	10.4	8.6	14.3
P2	2.9	-0.9	2.3	2.3	3.4	5.2
P3	2.1	1.4	1.4	1.5	1.7	5.2
P4	1.1	1.0	0.4	1.3	2.8	4.0
P5	6.5	1.4	0.2	2.0	1.9	3.0
P6	2.7	-0.3	-0.1	2.5	4.1	5.9
P7	0.3	-0.7	0.4	1.7	2.7	3.8
P8	2.5	1.0	1.4	1.4	0.9	3.0
P9	1.4	2.4	0.6	1.3	2.6	3.6
P10	3.4	3.0	1.2	1.9	2.3	4.7
P11 OP	1.8	2.2	1.1	1.1	2.8	4.6
P11 CL	3.4	3.0	1.2	1.9	2.3	4.7
P11 BA	3.0	3.4	2.5	3.0	4.4	6.6

G

	Frequency (Hz)					
	125	250	500	1000	2000	4000
Receiver	G - strength					
P1	21.6	19.0	19.1	20.0	18.0	22.0
P2	15.2	13.1	12.7	12.7	13.1	12.4
P3	11.8	9.0	11.0	11.6	11.2	11.2
P4	14.1	9.1	10.9	11.1	10.4	9.6
P5	14.2	9.5	10.8	12.3	11.2	9.9
P6	16.2	7.8	10.2	12.4	11.8	11.3
P7	12.4	8.3	10.2	11.4	10.9	10.1
P8	13.3	8.8	11.0	11.2	10.0	9.0
P9	11.9	9.2	10.8	11.3	11.1	9.8
P10	15.2	10.8	11.3	12.8	11.5	11.5
P11 OP	13.3	10.0	12.0	12.3	12.1	11.9
P11 CL	15.2	10.8	11.3	12.8	11.5	11.5
P11 BA	11.8	8.4	10.4	10.6	10.8	10.9

Firing schedules for foaming tested in the study

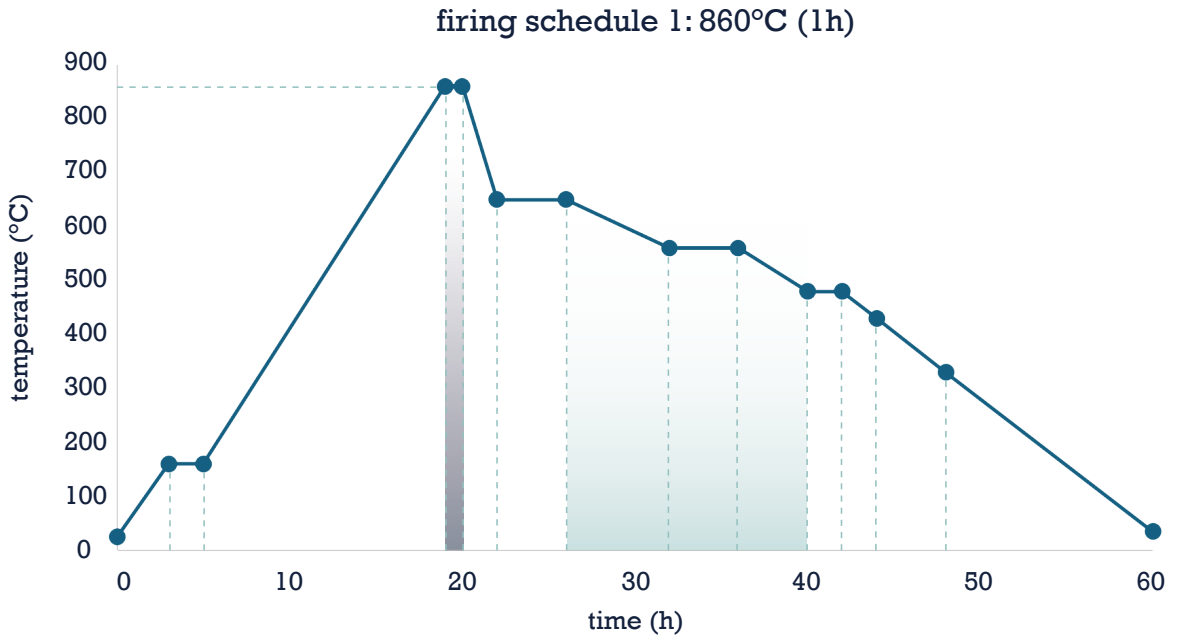

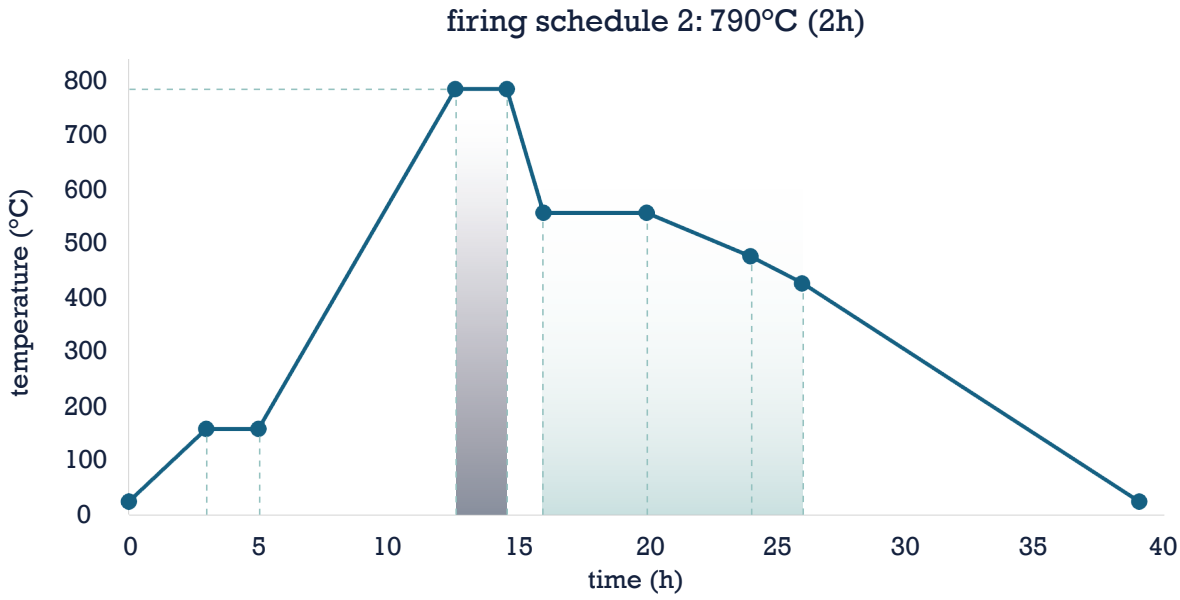

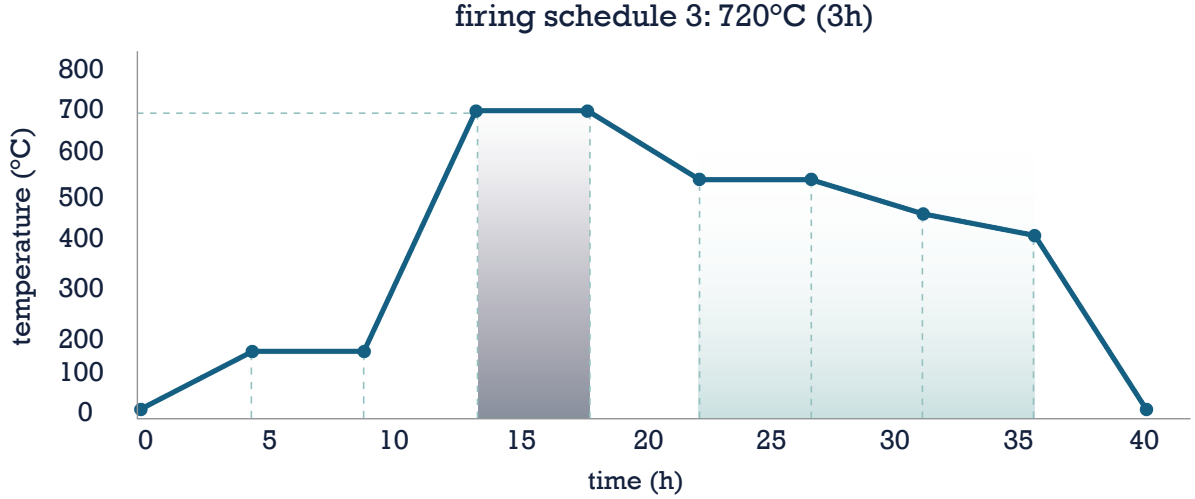

Photohgraphs of all the manufactured foam glass samples


SL5CCT1
AL5CCT1
SL5EST1
SL2.5CCT2
SLCCT2(2.5+5)
SL3.5CCT2
LB2.5EST2
SL2.5CCT1
SL2CCT2
SL5EST2
LB1EST2
SL2.5EST2
LB2.5EST3
SL2.5EST3
SL5CCT3
CM3CCT1
CM5CCT1
CM0.3C1.6HPT2
CL/CM50/50T2
CM3CCT2
SL/CM20/80T2
SLCCT2(2.5+5)
LB2.5EST2
M1EST2
SL2.5EST2
LB5EST1
AM5EST2
LB2.5EST1
CM0.3C3.2HPT2
M2.5EST2
SL10MDT2
SL2.5EST1
CM0.3C1.6HPT1
SL/CM20/80T2
SL2.5CCT3

Impedance tube measurements results

Comparison of single-layer and double-layer fused samples

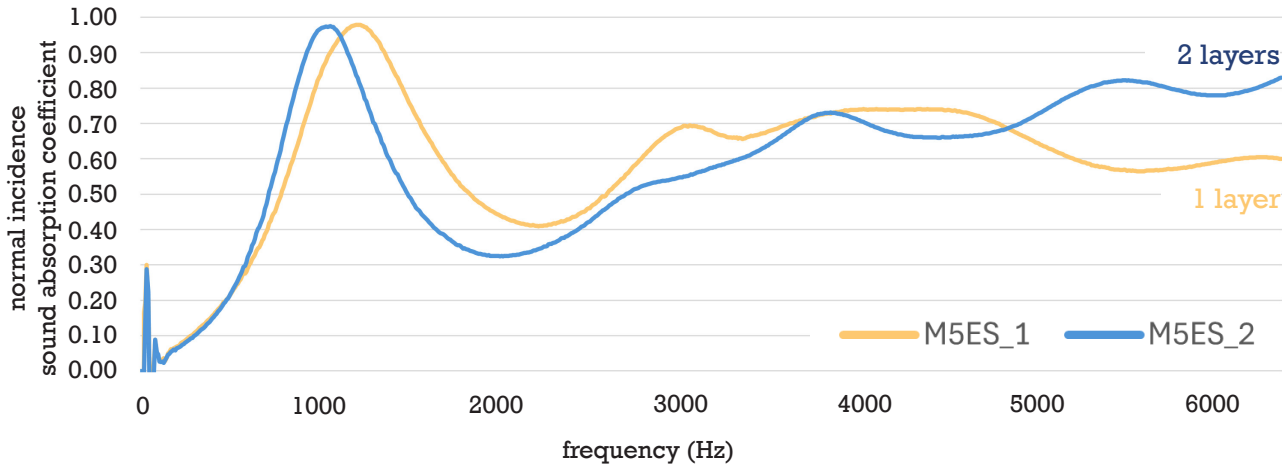

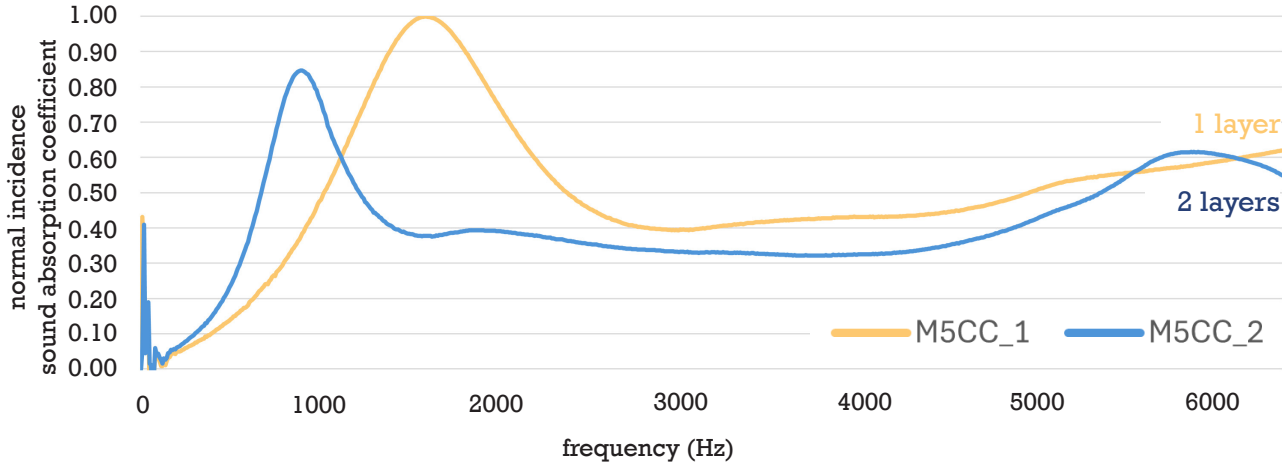

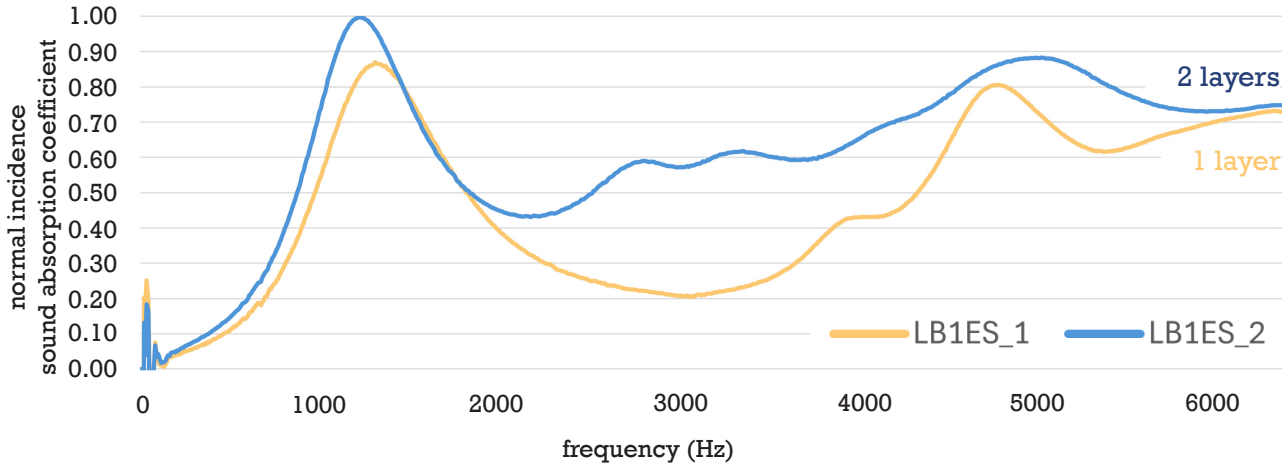

Comparison of single-layer and double-layer glued samples

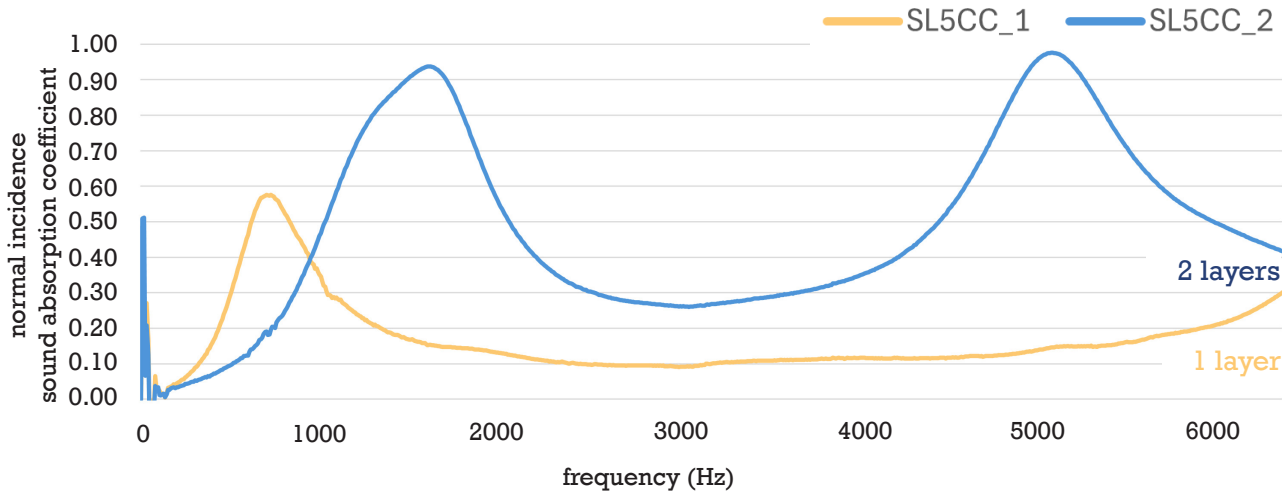

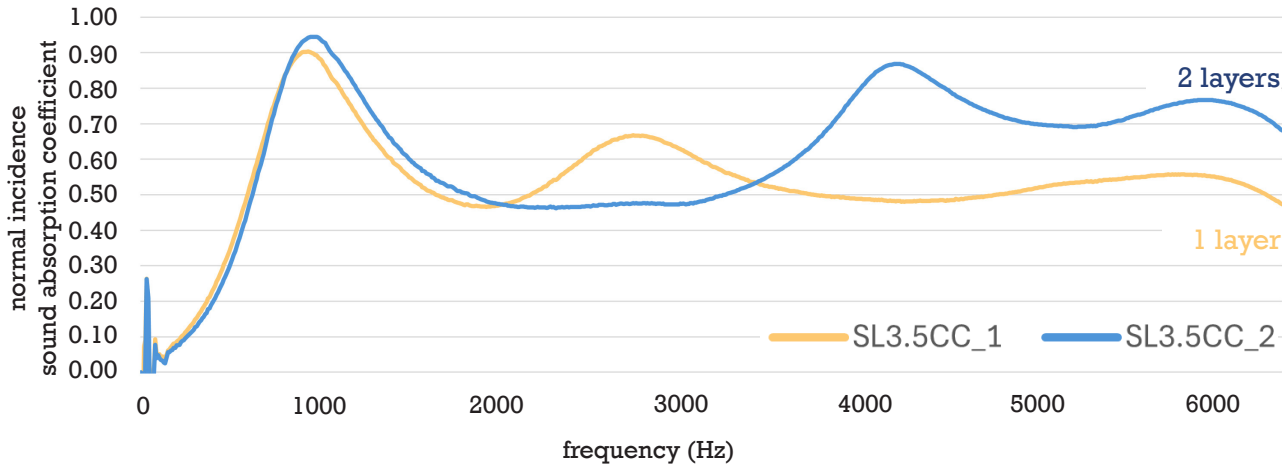

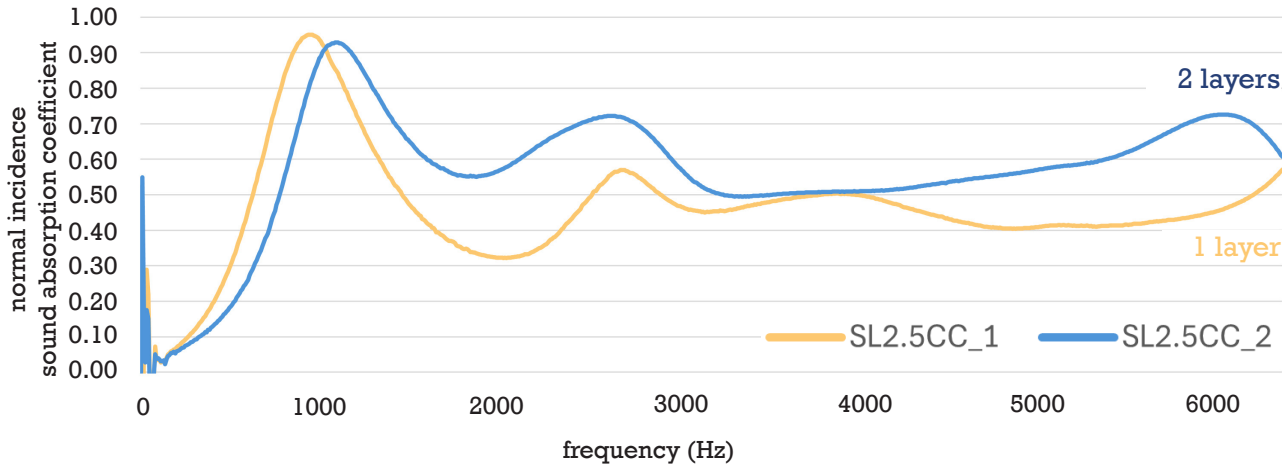

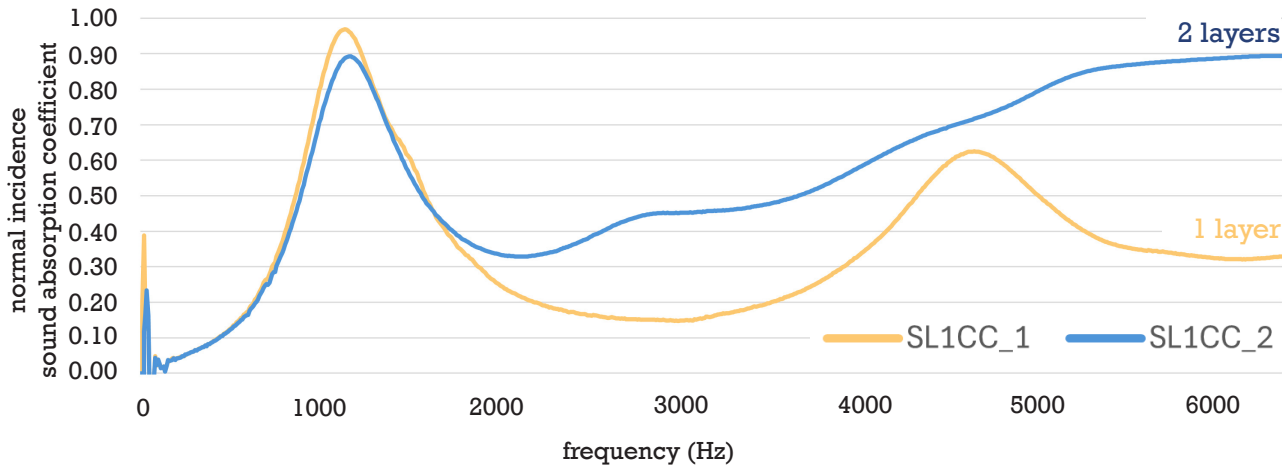

CATT-Acoustic absorption and scattering coefficients of materials used in simulations

```
ABS FLOOR = <2 3 2 3 4 5> L <5 5 10 10 10 15> {246 183 116}
ABS CEILING = <40 58 55 68 60 65> L <50 50 60 60 70 80> {246 183 116}
ABS WOOD_WALL = <30 28 20 10 11 12> L <10 10 10 15 15 15> {246 183 116}
ABS CONCRETE = <4 3 2 3 6 5> L <15 15 20 20 30 30> {116 116 116}
ABS GLASS = <8 12 1 6 5 4> L <15 20 25 30 30 30> {173 216 230}
ABS CURTAIN = <22 15 30 25 35 37> L <20 20 20 25 25 30> {0 0 0}
ABS RADIATOR = <8 12 4 7 5 8> L <10 15 15 20 20 20> {24 24 24}
ABS AUDITORIUM = <35 34 17 22 36 39> L <50 60 60 70 70 70> {116 116 116}
ABS BENCHES_EMPTY = <40 57 50 60 65 72> L <30 40 40 50 50 60> {255 0 0}
ABS ORCHESTRA = <27 53 67 93 87 8> L <80 80 80 80 80 80> {88 57 39}
ABS BENCHES_FULL = <41 58 80 90 92 89> L <60 60 70 70 75 80> {128 0 128}
```

Reflective panels solutions tested in CATT-Acoustic

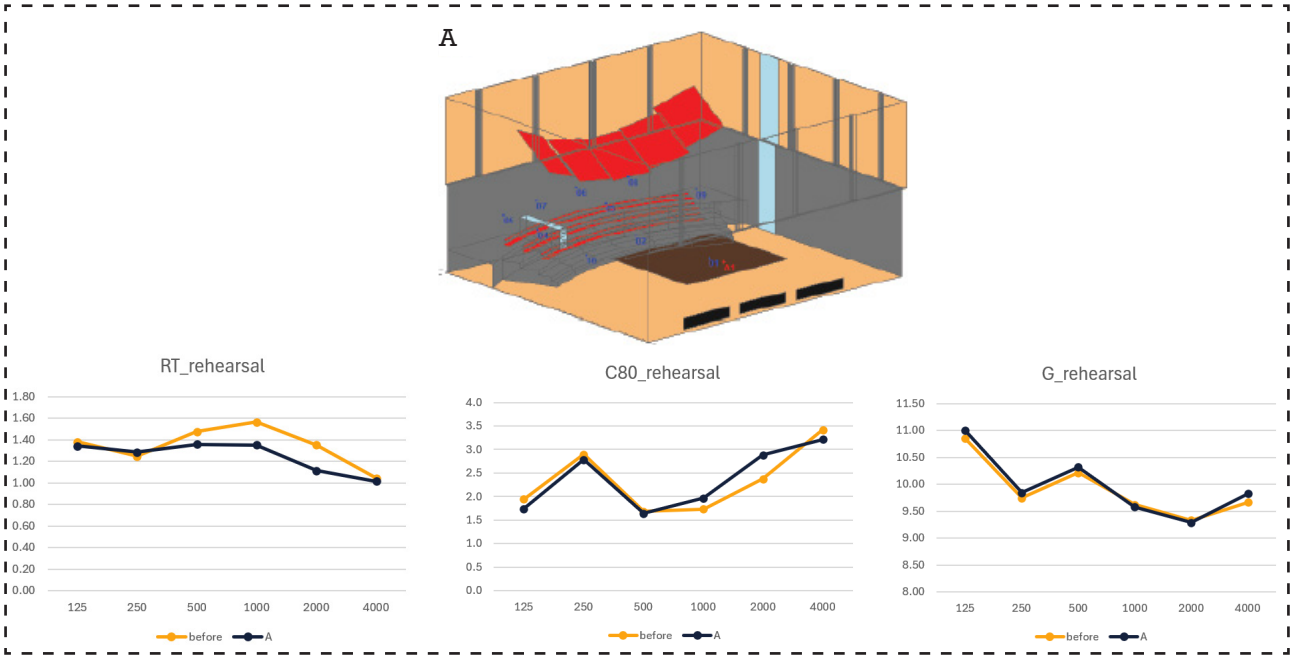

B1

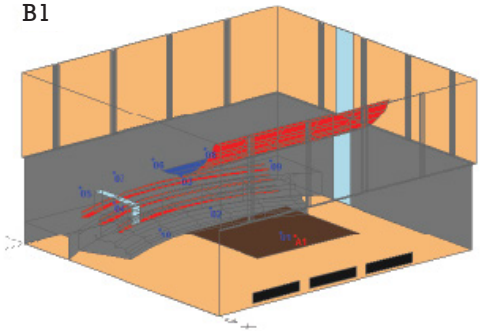

B2

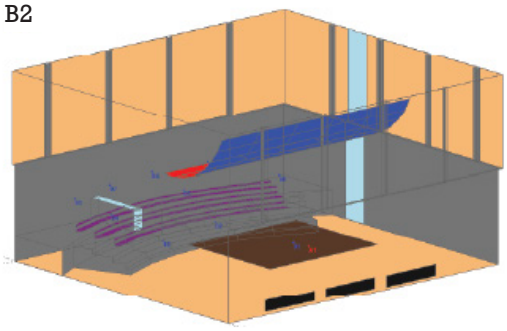

RT_rehearsal

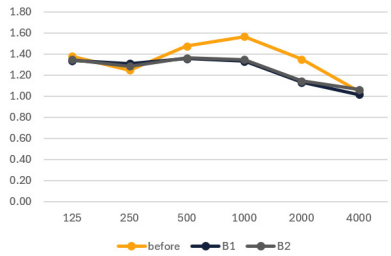

C80_rehearsal

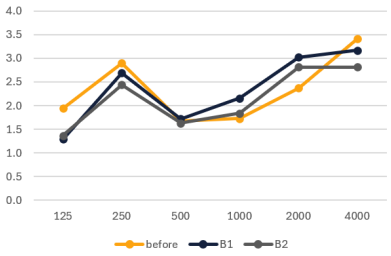

G_rehearsal

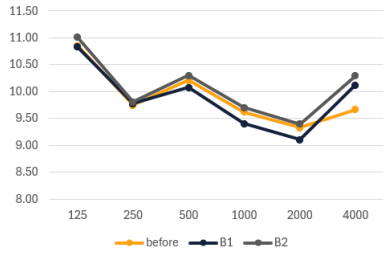

E

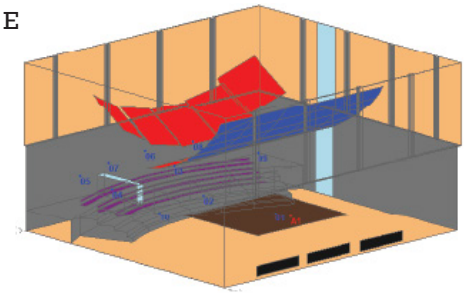

RT_performance

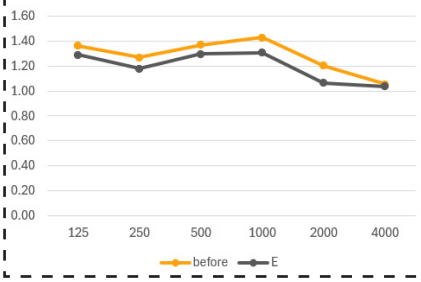

C80_performance

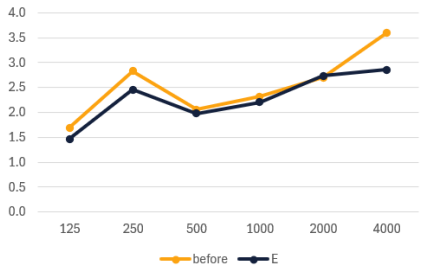

G_performance

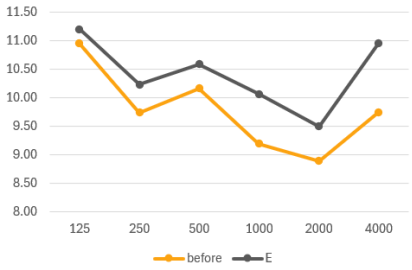

F2

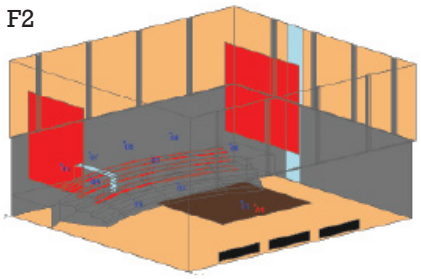

RT_rehearsal

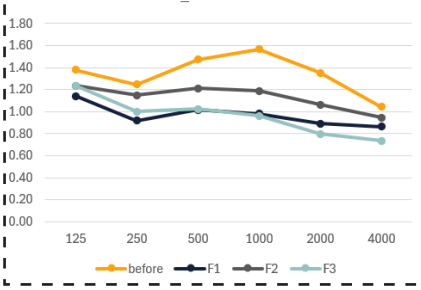

C80_rehearsal

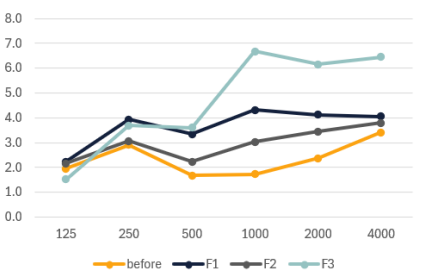

G_rehearsal

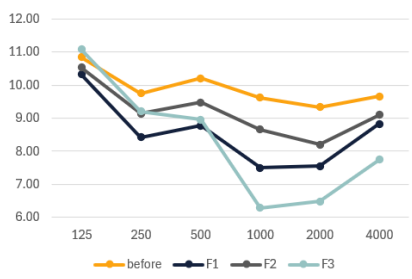

K1

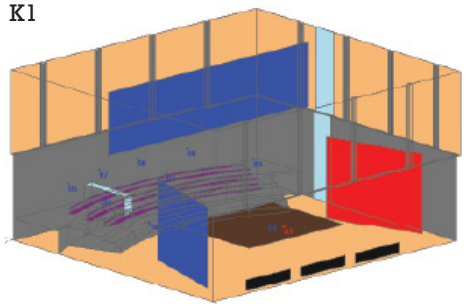

K2

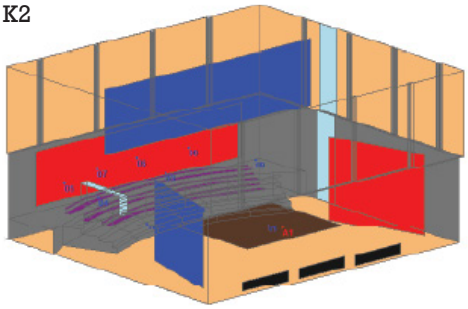

RT_performance

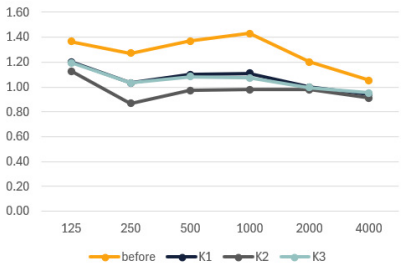

C80_performance

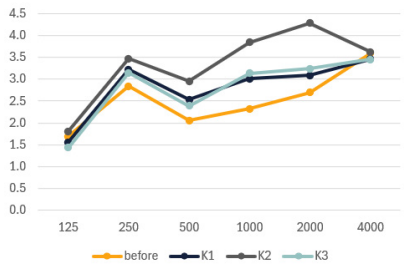

G_performance

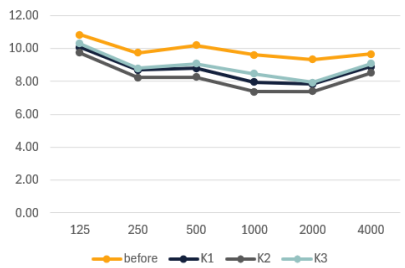

L1

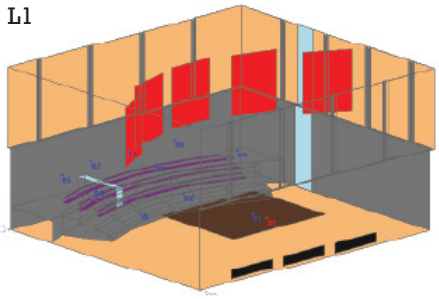

L5

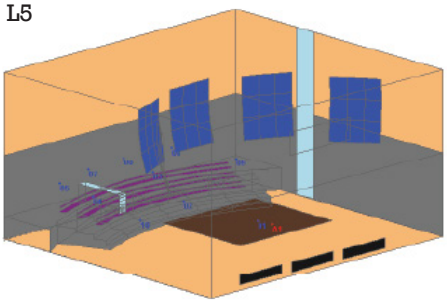

RT_performance

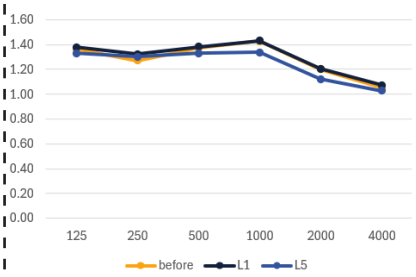

C80_performance

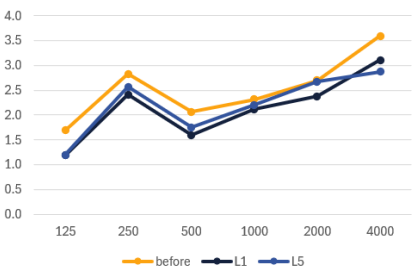

G_performance

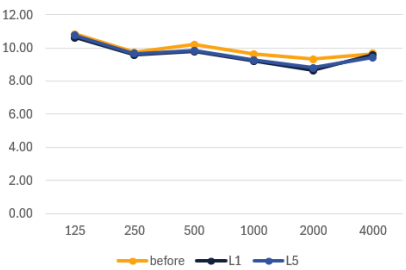

M1

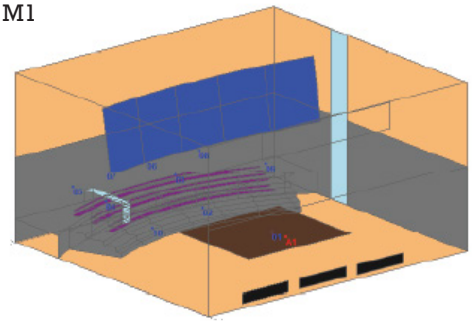

M4

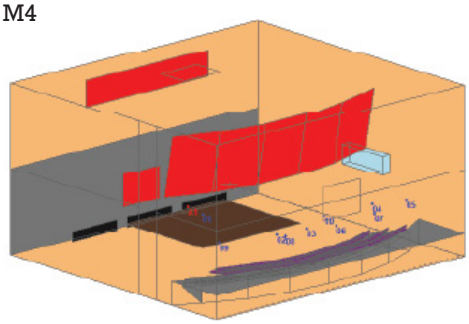

RT_performance

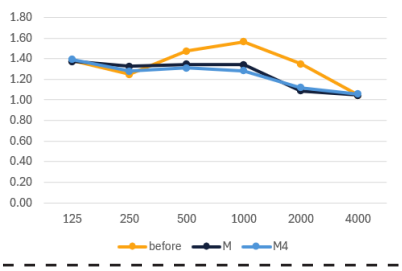

C80_performance

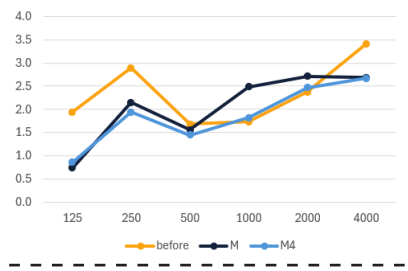

G_performance